

Synthesis of Processable High Performance Polymers

Thesis submitted to the

UNIVERSITY OF PUNE

For the degree of

DOCTOR OF PHILOSOPHY

in

CHEMISTRY

By

R. D. Shingte

Polymer Science and Engineering Division

National Chemical Laboratory

PUNE 411 008

March 2006

To my mentor

Dr. P. P. Wadgaonkar

Knowing him, one is touched by his

Natural simplicity and Infectious enthusiasm

Acknowledgements

As anyone who has earned a Ph.D. will attest, the research process has its moments of elation and difficulties. This research work has been no different. During this learning journey, it was my privilege to have been associated with the following people and to have received their advice, encouragement and support, without which this work would not have been possible:

First and foremost, with great pleasure I would like to dedicate this thesis to my advisor Dr. P. P. Wadgaonkar, who was and will be my mentor and role model. His technical and personal guidance has been invaluable in making me become a better professional and person. This work would not have been possible without your inspiration.

I would like to thank the Council of Scientific and Industrial Research, New Delhi for the award of fellowship and Director, NCL for providing facilities which enabled me to carry out my research in such a prestigious research laboratory.

I take this opportunity to express my deep sense of gratitude to Dr. Rajmohan, Dr. Narsimhaswamy (CLRI, Chennai), Prof. R. B. Mane (Shivaji University, Kolhapur), Prof. M. M. Salunkhe (Shivaji University, Kolhapur), Dr. Guru (GE, Bangalore), Dr. Srinu (GE, Bangalore), Prof. P. Ghosh (IIT, Mumbai), Dr. Mukundan (HEMRL, Pune), Prof. Ramkrishnan, (IISC, Bangalore), Dr. Ashish Lele, Dr. Mohan Bhadbhade, Dr. Guruswamy, Dr. Murali Sastry, Dr. Pedireddy, Dr. Radhakrishnan, Dr. C. Ramesh, Dr. Ulhas Kharul, Dr. Soney Verghese (TUE, Netherlands), Dr. (Mrs.) Vedavati Puranik and Dr. (Mrs.) Jyoti Jog for valuable discussions, which led to proper design of some of the experiments. I sincerely thank Dr. C. V. Avadhani and Dr. A. S. Jadhav who extended their help and support whenever it was required. Thanks are also due to all my teachers for making me eligible for research.

I express my sincere thanks to Dr. S. Sivaram for his inspiring guidance, stimulating discussions and encouragements.

With much pleasure I thank Sandhya, Sudhir, Nana, Vijay, Yogesh, Santosh, Depan, T. Raja, Makrand, Pritesh, Vaijyanti, Kishor Jadhav, and Sriram Karandikar for being my true friends during moments of both success and despair.

Many thanks go to my labmates Anjana, Snehalata, Sony, Pandurang, Arun and Arvind for their help. The help provided by, Nilesh (HEMRL, Pune), Rajiv (IIT, Mumbai), Santosh, Kuldip, Dr. Ramesh Ghadage, Kannan and Prathap cannot go unnoticed.

I thank Mrs. Dhoble, Mr. Menon, Dr. S. D. Patil, Dr. P. G. Shukla, Dr. N. N. Chavan, Dr. T. P. Mohandas, Dr. Khisti, Dr. R. A. Kulkarni, Dr. M. V. Badiger, Dr. R. P. Singh, Mr. A. S. Patil, Mr. K. G. Raut, Dr. B. B. Idage, Dr. B. D. Sarwade, Dr. (Mrs.) A. N. Bote and Dr. (Mrs.) S. B. Idage for their help on many occasions. I am thankful all my colleagues Anjali, Nirmala, Jinu, Ramnathan, Birajdar, Ranjit, Ganni, Neeta, Mahesh, Ravi, Smitha, Bhoje, Malli, PK, Raghu, Govind, Kamendra, Harshada, Rajkiran, Kedar and Subramaniam for their cooperation during my stay at NCL. With much pleasure I thank Siddheshwar and Jine for their help. I thank the members of central NMR facility, especially, Kavita and Mrs. Usha Phalgune, micro analysis, CMC, SMIS, glass blowing, stores, workshop and administrative section for their help.

I am blessed with a very caring and loving family. My special gratitude goes to my father, who instilled in me a desire to learn, strong work ethics and the value of common sense. I shall not have completed this thesis without the constant encouragement and motivation from my mother. I shall not fail to mention my grand parents, uncles, aunts, brothers and sisters for their immense love, support and patience beyond limits.

Rahul D Shingte

Declaration by the Supervisor

Certified that the work incorporated in the thesis entitled “**Synthesis of Processable High Performance Polymers**” subitted by Rahulkumar Diliprao Shingte was carried out under my supersivison. Such material as has been obtained from other sources has been duly acknowledged in this thesis.

March, 2006

Pune

**P. P. Wadgaonkar
(Research Guide)**

Declaration by the Candidate

I declare that the thesis entitled “**Synthesis of Processable High Performance Polymers**” is my own work conducted under the supervision of Dr. P. P. Wadgaonkar, at Polymer Science and Engineering Division, National Chemical Laboratory, Pune.

I further declare that to the best of my knowledge, this thesis does not contain any part of work, which has been submitted for the award of any degree either of this University or any other University without proper citation.

Research Guide

Student

(P. P. Wadgaonkar)

(R. D. Shingte)

CONTENTS

*	Abstract	i
*	List of Tables	iv
*	List of Schemes	vii
*	List of Figures	ix

CHAPTER 1 Introduction and Literature Survey

1.1	Introduction	1
1.2	Polyimides	3
1.2.1	Synthesis of polyimides	3
1.2.1.1	Classical two-step method <i>via</i> poly(amic acid)s	4
1.2.1.2	One-step high temperature solution synthesis of polyimides	12
1.2.1.3	Other synthetic routes to polyimides	13
1.2.1.3.1	Polyimides <i>via</i> derivatized poly(amic acid) precursors	13
1.2.1.3.2	Polyimides <i>via</i> polyisoimide precursors	15
1.2.1.3.3	Polyimides from diester-diacids and diamines (Ester-acid route)	15
1.2.1.3.4	Polyimides from tetracarboxylic acids and diamines	16
1.2.1.3.5	Polyimides from dianhydrides and diisocyanates	17
1.2.1.3.6	Polyetherimides <i>via</i> nucleophilic aromatic substitution reactions	18
1.2.1.3.7	Other routes to polyimide formation	19
1.2.2	Structure-property relationship in aromatic polyimides	19
1.2.2.1	Glass transition and solubility	20
1.2.2.2	Optical properties	21
1.2.2.3	Dielectric properties and moisture uptake	21
1.2.3	Applications of polyimides	21
1.2.3.1	Liquid crystal displays	22
1.2.3.2	Polyimides for LCD application	24
1.3	Polyesters	27
1.3.1	Synthesis of polyesters	27
1.3.1.1	Acid chloride route	27

1.3.1.1.1	Interfacial polycondensation	27
1.3.1.1.2	Low temperature solution polycondensation	29
1.3.1.1.3	High temperature solution polycondensation	30
1.3.1.2	Transesterification route	30
1.3.1.3	Miscellaneous routes for polyester synthesis	30
1.3.2	Structure- property relationship in polyesters	31
1.3.2.1	Gas separation	31
1.3.2.2	Aromatic polyesters for gas separation	34
1.3.3	Applications of aromatic polyesters	36
	References	37
CHAPTER 2 Scope and Objectives		49
<hr/>		
CHAPTER 3 Synthesis and Characterization of Condensation Monomers		
<hr/>		
3.1	Introduction	55
3.1.1	Cashew nut shell liquid (CNSL)	55
3.1.2	<i>p</i> -Cumylphenol	57
3.2	Experimental	58
3.2.1	Materials	58
3.2.2	Measurements	58
3.3	Synthesis	59
3.3.1	Synthesis of 1,1-bis(4-hydroxyphenyl)-3-pentadecylcyclohexane	59
3.3.1.1	Synthesis of 3-pentadecylphenol	59
3.3.1.2	Synthesis of 3-pentadecylcyclohexanol	59
3.3.1.3	Synthesis of 3-pentadecylcyclohexanone	59
3.3.1.4	Synthesis of 1,1-bis(4-hydroxyphenyl)-3-pentadecylcyclohexane	60
3.3.2	Synthesis of 1,1-bis(4-hydroxyphenyl)cyclohexane	60
3.3.3	Synthesis of 1,1-bis(4-hydroxyphenyl)-3-methylcyclohexane	61
3.3.4	Synthesis of 1,1-bis(4-aminophenyl)-3-pentadecylcyclohexane	61
3.3.5	Synthesis of 1,1-bis(4-hydroxyphenyl) -4-perhydrocumyl cyclohexane	62
3.3.5.1	Synthesis of 4-(1-cyclohexyl-1-methyl ethyl) cyclohexanol	62
3.3.5.2	Synthesis of 4-(1-cyclohexyl-1-methyl ethyl) cyclohexanone	62

3.3.5.3	Synthesis of 1,1-bis(4-hydroxyphenyl) -4-perhydrocumyl cyclohexane	63
3.3.6	Synthesis of 1,1-bis(4-hydroxy-3-methylphenyl) -4-perhydrocumyl cyclohexane	63
3.3.7	Synthesis of 1,1-bis(4-hydroxy-3,5-dimethylphenyl) -4-perhydrocumyl cyclohexane	63
3.3.8	Synthesis of 1,1-bis(4-hydroxy-3,5-dibromophenyl) -4-perhydrocumyl cyclohexane	64
3.3.9	Synthesis of 1,1-bis(4-hydroxy-3-methyl-5-bromophenyl) -4-perhydrocumyl cyclohexane	64
3.3.10	Synthesis of 1,1-bis(4-aminophenyl) -4-perhydrocumyl cyclohexane	65
3.3.11	Synthesis of 1,1-bis[4-(4-aminophenoxy)phenyl]-4-perhydrocumyl cyclohexane	65
3.3.11.1	Synthesis of 1,1-bis[4-(4-nitrophenoxy)phenyl]-4-perhydrocumyl cyclohexane	65
3.3.11.2	Synthesis of 1,1-bis[4-(4-aminophenoxy)phenyl]-4-perhydrocumyl cyclohexane	65
3.3.12	Synthesis of 1,1-bis[4-(4-carboxyphenoxy)phenyl]-4-perhydrocumyl cyclohexane	66
3.3.12.1	Synthesis of 1,1-bis[4-(4-cyanophenoxy)phenyl]-4-perhydrocumyl cyclohexane	66
3.3.12.2	Synthesis of 1,1-bis[4-(4-carboxyphenoxy)phenyl]-4-perhydrocumyl cyclohexane	66
3.4	Results and Discussion	
3.4.1	Synthesis and characterization of 1,1-bis(4-hydroxyphenyl)-3-pentadecylcyclohexane	67
3.4.2	Synthesis and characterization of 1,1-bis(4-hydroxyphenyl)-cyclohexane	80
3.4.3	Synthesis and characterization of 1,1-bis(4-hydroxyphenyl)-3-methylcyclohexane	82
3.4.4	Synthesis and characterization of 1,1-bis(4-aminophenyl)-3-pentadecylcyclohexane	84
3.4.5	Synthesis and characterization of bisphenols derived from <i>p</i> -cumyl phenol	86
3.4.5.1	Synthesis and characterization of 1,1-bis(4-hydroxyphenyl) -4-perhydrocumyl cyclohexane	90
3.4.5.2	Synthesis and characterization of 1,1-bis(4-hydroxy-3-methylphenyl) -4-perhydrocumyl cyclohexane	98

3.4.5.3	Synthesis of 1,1-bis(4-hydroxy-3,5-dimethylphenyl) -4-perhydrocumyl cyclohexane	100
3.4.5.4	Synthesis and characterization of 1,1-bis(4-hydroxy-3,5-dibromophenyl) -4-perhydrocumyl cyclohexane and 1,1-bis(4-hydroxy-3-methyl-5-bromophenyl) -4-perhydrocumyl cyclohexane	105
3.4.5.5	Conformational analysis of 1,1-bis(4-hydroxy-3,5-dibromophenyl) -4-perhydrocumyl cyclohexane	109
3.4.6	Synthesis and characterization of 1,1-bis(4-aminophenyl) -4-perhydrocumyl cyclohexane	112
3.4.7	Synthesis and characterization of 1,1-bis[4-(4-aminophenoxy)phenyl]-4-per-hydrocumyl cyclohexane	115
3.4.8	Synthesis and characterization of 1,1-bis[4-(4-carboxyphenoxy)phenyl]-4-per-hydrocumyl cyclohexane	121
3.5	Conclusions	125
	References	126

CHAPTER 4 Synthesis and Characterization of Processable High Performance Polymers Containing Cyclohexylidene Moiety with Flexible Pentadecyl Substituent

4.1	Introduction	128
4.2	Experimental	129
4.2.1	Materials	129
4.2.2	Measurements	129
4.2.3	Cell preparation for pretilt angle measurement	130
4.3	Synthesis of (co)polyesters and (co)polyimides containing pentadecyl-cyclohexylidene moiety	131
4.3.1	Synthesis of polyesters from 1,1-bis(4-hydroxyphenyl)-3-pentadecylcyclohexane and terephthalic acid chloride / isophthalic acid chloride	131
4.3.2	Synthesis of copolyesters from 1,1-bis(4-hydroxyphenyl)-3-pentadecylcyclohexane and BPA with terephthalic acid chloride	131
4.3.3	Synthesis of polyimides from 1,1-bis(4-aminophenyl)-3-pentadecylcyclohexane and commercial dianhydrides	132
4.3.4	Synthesis of copolyimides from 1,1-bis(4-aminophenyl)-3-pentadecylcyclohexane and 4,4'-oxydianiline with biphenyltetracarboxylic dianhydride	132
4.4	Results and Discussion	

4.4.1	Synthesis and characterization of polyesters from 1,1-bis(4-hydroxyphenyl)-3-pentadecylcyclohexane and terephthalic acid chloride/isophthalic acid chloride	133
4.4.1.1	Structural characterization	136
4.4.1.2	Solubility measurements	141
4.4.1.3	X-Ray diffraction studies	142
4.4.1.4	Thermal properties	143
4.4.2	Synthesis and characterization of copolyesters from 1,1-bis(4-hydroxyphenyl)-3-pentadecylcyclohexane and BPA with terephthalic acid chloride	145
4.4.2.1	Structural characterization	147
4.4.2.2	Solubility measurements	148
4.4.2.3	X-Ray diffraction studies	149
4.4.2.4	Thermal properties	150
4.4.3	Synthesis and characterization of polyimides from 1,1-bis(4-aminophenyl)-3-pentadecylcyclohexane and commercial dianhydrides	152
4.4.3.1	Structural characterization	154
4.4.3.2	Solubility measurements	156
4.4.3.3	X-Ray diffraction studies	157
4.4.3.4	Thermal properties	157
4.4.3.5	Optical properties	159
4.4.4	Synthesis and characterization of copolyimides from 1,1-bis(4-aminophenyl)-3-pentadecylcyclohexane and oxydianiline with biphenyltetracarboxylic dianhydride	163
4.4.4.1	Structural characterization	164
4.4.4.2	Solubility measurements	166
4.4.4.3	X-Ray diffraction studies	167
4.4.4.4	Thermal properties	167
4.4.4.5	Optical properties	170
4.5	Pretilt angle and electro-optical characteristics of copolyimide derived from 1,1-bis(4-aminophenyl)-3-pentadecylcyclohexane and oxydianiline with biphenyltetracarboxylic dianhydride	171
4.6	Conclusions	174
	References	175

**CHAPTER 5 Synthesis and Characterization of Processable High Performance
Polymers Containing Cyclohexylidene Moiety with Bulky
Perhydrocumyl Substituent**

5.1	Introduction	177
5.2	Experimental	178
5.2.1	Materials	178
5.2.2	Measurements	178
5.2.2.1	Film preparation for gas permeability measurement	179
5.2.2.2	Measurement of gas permeability	179
5.3	Synthesis of polyesters, polyimides and polyetherimides containing bulky perhydrocumyl substituted cyclohexylidene group	181
5.3.1	Synthesis of polyesters from bisphenols containing perhydrocumyl-cyclohexylidene and terephthalic acid chloride / isophthalic acid chloride	181
5.3.2	Synthesis of polyimides from 1,1-bis(4-aminophenyl) -4-perhydrocumyl cyclohexane and commercial dianhydrides	182
5.3.3	Synthesis of polyetherimides from 1,1-bis[4-(4-aminophenoxy)phenyl]-4-per-hydrocumyl cyclohexane and commercial dianhydrides	182
5.4	Results and Discussion	
5.4.1	Synthesis and characterization of polyesters from perhydrocumyl cyclohexylidene containing bisphenols and terephthalic acid chloride / isophthalic acid chloride.	183
5.4.1.1	Structural characterization	186
5.4.1.2	Solubility measurements	192
5.4.1.3	X-Ray diffraction studies	194
5.4.1.4	Thermal properties	195
5.4.2	Gas permeability studies on polyesters derived from bisphenols containing perhydrocumyl cyclohexylidene moiety and terephthalic acid chloride / isophthalic acid chloride.	199
5.4.2.1	Gas permeability analysis	200
5.4.3	Synthesis and characterization of polyimides from 1,1-bis(4-aminophenyl) -4-perhydrocumyl cyclohexane and commercial dianhydrides	205
5.4.3.1	Structural characterization	207
5.4.3.2	Solubility measurements	209
5.4.3.3	X-Ray diffraction studies	209
5.4.3.4	Thermal properties	210

5.4.3.5	Optical properties	212
5.4.4	Pretilt angle and electro-optical characteristics of polyimide derived from 1,1-bis(4-aminophenyl)-4-perhydrocumyl cyclohexane and commercial dianhydrides	215
5.4.5	Synthesis and characterization of polyetherimides from 1,1-bis[4-(4-aminophenoxy)phenyl]-4-per-hydrocumyl cyclohexane and commercial dianhydrides	217
5.4.5.1	Structural characterization	219
5.4.5.2	Solubility measurements	220
5.4.5.3	X-Ray diffraction studies	221
5.4.5.4	Thermal properties	221
5.4.5.5	Optical properties	223
5.5	Conclusions	225
	References	227
CHAPTER 6	Summary and Conclusions	229
	Appendix	
	SYNOPSIS	
	LIST OF PUBLICATIONS	

Abstract

Step-growth polymerization continues to receive intense academic and industrial attention for the preparation of polymeric materials used in a vast array of applications. In recent years much of the focus in step-growth polymers has been in the area of high performance polymers. High performance / high temperature polymers such as polyimides, polyamides, polyesters, etc. are of considerable interest because of their excellent mechanical and high-temperature properties. A large number of high performance polymers have been synthesized in the academic and industrial research laboratories. However, most of them usually exhibit very low solubilities and melting points far above their thermal decomposition temperatures, which limits their widespread applications. There are several reports describing approaches to improve the processability of high performance/ high temperature polymers by making use of structurally modified monomers.

The main objective of the present research was to design and synthesize processable high performance polymers such as polyimides and polyesters by making use of difunctional monomers containing pendent flexible alkyl chain or bulky “cardo” group. Another objective was to evaluate the applications of selected polymers as alignment layers for liquid crystal display devices and membrane materials for gas separation.

Thus, our synthetic research effort was directed towards structural modifications designed to aid improved processability to the polymers. New bisphenols and diamines containing substituted cyclohexylidene moiety were synthesized starting from cashew nut shell liquid (CNSL), a renewable resource material and *p*-cumylphenol by simple reaction sequences. These difunctional monomers provide the structural characteristics needed for the improvement of properties such as processability and specific properties like pretilt angle and gas permeability.

A detailed investigation of spectral and X-ray crystallography data of difunctional monomers containing substituted cyclohexylidene moiety showed the presence of distereotopic phenyl rings which are magnetically non-equivalent.

A series of polyesters and polyimides containing pentadecylcyclohexylidene moiety was synthesized from respective bisphenol (BPC₁₅) and diamine (BAC₁₅). Polyesters were synthesized by two-phase interfacial polycondensation whereas polyimides were synthesized by one-step high temperature solution polycondensation. Medium to high molecular weight polyesters and polyimides soluble in common organic solvents were obtained. Polyesters derived from BPC₁₅ exhibited constitutional isomerism which has its origin in the distereotopic nature of BPC₁₅. The incorporation of pentadecyl chain along the polymer backbone substantially decreased the glass transition temperature of polyesters and polyimides. The depression in glass transition temperature of pendant pentadecyl chain containing polyesters and polyimides demonstrated the “plasticizing” ability of pentadecyl chain.

A series of copolyesters and copolyimides containing pentadecylcyclohexylidene moiety were synthesized. Glass transition temperature of copolyesters and copolyimides decreased with the increasing content of BPC₁₅ or BAC₁₅, respectively. All of the (co)polyesters and (co)polyimides exhibited high thermal stabilities. A large window between glass transition and polymer degradation temperature was observed. This gives an opportunity for these (co)polymers to be melt-processed or compression molded.

Preliminary experiments for using copolyimides containing pentadecylcyclohexylidene moiety as alignment layer for liquid crystal display were carried out. Pretilt angles in the range 2.51-2.75° were observed which is adequate for display applications.

A series of new polyesters with a systematic variation of methyl and /or bromo substituent on phenyl rings was synthesized from bisphenols containing bulky perhydrocumyl cyclohexylidene “cardo” group by two-phase interfacial polycondensation technique. Moderate to high molecular weight polyesters soluble in common organic solvents were obtained. The presence of constitutional isomerism in polyesters containing substituted cyclohexylidene moieties was established by detailed NMR spectral analysis. The glass transition temperature of polyesters derived from isophthalic acid chloride were lower than their terephthalic acid chloride derived analogues. The effect of symmetric and asymmetric substitution of bisphenol rings on the polymer properties was studied. The utility of perhydrocumyl cyclohexylidene containing polyesters as membrane materials for gas separation was demonstrated.

A series of polyimides and polyetherimides was synthesized from perhydrocumyl cyclohexylidene containing diamines and commercial dianhydrides by one-step high temperature solution polycondensation in *m*-cresol.

Application of organo-soluble polyimides containing perhydrocumyl cyclohexylidene moiety as alignment layer for liquid crystal display was evaluated in brief. A pretilt angle of 2.43° was observed for polyimide synthesized from BAPCP and BTDA, which is adequate for display applications.

Overall, polymer processability / solubility was improved by the incorporation of pendant pentadecyl chain *via* internal “plasticization”. The incorporation of bulky perhydrocumyl substituted cyclohexylidene “cardo” group resulted into polyimides and polyesters with improved solubility in common organic solvents and higher thermal properties.

List of Tables

1.1	Relative rate constants for reactions pathways involved in poly(amic acid) synthesis	8
1.2	Effect of chemical structure on solubility and glass transition	20
1.3	Minimum kinetic diameter of various penetrants	32
1.4	Representative examples of polyesters used for gas permeation measurements	35
3.1	X-Ray crystal data for 1,1-bis(4-hydroxyphenyl)-3-pentadecylcyclohexane	77
3.2	Analysis of potential hydrogen bonds in 1,1-bis(4-hydroxyphenyl)-3-pentadecylcyclohexane	77
3.3	X-Ray crystal data for 1,1-bis(4-hydroxyphenyl) -4-perhydrocumyl cyclohexane	95
3.4	Analysis of potential hydrogen bonds in 1,1-bis(4-hydroxyphenyl) -4-perhydrocumyl cyclohexane	95
3.5	X-Ray crystal data for 1,1-bis(4-hydroxy-3,5-dimethylphenyl) -4-perhydrocumyl cyclohexane	103
3.6	Analysis of potential hydrogen bonds in 1,1-bis(4-hydroxy-3,5-dimethylphenyl) -4-perhydrocumyl cyclohexane	103
3.7	X-Ray crystal data for 1,1-bis(4-hydroxy-3,5-dibromophenyl) -4-perhydrocumyl cyclohexane	108
3.8	Bond lengths and bond angles for 1,1-bis(4-hydroxy-3,5-dibromophenyl) -4-perhydrocumyl cyclohexane and its B3LYP/6-31G** level geometry optimized structure 1a	110
3.9	X-ray crystal data for 1,1-bis(4-aminophenyl) -4-perhydrocumyl cyclohexane	114
3.10	X-Ray crystal data for 1,1-bis[4-(4-aminophenoxy)phenyl]-4-per hydrocumyl cyclohexane	119
3.11	Analysis of potential hydrogen bonds in 1,1-bis[4-(4-aminophenoxy)-phenyl]-4-per hydrocumyl cyclohexane	119
4.1	Synthesis of polyesters from 1,1-bis(4-hydroxyphenyl)-3-pentadecyl-cyclohexane and terephthalic acid chloride / isophthalic acid chloride	135
4.2	Synthesis of polyesters from BPA, BPC and BPC ₁ with terephthalic acid chloride / isophthalic acid chloride	135
4.3	GPC data for polyesters derived from 1,1-bis(4-hydroxyphenyl)-3-pentadecylcyclohexane and terephthalic acid chloride / isophthalic acid chloride	135
4.4	Solubility data of polyesters derived from bisphenols and terephthalic acid chloride / isophthalic acid chloride	141

4.5	Thermal properties of the polyesters derived from bisphenols and terephthalic acid chloride / isophthalic acid chloride	144
4.6	Synthesis of copolyesters from BPC ₁₅ and BPA with terephthalic acid chloride	146
4.7	Solubility data of copolyesters derived from BPA and BPC ₁₅ with terephthalic acid chloride	149
4.8	Thermal properties of the copolyesters derived from BPA and BPC ₁₅ with terephthalic acid chloride	151
4.9	Synthesis of polyimides from 1,1-bis(4-aminophenyl)-3-pentadecylcyclohexane and commercial dianhydrides	154
4.10	Solubility data of polyimides synthesized from 1,1-bis(4-aminophenyl)-3-pentadecylcyclohexane and commercial dianhydrides	156
4.11	Thermal properties of polyimides derived from 1,1-bis(4-aminophenyl)-3-pentadecylcyclohexane and commercial dianhydrides	158
4.12	Optical properties of polyimides derived from 1,1-bis(4-aminophenyl)-3-pentadecylcyclohexane and commercial dianhydrides	162
4.13	Synthesis of copolyimides from BAC ₁₅ and ODA with BPDA	164
4.14	Solubility data of polyimides derived from BAC ₁₅ and ODA with BPDA	166
4.15	Thermal properties of copolyimides derived from BAC ₁₅ and ODA with BPDA	168
4.16	Optical properties of the copolyimides derived from BAC ₁₅ and ODA with BPDA	170
5.1	Synthesis of polyesters from perhydrocumyl cyclohexylidene containing bisphenols and terephthalic acid chloride / isophthalic acid chloride	185
5.2	GPC data of polyesters derived from perhydrocumyl cyclohexylidene containing bisphenols and terephthalic acid chloride / isophthalic acid chloride	186
5.3	C=O Absorption frequencies for polyesters derived from perhydrocumyl cyclohexylidene containing bisphenols and terephthalic acid chloride / isophthalic acid chloride	187
5.4	Solubility data of polyesters derived from bisphenols containing perhydrocumyl cyclohexylidene and terephthalic acid chloride / isophthalic acid chloride	193
5.5	Thermal properties of polyesters derived from perhydrocumyl-cyclohexylidene containing bisphenols and terephthalic acid chloride / isophthalic acid chloride	196
5.6	Physical and thermal properties of polyesters derived from perhydrocumyl cyclohexylidene containing bisphenols and terephthalic acid chloride / isophthalic acid chloride.	201

5.7	Permeability coefficients and ideal selectivities for polyesters derived from perhydrocumyl cyclohexylidene containing bisphenols / terephthalic acid chloride and isophthalic acid chloride at $35\pm 0.1^{\circ}\text{C}$	203
5.8	Synthesis of polyimides from 1,1-bis(4-aminophenyl)-4-perhydrocumyl cyclohexane and commercial dianhydrides	206
5.9	Solubility data of polyimides derived from 1,1-bis(4-aminophenyl)-4-perhydrocumyl cyclohexane and commercial dianhydrides.	209
5.10	Thermal properties of polyimides derived from 1,1-bis(4-aminophenyl)-4-perhydrocumyl cyclohexane and commercial dianhydrides	211
5.11	Optical properties of polyimides derived from 1,1-bis(4-aminophenyl)-4-perhydrocumyl cyclohexane and commercial dianhydrides	214
5.12	Synthesis of polyetherimides from 1,1-bis[4-(4-aminophenoxy)phenyl]-4-perhydrocumyl cyclohexane and commercial dianhydrides	218
5.13	Solubility data for polyetherimides derived from 1,1-bis[4-(4-aminophenoxy)phenyl]-4-perhydrocumyl cyclohexane and commercial dianhydrides	220
5.14	Thermal properties of polyetherimides derived from 1,1-bis[4-(4-aminophenoxy)phenyl]-4-perhydrocumyl cyclohexane and commercial dianhydrides	222
5.15	Optical properties of polyetherimides derived from BAPPHC and commercial dianhydrides	224

List of Schemes

1.1	Preparation of Kapton® polyimide	4
1.2	Major reaction pathways involved in poly(amic acid) synthesis	7
1.3	Possible imide formation mechanisms	9
1.4	Mechanism involved in chemical dehydration of amic acid	11
1.5	Postulated mechanism for amic acid back reaction to anhydride and amine.	14
1.6	Polyimide synthesis from tetracarboxylic acid-amine salt	16
1.7	Polyimide synthesis from dianhydrides and diisocyanates <i>via</i> an imide-anhydride seven-membered intermediate	17
1.8	Synthesis of polyetherimides by nucleophilic aromatic substitution (a) and delocalization of negative charge in Meisenheimer transition state in imide system (b)	18
1.9	Synthesis of polyimides by Pd-catalyzed carbon-carbon coupling reaction	19
1.10	Phase-transfer catalyzed interfacial polycondensation	28
1.11	Solution polycondensation of bisphenol and diacid chloride	29
3.1	Synthesis of 1,1-bis(4-hydroxyphenyl)-3-pentadecylcyclohexane	68
3.2	Synthesis of 1,1-bis(4-hydroxyphenyl)cyclohexane	80
3.3	Synthesis of 1,1-bis(4-hydroxyphenyl)-3-methylcyclohexane	82
3.4	Synthesis of 1,1-bis(4-aminophenyl)-3-pentadecylcyclohexane	84
3.5	Synthesis of bisphenols starting from <i>p</i> -cumylphenol	87
3.6	Synthesis of 1,1-bis(4-aminophenyl)-4-perhydrocumyl cyclohexane	112
3.7	Synthesis of 1,1-bis[4-(4-aminophenoxy)phenyl]-4-per-hydrocumyl cyclohexane	115
3.8	Synthesis of 1,1-bis[4-(4-carboxyphenoxy)phenyl]-4-per-hydrocumyl cyclohexane	121
4.1	Synthesis of polyesters from bisphenols and terephthalic acid chloride / isophthalic acid chloride	134
4.2	Synthesis of aromatic copolyesters based on BPC ₁₅ and BPA with terephthalic acid chloride	146
4.3	Synthesis of polyimides from 1,1-bis(4-aminophenyl)-3-pentadecylcyclohexane and commercial dianhydrides	153
4.4	Synthesis of copolyimides from BAC ₁₅ and ODA with BPDA	163
5.1	Synthesis of polyesters from perhydrocumyl cyclohexylidene containing bisphenols and terephthalic acid chloride / isophthalic acid chloride.	184

5.2	Synthesis of polyimides from 1,1-bis(4-aminophenyl)-4-perhydrocumyl cyclohexane and commercial dianhydrides	205
5.3	Synthesis of polyetherimides from 1,1-bis[4-(4-aminophenoxy)phenyl]-4-perhydrocumyl cyclohexane and commercial dianhydrides	217

List of Figures

1.1	Approaches for improving processability of high performance polymers	2
1.2	Structure of twisted nematic display in normally white mode (off-state)	22
1.3	Structure of twisted nematic display in normally white mode (on-state)	23
1.4	Alignment and pretilt of liquid crystal molecules	24
1.5	Effect of alkylene chain length on pretilt angle	25
1.6	Generalized representation of an ideal membrane separation process	32
3.1	Nut of Cashew	56
3.2	Constituents of CNSL	56
3.3	^1H -NMR spectrum of 3-pentadecylcyclohexanol	69
3.4	^{13}C -NMR spectrum of 3-pentadecylcyclohexanol	70
3.5	^1H -NMR spectrum of 3-pentadecylcyclohexanone	71
3.6	HPLC trace of 1,1-bis(4-hydroxyphenyl)-3-pentadecylcyclohexane	72
3.7	FTIR spectrum of 1,1-bis(4-hydroxyphenyl)-3-pentadecylcyclohexane	72
3.8	^1H -NMR spectrum of 1,1-bis(4-hydroxyphenyl)-3-pentadecylcyclohexane	73
3.9	COSY spectrum of 1,1-bis(4-hydroxyphenyl)-3-pentadecylcyclohexane	74
3.10	NOESY spectrum of 1,1-bis(4-hydroxyphenyl)-3-pentadecylcyclohexane	74
3.11	^1H - ^{13}C HETCOR spectrum of 1,1-bis(4-hydroxyphenyl)-3-pentadecylcyclohexane	75
3.12	Partial ^1H -NMR spectrum of 1,1-bis(4-hydroxyphenyl)-3-pentadecylcyclohexane in C_6D_6	76
3.13	^{13}C -NMR spectrum of 1,1-bis(4-hydroxyphenyl)-3-pentadecylcyclohexane	76
3.14a	ORTEP diagram for 1,1-bis(4-hydroxyphenyl)-3-pentadecylcyclohexane. Ellipsoids are drawn at 50% probability level	79
3.14b	Packing diagram for 1,1-bis(4-hydroxyphenyl)-3-pentadecylcyclohexane molecules	79
3.15	^1H -NMR spectrum of 1,1-bis(4-hydroxyphenyl)cyclohexane in CD_3OD	81
3.16	^{13}C -NMR spectrum of 1,1-bis(4-hydroxyphenyl)cyclohexane in CD_3OD	81

3.17	¹ H-NMR spectrum of 1,1-bis(4-hydroxyphenyl)-3-methylcyclohexane in CD ₃ OD	83
3.18	¹³ C-NMR spectrum of 1,1-bis(4-hydroxyphenyl)-3-methylcyclohexane in CD ₃ OD	83
3.19	FTIR spectrum of 1,1-bis(4-aminophenyl)-3-pentadecylcyclohexane	85
3.20	¹ H-NMR spectrum of 1,1-bis(4-aminophenyl)-3-pentadecylcyclohexane	85
3.21	¹³ C-NMR spectrum of 1,1-bis(4-aminophenyl)-3-pentadecylcyclohexane	86
3.22	FTIR spectrum of perhydrocumylcyclohexanol	88
3.23	¹ H-NMR spectrum of perhydrocumylcyclohexanol	89
3.24	FTIR spectrum of perhydrocumylcyclohexanone	89
3.25	¹ H-NMR Spectrum of perhydrocumylcyclohexanone	90
3.26	HPLC trace of 1,1-bis(4-hydroxyphenyl) -4-perhydrocumyl cyclohexane	90
3.27	¹ H NMR spectrum of 1,1-bis(4-hydroxyphenyl) -4-perhydrocumyl cyclohexane in CD ₃ CN	91
3.28	¹³ C NMR spectrum of 1,1-bis(4-hydroxyphenyl) -4-perhydrocumyl cyclohexane	92
3.29	COSY spectrum of 1,1-bis(4-hydroxyphenyl) -4-perhydrocumyl cyclohexane	92
3.30	NOESY spectrum of 1,1-bis(4-hydroxyphenyl) -4-perhydrocumyl cyclohexane	93
3.31	¹ H- ¹³ C-HETCOR spectrum of 1,1-bis(4-hydroxyphenyl) -4-perhydrocumyl cyclohexane	93
3.32	Partial TOCSY spectrum of 1,1-bis(4-hydroxyphenyl) -4-perhydrocumyl cyclohexane	94
3.33a	ORTEP diagram for 1,1-bis(4-hydroxyphenyl) -4-perhydrocumyl cyclohexane. Ellipsoids are drawn at 50% probability level	97
3.33b	Packing diagram for 1,1-bis(4-hydroxyphenyl) -4-perhydrocumyl cyclohexane.	97
3.34	DSC curve for 1,1-bis(4-hydroxyphenyl) -4-perhydrocumyl cyclohexane	98
3.35	HPLC trace of 1,1-bis(4-hydroxy-3-methylphenyl) -4-perhydrocumyl cyclohexane	99
3.36	¹ H NMR spectrum of 1,1-bis(4-hydroxy-3-methylphenyl) -4-perhydrocumyl cyclohexane	99
3.37	¹³ C NMR spectrum of 1,1-bis(4-hydroxy-3-methylphenyl) -4-perhydrocumyl cyclohexane	100

3.38	HPLC trace of 1,1-bis(4-hydroxy-3,5-dimethylphenyl) -4-perhydrocumyl cyclohexane	101
3.39	¹ H NMR spectrum of 1,1-bis(4-hydroxy-3,5-dimethylphenyl) -4-perhydrocumyl cyclohexane	101
3.40	¹³ C NMR spectrum of 1,1-bis(4-hydroxy-3,5-dimethylphenyl) -4-perhydrocumyl cyclohexane	102
3.41a	ORTEP diagram for 1,1-bis(4-hydroxy-3,5-dimethylphenyl) -4-perhydrocumyl cyclohexane. Ellipsoids are drawn at 50% probability level	104
3.41b	Packing diagram for 1,1-bis(4-hydroxy-3,5-dimethylphenyl) -4-perhydrocumyl cyclohexane	104
3.42	¹ H NMR spectrum of 1,1-bis(4-hydroxy-3-methyl-5-bromophenyl) -4-perhydrocumyl cyclohexane	106
3.43	¹³ C NMR spectrum of 1,1-bis(4-hydroxy-3-methyl-5-bromophenyl) -4-perhydrocumyl cyclohexane	106
3.44	¹ H NMR spectrum of 1,1-bis(4-hydroxy-3,5-dibromophenyl) -4-perhydrocumyl cyclohexane	107
3.45	¹³ C NMR spectrum of 1,1-bis(4-hydroxy-3,5-dibromophenyl) -4-perhydrocumyl cyclohexane	107
3.46	ORTEP diagram for 1,1-bis(4-hydroxy-3,5-dibromophenyl) -4-perhydrocumyl cyclohexane. Ellipsoids are drawn at 50% probability level	108
3.47	Conformers of 1,1-bis(4-hydroxy-3,5-dibromophenyl) -4-perhydrocumyl cyclohexane	109
3.48	Energy comparison graph for conformers of 1,1-bis(4-hydroxy-3,5-dibromophenyl) -4-perhydrocumyl cyclohexane	112
3.49	¹ H-NMR spectrum of 1,1-bis(4-aminophenyl) -4-perhydrocumyl cyclohexane	113
3.50	¹³ C-NMR spectrum of 1,1-bis(4-aminophenyl) -4-perhydrocumyl cyclohexane	113
3.51	ORTEP diagram for 1,1-bis(4-aminophenyl) -4-perhydrocumyl cyclohexane. Ellipsoids are drawn at 50% probability level	114
3.52	FTIR spectrum of 1,1-bis[4-(4-nitrophenoxy)phenyl]-4-perhydrocumyl cyclohexane and 1,1-bis[4-(4-aminophenoxy)phenyl]-4-perhydrocumyl cyclohexane	116
3.53	¹ H NMR spectrum of 1,1-bis[4-(4-nitrophenoxy)phenyl]-4-perhydrocumyl cyclohexane and 1,1-bis[4-(4-aminophenoxy)phenyl]-4-perhydrocumyl cyclohexane	117
3.54	¹³ C NMR spectrum of 1,1-bis[4-(4-nitrophenoxy)phenyl]-4-perhydrocumyl cyclohexane and 1,1-bis[4-(4-aminophenoxy)phenyl]-4-perhydrocumyl cyclohexane	118

3.55a	ORTEP diagram for 1,1-bis[4-(4-aminophenoxy)phenyl]-4-per hydrocumyl cyclohexane. Ellipsoids are drawn at 50% probability level	120
3.55b	Packing diagram for 1,1-bis[4-(4-aminophenoxy)phenyl]-4-per hydrocumyl cyclohexane	120
3.56	FTIR spectrum of 1,1-bis[4-(4-cyanophenoxy)phenyl]-4-per hydrocumyl cyclohexane and 1,1-bis[4-(4-carboxyphenoxy)phenyl]-4-per hydrocumyl cyclohexane	122
3.57	¹ H NMR spectrum of 1,1-bis[4-(4-cyanophenoxy)phenyl]-4-per hydrocumyl cyclohexane and 1,1-bis[4-(4-carboxyphenoxy)phenyl]-4-per hydrocumyl cyclohexane	123
3.58	¹³ C NMR spectrum of 1,1-bis[4-(4-cyanophenoxy)phenyl]-4-per hydrocumyl cyclohexane and 1,1-bis[4-(4-carboxyphenoxy)phenyl]-4-per hydrocumyl cyclohexane	124
4.1	FTIR spectrum of polyester derived from 1,1-bis(4-hydroxyphenyl)-3-pentadecylcyclohexane and terephthalic acid chloride	136
4.2	¹ H and ¹³ C-NMR spectra of polyester derived from BPC ₁₅ and terephthalic acid chloride	137
4.3	Partial ¹ H-NMR and ¹³ C NMR spectra of 4-cumylphenyl terephthalate at 300 MHz	138
4.4	¹ H and ¹³ C-NMR spectra of polyester derived from 1,1-bis(4-hydroxyphenyl)-3-pentadecylcyclohexane and isophthalic acid chloride	139
4.5	Comparison of partial ¹ H-NMR spectra of 4-cumylphenyl isophthalate with polyester derived from isophthalic acid chloride and BPC ₁₅	140
4.6	X-Ray diffraction patterns of polyesters derived from bisphenols and terephthalic acid chloride / isophthalic acid chloride	142
4.7	TG curves of polyesters derived from bisphenols and terephthalic acid chloride / isophthalic acid chloride	143
4.8	DSC curves of the polyesters derived from bisphenols and terephthalic acid chloride / isophthalic acid chloride	145
4.9	FT-IR spectrum of copolyester derived from BPC ₁₅ and BPA with terephthalic acid chloride (P-10)	147
4.10	¹ H-NMR spectrum of copolyester derived from BPC ₁₅ and BPA with terephthalic acid chloride (P-10)	148
4.11	¹³ C-NMR spectrum of copolyester derived from BPC ₁₅ and BPA with terephthalic acid chloride (P-10)	148
4.12	X-ray diffraction patterns of copolyesters derived from BPC ₁₅ and BPC with terephthalic acid chloride	150
4.13	TG curves of the copolyesters derived from BPA and BPC ₁₅ with terephthalic acid chloride	150

4.14	DSC curves of copolyesters derived from BPA and BPC ₁₅ with terephthalic acid chloride	152
4.15	FT-IR spectrum of polyimide derived from BAC ₁₅ and BPDA (PI-2)	155
4.16	¹ H-NMR spectrum of polyimide derived from 1,1-bis(4-aminophenyl)-3-pentadecylcyclohexane and BPDA (PI-2)	155
4.17	¹³ C-NMR spectrum of polyimide derived from 1,1-bis(4-aminophenyl)-3-pentadecylcyclohexane and BPDA (PI-2)	156
4.18	Wide-angle X-ray diffraction patterns of polyimides derived from 1,1-bis(4-aminophenyl)-3-pentadecylcyclohexane and commercial dianhydrides	157
4.19	TG curves of polyimides derived from 1,1-bis(4-aminophenyl)-3-pentadecylcyclohexane and commercial dianhydrides	158
4.20	DSC curves of the polyimides derived from 1,1-bis(4-aminophenyl)-3-pentadecylcyclohexane and commercial dianhydrides	159
4.21	UV-vis absorption spectra of polyimide films derived from 1,1-bis(4-aminophenyl)-3-pentadecylcyclohexane and commercial dianhydrides	160
4.22	FT-IR spectrum of copolyimide derived from BAC ₁₅ and ODA with BPDA (PI-9)	165
4.23	¹ H-NMR spectrum of copolyimide derived from BAC ₁₅ and ODA with BPDA (P-9)	165
4.24	¹³ C-NMR spectrum of copolyimide derived from BAC ₁₅ and ODA with BPDA (P-9)	166
4.25	Wide angle X-ray diffraction patterns for copolyimides derived from 1,1-bis(4-aminophenyl)-3-pentadecylcyclohexane and BPDA	167
4.26	TG curves of copolyimides derived from BAC ₁₅ and ODA with BPDA	168
4.27	DSC curves of copolyimides derived from BAC ₁₅ and ODA with BPDA	169
4.28	Glass transition temperature vs mol% of BAC ₁₅ for copolyimides derived from BPDA with ODA and BAC ₁₅	169
4.29	UV-vis absorption spectra of copolyimide films derived from BAC ₁₅ and ODA with BPDA	170
4.30	Twisted nematic cell made from polyimide PI-8. (a) cell between crossed polarizers (b) cell between parallel polarizers (c) cell at 45° between crossed polarizers.	172
4.31	A) Electro-optical characteristics of copolyimide orientation layer B) Response and relaxation times for copolyimide orientation layer from the non-select to the select state (5V) at a frequency of 1000 Hz	173
5.1	Schematic diagram for gas permeability measurement	180

5.2	FT-IR spectra (Film) of polyesters derived from BPPCP and terephthalic acid chloride and isophthalic acid chloride	187
5.3	¹ H-NMR and ¹³ C-NMR spectra of polyester derived from BPPCP and terephthalic acid chloride	188
5.4	Partial ¹ H-NMR spectrum of polyester P-1 at three different magnetic field strengths viz, 200, 400 and 500 MHz	189
5.5	Microstructure of polyester derived from BPPCP and terphthalic acid chloride	190
5.6	¹ H-NMR and ¹³ C-NMR spectra of polyester derived from BPPCP and isophthalic acid chloride	191
5.7	Partial ¹³ C-NMR spectra of polyesters synthesized from bisphenols containing perhydrocumylcyclohexylidene group with terephthalic acid chloride / isophthalic acid chloride	192
5.8	X-Ray diffraction patterns of polyesters derived from perhydrocumyl cyclohexylidene containing bisphenols and terephthalic acid chloride / isophthalic acid chloride	194
5.9	TG curves of polyesters derived from perhydrocumyl cyclohexylidene containing bisphenols with terephthalic acid chloride / isophthalic acid chloride	195
5.10	DSC curves of polyesters derived from perhydrocumyl cyclohexylidene containing bisphenols and terephthalic acid chloride	198
5.11	DSC curves of polyesters derived from perhydrocumyl cyclohexylidene containing bisphenols and isophthalic acid chloride	198
5.12	FTIR spectrum of polyimide derived from 1,1-bis(4- aminophenyl)-4-perhydrocumyl cyclohexane and 6-FDA (PI-5)	207
5.13	¹ H and ¹³ C-NMR spectra of polyimide derived from 1,1-bis(4-aminophenyl)-4-perhydrocumyl cyclohexane and FDA (PI-5)	208
5.14	X-ray diffraction patterns of polyimides derived from 1,1-bis(4-aminophenyl)-4-perhydrocumyl cyclohexane and commercial dianhydrides	210
5.15	TG curves of polyimide derived from 1,1-bis(4- aminophenyl)-4-perhydrocumyl cyclohexane and commercial dianhydrides	211
5.16	DSC curves of polyimides derived from 1,1-bis(4- aminophenyl)-4-perhydrocumyl cyclohexane and commercial dianhydrides	212
5.17	UV-vis absorption spectra of polyimide films derived from 1,1-bis(4-aminophenyl)-4-perhydrocumyl cyclohexane and commercial dianhydrides	213
5.18	(a) Electro-optical characteristics of polyimide orientation layer (b) Response and relaxation times for polyimide orientation layer from the non-select to select state (5V) at a frequency of 1000 Hz	216
5.19	FT-IR spectrum of polyetherimide derived from 1,1-bis[4-(4-aminophenoxy)phenyl]-4-per-hydrocumyl cyclohexane and BPDA	219

	(PEI-1)	
5.20	¹ H-NMR spectrum of polyetherimide derived from 1,1-bis[4-(4-aminophenoxy)phenyl]-4-per-hydrocumyl cyclohexane and BPDA (PEI-1)	220
5.21	Wide angle X-ray diffraction of polyetherimides synthesized from 1,1-bis[4-(4-aminophenoxy)phenyl]-4-per-hydrocumyl cyclohexane and commercial dianhydrides	221
5.22	TG curves of polyetherimides derived from 1,1-bis[4-(4-aminophenoxy)phenyl]-4-per-hydrocumyl cyclohexane and commercial dianhydrides	222
5.23	DSC curves of polyetherimides derived from 1,1-bis[4-(4-aminophenoxy)phenyl]-4-per-hydrocumyl cyclohexane and commercial dianhydrides	223
5.24	UV-visible absorption spectra of polyetherimides derived from 1,1-bis[4-(4-aminophenoxy)phenyl]-4-per-hydrocumyl cyclohexane and commercial dianhydrides	223

Chapter 1. Introduction and Literature Survey

1.1 Introduction

The use of polymers is widespread in modern society, and their applications continue to grow. Many of the important advances in the polymeric materials involve imparting desirable properties through the control of polymer structure. In recent years much of the focus has been in the area of high performance polymers (HPPs), in which tailoring polymer structure to give specific set of properties is paramount. It has been observed that high performance, like beauty, is in the eye of the beholder, its definition changing with context. Indeed, although HPPs can be broadly defined as materials that exhibit properties superior to those of state-of-the-art materials, many scientists and technologists prefer more specific definitions. Such definitions may refer to materials, which exhibit not only a unique combination of properties (e.g., high strength, high stiffness and high impact resistance, high resistivity, low dielectric constant, excellent chemical and solvent resistance, and low flammability and smoke generation, etc.) superior to those of state-of-the-art materials but also better elevated temperature behavior.

Many of the currently used HPPs have their roots in the research and development work in the 1960s. Then, as now, the aerospace industry was a significant driving force behind the development of new materials for demanding environments and it remains their largest user. The most prolific decade for HPPs was 1960-1970 where most thermally stable heterocyclic rings were incorporated within polymers. The drive during the early part of this era was directed primarily towards thermal stability; little attention was paid to processability. 1970s saw the commercialization of several HPPs. In the 1980s, work focused on exploring ways to make polymers more processable and on developing more cost-effective routes to convert them into various useful forms.

The research continues in many other areas such as microelectronics (photoresists, interlayer dielectrics), alignment films for liquid crystal display devices, electroactive actuators and devices, optical fiber waveguides, proton exchange membranes for fuel cells, separation/barrier materials, etc.

Polyimides, polyamides polyamideimides and aromatic polyesters are the important classes of high performance polymers. The high regularity and high rigidity of the backbones of HPPs result in strong chain-chain interactions, high crystallinity, high

melting points and low solubility. Thus, processing of HPPs is often difficult. In order to increase processability and systematically understand HPPs, a wide variety of modified HPPs have been synthesized. Several approaches have been used (**Figure 1.1**) to modify HPPs including: (1) the insertion of flexible spacers between the rigid units; (2) the insertion of bent or ‘crankshaft’ units along the aromatic backbones to form random or alternative copolymers; and (3) the appending of bulky side groups or flexible side chains to the aromatic backbones.

Rod-like polymers

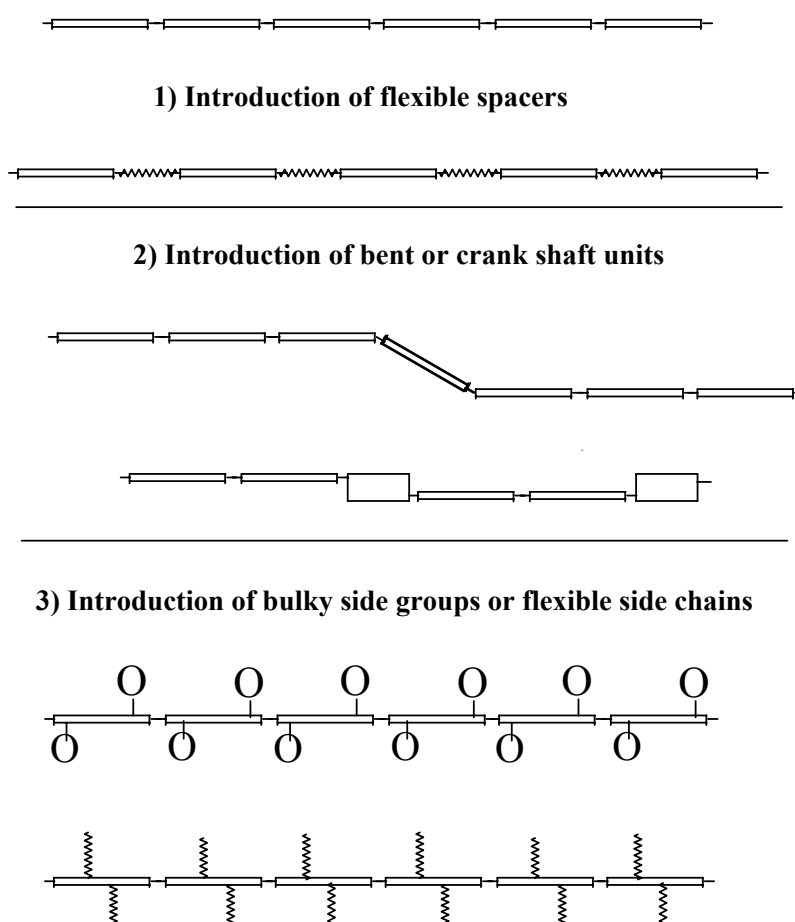
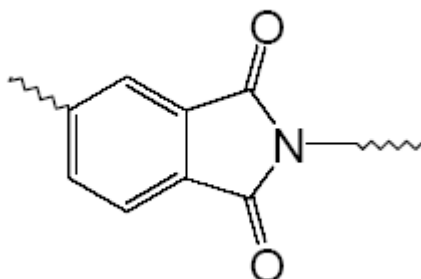


Figure 1.1: Approaches for improving processability of high performance polymers.

This chapter will discuss some topics relevant to this dissertation, including common synthetic chemistry and methods used to prepare polyimides and polyesters, important characteristics and their applications.

1.2 Polyimides

Polyimides are a class of polymers containing a heterocyclic imide unit



in the polymer backbone

Historically, the first report concerning polyimides was made by Bogert and Renshaw in 1908.¹ However, only in the early 1960s were polyimides successfully introduced as commercial polymeric materials (Kapton) by DuPont.² Since that time, an impressive variety of polyimides have been synthesized and reported in the literature.³⁻⁷

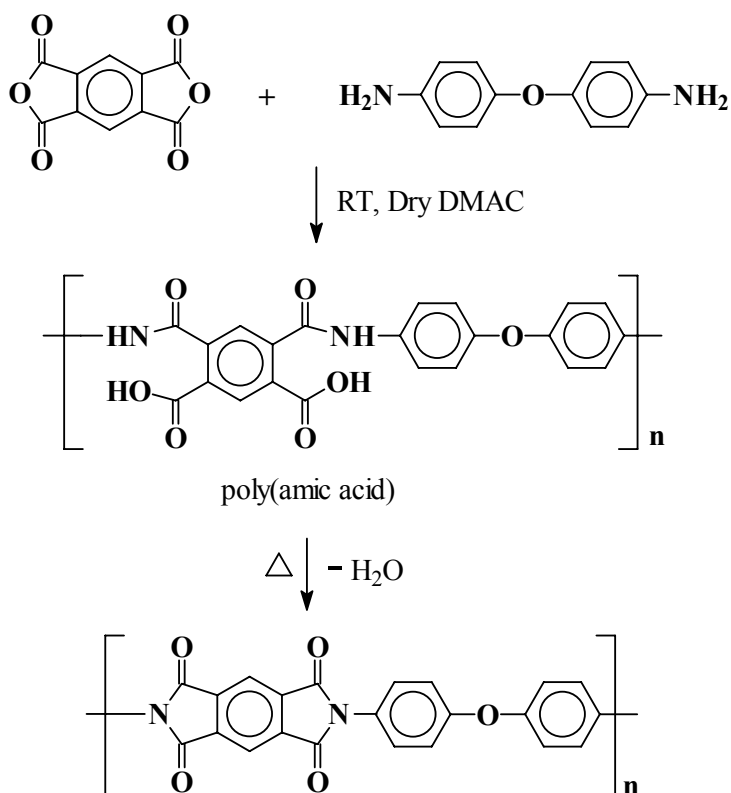
Polyimides are important, both scientifically and commercially, because of their combination of outstanding key properties, including thermal, thermo-oxidative stability, high mechanical strength, high modulus, excellent electrical properties, and superior chemical resistance. Therefore, in spite of their general difficulty in processing and high cost, polyimides are widely used as matrix resins, adhesives, coatings, printed circuit board and insulators for high performance applications in the aerospace, automotive, electrical, electronics and packaging industries.

1.2.1 Synthesis of polyimides

The design and the synthetic pathway are important constituents in the development of high performance polyimide materials. Polyimides are generally derived from the step or condensation reaction of organic diamines and tetracarboxylic dianhydrides. In this section, the fundamental aspects and new developments in the chemistry of polyimide synthesis will be discussed.

1.2.1.1 Classical two-step method *via* poly(amic acid)s

The classical synthetic pathway pioneered at DuPont de Nemours and Co. to cope with the infusibility and insolubility of aromatic polyimides is still the most popular technique for the preparation of polyimides. As shown in **Scheme 1.1**, with the example of Kapton synthesis, this preparative approach consists of the formation of soluble, and thus processable, poly(amic acid) (PAA) precursors from diamines and tetracarboxylic dianhydrides, followed by the conversion of PAAs to the desired polyimide *via* imidization.



Scheme 1.1: Preparation of Kapton® polyimide.

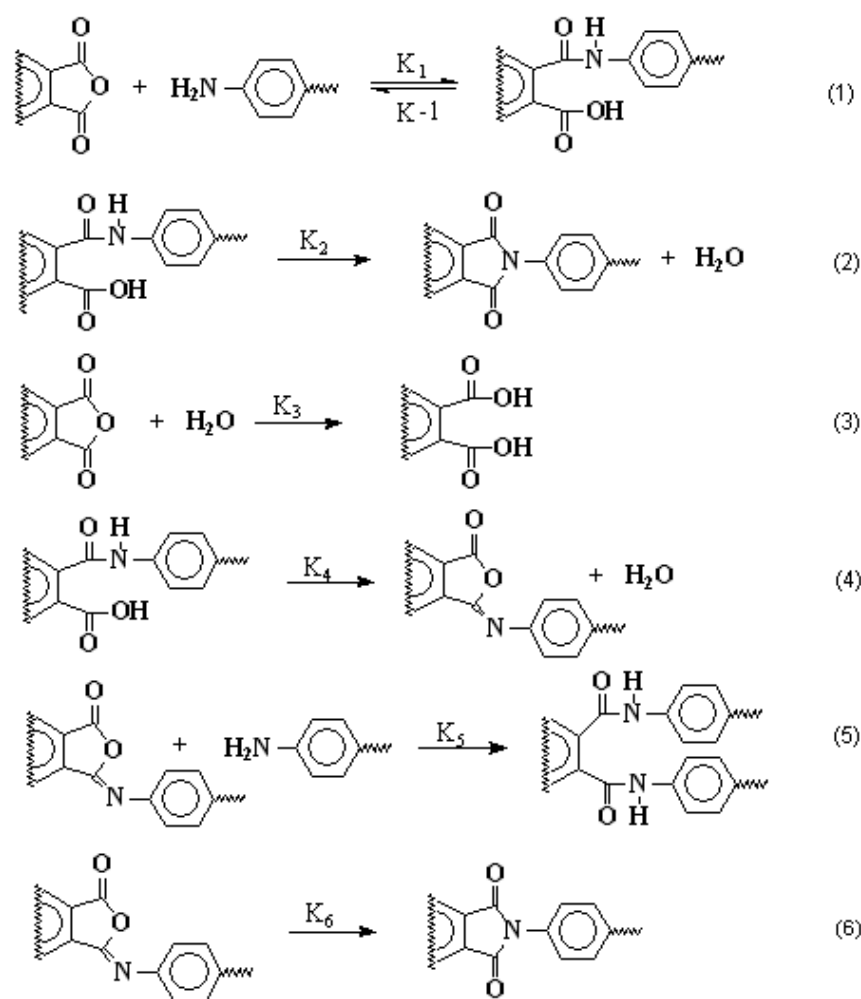
a) Formation of poly(amic acid)s

The formation of poly(amic acid) is achieved *via* the reaction of a dianhydride and a diamine in a dry aprotic solvent at or below room temperature. The reaction mechanism involves the nucleophilic attack of the amino group on the carbonyl carbon of the anhydride group, followed by the opening of the anhydride ring to form an amic acid

group. In this equilibrium reaction, the forward reaction is often much faster than the reverse reaction. The acylation reaction of amine is an exothermic reaction.⁸ The forward reaction in a dipolar solvent is a second-order reaction and the reverse reaction is a first-order reaction. Therefore, the equilibrium is favored at low temperature and high monomer concentration to form high molecular weight poly(amic acid).⁹ The reactivity of the monomers is an important factor governing the rate of amic acid formation. It is expected that the nucleophilicity of the amino nitrogen atom of the diamine and the electrophilicity of the carbonyl group of the dianhydride are important factors in this process. However, structure of the diamine seems to influence the rate of the acylation reaction more than the variation in dianhydride.¹⁰ The high nucleophilicity of the diamine results in high reactivity. The reactivity of diamines correlates well with their basicities (pK_a) as expressed by Hammett relation.¹¹ However, very high basic diamines, e.g. aliphatic diamines, have an unfortunate tendency to form ionic salts with the carboxyl group of the formed amic acid linkage, while the protonation of the amine group prevents its reaction with the anhydride. Thus, these diamines are not suited for this preparative pathway. On the other hand, diamines of very low basicity have poor nucleophilic ability and thus do not react well with dianhydrides. It has been suggested that an optimal diamine should have a pK_a of 4.5-6.¹² The effect of the reactivities of anhydrides is manifested by the fact that the reaction rate increases with increasing affinity for the electron by the dianhydride. Earlier investigators¹³ quantified electron affinity (E_a) for various dianhydrides by polarographic measurements and demonstrated that the rate of an acylation reaction of 4,4'-diaminodiphenyl ether and a model compound, 4-aminodiphenyl ether, was closely correlated with these E_a values. In addition to the inherent characteristics of the monomers, the properties of the solvent utilized are also critical. For example, the use of polar aprotic solvents that can form strongly hydrogen-bonded complexes with the carboxyl group, plays a major role in driving the equilibrium to amic acid. Dimethyl sulfoxide (DMSO), N,N-dimethylacetamide (DMAc), N,N-dimethylformamide (DMF) and 1-methyl-2-pyrrolidinone (NMP) are the solvents most generally used. The rate of poly(amic acid) formation measured for phthalic anhydride and 4-phenoxyaniline increased with solvent in the order of tetrahydrofuran (THF) < acetonitrile < DMAc.¹⁴

Several minor, but important, reactions also occur during poly(amic acid) formation. These side reactions may become significant under certain conditions, particularly when

the acylation reaction of the diamine is relatively slow because of low monomer reactivity or low monomer concentration. In addition to the amic acid propagation route, five additional potential reaction pathways are possible and are illustrated in **Scheme 1.2**. Their relative rate constants are listed in **Table 1.1**.¹⁵ The formation of poly(amic acid) is an equilibrium reaction determined by acylation (k_1) and deacylation (k_{-1}) reactions. The latter is also described as an intramolecular acidolysis, forming an anhydride. Poly(amic acid)s are known to undergo hydrolytic degradation even at ambient temperatures. When poly(amic acid)s are in solution, a small amount of the anhydride is always present in an equilibrium concentration. However small, it plays an important role in the hydrolytic degradation of poly(amic acid). In the presence of water, the anhydride group is hydrolyzed to form an *ortho* dicarboxylic group as shown in (3). The reaction is driven by the enhanced nucleophilicity of the water in a dipolar aprotic solvent and by the strong acid-base interaction of the material with the dipolar solvent. The effects of water on the molecular weight of poly(amic acid)s during polymerization, and the effect of added water on the molecular weight of poly(amic acid)s in solution, are well documented.¹⁶ It should be noted that water formed *in situ* by the imidization of amic acid, as shown by equation (2), is important. Even if the rate of imidization, and therefore the formation of water, is relatively low at ambient temperatures, it is still significant enough to cause a gradual decrease in molecular weight over a long period of time. For example, Frost and Kesse¹⁷ studied aging of a 11% DMAc solution of pyromellitic dianhydride-4,4'-diaminodiphenyl ether (ODA) poly(amic acid) at 35°C. After 21 days, approximately 20% of the amic acid was converted to the imide, generating the corresponding amount of water, which was equivalent to having 0.19% water in the solvent. When long-term storage is necessary, poly(amic acid) solutions should be kept refrigerated to maintain the properties essential to further processing.



Scheme 1.2: Major reaction pathways involved in poly(amic acid) synthesis.¹⁵

Table 1.1: Relative rate constants for reactions pathways involved in poly(amic acid) synthesis (Scheme1.2).¹⁵

Reaction	Rate constant (s ⁻¹)*
Propagation (k ₁)	0.1-0.5
Depropagation (k ₋₁)	10 ⁻⁵ -10 ⁻⁶
Spontaneous imidization (k ₂)	10 ⁻⁸ -10 ⁻⁹
Hydrolysis (k ₃)	10 ⁻¹ -10 ⁻²
Isoimide formation (k ₄)	—
Diamide formation (K ₅)	—
Isomerization (k ₆)	—

*Rate constants are estimated for a typical polymerization at ca. 10 wt.% concentration, i.e. 0.5M.

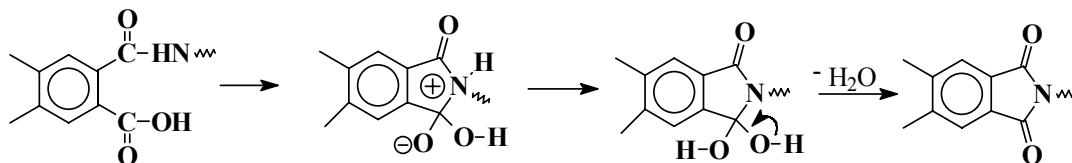
b) Thermal imidization of poly(amic acid)s

The first pathway for the cyclization of an amic acid moiety into an imide involves gradual heating of the PAA to 250-350°C, depending upon the stability and the glass transition temperature of the polymer. The events occurring during the heating include evolution of solvent and dehydrative cycloimidization. The imidization is accomplished through nucleophilic attack of the amide nitrogen on the acid carbonyl carbon with elimination of water. **Scheme 1.3** shows two amic acid cyclization mechanisms proposed by Harris.⁸ The main difference between the two mechanisms is when the loss of the amic acid proton occurs. Harris suggested that mechanism 2 is more likely, since the conjugated base of the amic acid is a more potent nucleophile than the amide. On the other hand, extremely small amide dissociation constants and the demonstrated effectiveness of acid catalyzed reactions^{10,18,19} tend to support mechanism-1.

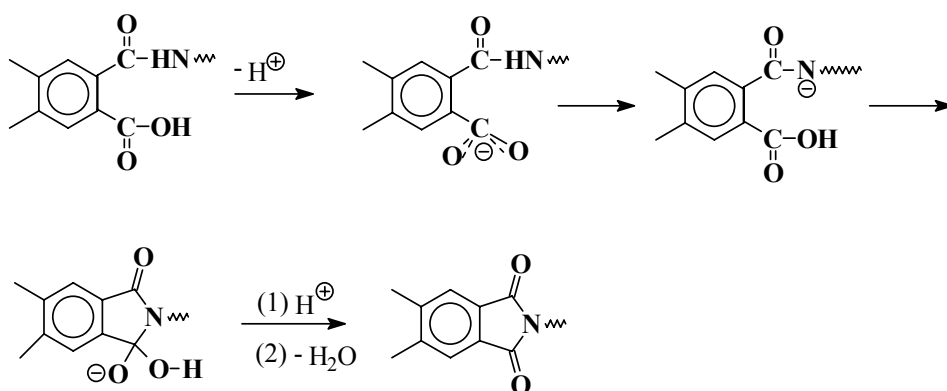
Thermal imidization is particularly effective for the preparation of thin materials such as films, coatings, fibers, and powders because it allows the diffusion of the by-product and

the solvent without forming bristles and voids. The problem of film cracking as a result of shrinkage stress can be avoided by carefully controlling the curing profile. A typical heating schedule includes a stage below 150°C, followed by a relatively rapid temperature ramp to a second stage above the T_g of the resulting polyimide. The majority of the solvent is slowly driven off in the first stage, while imidization essentially occurs in the second stage, where curing shrinkage stress is releasable.¹⁵ Such a heating cycle allows the conversion of polyamic acid to polyimide with degree of imidization of about 92-99%, and this is considered to be the maximum that can be achieved *via* thermal imidization. Further heating at 300°C or higher does not result in 100% conversion because of the so-called “kinetic interruption” effect.⁸ It should be noted that the hydrolytically unstable residual amic acid units resulting from kinetic interruption are considered as defect sites. Their presence at concentrations of 1-8% in the resulting polyimide can noticeably reduce hydrolytic stability. This is particularly evident for the rigid-rod like polyimides, for which full imidization is considered the most difficult to achieve.³

Mechanism 1



Mechanism 2



Scheme 1.3: Possible imide formation mechanisms.⁸

Another important consideration of thermal imidization is the occurrence of side reactions. Compared with polyimides produced from solution imidization, bulk thermal imidization results in polyimides of significantly different properties as a result of these side reactions. A partially reversible decrease in molecular weight in the early stage of imidization was

observed as a result of the depolymerization reaction. This effect has been monitored in insoluble polyimide, by both changes in their mechanical properties during imidization and by temporary appearance of the anhydride carbonyl absorption band near 1860 cm^{-1} between $100\text{-}250^\circ\text{C}$.²⁰⁻²² Evidence of this effect was later verified by measuring the molecular weight of the soluble polymer at different stages of the thermal imidization.²³ The molecular weight gradually regained at high temperature. The side reactions associated with thermal imidization can also lead to some form of crosslinking.²⁴ Amine-terminated model imide compounds were monitored by Raman spectroscopy while heating.^{25,26} The appearance of Raman absorption at 1665 cm^{-1} (C=N) confirmed that imide-imine conversion was occurring, which was predicted by a proposed crosslink reaction mechanism²⁷ involving the attack of terminal amino groups to imide carbonyl groups, with the resulting formation of imine. A study by Schulze et. al,²⁸ however, showed that the imine bond formation is only significant when small amine-terminated species were present. The probability of imine formation decreased with the chain length. Side reactions also include isoimide formation, which thermally isomerizes to the normal imide at later stages.

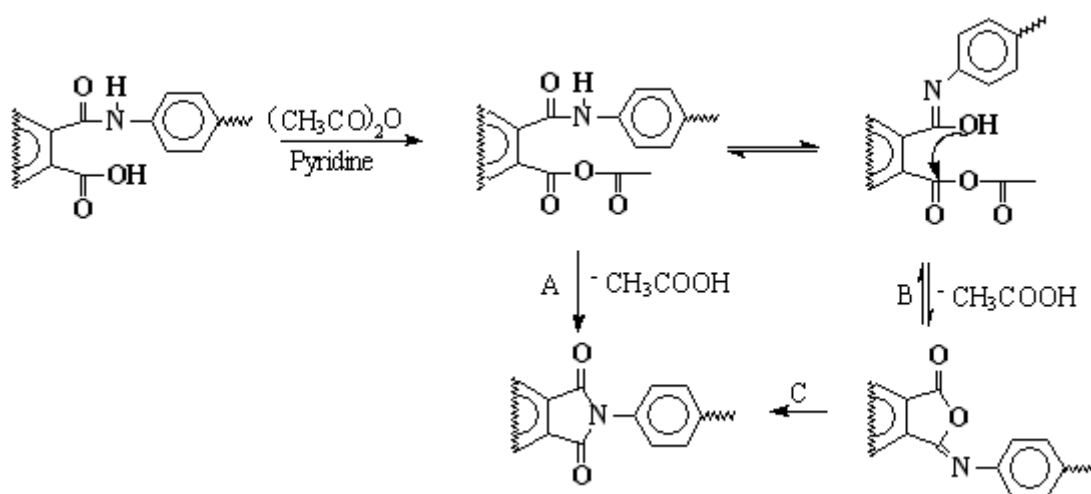
c) **Chemical imidization of poly(amic acid)s**

The second pathway of cyclodehydration of amic acid to imide involves the use of a chemical dehydrating agent to promote ring closure reactions in temperature ranges of $20\text{-}80^\circ\text{C}$, which is effective for either soluble or insoluble polyimides.^{29,30} Commonly used reagents include acid anhydrides in the presence of tertiary amines. Among the dehydrating agent used were acetic anhydride, propionic anhydride, n-butyric anhydride, benzoic anhydride, as well as others. The amine catalysts used include pyridine, methylpyridine, lutidine, N-methylmorpholine, trialkylamines and others.

The outcome of the reaction can be very different depending on the type of dehydrating agent used, the monomer components of poly(amic acid)s, and the reaction temperature. For example, in the presence of trialkylamines with high pK_a (>10.65), high molecular weight polyimides were obtained. On the other hand, the use of a less basic tertiary amine resulted in the formation of polyimides with lower molecular weight. Different results, however, were obtained for heteroaromatic amines. Despite their lower basicity, high molecular weight polymers were formed when pyridine, 2-methylpyridine and

isoquinoline ($5.2 < \text{pK}_a < 5.7$) were used as catalysts.²⁹ The use of acetyl chloride as a dehydrating agent afforded isoimides.³¹ The use of N,N-dicyclohexylcarbodiimide (DCC) also resulted in essentially quantitative conversion of amic acid to isoimides.³² On the other hand, a mixture of imide and isoimide was formed when pyridine was used as the catalyst.³³ However, when pyridine was replaced with triethylamine, isoimide formation was practically eliminated, which also resulted in a significantly faster reaction rate. In examining the conversion of benzophenone tetracarboxylic dianhydride/9,9-fluorenedianiline based poly(amic acid) to the corresponding soluble polyimide, it was found that the cyclizing agent is most effective when employing 4-9 moles per repeat unit of the poly(amic acid). Increasing the temperature from 20°C to 100°C decreased the reaction time from 15 h to 2 h to achieve complete imidization.³⁴

A kinetic study of chemical imidization process has resulted the mechanism shown in **Scheme 1.4**.^{15, 35} A mixed anhydride intermediate is formed by the reaction of the amic acid linkage with acetic anhydride, which is promoted by the presence of a base. The mixed anhydride can further tautomerize from the amide to the iminol form. The amide tautomer cyclizes to the imide (pathway A), the thermodynamically favored product, whereas the iminol tautomer yields the kinetically favored isoimide form (pathway B). Although isoimides are known to thermally isomerize to imides (pathway C), in this case, isomerization occurs *via* the back reaction. This back reaction is apparently initiated by the nucleophilic attack of the acetate ion on the isoimide.³⁶ Such behavior is consistent with the fact that a stronger amine, such as triethylamine, promotes acetate formation, and thus increases the back reaction that results in exclusive imide formation.



Scheme 1.4: Mechanism involved in chemical dehydration of amic acid.^{15,35}

In contrast to thermal imidization, the chemical imidization of poly(amic acid)s occurs without the depolymerization reaction, and thus the molecular weight of the polymer remains constant.³⁷ However, chemical imidization is less attractive for commercial applications because of the expense and process complexity.

d) High temperature solution imidization of poly(amic acid)s

Polyimides resulting from solid state thermal imidization often demonstrate insolubility, infusibility and thus poor processability.³⁸ To overcome these drawbacks, high temperature solution imidization has been successfully utilized.^{10,39,40} Cyclodehydration is conducted by heating a poly(amic acid) solution in a high boiling solvent at temperatures of 160-200°C, in the presence of an azeotropic agent. Compared with bulk thermal imidization, the lower process temperatures and greater mobility in solution ensured the avoidance of degradation and side reactions.

Studies^{10,41} were conducted investigating the kinetics and mechanisms of the solution imidization process. Second order kinetics were determined by monitoring amic acid concentrations using non-aqueous titration and an acid-catalyzed imidization mechanism was suggested. It was clearly demonstrated by 2D-¹H NMR and intrinsic viscosity measurements that the poly(amic acid) chain cleaved to form anhydride and amine end groups at the initial stage of the reaction. As the reaction proceeded, the end groups recombined or the chains “healed” to form polyimides of higher molecular weight.

1.2.1.2 One-step high temperature solution synthesis of polyimides

Soluble polyimides can also be prepared *via* a one-step high temperature solution polycondensation of tetracarboxylic dianhydrides and diamines. In this process, the dianhydride and diamine monomers are heated in a high boiling solvent, or a mixture of solvents, at temperature in excess of 140°C, which permits the imidization reaction to proceed rapidly. Commonly used solvents are dipolar aprotic amide solvents, nitrobenzene, benzonitrile, α -chloronaphthalene, *o*-dichlorobenzene, trichlorobenzenes, and phenolic solvents such as *m*-cresol and chlorophenols. Toluene, *o*-dichlorobenzene, 1-cyclohexyl-2-pyrrolidinone (CHP) are often used as cosolvents to remove the water resulting from condensation *via* azeotroping.⁴²⁻⁴⁵ Unlike the methods described earlier, the

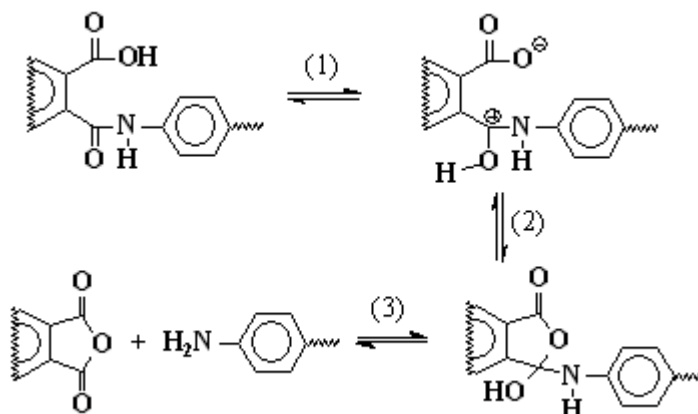
preparation of a high molecular weight poly(amic acid) is not required for this procedure. Imidization can still proceed *via* an amic acid intermediate. However, the presence of the amic acid group is relatively small during polymerization because it is short-lived at high temperatures and either rapidly imidizes or converts to amine and anhydride. The kinetic profile consists of second-order amic acid formation and first- or second-order imide formation with amic acid formation as the rate-limiting step.^{46,47} Under such conditions, steady-state approximation can be applied to the amic acid formation and the entire process can be expected to follow second-order kinetics. However, this predicted behavior is observed only at low conversions (< 30%) and is likely to be complicated by increased molecular weight at higher conversions. In much of the literature, the reaction was shown to be catalyzed by acid.^{48,49} Kreuz et al.,⁵⁰ however, observed that thermal imidization of poly (amic acid)s could be catalyzed by tertiary amines. High temperature solution polymerization in *m*-cresol could be achieved in the presence of high boiling tertiary amines, e.g., using quinoline as the catalyst. Dialkylaminopyridines and other tertiary amines were effective catalysts in neutral solvent such as dichlorobenzene.⁵¹⁻⁵³ The rate of imidization achieved *via* one-step high temperature solution synthesis was essentially complete, or 100%. No “defect sites,” of either amic acid or isoimide type, were detected in the resulting polymers, which can likely account for the differences in the physical properties observed between polyimides produced by solution synthesis and those obtained by the conventional two-step technique.^{42,54} Another advantage of the high temperature solution method is that it allows high molecular weight polyimides to be prepared from monomers with sterically or electronically-hindered groups that would otherwise be hard to successfully polymerize *via* the two-step route. Polyimides whose T_m is $\leq 300^\circ\text{C}$ or whose T_g is $\leq 250^\circ\text{C}$ can be prepared by one-step melt polycondensation using the extrusion molding method.⁵⁵

1.2.1.3 Other synthetic routes to polyimides

1.2.1.3.1 Polyimides *via* derivatized poly(amic acid) precursors

As discussed in Section 1.2.1.1 solutions of poly(amic acid)s are susceptible to hydrolytic degradation. This process breaks down the molecular weight of the amic acid and resulting polyimide.⁵⁶ It is believed that hydrolysis occurs through the acid-catalyzed formation of

an anhydride, as shown in **Scheme 1.5**,¹⁵ rather than through direct hydrolysis of the amide linkage. To prevent this, efforts have been made to derivatize the amic acid to exclude the proton transfer from the acid group.



Scheme 1.5: Postulated mechanism for amic acid back reaction to anhydride and amine.

The simplest way to eliminate the proton transfer step is to neutralize the acid group with a base, such as a tertiary or a secondary amine, to form a polymeric salt.⁵⁰ However, the viscosity of the solution is very high due to the presence of ionic polymer chains. Alternatively, a more complex approach involves converting the acid group into either an amide or ester moiety. The *ortho*-carboxylic group in poly(amic acid)s can be chemically modified to either an ester or an amide moiety. The ester and amide derivatives of poly(amic acid)s are stable, unable to form carboxylate anion which prevents the creation of degradation intermediate (reaction 1 in **Scheme 1.5**). Poly(amic ester)s can be isolated by precipitation without degradation and can be stored for an indefinite period at ambient temperatures. Such stability is highly desirable for some applications, such as microelectronics. In the preparation of photosensitive polyimides, the photocurable functionality is usually incorporated through derivatizing the poly(amic acid) to poly(amic ester).

The preparation of derivatized poly(amic acid)s can be achieved by one of two general pathways: 1) Formation of the poly(amic acid) followed by derivatization of the *ortho*-carboxylic acid groups along the polymer backbone; and 2) Derivatization of the monomer and subsequent activation to allow the monomer to enter a polymer forming reaction to yield the desired polymer. Conversion of esters of poly(amic acid) to polyimides readily proceeds thermally but at a slower rate and generally requires a temperature significantly

higher than 200°C. The increased imidization temperature regime offers a wider processing window.

1.2.1.3.2 Polyimides *via* polyisoimide precursors

In general, polyisoimides are significantly more soluble and possess lower melt viscosities and lower glass transition temperatures than the corresponding polyimides, mainly because of their lower symmetry and structural irregularity.⁵⁷ These features make it possible to prepare rigid rod-like polyimides using soluble and processable polyisoimides.⁵⁸ Polyisoimides are formed from the corresponding poly(amic acid), using a dehydrating agent, such as trifluoroacetic anhydride, in conjunction with triethylamine. N, N-Dicyclohexylcarbodiimide (DCC) and acetyl chloride by themselves were reported to form polyisoimides from poly(amic acid)s in high yield.^{31,32,59} A polyisoimide can easily be converted to the corresponding polyimide *via* thermal treatment at >250°C. Alternately, polyisoimides have been reacted with alcohol to produce poly(amic ester)s, which could then be thermally converted to polyimides.⁶⁰ On treatment with amines, polyisoimides likewise give poly(amic amide)s quantitatively. Poly(amic amide)s were also thermally converted to polyimides.⁶¹

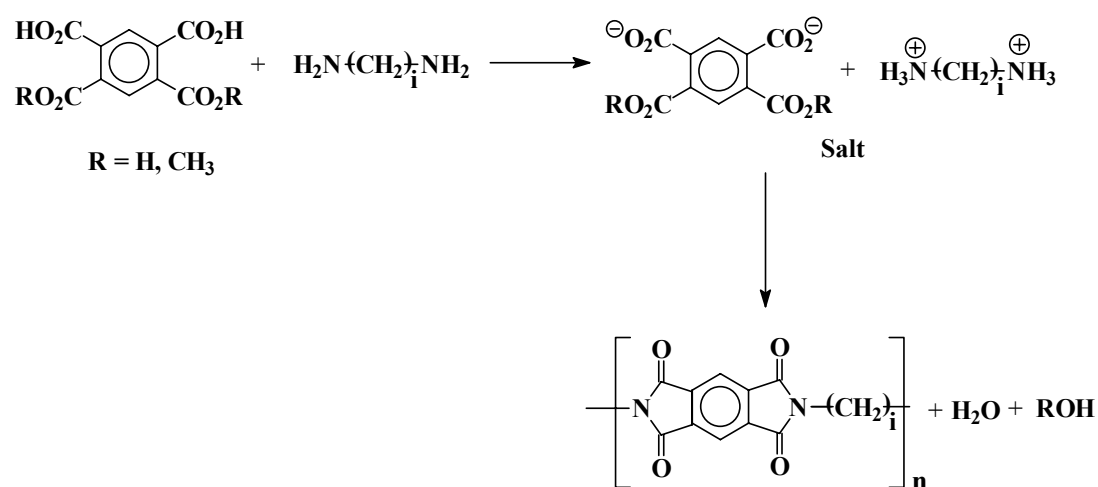
1.2.1.3.3 Polyimides from diester-acids and diamines (Ester-acid route)

Synthesizing polyimides *via* the ester-acid route involves derivatizing the anhydrides to ester-acid and subsequently allowing the diamines to react, which yields the desired poly(amic acid) and polyimide. Polyimides are frequently synthesized *via* the ester-acid monomer route because this process is relatively tolerant of water in solvents and reactors.^{61,63} In the initial stage of esterification, the dianhydride is simply refluxed in an excess of alcohol. It should be noted that the rate is greatly enhanced by addition of an amine catalyst, e.g., triethylamine, which acts as an acid acceptor. Once the excess alcohol has been evaporated, the resulting diester diacid is then reacted in solution with a suitable diamine to form a poly(amic acid). A polar, aprotic solvent is needed for the similar reason as for poly(amic acid) route. The polyimide is obtained by thermal or high temperature solution imidization described earlier. Previously, it was thought that that the mechanism of amic acid formation from diester-diacid and diamine proceeds by the nucleophilic

attack of ester carbonyl by amine resulting in poly(amic acid) with the elimination of alcohol. However, it was later discovered that the anhydride functional group was formed at elevated temperatures *in situ* from the *ortho* ester-acid.⁶²⁻⁶⁴ The anhydride then reacts with the diamine to yield a poly(amic acid).

1.2.1.3.4 Polyimides from tetracarboxylic acids and diamines

This synthetic route for producing aliphatic-aromatic polyimides with high molecular weight involves combining aromatic tetracarboxylic acids and aliphatic diamines to form salts, similar to the synthesis of nylon *via* nylon salts. The salts are thermally imidized under high pressure at temperatures above 200°C to form polyimides (**Scheme 1.6**). It should be pointed out that the intermediate poly(amic acid)s are not detected during the polycondensation stage. Rather, it appears that the imidization and formation of poly(amic acid)s takes place at the same time. This means that the imidization rate is very fast.⁶⁵



Scheme 1.6: Polyimide synthesis from tetracarboxylic acid-amine salt.

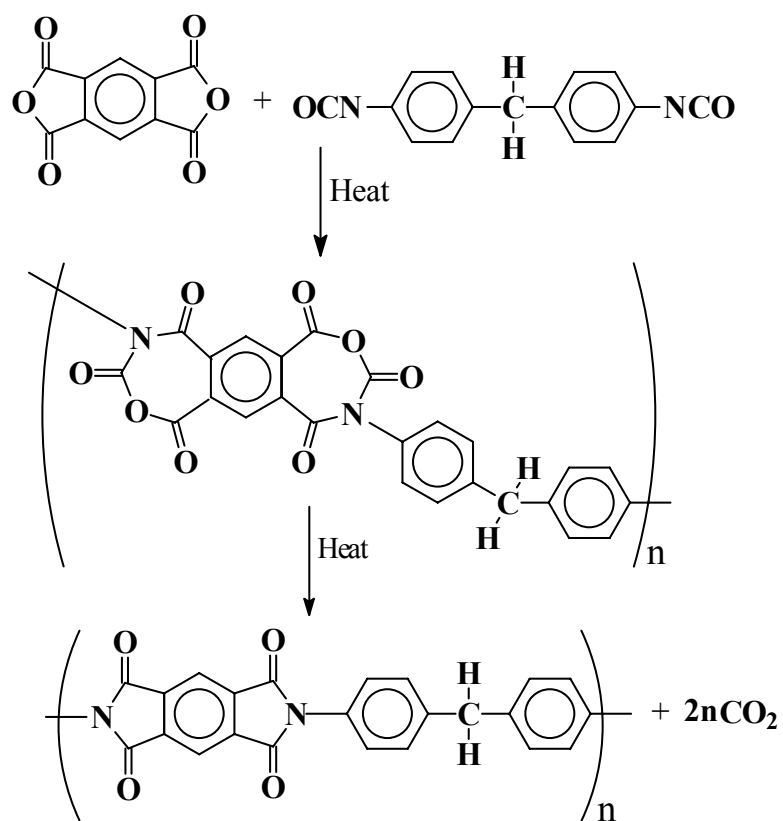
In the one-step melt polymerization of polyimides, it is advantageous to use tetracarboxylic acids because high molecular weight poly(amic acid) intermediates of very high melt viscosities are not formed during the initial heating stage. Another advantage of using tetracarboxylic acids is their stability and ease of purification. Many of them can be readily recrystallized from hot water.

1.2.1.3.5 Polyimides from dianhydrides and diisocyanates

It has long been known that phthalic anhydride reacts with aromatic and aliphatic isocyanates to give n-aryl - and n-alkylphthalimides,⁶⁶ respectively. The reaction of aromatic diisocyanates with dianhydrides has been utilized to synthesize polyimides.⁶⁷⁻⁷⁹

Reaction of isocyanate with anhydride involves formation of a 7-membered cyclic intermediate (**Scheme 1.7**).^{77,79} This intermediate is believed to split off carbon dioxide when heated to form 5-membered imide rings.

High molecular weight polyimides have been synthesized by reacting blocked isocyanates with anhydrides.⁸⁰

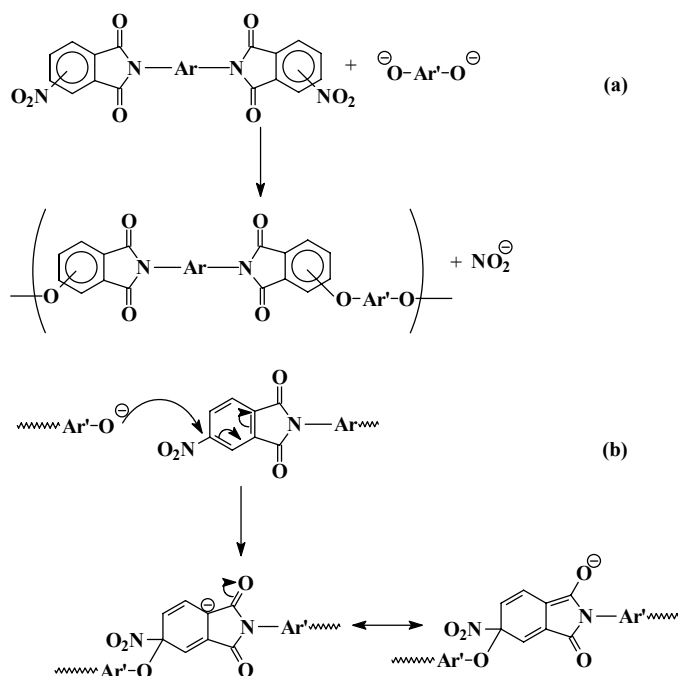


Scheme 1.7: Polyimide synthesis from dianhydrides and diisocyanates *via* an imide-anhydride seven-membered intermediate

1.2.1.3.6 Polyetherimides *via* nucleophilic aromatic substitution reactions

Aromatic nucleophilic substitution of bishalo- and bisnitro- substituted aromatic ketones and sulfones with bisphenolates can produce polyetherketones⁸¹ and polyethersulfones,⁸² respectively. Aromatic halo- and nitro-groups are also strongly activated by imide groups toward nucleophilic aromatic substitution⁸³⁻⁸⁶ with anhydrous bisphenol salts in polar aprotic solvents. The polymer chain is generated by the formation of successive aromatic ether bonds. A general synthetic pathway is depicted in **Scheme 1.8(a)**. Halo- and nitro-substituted imides are more reactive than the corresponding sulfones and ketones. This is due to the fact that the phthalimide ring is not only activated by the additional carbonyl group, but the two carbonyl groups are locked in a coplanar conformation with the phenyl ring, providing more effective resonance. Because of the favorable carbonyl conformation, the Meisenheimer type transition state is stabilized by the effective delocalization of the negative charge as shown in **Scheme 1.8(b)**.⁸⁷

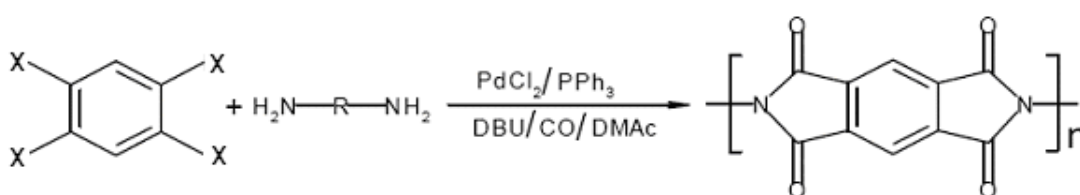
This process is commercially being used by GE, for the production of ULTEM[®], a polyether imide.



Scheme 1.8: Synthesis of polyetherimides by nucleophilic aromatic substitution (a) and delocalization of negative charge in Meisenheimer transition state in imide system (b).⁸⁷

1.2.1.3.7 Other routes to polyimide formation

Many other polyimide preparation methods have been reported in addition to the aforementioned routes. Due to the improved stability and solubility of derivatized PAAs, a number of techniques have been developed to form alkyl esters,⁸⁸⁻⁹² silyl esters,^{93,94} and ammonium salts^{95,96} of PAAs, all of which can be thermally cyclized to form polyimides. The alkyl esters are formed from the reaction of an ester-acid chloride and the silylated esters are formed in the reaction of N,N'-bis(trialkylsilyl) diamines with various dianhydrides. The ammonium salts of PAA's can be formed by reaction with a secondary or tertiary amine. The resulting polyelectrolyte can then be dispersed in an aqueous medium and used to fabricate carbon fiber composites.⁹⁶ Polyimides can also be prepared by Diels-Alder⁹⁷⁻¹⁰⁰ and Michael^{101,102} cycloaddition reactions. Palladium¹⁰³⁻¹⁰⁵ (Scheme 1.9) and nickel¹⁰⁶ catalyzed carbon-carbon coupling reactions have also been reported in the literature. Thin films of polyimides for microelectronic applications have been prepared by vapor-phase polymerization of PMDA and ODA^{7a, 107}. Solventless synthesis of polyimids via a monomeric salt has been carried out with aromatic dianhydrides and aliphatic diamines¹⁰⁸. Though the polyamic acid, intermediate of polyimide, is moisture sensitive, the reports are available for use of water as a solvent for polyimide synthesis,^{109a, b} which might be possible by formation of stable polyamic acid salt, as evidenced by Imai et al.^{109c}



Scheme 1.9: Synthesis of polyimides by Pd-catalyzed carbon-carbon coupling reaction.¹⁰³

1.2.2 Structure-property relationship in aromatic polyimides

The properties of polyimides, as for polymers in general, are governed by three fundamental characteristics: chemical structure, average molecular weight and molecular weight distribution.¹¹⁰ The chemical structure relates to the chemical composition of the repeat unit and the end groups. It also encompasses the composition of any branches,

crosslinks or defects in the structural sequence. The average molecular weight describes the average polymer chain size. The molecular weight distribution relates to the degree of regularity in the molecular size.

Extensive literature has been published describing alterations in the structure and the size of the polyimide backbone and how these changes affect the physical and mechanical properties¹¹¹ and in this section we will discuss the relationships between structure and properties such as thermal transitions and optical and dielectric properties.

1.2.2.1 Glass transition and solubility

Interchain interactions define the solubility and processability of polymers. In case of polyimides these interactions are basically charge transfer complexes formed between polyimide chains. To address the interchain interactions in polyimides, electron affinity of dianhydrides and ionization potential of diamines should be taken into consideration. Polyimide derived from dianhydride with highest electron affinity and diamaine with lowest ionization potential will have strongest interchain interactions. The strongest inetrchain interaction leads to polymers with high Tg and low solubility.⁶

Different methods have been studied to reduce the chain interactions or to promote better interactions between solvent and polymeric chains.

1. Reactants with asymmetric structures (*meta* instead of *para*-catenation).^{6, 112a}
2. Reactants with flexible links (O, CH₂, etc) which disrupt conjugation and increase the chain flexibility.^{6, 112a}
3. Introduction of polar groups in the repeating units.^{112b-c}
4. Introduction of bulky substituents.^{4,6,7-9, 112a}

The general effects of these approaches are summarized in **Table 1.2**

Table 1.2 Effect of chemical structure on solubility and glass transition

Structure modification	Solubility	Tg	References
<i>o, m</i> verses <i>p</i> attachment	↗	↘	6, 112a
Flexible links	↗	↘	6,112a
Polar groups	↗	↘	112d,e
Bulky substituents	↗	↗	4, 6, 7-9, 112a

1.2.2.2 Optical properties

As for the other polymeric materials, amorphous polyimides exhibit a good transparency. Colorless polyimides can be obtained by minimizing the electronic conjugation or charge transfer complexes. Typical approaches include a) use of fluorinated diamines or dianhydrides, b) introduction of bulky “cardo” groups along the polymer backbone, etc. In addition to fluorinated and cardo polyimides, semiaromatic polyimides were synthesized from cycloaliphatic dianhydrides and aromatic diamines. Various cycloaliphatic dianhydrides and diamines have been synthesized to obtain colorless polyimides. UV cutoff of the polyimides derived from cycloaliphatic dianhydrides is around 320 nm with higher transmittance of light.

Controlling the refractive index of colorless polyimides is an important requirement for optical waveguides. It is performed by the copolymerization of fluorinated dianhydride with a mixture of fluorinated and nonfluorinated diamine. Refractive index of the polymer increases when the molar fraction of nonfluorinated diamine increases, which leads to undesirable optical loss. Use of chlorinated diamines instead of non fluorinated diamines showed increase in refractive index without optical loss.

1.2.2.3 Dielectric properties and moisture uptake

The chemical requirements leading to a low dielectric constant (below 3) and low moisture uptake are the same which were discussed in **Section 1.2.2a** and **1.2.2b**. Substituents like fluoroalkyl, fluoroalkoxyl or cardo groups allow the dielectric constant to drop to 2.6-2.7. The moisture uptake is also minimized for these polymers. Similar results were obtained with cycloaliphatic imides but with low thermal stability.^{4,6,7-9, 110,112a}

1.2.3 Applications of polyimides

The list of polyimide applications is unending and it still keeps growing with the increasing demands of growing technologies.

Polyimides find applications as alignment layers for liquid crystal displays. In the following section sampling of literature will be reviewed with particular emphasis on liquid crystal alignment properties of polyimides. A brief introduction of liquid crystal displays (LCDs) and alignment layers for LCDs is provided followed by summary of literature on use polyimides for this application.

1.2.3.1 Liquid crystal displays

Liquid crystal displays (LCDs) are a passive display technology. This means they do not emit light; instead, they use the ambient light in the environment. By manipulating this light, they display images using very little power. This has made LCDs the preferred technology whenever lower power consumption and compact size are critical. Few of the LCDs applications involve, laptop computers, camcorders, portable TVs, etc.

Liquid crystal (LC) is an organic substance that has both a liquid and a crystal molecular structure. In this liquid, the rod-shaped molecules are normally in a parallel array, and an electric field can be used to control the molecules. Most LCDs today use type of liquid crystal called Twisted Nematic (TN). A Liquid Crystal Display (LCD) consists of two substrates that form a “flat bottle” that contains liquid crystal mixture. The inside surfaces of the bottle or cell are coated with a polymer that is rubbed in one direction to align the molecules of liquid crystals, which is called as an alignment layer. The LC molecules align on the surface in the direction of buffing. For TN devices, the two surfaces are buffed orthogonal to one another, forming a 90° twist from one surface to the other (Figure 1.2).

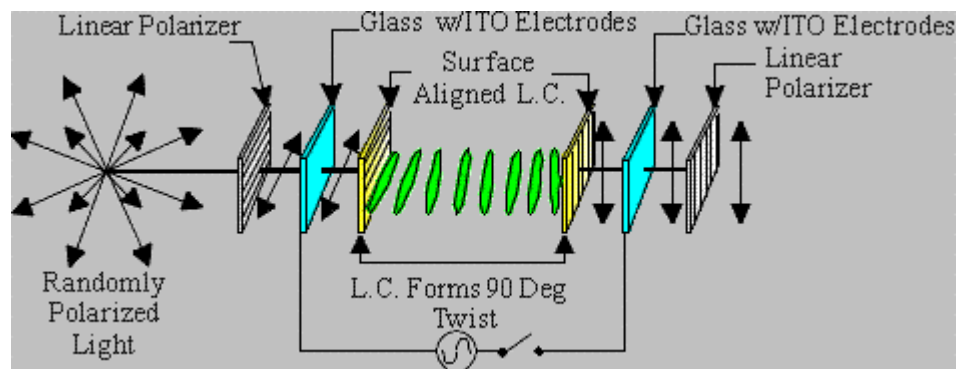


Figure 1.2: Structure of twisted nematic display in normally white mode (off-state).

This helical structure has the ability to control light. A polarizer is applied to the front and an analyzer/reflector is applied to the back of the cell. When randomly polarized light passes through the front polarizer it becomes linearly polarized. It then passes through the front glass and is rotated by the liquid crystal molecules and passes through the rear glass. If the analyzer is rotated 90° to the polarizer, the light will pass through the analyzer and be reflected back through the cell. The observer will see the background of the display, which in this case is the silver gray of the reflector.

The LCD glass has transparent electrical conductors plated onto each side of the glass in contact with the liquid crystal fluid and they are used as electrodes. These electrodes are made of Indium-Tin Oxide (ITO). When an appropriate drive signal is applied to the cell electrodes, an electric field is set up across the cell. The liquid crystal molecules will rotate in the direction of the electric field. The incoming linearly polarized light passes through the cell unaffected and is absorbed by the rear analyzer. The observer sees a black character on a silver gray background (**Figure 1.3**). When the electric field is turned off, the molecules relax back to their 90° twist structure. This is referred to as a positive image, reflective viewing mode. Carrying this basic technology further, an LCD having multiple selectable electrodes and selectively applying voltage to the electrodes, a variety of patterns can be achieved.¹¹⁴

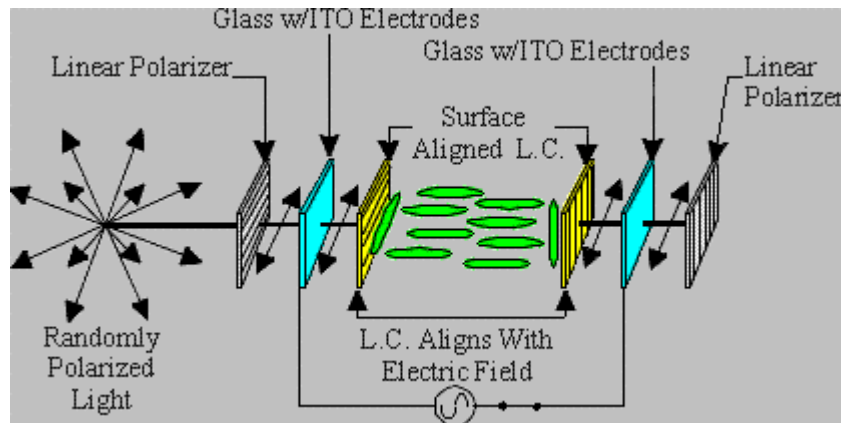


Figure 1.3: Structure of twisted nematic display in normally white mode (on-state).

The alignment layers not only align the liquid crystal molecules unidirectionally, but they also generate a slight tilt to the molecules (**Figure 1.4**). Either end of liquid crystal molecules may rise when the voltage is applied if the molecules lie flat on the surface. The slight tilt, thus, results in a fast response to the applied voltage. The angle between the axis of the liquid crystal molecules and the alignment layer is called pretilt angle.

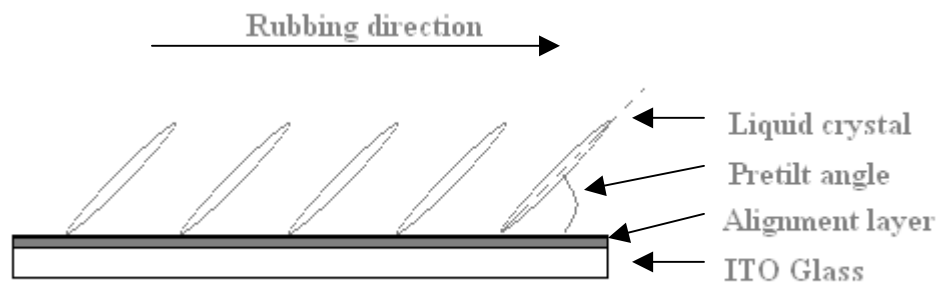


Figure 1.4: Alignment and pretilt of liquid crystal molecules.

1.2.3.2 Polyimides for LCD application

Rubbed polymer films are used in flat-panel displays to control the alignment of liquid crystals in contact with the polymer, a phenomenon first discovered by Maugin in 1911.¹¹⁵ Polyimide and polyamideimide films have been used as alignment layers in LCDs because of their good adhesive properties, insulation ability and orientational ability. A solution of poly(amic acid) is first spin coated on to a ITO glass plate. The resulting film is cured at 150 to 250°C to form a thin polyimide layer. With soluble polyimides, a thin film is spin coated onto a ITO glass plate and baked to evaporate solvent at relatively low temperature. The polyimide surface is then repeatedly rubbed in the same direction with a cotton, silk or velvet cloth. When liquid crystal molecules are placed on this layer, they will align in the same direction as the rubbing direction. The actual tilt angle obtained is a function of polymer ordering on the surface, the resulting surface energy, the nature of the cloth used to buff the surface and the amount of buffing work. In addition to these variables, each of the hundreds of commercial liquid crystal formulations interact differently with a given surface. In general, however, the single most important factor determining the value range of the tilt angle is the intrinsic character of the polymer used to control this angle. Berreman proposed that liquid crystal molecules are oriented and a pretilt induced by small mechanical grooves.¹¹⁶ Uchida proposed that the alignment of polyimide chains induced the pretilt.¹¹⁷

The pretilt angle is critically important to the manufacture of LCDs. For most standard twisted nematic (TN) LCDs (off = white) a small pretilt angle of 2-3° is enough, which can be generated by simply rubbing several commercial polyimide films. For more sophisticated supertwisted nematic (STN) LCDs higher tilt angles of greater than 5° are

required because of the higher twist angles in the liquid crystal molecules.¹¹⁸ There are, however, other LCD applications which require lower tilt angles of less than 2° while maintaining good and stable alignment properties. For example, normally black LCDs (off = black) require tilt angles lower than that achieved using conventional polyimides.¹¹⁹

The effect of several alignment layer chemical structures on pretilt angles generated were determined by Nozaki and coworkers.¹²⁰ High pretilt angles were obtained with 1) high level of imidization, 2) rigid tetracarboxylic anhydride moiety and 3) uneven distribution of fluorine atoms in polymer film. It has been also found that the orientation of polyimide film on thin layer surface played an important role in aligning liquid crystal molecules on the surface.

Liu et al¹²¹ in their study of molecular design of liquid crystal alignment polyimide layer (LCAL) showed that LCAL should have flexible moieties in the polymer backbone and some long-chain alkyl groups should be introduced into the main chain or as the side chain so as to raise the LC pretilt angle. Polyimides derived from aliphatic diamines with different lengths and BPDA, displayed odd even effect. The higher pretilt angle in the range 3-6° were obtained with polymers containing even-numbered aliphatic segments. However, lower pretilt angles of 0.5° were obtained with polyimides containing odd-numbered segments (**Figure 1.5**).¹²²

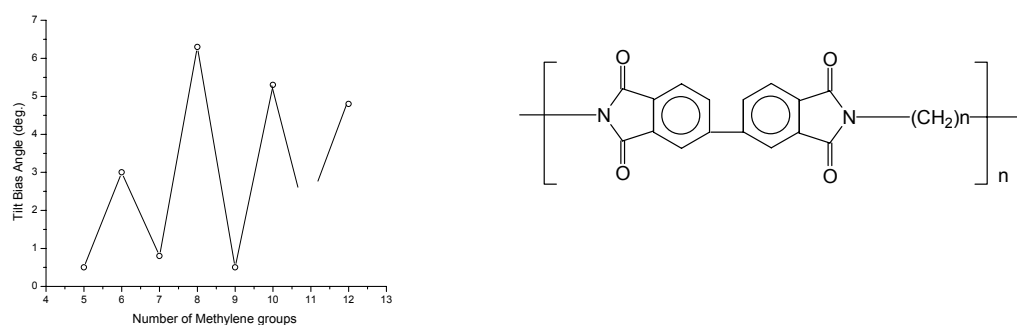


Figure 1.5: Effect of alkylene chain length on pretilt angle.

It has been observed that polyimides with long alkyl and fluorinated alkyl side branches generate high pretilt angle of LCs by rubbing.¹²³⁻¹²⁶ Thus, they have suggested that the high pretilt angles are attributed to steric interactions between LCs and neatly aligned branched chains.

Recently, series of polyimides with side chains containing the mesogens has been prepared.¹²⁷⁻¹²⁸ In this case the mesogen is supposed to act together with LCs in their alignment.

The thermal requirements in the case of LCDs are not stringent and therefore the use of polyimides derived from alicyclic monomers¹²⁹⁻¹³⁰ and monomers with alkyl groups have gained importance.¹³¹⁻¹³⁴

Aerospace industry has been and still continues to be the major user of polyimides in various forms, such as, adhesives, coatings, matrix for composites, etc. Polyimides are used in the electronics field in the areas such as wafer fabrication, adhesion, chip packaging and assembly.¹³⁵⁻¹⁴² They can be used as optical waveguides in optoelectronic devices.¹⁴³

1.3 Polyesters

Polyesters are polymers with recurring ester groups $\text{—}\overset{\text{O}}{\parallel}\text{—}\text{—}$ as an integral part of the main polymer chain.

The reaction of aromatic dicarboxylic acids and diphenols was first noted by Conix¹⁴⁴ in 1957. The literature on polyarylates based on aromatic dicarboxylic acids is extensive. Before the production of first commercial aromatic polyester, U-polymer (a polyarylate based on bisphenol A and tere/isophthalates) by Unitica, in 1974, 140 different chemical compositions of polyarylates were listed.¹⁴⁵

Polyarylates have found applications in wide variety of areas by virtue of their attractive electrical and mechanical properties. However, polyarylates are generally difficult to process because of their limited solubility in organic solvents and high glass transition and melting temperatures. The melt viscosity of BPA-based polyesters is noted to be high and thus it's injection mouldability is considered to be a limitation. Therefore, a great deal of effort has been expended to try to improve processability of polyarylates.

1.3.1 Synthesis of Polyesters

High molecular weight aromatic polyesters are prepared by two chemical routes.

1. Acid chloride route
2. Transesterification route

1.3.1.1 Acid chloride route

This route is generally applicable and mostly used for the synthesis of polyarylates. The diacids are converted into diacid chlorides followed by condensation with diphenols. The reaction can be performed by three different processes

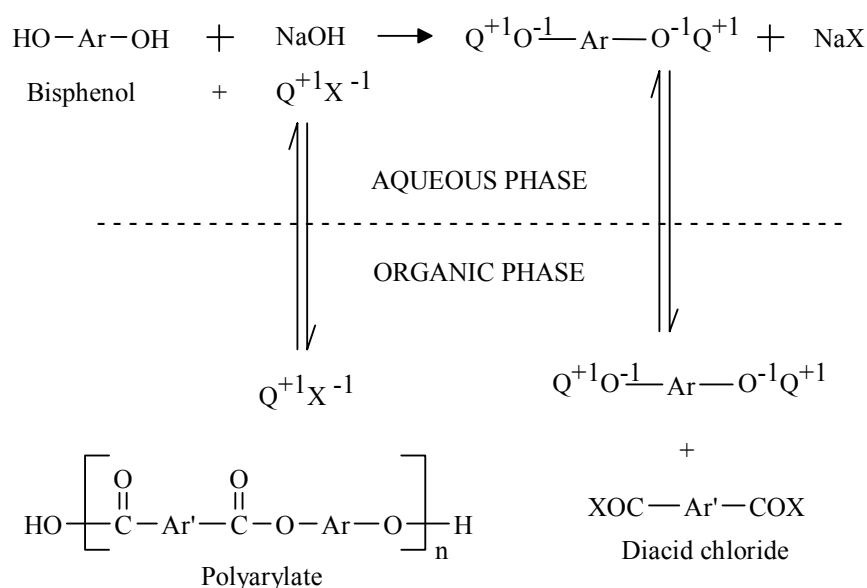
1.3.1.1.1 Interfacial polycondensation

The interfacial process for the preparation of polyarylates was first described by Eareckson¹⁴⁶ and Conix.¹⁴⁴ Basically, the interfacial polymerization involves the reaction of dialkali metal salt of a diphenol with diacid chloride(s) in systems such as water-

dichloromethane or water-chlorobenzene. The acid chloride, which can be either aliphatic or aromatic is dissolved in the water-immiscible organic phase and is reacted with the aqueous alkaline bisphenolates under high speed stirring. Aliphatic diols do not form alcoholate ions in aqueous solutions and are, therefore, not suitable monomers for the preparations of polyesters by interfacial technique.

Since reaction takes place at the interface or near the interface, factors such as stirring speed, the relative volume of organic and aqueous phases, monomer concentrations and the nature and concentration of phase transfer catalyst exert a marked influence on reaction kinetics and on the resulting polymer yield and molecular weight^{147b, c}. Phase transfer catalyst (PTC) facilitates the transportation of phenolate ions in the organic phase and can also act as a surfactant, which increases the total interfacial area and consequently overall reaction rate^{147b, d}.

A typical phase -transfer catalyzed interfacial polycondensation is shown in **Scheme 1.10**.



Scheme 1.10: Phase-transfer catalyzed interfacial polycondensation.

The basic function of PTC is to transfer the anions of the reacting salt into the organic medium in the form of ion pairs. These ion pairs react with chloride ions in the organic phase producing the desired product. The regenerated PTC is transferred back into the aqueous medium.^{147,148} The most commonly used PTC's are benzyltriethyl-ammonium chloride (BTEAC), tetraethylammonium chloride (TEAC), tetramethylammonium

chloride (TMAC), benzyltriphenyl phosphonium chloride (BTTPC), 15-crown-5 (15-C-15), and 18-crown-6 (18-C-6).

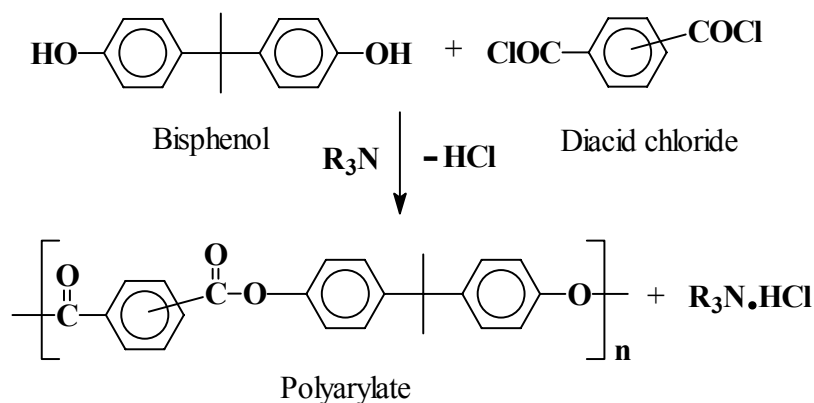
The choice of organic solvent is very important in interfacial polycondensation. It is advantageous that polyarylate formed during the polymerization should remain in the solution form to obtain the high molecular weight polymers. The precipitation of polymer lowers the reaction rates, hence, low molecular weight polymers are obtained.

In contrast to polyesterification carried out in homogeneous media, the maximum molecular weight is not necessarily obtained at the equimolar ratio of reactants. The actual optimum stoichiometric ratio depends on the rate of diffusion of individual reactants to the reaction zone. The synthesis of high molecular weight polyesters have been reported for diacid chloride-bisphenol stoichiometric ratios ranging between 0.58 and 2, depending on reactants and experimental conditions.^{148b, c}

Interfacial polymerization is commercially applied the synthesis of bisphenol-A polyester such as Unitika's U-polymer.

1.3.1.1.2 Low temperature solution polycondensation

Low temperature solution polycondensations are generally run at room temperature or between -10°C to +30°C. Polyarylates are synthesized by the reaction of equivalent amounts of a diacid chloride and a dihydroxy compound in an inert solvent such as THF or dichloromethane in the presence of tertiary amines such as triethyl amine or pyridine, which plays a role of both reaction catalyst and HCl acceptor. This synthetic method is also termed acceptor-catalytic polyesterification.^{150b, c} **Scheme 1.11** depicts the synthesis of polyester from bisphenol-A and terephthalic acid chloride/ isophthalic acid chloride.



Scheme 1.11: Solution polycondensation of bisphenol and diacid chloride.

High molecular weight polyarylates are successfully synthesized in pyridine alone or in combination with a tertiary amine in an inert organic solvent.^{144,146,150-152}

1.3.1.1.3 High temperature solution polycondensation

The polycondensation of a diacid chloride with a bisphenol without an acid acceptor is slow at room temperature. The rate of polycondensation increases with increasing temperature. The high temperature solution polycondensation is carried out at elevated temperatures (~200°C) in an inert high boiling solvent. The high boiling solvents used are nitrobenzene or o-dichlorobenzene.¹⁵³ The o-dichlorobenzene and pyridine system is the most effective one to produce the polymer with high molecular weight.¹⁵⁴ Polyarylates are also prepared in good yields at 215-220°C in dichloroethylbenzene.^{155,156} No acid acceptor is needed because the evolved hydrogen chloride is continuously removed from the system with the aid of an inert gas. A wide variety of other solvents are useful and include chlorinated benzenes (tetrachlorobenzene), chlorinated biphenyls or diphenylethers, chlorinated naphthalenes, as well as non-chlorinated aromatics such as terphenyl, benzophenones, dibenzylbenzenes, and the like.

1.3.1.2 Transesterification route

Transesterification reactions can be carried out by reaction of,

- 1) Diphenyl ester of an aromatic dicarboxylic acid and bisphenol¹⁵⁷⁻¹⁶¹,
- 2) Aromatic dicarboxylic acid and diacetate derivative of bisphenol^{144,162-164},
- 3) Dialkylester of dicarboxylic acid and diacetate derivative of bisphenol¹⁶⁵⁻¹⁶⁷,

1.3.1.3 Miscellaneous routes for polyester synthesis

Various routes other than the routes mentioned above have been used for polyester synthesis. Phenol silyl ether route demonstrated by Kricheldorf¹⁶⁸⁻¹⁷¹, direct esterification route using activated diacid intermediate¹⁷²⁻¹⁸¹, palladium-catalyzed carbonylation of aromatic dihalides with bisphenols¹⁸²⁻¹⁸⁵, are few of them.

1.3.2 Structure-property relationship in polyesters

Effect of monomer structure on the polyester properties has been reviewed.^{145,165} Structure-property relationship in view of gas separation will be discussed in this Section.

1.3.2.1 Gas separation

Gas separation using polymeric membranes was first reported by Mitchell in a study with hydrogen and carbon dioxide mixture in 1831.¹⁸⁶ Thomas Graham, in 1866, made next important step in understanding the permeation process. He postulated that permeation is a three step process: the solution of the gas flows onto the upstream (high-pressure) surface of the membrane, gas diffuses through the membrane and finally, gas evaporates from the downstream (low-pressure) surface of the membrane.¹⁸⁷ This early description of gaseous transport is considered to be the basis for today's "solution-diffusion model", which is used to explain many membrane separations.

The separation of oxygen and nitrogen from air, and hydrogen from carbon monoxide, methane or nitrogen are large consumers of energy in the chemical processing industry. In general, purified gases are more valuable than arbitrary mixtures of two or more components since pure components provide the option of formulating an optimum mixture for particular applications.

Energy-intensive compression of feed system is often needed to provide the driving force for permeation in membrane based separations. In their simplest ideal forms, membranes appear to act as molecular scale filters that take a mixture of two gases, A and B, into the feed port of the module and produce a pure permeate containing pure A and a nonpermeate containing pure B (**Figure 1.6**). Real membranes can approach the simplicity and separation efficiency of such idealized devices, but generally complex recycling of some of the permeate or nonpermeate stream may be needed because perfect selection of A and B molecules cannot be achieved in a single pass.

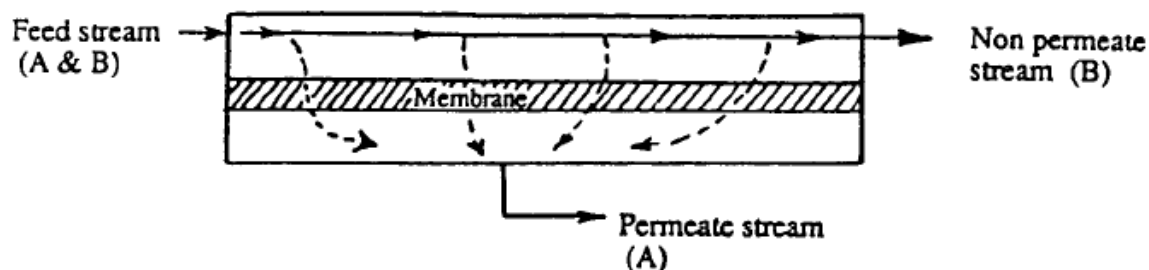


Figure 1.6: Generalized representation of an ideal membrane separation process.

Solution-diffusion membranes rely on the thermally agitated motion of chain segments comprising the polymer matrix to generate transient penetrant-scale gaps that allows diffusion from upstream to the downstream face of the membrane. By varying the chemical nature of the polymer one can change the size distribution of the randomly occurring gaps to retard the movement of one species while allowing the movement of the other. If one could perfectly control this distribution, a true molecular sieving process would occur and infinite selectivity would be achieved. The essential impossibility of such a situation is suggested by kinetic diameter data of various important penetrants (**Table 1.3**). The ability to regulate the distribution of transient-gap sizes in solution diffusion membrane is achieved by the use of molecules with highly hindered segmental motions and packing. Typically these materials are amorphous and are referred to as glassy polymers.

Table 1.3: Minimum kinetic diameter of various penetrants.¹⁸⁸

Penetrant	He	H ₂	NO	CO ₂	O ₂	N ₂	CO	CH ₄	C ₂ H ₄	Xe	C ₃ H ₈
Kinetic diameter (Å)	2.6	2.89	3.17	3.3	3.46	3.64	3.76	3.8	3.9	3.96	4.3

Permeation is a function of two parameters: the solubility constant, S , and the diffusion coefficient, D . The solubility constant is a thermodynamic term based on specific polymer-penetrant interactions and condensability of the penetrant. The diffusion coefficient is a kinetic term referring to the movement of gas molecules inside the polymer matrix.¹⁸⁹ The diffusion coefficient determines “how frequently, on a time-averaged basis, a hole of sufficient volume appears next to the gas penetrant, enabling it to jump further through the membrane”.¹⁹⁰

The permeability coefficient of penetrant molecule A (P_A) can be expressed in terms of the mean diffusion coefficient (D_A) and the solubility coefficient (S_A)^{191,192}

$$P_A = D_A \times S_A$$

The permeability coefficient of penetrant molecule A (P_A) through a dense polymer membrane, having an effective membrane thickness of l , can be derived from the steady state flux, F_A

$$P_A = F_A \times \frac{l}{\Delta p}$$

where, Δp is the partial pressure difference between the upstream and downstream pressure of penetrant molecules A across the membrane. Several methods have been devised to determine the permeability coefficient of gases through membranes and, thus, a number of different units have been used to express the permeability coefficient. The permeability coefficient is expressed in units of Barrers, where 1 Barrer is $10^{-10} \cdot [\text{cm}^3 (\text{STP}) \cdot \text{cm}/\text{cm}^2 \cdot \text{s} \cdot \text{cmHg}]$.

The selectivity, $\alpha(A/B)$ or the so-called separation factor, of a dense polymer membrane between two penetrant gas molecules A and B is the ratio of the permeability coefficients of both penetrant gases. When the downstream pressure is negligible relative to the upstream pressure and when strong interactions between the polymer and both penetrant molecules are not observed, $\alpha(A/B)$ is almost equal to the “ideal” separation factor, $\alpha(A/B)^*$. This ideal separation factor can be decomposed into contributions of solubility selectivities (S_A/S_B) and diffusivity selectivities (D_A/D_B). Therefore,

$$\alpha = \frac{P_A}{P_B} = \left(\frac{D_A}{D_B} \right) \left(\frac{S_A}{S_B} \right)$$

The solubility selectivity (S_A/S_B) is determined primarily by the difference in inherent condensability between both penetrant molecules A and B and by their interactions with the membrane boundary. The diffusivity selectivity (D_A/D_B) is determined by the ability of the polymer matrix to function as size and shape selective media through segmental mobility and intersegmental packing factors. In the absence of strong polymer-penetrant interactions, the diffusivity selectivity tends to be the major factor in the separation process. For commonly available polymers, it has been found that the permeability

coefficient and the selectivity are interdependent. Higher gas permeability coefficients are usually accompanied by lower selectivities, and vice versa.

Usually the gas transport properties behavior is analyzed and correlated to the polymer properties such as glass transition temperature (T_g), d -spacing and fractional free volume (FFV). The d -spacing, the average distance between adjacent segmental backbones is determined by X-ray diffraction analysis and can be used as an index of “openness” of polymer matrix. The FFV takes into account the specific and occupied volumes and generally seems to give better representation of the “non-occupied space” in the polymer available for transport than does the d -spacing.

1.3.2.2 Aromatic polyesters for gas separation

A major objective in macromolecular science is to properly design and optimize the polymeric repeat unit, since this allows one to selectively tailor certain material properties. Gas permeation science investigates inter- and intra-chain interactions of the polymer with respect to penetration by gas molecules, and on the microscopic level it is a sensitive probe to slight modifications in molecular structure.

There is a general relationship reported in the literature that as the permeability of gas A increases, its selectivity decreases.¹⁹³ This behavior is easily understood if the matrix is capable of tightly packing since the free volume, or unoccupied space, is reduced thereby decreasing its ability to transport permeants. Concurrently, the same material shows an improved “sieving” or higher selecting ability between gases of different sizes, shapes and electronic environments. While this general trend is true of polyesters, as well as most other polymers, there is a continuing goal to synthesize materials which can simultaneously achieve both higher permeability and higher selectivity, or which can attain higher permeability with only a slight reduction in selectivity.

Several researchers have reported on the differences observed by the varying the monomer linkages from *meta* to *para*.¹⁹⁴⁻¹⁹⁷ It has been found that *meta*-catenation tends to decrease permeability and increase selectivity due to impeded intra- and inter-segmental motion. The gas permeabilities of various polyarylates have been studied by several researchers. The representative examples of polyesters used for gas separation are given in **Table 1.4**

Table 1.4: Representative examples of polyesters used for gas permeation measurements

No	Polyester	Reference
1		198
2	<p style="text-align: right;">$R = H/C(CH_3)_3$</p>	199
3	<p style="text-align: right;"> $R_1 = CH_3, R_2 = H$ $R_1 = R_2 = CH_3$ $R_1 = CH(CH_3)_2, R_2 = H$ $R_3 = H/C(CH_3)_3$ $R_1 = CH_3, R_2 = Br$ $R_1 = Br, R_2 = Br$ </p>	201
4	<p style="text-align: right;">$R_1 = H/Br, R_2 = H/C(CH_3)_3$</p>	199,200
5	<p style="text-align: right;">$R_1 = H/Br, R_2 = H/C(CH_3)_3$</p>	199,200
6		202
7	<p style="text-align: right;"> $R_1 = R_2 = H$ $R_1 = R_2 = Br$ $R_1 = CH_3, R_2 = H$ $R_1 = R_2 = Cl$ $R_1 = R_2 = CH_3$ $R_1 = CH_3, R_2 = Br$ </p>	203
8		204

In all above mentioned examples the permselectivities of isophthalic acid - based polyarylates are higher than terephthalic acid based ones.

1.5.3 Applications of polyarylates

Polyarylates are excellent in their UV stability and suggests utility in exterior glazing, solar energy collectors, transparent signs, automotive lenses, lighting housing, safety lamp housings, transparent lamp diffusers, traffic lights, etc. They find applications in the field of electronics as electrical connectors and capacitors. Additional suggested applications include bearings, bushings, heater element holders, high temperature valves, and ball joint seals in automotive industry.

The foregoing description reveals that polyimides and aromatic polyesters constitute an extremely promising examples of high performance polymers, which have been successfully put to use in many branches of emerging technologies where properties such as high heat resistance, mechanical strength, photostability, electrical insulation, barrier properties, etc. are needed.

The knowledge of characteristic features of the formation of polyimides and aromatic polyesters and the relation between their structure and properties has led to enormous prospects for specific design of the polymer chain and hence for imparting a set of desired properties to such polymers.

References

1. Bogert, M. T.; Renshaw, R. R. *J. Am. Chem. Soc.* **1908**, *30*, 1135.
2. Sroog, C. E.; Endrey, A. L.; Abramo, S. V.; Edwards C. E.; Olivier, K. L. *J. Polym. Sci.* **1965**, *3*, 1373
3. Sroog, C. E. *Prog. Polym. Sci.* **1991**, *16*, 561
4. *Polyimides: Synthesis, Characterization and Applications, Vols.1 and 2*, Mittal, K. L. (Ed.), Plenum Press: New York, 1984.
5. *Polyimides: Materials, Chemistry and Characterization*, Feger, C.; Khojasteh M. M.; McGrath, J. E. (Eds.), Elsevier:Amsterdam, 1989.
6. *Polyimides* Wilson, D.; Stenzenberger, H. D.; Hergenrother, P. (Eds.), Blackie & Sons Ltd.: Glasgow and London, 1990.
7. a) *Polyimides, Fundamentals and Applications*, Ghosh, M. K.; Mittal, K. L. (Eds.), Marcel Dekker: New York, 1996. b) *Thermally Stable Polymers*, Cassidy, P. E., Marcel Dekker: New York 1980. c) *High Performance Polymers: Their Origin and Developments* Seymour, R. B.; Krishenbaum, G. S., Elsevier: New York, 1986. d) Jaquiss, D. B. G.; Borman, W. F. H.; Campbell, R. W., *Encyclopedia of Chemical Technology* Grayson, M. (Ed.), John Wiley and Sons: New York ,1982. e) *Engineering Thermoplastics: Properties and Applications*, Margolis, J. M. (Ed.), Marcel Dekker Inc.: New York 1985.
8. Harris F. W. in *Polyimides*, Wilson, D.; Stenzenberger, H. D.; Hergenrother, P. M. (Eds.), Blackie & Sons Ltd.: Glasgow and London, 1990.
9. Takekoshi, T. in *Polyimides, Fundamentals and Applications*, Ghosh M. K.; Mittal, K.L. (Eds.), , Marcel Dekker: New York, 1996, p7.
10. Kim, Y. J.; Glass, T. E.; Lyle, G. D.; McGrath, J. E. *Macromolecules* **1993**, *26*, 1344
11. Zubkov, V. A.; Koton, M. M.; Kudryavtsev, V. V.; Svetlichnyi, V. M. *Zh. Org. Khim*, **1981**, *17*(8), 1501
12. Hodgkin, J. H. *J. Polym. Sci. Polym.Chem.* **1976**, *14*, 409.
13. Svetlichnyi, V. M.; Kalnins, K.; Kudryavtsev, V. V.; Koton, M. M. *Dokl. kad. Nauk SSSR (Engl. Transl.)* **1977**, *237*(3), 693.
14. Solomin, V. A.; Kardash, I. E.; Snagovskii, Yu. S.; Messerle, P. E.; Zhubanov, B. A.; Pravendnikov, A. N. *Dokl. Akad. Nauk SSSR (Engl. Transl.)* **1977**, *236*(1), 510.
15. Volksen, W. *Adv. Polym. Sci.* **1994**, *117*, 111.

16. Bessonov, M. I.; Koton, M. M.; Kudryavtsev, V. V.; Laius, L. A. in *Polyimides: Thermally Stable Polymers*, Plenum Press: New York, 1987.
17. Frost, L. W.; Kesse, I. *J. Appl. Polym. Sci.* **1964**, *8*, 1039.
18. Lavrov, S. V.; Ardashnikov, A. Ykardash, I. Y.; Pravednikov, A. N. *Polym. Sci. USSR(Engl. Transl.)*, **1977**, *19*, 1212
19. Lavrov, S. V.; Talankina, O. B.; Vorob'yev, V. D.; Izyumnikov, A. L.; Kardash, I. Y.; Pravednikov, A. N. *Polym. Sci. USSR (Engl. Transl.)*, **1980**, *22*, 2069.
20. Fjare, D. E.; Roginski, R. T. in *Advances in Polyimide Science and Technology*, Feger, C.; Khojasteh, M. M.; Htoo, M. S. (Eds.), Technomic: Lancaster, PA, **1993**, p326.
21. Dine-Hart, R.A.; Wright, W. W. *J. Appl. Polym. Sci.* **1967**, *11*, 609.
22. Laius, L. A.; Tsapovetskii, M. I. in *Polyimides: Synthesis, Characterization and Applications*, Mittal, K. L. (Ed.), Vol. 1, Plenum Press: New York, 1984, p1.
23. Young, P. R.; Davis, J. R.; Chang, A. C.; Richardson, J. N. *J. Polym. Sci. Polym.Chem.* **1990**, *28*, 3107.
24. Snyder, R. W.; Thomson, B.; Bartges, B.; Czerniowski, D.; Painter, P. C. *Macromolecules* **1989**, *22*, 4166.
25. Saini, A. K.; Carlin, C. M.; Patterson, H. H. *J. Polym. Sci. Polym.Chem.* **1992**, *30*, 419.
26. Saini, A. K.; Carlin, C. M.; Patterson, H. H. *J. Polym. Sci. Polym.Chem.* **1993**, *31*, 2751.
27. Kundryavsev, V. V.; Koton, M. M.; Meleshko, T. M.; Skilzkova, V. P. *Vysokomol. Soedin.* **1975**, *A17*, 1764.
28. Schulze, T.; Saini, A. K.; Labreque, D.; Patterson, H. H. *J. Mater. Sci.* **1997**, *A34*, 1535.
29. Vinogradova, S. V.; Vygodskii, Ya. S.; Vorob'ev, V. D.; Churochkina, N. A.; Chudina, L. I.; Spirina, T. N.; Korshak, V. V. *Polym. Sci. USSR (Engl. Transl.)*. **1974**, *16*, 584.
30. Ranney, M. W. in *Polyimide Manufacture*, Noyes Data Corp., Park Ridge, NJ, 1971.
31. Hoogewerff, S.; Van Dorp, W.A. *Rec. Trav. Chem*, **1986**, *13*, 93.

32. Angelo, R. J.; Golike, R. C.; Tatum, W. E.; Kreuz, J. A. in *Advances in Polyimide Science and Technology*, Weber, W. D.; Gupta, M. R. (Eds.), *Plast. Eng.*, Brookfield, CT, 1985, p67.
33. Koton, M. M.; Meleshko, T. K.; Duryavtsev, V. V.; Nechayev, P. P.; Kamzolkina, Ye. V.; Bogorad, N. N. *Polym. Sci. USSR (Engl. Transl.)*, **1982**, *24*, 791.
34. Riderick, W. R. *J. Am. Chem. Soc.* **1957**, *79*, 1710.
35. Koton, M. M.; Kudryavtsev, V. V.; Zubkov, V. A.; Yakimanskii, A. V.; Meleshko, T. K.; Bogorad, N. N. *Polym. Sci. USSR (Engl. Transl.)*, **1984**, *26*, 2839.
36. Riderick, W. R. *J. Org. Chem.*, **1964**, *29*, 745.
37. Wallach, M. L. *J. Polym. Sci. Part A-2* **1969**, *7*, 1995.
38. Snyder, R. W.; Thomson, B.; Bartges, B.; Czerniowski, D.; Painter, P. C. *Macromolecules* **1989**, *22*, 4166.
39. McGrath, J. E.; Grubbs, H.; Rogers, M. E.; Güngör, A.; Joseph, W. A.; Mercier, R.; Rodrigues, D.; Wilkes, G. L.; Brennan, A. *Int. SAMPE Tech. Conf.* **1991**, *23*, 119.
40. Arnold, C. A.; Summers, J. D.; Chen, Y. P.; Bott, R. H.; Chen, D.; McGrath, J. E. *Polymer* **1989**, *30*, 986.
41. Yilmaz, T.; Güçlü, H.; Özarslan, Ö.; Yidiz, E.; Kuyulu, A.; Ekinçi, E.; Güngör, A.; *J. Polym. Sci. Polym. Chem.* **1997**, *35*, 2981.
42. Harris, F. W.; Hsu, S. L.-C. *High Perf. Polym.* **1989**, *1*, 3.
43. Summers, J. D.; Arnold, C. A.; Bott, R. H.; Taylor, L. T.; Ward, T. C.; McGrath, J. E. *Int. SAMPE Symp. Exhib.* **1987**, *32*, 613.
44. Arnold, C. A.; Rogers, M. E.; Smith, C. D.; Lyle, G. D.; York, G. A.; Jurek, M. J.; McGrath, J. E. *Int. SAMPE Symp. Exhib.* **1989**, *34*, 1255.
45. Takekoshi, T.; Kochanowski, J. E.; Manello, J. S.; Webber, M. J. *J. Polym. Sci. Polym. Lett.* **1986**, *74*, 93.
46. Sonnett, J. M.; Gannett, T. P. in *Polyimides, Fundamentals and Applications*, Ghosh, M.K.; Mittal, K. L. (Eds.), Marcel Dekker: New York, 1996, p151.
47. Gerashchenko, Z. V.; Vygodskii, Ya. S.; Slonimskii, G. L.; Askadskii, A. A.; Papkov, V. S.; Vinogradova, S. V.; Dashevskii, V. G.; Klimova, V. A.; Sherman, F. B.; Korshak, V. V. *Polym. Sci. USSR (Engl. Transl.)* **1973**, *15*, 1927.

48. Solomin, V. A.; Kardash, I. E.; Snagovskii, Yu. S.; Messerle, P. E.; Zhubanov, B. A.; Pravendnikov, A. N. *Dokl. Akad. Nauk USSR (Engl. Transl.)*, **1977**, 236(1), 510.
49. Lavrov, S. V.; Ardashnikov, A. Ya.; Kardash, I. Ye., Pravendnikov, A. N. *Polym. Sci. USSR (Engl. Transl.)* **1977**, 19, 1212.
50. Kreuz, J. A.; Endrey, A. L.; Gay, F. P.; Sroog, C. E. *J. Polym. Sci. Polym. Chem.* **1966**, 4, 2607.
51. White, D. M.; Keyes, D. G. U. S. Patent Number 4,324,884, (to General Electric Co.), 1982.
52. White, D. M.; Keyes, D. G. U. S. Patent Number 4,324,885, (to General Electric Co.), 1982.
53. White, D. M.; Keyes, D. G., U. S. Patent Number 4,330,666, (to General Electric Co.), 1982.
54. Oishi, Y. ; Ishida, M.; Kakimoto, M.-A. ; Imai, Y.; Kurosaki, T. *J. Polym. Sci. Polym. Chem.* **1992**, 30, 1027.
55. Schmidt, L. R.; Lovgren, E. M.; Meissner, P. G. *Int. Polym. Process*, **1989**, 4, 270.
56. Hasegawa, M.; Shindo, Y.; Sugimura, T.; Horie, K.; Yokota, R.; Mita, I. *J. Polym. Sci. Polym. Chem.* **1991**, 29, 1515.
57. Mochizuki, A.; Teranishi, T.; Ueda, M. *Polymer J.* **1994**, 26, 315.
58. Wallace, J. S.; Arnold, F. E.; Tan, L. S. *Polym. Prepr.* **1987**, 28(2), 316.
59. William, E. T. U. S. Patent Number 3,261,811, (to Du Pont Co.), 1966.
60. Tan, L.; Arnold, F. E. *Polym. Prepr.* **1988**, 29(2), 316.
61. Delvigis, P.; Hsu, L. C. ; Serafini, T. T. *J. Polym. Sci. Polym. Lett.* **1970**, 8, 29.
62. Moy, T. M.; DePorter, C. D.; McGrath, J. E. *Polymer* **1993**, 34, 819.
63. Moy, T. M. *Ph.D. Dissertation*, Virginia Tech, 1993.
64. Johnston, J. C.; Meador, M. A. B.; Alston, W. B. *J. Polym. Sci. Polym. Chem.* **1987**, 25, 2175.
65. Sato, M. in *Handbook of Thermoplastics*, O. Olabisi, (Ed.), Marcel Dekker: New York, 1997, p 665.
66. Hurd, C. D.; Prapas, A. G. *J. Org. Chem.* **1959**, 24, 388.
67. Farrissey, W.J.; Rose, J.S.; Carleton, P.S. *J. Appl. Polym. Sci.* **1970**, 14, 1093.
68. Carleton, P.S.; Farrissey, W.J.; Rose, J.S. *J. Appl. Polym. Sci.* **1972**, 16, 2983.
69. Alvino, W.M.; Edelman, L.E. *J. Appl. Polym. Sci.* **1975**, 19, 2961.

70. Alvino, W.M.; Edelman, L.E. *J. Appl. Polym. Sci.* **1978**, *22*, 1983.
71. Ghatge, N.D.; Mulik, U.P. *J. Polym. Sci. Polym. Chem.* **1980**, *18*, 1905.
72. Shinde, B.M.; Ghatge, N.D.; Patil, N.J. *J. Appl. Polym. Sci.* **1985**, *30*, 3505.
73. Wenzel, M.; Ballauff, M.; Wegner, G. *Makromol. Chem.* **1987**, *188*, 2865.
74. Helmer-Metzmann, F.; Ballauff, M.; Schulz, R.C.; Wegner, G. *Makromol. Chem.* **1989**, *190*, 985.
75. Kakimoto, M.-A.; Akiyama, R.; Negi, Y.S.; Imai, Y. *J. Polym. Sci. Polym. Chem.* **1988**, *26*, 99.
76. Sendijarevic, A.; Sendijarevic, V.; Frisch, K.C. *J. Polym. Sci. Polym. Chem.* **1990**, *28*, 3603.
77. Avadhani, C.V.; Wadgaonkar, P.P.; Vernekar, S.P. *J. Polym. Sci. Polym. Chem.* **1990**, *28*, 1681.
78. Kilic, S.; Mohanty, D.K.; Yilgor, I.; McGrath, J.E. *Polym. Prepr.* **1986**, *27*(1), 318.
79. Volksen, W. *Adv. Polym. Sci.* **1994**, *117*, 111.
80. Iyer, N. P.; Radhakrishnan, G. *Polym. Int.* 2000, *49*, 546.
81. Attwood, T. A.; Dawson, P. C.; Freeman, J. L.; Hoy, L.R. J.; Rose, J. B.; Staniland, P. A. *Polymer* **1981**, *22*, 1096.
82. Johnson, R. N.; Farnham, A. G.; Clendinning, R. A.; Hale, W. F.; Merriam, C. N. *J. Polym. Sci. Polym. Chem.* **1967**, *5*, 2375.
83. Wirth, J. G.; Health, D. R. U. S. Patent Number 3,787,364, (to General Electric Co.), 1974.
84. Williams, F. J. U. S. Patent Number 3,847,869, (to General Electric Co.), 1974.
85. Wirth, J. G.; Health, D. R. U. S. Patent Number 3,838,097, (to General Electric Co.), 1974.
86. Takekoshi, T.; Wirth, J. G.; Health, D. R.; Kochanowski, J. E.; Manello, J. S.; Webber, M. J. *J. Polym. Sci. Polym. Chem.* **1980**, *18*, 3069.
87. Takekoshi, T. in *Polyimides*, Wilson, D.; Stenzenberger, H. D.; Hergenrother, P. M. (Eds.), Blackie & Sons Ltd.: Glasgow and London, 1990, p38.
88. Volksen, W.; Hofer, D.; Cheng, Y.Y.; *Polyimides and Other High-Temperature Polymers*, Abadie, M.J.M.; Sillon, B. (Eds.), Elsevier: Amsterdam, 1991, p 45.
89. Becker, K.H.; Schmidt, H.W., *Macromolecules* **1992**, *25*, 6784.
90. Stoffel, N.C.; Kramer, E.J.; Volksen, W.; Russel, T.P.; *Polymer* **1993**, *34*, 4524.

91. Stoffel, N.C.; Kramer, E.J.; Volksen, W.; Russel, T.P.; *J. Polym. Sci. Polym. Phys.* **1998**, *36*, 2247.
92. Carter, K.R.; DiPietro, R.A.; Sanchez, M.I.; Russell, T.P.; Lakshmanan, P.; McGrath, J.E.; *Chem. Mater.* **1997**, *9*, 105.
93. Boldebeck, E.M.; Klebe, J.F., US Patent Number 3,303,157, 1967.
94. Korshak, V.V., Vinogradova, S.V.; Vygodskii, Ya.S.; Nagiev, Z.M.; Urman, Ya.G.; Alekseeva, S.G.; Slonium, I.Ya.; *Makromol. Chem.* **1983**, *184*, 235.
95. Yoda, N.; Hiramoto, H., *J. Macromol. Sci. Chem. Phys.* **1984**, *A21* (13&14), 1641.
96. Facinelli, J.V.; Gardner, S.L.; Dong, L.; Sensenich, C.L.; Davis, R.M.; Riffle, J.S. *Macromolecules* **1996**, *29*, 7342.
97. Kuramoto, N.; Hayashi, K.; Nagai, K. *J. Polym. Sci. Polym. Chem.* **1994**, *32*, 2501.
98. Alhakimi, G.; Klemm, E. *J. Polym. Sci. Polym. Chem.* **1995**, *33*, 767.
99. Alhakimi, G.; Klemm, E.; Gorus, H. *J. Polym. Sci. Polym. Chem.* **1995**, *33*, 1133.
100. Cella, J.A.; Grade, M.M.; Nye, S.A.; Valkenburgh, V.M.; Wengrovius, J.H. *Macromolecules* **1992**, *25*, 6355.
101. Kurmanaliev, M.; Ergozhin, E.E.; Izteleuova, I.K. *Makromol. Chem.* **1993**, *194*, 2655.
102. Laurienzo, P.; Malinconico, M.; Perenze, N.; Segre, A.L. *Macromol. Chem. Phys.* **1994**, *195*, 3057.
103. Perry, R. J., Ternner, S. R. *J. Org. Chem.* **1991**, *56*, 6573.
104. Perry, R. J., Ternner, S. R. *J. Macromol. Sci. Chem.* **1991**, *A 28*, 1213.
105. a) Helmer-Metzmann, F.; Rehahn, M.; Schmitz, L.; Ballauff, M.; Wegner, G. *Makromol. Chem.* **1992**, *193*, 1847. b) Schmitz, L.; Rehahn, M.; Ballauff, M. *Polymer* **1993**, *34*, 646. c) Perry, R. J., Tunney, S. E., Wilson, B. D. *Macromolecules* **1996**, *29*, 1014.
106. a) Gao, C.; Zhang, S.; Gao, L.; Ding, M. *Macromolecules* **2003**, *36*, 5559. b) Gao, C.; Wu, X.; Lv, G; Ding, M.; Gao, L. *Macromolecules* **2004**, *37*, 2754
107. a) Salem, J. R.; Sequeda, F.O.; Duran, J.; Lee, W.Y.; Yang, R.M. *J. Vac. Sci. Technol* **1986**, *A4*, 369. b) Roberts, C.C.; Letts, S.A.; Saculla, M.D.; Hsieh, E.J.; Cook, R.C. *Fusion Technol.* **1999**, *35*, 138. c) Alfonso, E.L.; Tsai, F.Y.; Chen, S.H.; Gram, R.Q.; Harding, D.R. *Fusion Technol.* **1999**, *35*, 131.

108. a) Edwards, W.M.; Robinson, I. M. U. S. Patent Number 2,710,853, 1955. b) Inoue, T.; Kumagai, Y.; Kakimoto, M.; Imai, Y.; Watanabe, J. *Macromolecules* **1997**, 30, 1921.
109. a) Chiefari, J.; Dao, B.; Groth, A.M.; Hodgkin, J.H. *High Perf. Poly.* **2006**, 18, 31. b) Kreuz, J.A.; Endrey, A.L.; Gay, F.P.; Sroog, C.E. *J. Polym. Sci. Polym.Chem.* **1966**, 4, 2607. c) Imai, Y.; Fueki, T.; Inoue, T.; Kakimoto, M. *J. Polym. Sci. Polym. Chem.* **1998**, 36, 2663.
110. Van Krevelen, D.W. *Properties of Polymers: Their Estimation and Correlation with Chemical Structure*; Elsevier: 1976, p111.
111. a) de Abajo, J.; de la Campa, J.G. *Adv. Polym. Sci.* **1999**, 140, 23. b) Sillion, B. in *Comprehensive Polymer Science, Vol. 5*, Eastmond, G.C.; Ledwith, A.; Russo, S.; Sigwalt, P. (Eds.), Pergamon Press, New York: 1989, p 499. c) Chung, T.-S.; Pan, J.; Liu, S.L.; Mullick, S.; Vora, R.H. in *Advanced Functional Molecules and Polymers, Vol. 4, Physical Properties and Applications*, Nalwa, H.S. (Ed.), Gordon and Breach Science Publishers, 2001, p 157.
112. a) Sillion, B.; Rabilloud, G. in *New Methods in Polymer Synthesis, Vol. 2*, Ebdon, J.R.; Eastmond, G.C. (Eds.), Blackie, London, **1995**. b) Brandom, D.K.; Desoura, J.P.; Baird, D.J.; Wilkes, G.L. *J. Appl. Polym. Sci.* **1997**, 66, 1543. c) Imai, Y. *Adv. Polym. Sci.* **1999**, 140, 1. d) Malinge, J.; Garapon, J; Sillion, B. *Br. Polym. J.* **1988**, 20, 431. e) Liaw, D.J.; Liaw, B.-Y.; Li, L.-J; Sillion B.; Mercier, R.; Thiria, R. *Chem. Mat.* **1998**, 10, 734
113. a) Saint, A.K.; Slem, W.S. *SAMPE J.* **1985**, 21, 28. b) Han, K.; Lee, H.J.; Rhee T.H. *J. Appl. Polym. Sci.* **2000**, 74, 107. c) Li, B.; Prexta, L.A.; Zhihao, S.; Cheng, Z.D. *Polym. Prep.* **1996**, 41, 105. d) Liaw, D.J.; Liaw, B. Y. *Polymer.* **1999**. 40, 3183. e) Volsken, W.; Cha, H.J.; Sanchez, M.I.; Yoon, D.Y. *React. Funct. Polym.* **1996**, 30, 61. f) Suzuki, H.; Abe, K.; Takaishi, M. Narita.; Hamada, I. *J. Polym. Sci.Polym. Chem.* **2000**, 38, 108. g) Ichino, T.; Suzuki, S.; Matsuura, T.; Nishi, S.; *J. Polym. Sci. Polym. Chem.* **1990**, 28, 323. h) Auman, B.C.; Myers, T.L.; Higley, D.P. *J. Polym. Sci., Part A: Polym. Chem.* **1997**, 35, 2441.
114. Morozumi, S. in *Liquid Crystals: Applications and Uses*, Bahadar, D. (Ed.); World Scientific: London 1990, chap 7.
115. Mauain, C. *Bull. Soc. Fr. Miner.* **1911**, 34, 71.
116. Berreman, D. W. *Phys. Rev. Lett.* **1984**, 45, 1021.

- 117 Uchida, T. *Mol. Cryst. Liq. Cryst.* **1985**, *123*, 15.
- 118 Wang, H. *Ph.D. Dissertation*; UMI No. 9925168, The University of Akron, USA, 1999.
- 119 Auman, B. C.; Bohm, E. U.S. Patent Number 5,731,404, 1998.
120. Nozaki, C.; Imamara, N.; Sano, Y. *Jpn. J. Appl. Phys.* **1993**, *32*, 4352.
121. Liu, J.; Wana, Q.; Zha, P.; Li, Z. *Hebei Gonaye Daxue Xuebao* **1998**, *27*, 15.
122. Yokokura, H.; Oh-E., M.; Kondo, K.; Oh-Hara, S. *Mol. Cryst. Liq. Cryst.* **1993**, 253.
123. Lee, K.-W.; Peak, S. H.; Lien, A.; Daring, C.; Fakuro, H. *Macromolecules* **1996**, *29*, 8894.
124. Fshibashi, S.; Hirayama, M.; Matsuura, T. *Mol. Cryst. Liq. Cryst.* **1973**, *99*, 225.
125. Hwana, J. Y.; Li, J. S.; Juana, Y. S.; Chen, S. H. *Jpn. J. Appl. Phys.* **1995**, *34*, 3163.
126. Seo, D.-S.; Araya, K.; Yoshida, N.; Nishikawa, M.; Yabe, Y.; Kobayashi, S. *Jpn. J. Appl. Phys.* **1995**, *34*, L503.
127. Kim, S. I.; Ree, M.; Shin, T. J.; Jana, J. C. *J. Polym. Sci. Polym. Chem.* **1999**, *37*, 2909.
128. Ge, J.J.; Li, C.Y.; Xue, G.; Mann, I.K.; Zhang, D.; Wang, S.-Y.; Harris, F.W.; Chang, S.Z.D.; Hong, S.-C.; Zhuang, X.; Shen, Y.R. *J. Am. Chem. Soc.* **2001**, *123*, 5768.
129. Zhang, W.; Xu, H.-J.; Yin, J.; Guo, X.-X.; Ye, Y.-F.; Fang, J.-H.; Sui, Y.; Zhu, Z.-K. *J. Appl. Polym. Sci.* **2001**, *81*, 2814.
130. Li, L.; Yin, J.; Sui, Y.; Xu, H.-J.; Fang, J.-H.; Zhu, Z.-K.; Wang, Z.-G. *J. Polym. Sci. Polym. Chem.* **2000**, *38*, 1943.
131. Kim, D. H.; Jung, J. C. *Polym. Bull.* **2003**, *50*, 311.
132. Lee, S. W.; Chae, B.; Lee, B.; Choi, W.; Kim, S. B.; Kim, S. I.; Park, S.-M.; Jung, J. C.; Lee, K. H.; Ree, M. *Chem. Mater.* **2003**, *15*, 3105.
133. Shizuo, M.; Kenji, F.; Minoru, N.; Ryuji, K. EP 0389092 B1, (1994).
134. Lee, S. J.; Jung, J.C.; Lee, S.W.; Ree, M. *J. Polym. Sci. Polym. Chem.* **2004**, *42*, 3130.
135. Wong, C.P. *Mater. Chem. Phys.* **1995**, *42*, 25.
136. Bluestein, S.D.; Bramono, D.P.Y.; Miaoulis, I.N.; Wong, P.Y. *Mater. Res. Soc. Symp.Proc.* **1997**, *445*, 185.

137. Clearfield, H.M.; Furman, B.K.; Callegari, A.; Graham, T.; Purushothaman, S.; *Mater. Res. Soc. Symp. Proc.* **1994**, 323, 321.
138. Malba, V.; Liberman, V.; Berhardt, A.F.; *J. Vac. Sci. Technol.* **1997**, A 15(3), 844.
139. *Polymers in Microlithography: Materials and Processes*, Reichmanis, E.; MacDonald, S.A.; Iwayanagi, T. (Eds.), ACS Symp. Ser. (1989).
140. Jensen, R.J. in *Polyimides as Interlayer Dielectrics for High-Performance Interconnections of Integrated Circuits*, in *Polymers for High Technology: Electronics and Photonics*, Bowden, M.J.; Turner, S.R. (Eds.), 1987, p 466.
141. Senturia, S.D. *Polyimides in Microelectronics*, in *Polymers for High Technology: Electronics and Photonics*, Bowden, M.J.; Turner, S.R. (Eds.), 1987, p 428.
142. *Introduction to Microlithography*, Thompson, L.F.; Wilson, C.G.; Bowden, M.J. (Eds.), ACS Symp. Ser. 219, 1983.
143. Brown, H.R.; Yang, A.C.M.; Russell, T.P.; Volksen, W.; Kramer, E.J. *Polymer* **1988** 29, 1807.
144. Conix, A. J. *Ind. Chim. Belg.* **1957**, 22, 1457.
145. Korshak, V. V. *The Chemical Structure and Thermal Characterization of Polymers*, Israel Program for Scientific Translations, Keter, London, 1971.
146. a) Eareckson, W.H., *J. Polym. Sci. Polym. Chem.* **1959**, 40, 399. b) Vinogradova, S.V.; Vasnev, V.A.; Valetskii, P.M. *Russ. Chem. Rev.* **1994**, 63, 833. c) Villegas-Coss, I.; Ruiz-Trivino, F.A.; Hernandez-Loez, S. *J. Polym. Sci. Polym. Phys.* **2006**, 44, 256. d) Bucio, E.; Lara-Estevez, J.C.I.; Ruiz-Trivino, F.A.; Acosta-Huerta, A. *Polym. Bull.* **2006**, 56, 163. e) Bucio, E.; Fitch, J.W.; Venumbaka, S.R.; Cassidy, P.E. *Polymer* **2005**, 46, 3971.
147. a) Starks, C.M. *J. Am. Chem. Soc.* **1971**, 93, 195. b) Temin, S.C. in *Interfacial Synthesis*, Vol II: *Polymer Applications and Technology*, Millich, F.; Carraher, C.E.J. (Eds.), Marcel Dekker, New York, **1977**. c) Tsai, H.B.; Lee, Y.D. *J. Polym. Sci. Polym. Chem.* **1987**, 25, 2195. d) Wang, C. Y.; Wang, D.C.; Chiu, W.Y.; Chen, L.W. *Angew. Makromol. Chem.* **1997**, 248, 123.
148. Starks, C.M.; Liotta, C. *Phase Transfer Catalysts, Principles and Techniques*, Academic Press: New York, 1978. b) Sokolov, L.B. *Polymer Sci. USSR*, **1970**, 12, 1097. c) Borissov, G.; Sivriev, H. *Makromol. Chem.* **1972**, 158, 215
149. Freitag, D.; Bottenbruch, L.; Hucks, U. U.S. Patent Number 4,617,368, 1986 (to Bayer A.G.).

150. a) Kwolek, S.W.; Morgan, P.W. *J. Polym. Sci. Polym. Phys.* **1964**, 2, 2693. b) Vasnes, V.A.; Ignatov, V.N.; Vinogradova, S.V.; Tseitlin, H.M. *Makromol. Chem.* **1990**, 191, 1759. c) Vasnev, V.A.; Vinogradova, S.V. *Russ. Chem. Rev.* 1979, 48, 16.
151. Korkshak, V.V.; Vinogradova, S.V.; Lebedeva, A.S. *Vysokomol. Soedin Ser. A.* **1960**, 2, 1162.
152. Magat, E. E.; Strachen, D.R. U.S. Patent Number 2,708,617, 1955, (to Dupont Co.).
153. Turska, E.; Pietrzak, L.; Jantas, R. *J. Appl. Polym. Sci.* **1979**, 23, 2409.
154. Jeong, H.-J.; Iwasaki, K. M.; Kakimoto, M.-A.; Imai, Y. *Polym. J.* **1994**, 26, 379.
155. Korkshak, V.V.; Vinogradova, S.V. and Lebedeva, A.S., *Vysokomol. Soedin. Ser. A*, **1959**, 1, 1482.
156. Heck, M.H., U.S. Patent Number 3,133,898, 1964, (to Good Year Tyre and Rubber Co.).
157. Blaschke, F.; Ludwing, W. U.S. Patent Number 3,395,119, 1968.
158. Schnell, H.; Boilert, V.; Fritz, G. U.S. Patent Number 3,335,167, 1971, (to Farbenfabriken Bayer).
159. Eise, K.; Friedrich, R.; Goemar, H.; Schade, G.; Wolfes, W. Ger. Pat. 2,232,877, 1974 (to Werner Pffeidereer and Dynamit Nobel A. G.).
160. Inata, H.; Kawase, S.; Shima, T. U. S. Patent Number 3,972,852, 1974 (to Teijin Ltd.)
161. Kosanovich, G. M.; Salee, G. U. S. Patent Number 4,465,819, 1984, (to Occidental Chemical Corp.).
162. Levine, M.; Temin, S. C. *J. Polym. Sci. Polym. Chem.* **1958**, 28, 179.
163. Riecke, E. E.; Hamb, F. L. *J. Polym. Sci. Polym. Chem.* **1977**, 15, 593.
164. Chung, T. S. *Polym. Eng. Sci.* **1986**, 26, 901.
165. Bier, G., *Polymer* **1974**, 15, 527.
166. Peter, T.; Ludwing, B.; Josef, B. H.; Ulrich, G.; Wolfgang, A. Ger. Pat. 3,824,069 (Bayer A. G.).
167. Mahajan, S. S.; Idage, B. B.; Chavan, N. N.; Sivaram, S. *J. Appl. Polym. Sci.* **1996**, 61, 2297.
168. Kricheldorf, H. R.; Schwarz, G. *Polym. Bull.* **1979**, 1, 383.
169. Kricheldorf, H. R.; Zang, Q. Z.; Schwarz, G. *Polymer* **1982**, 23, 1821.
170. Kricheldorf, H. R. and Schwarz, G., *Makromol. Chem.* **1983**, 184, 475.

171. Thames, S. F.; Malone, K. G. *J. Polym. Sci. Polym. Chem.* **1993**, *31*, 521.
172. Higashi, F. *Polym. Appl. (Jpn.)* **1984**, *33*, 171.
173. Kajiyama K.; Hayama, K.; Morito, N.; Wayo, J.; Daigaku. K. *Kaseikei-hen.* **1995**, *35*, 125, (Japan) Chem. Abstract: 124: 290425k (1996).
174. Kitayama, S.; Sanui-K.; Ogata, N. *J. Polym. Sci. Polym. Chem.* **1984**, *22*, 2705.
175. Higashi, F.; Akiyama, N.; Koyama, T. *J. Polym. Sci. Polym. Chem.* **1983**, *21*, 3233.
176. Higashi, F.; Hoshio, A.; Kiyoshige, J. *J. Polym. Sci. Polym. Chem.* **1983**, *21*, 3241.
177. Higashi, F.; Hoshio, A.; Yamada, Y.; Ozawam, M. *J. Polym. Sci. Polym. Chem.* **1985**, *23*, 69.
178. Higashi, F.; Fujiwara, Y.; Yamada, Y. *J. Polym. Sci. Polym. Chem.* **1986**, *24*, 589.
179. Higashi, F.; Mashimo, T. and Takahashi, I. *J. Polym. Sci. Polym. Chem.* **1986**, *24*, 97.
180. Liaw, D. J. *J. Polym. Sci. Polym. Chem.* **1995**, *33*, 605.
181. Matsukawa, K.; Inoue, H. *J. Polym. Sci. Polym. Lett.* **1990**, *28*, 13.
182. Schenberg, A.; Bartoletti, I.; Heck, R. F. *J. Org. Chem.* **1974**, *39*, 3318.
183. Stille, J. K.; Wang, P. K. *J. Org. Chem.* **1975**, *40*, 532.
184. Yoneyama, M.; Kakimoto, M.-A.; Imai, Y. *Macromolecules* **1989**, *22*, 2293.
185. Jun, C. L.; Park, N. J.; *Pollimo*, **1995**, *19* (5), 676 ,(Korean), Chem. Abstr.: 124:88036d (1996).
186. Mitchel, J.K.; *Philadelphia J. Med. Sci.* **1831**, *13*, 36.
187. Graham, T. *Philos. Mag.* **1866**, *32*, 401.
188. Berch, D.W. *Zeolite Molecular Seives*, John Wiley and Sons: NewYork, 1974.
189. Koros, W.J.; Chern, R.T. *Handbook of Separation Process Technology*, Rousseau, R.W. (Ed.), 1987.
190. Kestina, R.G.; Fritzsche, A.K. *Polymer Gas Separation Membranes*, John Wiley and Sons: NewYork, 1993.
191. Koros, W.J.; Hellums, M.W. in *Encyclopaedia of Polymer Science and Engineering*, Suppl. Vol., 2nd Ed., John Wliey And Sons: NewYork, **1989**.
192. Walker, D.R.B.; Koros, W.J. *J. Memb. Sci.* **1993**, *55*, 99.
193. Koros, W.J.; Fleming, G.K. *J. Memb. Sci.* **1993**, *83*, 1.
194. Coleman, M.R.; Koros, W.J. *J. Memb. Sci.* **1990**, *50*, 2285.
195. Matsumoto, K.; Xu, P. *J. Memb. Sci.* **1993**, *81*, 23.

196. Kawakami, H.; Ansai, J.; Nagaoka, S. *J. Appl. Polym. Sci.* **1995**, *57*, 789.
197. Stern, S.A.; Mi, Y.; Yamamoto, H.; St. Clair, A.K. *J. Polym. Sci. Polym. Phys.* **1989**, *27*, 1887.
198. Pessan, L.A.; Koros, W.J. *J. Polym. Sci. Polym. Phys.* **1993**, *31*, 1245.
199. Pixton, M.R.; Paul, D.R. *J. Polym. Sci. Polym. Phys.* **1995**, *33*, 1135.
200. Pixton, M.R.; Paul, D.R. *J. Polym. Sci. Polym. Phys.* **1995**, *33*, 1353.
201. Pixton, M.R.; Paul, D.R. *Macromolecules* **1995**, *28*, 8277.
202. Kharul, U.K.; Kulkarni, S.S. *Bull. Mater. Sci.* **1994**, *17*(6), 1071.
203. Jager, J.; Hendriks, J.J. *J. Appl. Polym. Sci.* **1995**, *58*, 1465.
204. Sheu, F.R.; Chern, R.T. *J. Polym. Sci. Polym. Phys.* **1989**, *27*, 1121

Chapter 2. Scope and Objectives

From the time of Carothers to the present, the chemistry of step-growth polymerization has been constantly dominated by the synthetic organic chemist's viewpoint, whose focus is the synthesis of new polymer materials. This is probably one of the points that contrast it the most with the chemistry of the polymerization of unsaturated monomers, where physical chemists have played a much more substantial role. The fact that the chemistry of step-growth polymerization has long been the province of synthetic organic chemists is not difficult to explain. On the one hand, condensation reactions are among the most classic and most thoroughly investigated reactions in organic chemistry, and it so happens that polycondensation simply involves stepwise condensation reactions of difunctional monomers. On the other hand, the temptations have been strong for organic chemists to design new polymers by assembling various organic compounds to see what they would be.

Step-growth polymerization continues to receive intense academic and industrial attention for the preparation of polymeric materials used in a vast array of applications. In recent years much of the focus in step-growth polymers has been in the area of high performance polymers. High performance / high temperature polymers such as polyimides, polyamides, polyesters, etc. are of considerable interest because of their excellent mechanical and high-temperature properties.¹⁻⁸ A large number of high performance polymers have been synthesized in the academic and industrial research laboratories. However, most of them usually exhibit very low solubilities and melting points far above their thermal decomposition temperatures, which limits their widespread applications. There are several reports describing approaches to improve the processability of high performance/ high temperature polymers by making use of structurally modified monomers.⁹⁻²⁰ These approaches include (1) introduction of flexible segments or groups into the polymer backbone which reduces chain stiffness, (2) introduction of bulky side groups which help in the separation of polymer chains and hinder the molecular packing and crystallization, (3) use of enlarged monomers containing angular bonds which suppress coplanar structures, (4) use of 1,3-disubstituted monomers instead of

1,4-disubstituted ones, and / or asymmetric monomers which lower regularity and molecular ordering, and (5) attachment of flexible chains as pendant groups.

Using the above-mentioned chemical functions, a wide variety of monomers have been prepared and used to synthesize processable high performance polymers. The development of high performance / high temperature polymers either matching different processability requirements or exhibiting new, specific properties is the driving force for the research in new monomers. The research efforts during the last three decades to develop new monomers has enriched the chemistry of high performance polymers to such an extent that it would be difficult to find another field of macromolecular chemistry where the investigations have produced a similar variety of new species with wide range of properties.

It is reported that the use monomers that bear pendent flexible groups greatly reduces strong molecular interactions of stiff-chain aromatic polymers, producing an effective chain separation effect. In general, such pendent groups not only bring about improved solubility but also help lower the melting and glass transition temperatures *via* “internal plasticization”.^{14,18}

The introduction of bulky “cardo” groups is known to reduce the strong molecular interaction of stiff-chain aromatic polymers, producing an effective chain separation effect and lowering the cohesive energy density, thereby improving the solubility of these polymers. Additionally, the presence of bulky “cardo” group causes the lowering of polymer chain’s torsional mobility and generally an increment of the glass transition temperature.^{4,10,11,16,19-25}

Thus, our synthetic research effort was directed towards structural modifications designed to disturb regularity and chain packing thus providing better processability / solubility to the polymers. The major goal of the present research was to improve polymer processability and towards this goal two approaches were investigated. The first approach involves improving polymer processability *via* internal plasticization, whereas, second approach involves improvement of polymer solubility by incorporation of bulky “cardo” groups.

Plasticization normally involves the incorporation of a low molecular weight plasticizer, which improves polymer flow and processability. In internal plasticization, the plasticizer is chemically attached to or incorporated in the polymer backbone.²⁶⁻²⁹

It was of interest to design and synthesize new monomers containing flexible alkyl chain or bulky “cardo” group starting from cheap, commercially available raw materials. Cashew nut shell liquid (CNSL), a renewable resource material, contains compounds having 15 carbon alkyl /alkenyl chain, which are useful in various aspects of chemical industry.³⁰⁻³³ The 15 carbon chain could be exploited for the internal plasticization. *p*-Cumylphenol, a cheap raw material used as endcapping agent for polycarbonate resins³⁴ can be used to synthesize bulky "cardo" group containing monomers.

The first objective of this research was to develop a synthetic scheme that would allow the introduction of pendant pentadecyl chain as plasticizing group or bulky “cardo” group into the high performance polymers such as polyimides and polyesters. The approach involved synthesis of bisphenol and diamine containing pendant pentadecyl chain starting from CNSL and bisphenols and diamines containing bulky “cardo” group starting from *p*-cumylphenol. By relatively easy and inexpensive chemical routes, these monomers could be prepared that provide the structural characteristics needed for the improvement of processability.

The second objective of this research was to synthesize and characterize polyimides and polyesters containing pendant pentadecyl chain or bulky “cardo” group. In order to investigate the effect of incorporation of pendant pentadecyl chain on the properties of polymers, properties, such as solubility, thermal transitions and heat resistance were evaluated and compared with control polymers without alkyl or “cardo” groups. For this study, polymers such as polyimides and polyesters were synthesized and characterized, thus, permitting the establishment of a reliable structure-property relationship.

It is well known that polymer solubility and in-turn processability can be improved *via* copolymerization.^{1,35} Therefore, it was of interest to study the effect of pentadecyl chain containing bisphenol and diamine as a comonomer on the properties of copolyesters and copolyimides, respectively. It was of further interest to vary the comonomer content systematically to investigate the amount of comonomer required for aiding processability/solubility to copolymers. Based on these objectives the following specific problems were chosen for the present work.

1. Design and synthesis of difunctional monomers such as bisphenol and diamine starting from CNSL.
2. Design and synthesis of difunctional monomers such as bisphenols with systematic variation of substituents on phenyl rings and a diamine starting from *p*-cumylphenol.
3. Synthesis of polyesters and polyimides containing pendant pentadecyl chain from respective bisphenol and diamine and study the effect of pentadecyl chain on the polymer properties.
4. Synthesis of (co)polyesters and (co)polyimides from comonomers containing pentadecyl chain and study the effect of comonomer content on polymer properties / processability.
5. Synthesis of polyesters, polyimides and polyetherimides containing bulky “cardo” group from respective bisphenol and diamine and study the effect of incorporation of bulky “cardo” group on polymer properties.
6. Study the applications of selected (co)polyimide as alignment layers for liquid crystals.
7. Evaluation of polyesters containing bulky “cardo” group as membrane materials for gas separations and investigate the effect of different substituents on aromatic rings of bisphenol on the gas permeation properties of the polyesters.

1. References

2. *Synthetic Methods in Step Growth Polymers*; Rogers, M. E.; Long, T. E., Eds.; John Wiley and Sons: New York, 2003.
3. *Polyimides and Other High Temperature Polymers Vol. I*; Mittal, K. L., Ed.; VSP BV: The Netherlands, 2001.
4. *Polyimides: Fundamentals and Applications*; Ghosh, M. K.; Mittal, K. L. Eds.; Marcel Dekker: New York, 1996.
5. Vinogradova, S.V.; Vasnev, V.A.; Valetskii, P.M. *Russ. Chem. Rev.* **1994**, 63 (10), 833.
6. Lin, J.; Sherrington, D. C. *Adv. Polym. Sci.* **1994**, 111, 177.
7. Wartusch, J. *Makromol. Chem. Macromol. Symp.* **1993**, 75, 67.
8. Sroog, C. E. *Prog. Polym. Sci.* **1991**, 16, 561.
9. *Heat Resistant Polymers: Technologically Useful Materials*; Critchley, J. P.; Knight, G. J.; Wright, W. W. Plenum Press: New York, 1983.
10. Hergenrother, P. M. *High Perform. Polym.* **2003**, 15, 3.
11. Sillion, B. *High Perform. Polym.* **1999**, 11, 417.
12. de Abajo, J.; de la Campa, J. G. *Adv. Polym. Sci.*, **1999**, 140, 23.
13. Shifrina, Z. B.; Rusanov, A. L. *Russ. Chem. Rev.* **1996**, 65, 599.
14. Hergenrother, P. M.; Havens, S. J. *Macromolecules* **1994**, 27, 4659.
15. Sathav, J. R.; Harris, F. W. *Polymer* **1995**, 36, 4911.
16. Garcia, C.; Lozano, A. E.; de la Campa, J. G.; de Abajo, J. *Macromol. Rapid Commun.* **2003**, 24, 686.
17. Liaw, D. J.; Liaw, B. Y.; Yang, C. M. *Macromolecules* **1999**, 32, 7248.
18. Spiliopoulos, I.K.; Mikroyannidis, J.A. *Macromolecules* **1998**, 31, 1236.
19. Wang, H.; Shen, Z.; Cheng, S.Z.D.; Harris, F.W. *Polym. Prepr.* **1999**, 40(1), 88.
20. Morgan, P.W. *Macromolecules* **1970**, 3, 536.
21. Liaw, D.J.; Hsu, C.-Y.; Liaw, B.-Y. *Polymer* **2001**, 42, 7993.
22. Liaw, D.J.; Liaw, B.-Y. *Polym. Prepr.* **2000**, 41, 79.
23. Choi, K. Y.; Yi, M. H. *Macromol. Symp.* **1999**, 142, 193.
24. Liaw, D.J.; Liaw, B.-Y.; Lai, S.-H. *Macromol. Chem. Phys.* **2001**, 202, 807.
25. Yang, C.P.; Chen, J.-A. *Polym. Int.* **2000**, 49, 103.

26. *Prediction of Polymer Properties*; Bicerano, J., Marcel Dekker Inc.: New York, 1996.
27. *The Behavior of Plasticizers*; Mellan, I, Pregamon Press: New York, 1961.
28. *The Technology of Plasticizers*; Sears, J.K.; Darby, J.R., John Wiley and Sons : New York, 1981.
29. Sasthav, J.R.; Harris, F.W. *Polymer*, **1995**, 26, 4911.
30. Harvey, M.T.; Caplan, C. *Ind. Eng. Chem.* **1940**, 10, 1306.
31. Lubi, M.C.; Thachil, E.T. *Designed Monomers and Polymers* **2000**, 3, 123.
32. Suresh, K.I.; Kishanprasad, V.S. *Ind. Eng. Chem. Res.* **2005**, 44, 4504
33. Shingte, R.D.; Wadgaonkar, P.P. U.S. Patent Number 6,790,993, **2004**.
34. *Kirk-Othmer Encyclopedia of Chemical Technology, Vol. 2*, Kroschwitz, J.I.; Seidel, A.; Backford, M.; Eds.; Wiley Interscience : Hoboken, 2004.
35. Overberger, C.G. *J. Polym. Sci. Polym. Symp.* **1985**, 72, 67.

3.1 Introduction

One of the most important criteria that decides the final properties of a polymer is the structure of monomers and by selecting suitable monomers existing properties of a polymer could be tailored.¹⁻³ Therefore, in the synthesis of polymer the first step constitutes the synthesis of desired monomers, which can give rise to polymers with expected / targeted properties.

In the area of high performance polymers such as polyimides, polyamides, polyesters, etc., a large number of difunctional monomers have been synthesized in the past three decades with a view to overcome the traditional processing problems caused by the limited solubility and poor processability of these polymers. Efforts devoted to incorporating the structural features that improve processability have led to an outstanding enrichment of the chemistry of high performance polymers, and have allowed the opening of new investigations and application areas for these polymers.^{4,5}

In the present work, new monomers viz. bisphenols and diamines were designed and synthesized starting from cheap, commercially available raw materials, viz., cashew nut shell liquid and *p*-cumylphenol.

3.1.1 Cashew Nut Shell Liquid (CNSL):

Renewable organic resources continue to be in the common interest of both academic and industrial laboratories at all the times. The topic has attained a renewed interest for reasons of economy and environmental friendliness and contributes well to green chemistry practices. Among the renewable resources, cashew nut shell liquid (CNSL), a by-product of the cashew processing industry, is available abundantly worldwide (1,25,000 tpa). Cashew nut is a product of cashew tree, *Anacardium occidentale*.⁶ Cashew nut shell liquid (CNSL) occurs as a greenish-yellow viscous liquid in the soft honeycomb of the shell of the cashew nut. Cashew nut consists of an ivory colored kernel covered by a thin brown membrane (testa) and enclosed by an outer porous shell, the mesocarp which is about 3 mm thick with a honeycomb structure, where CNSL is stored (**Figure 3.1**). CNSL is

abundantly available in many parts of the world, such as, India, Brazil, Bangladesh, Tanzania, Kenya, tropical regions of Africa and South-East and Far-East Asia. Traditionally, a number of methods are employed to extract the oil from the nuts. Hot oil bath method where raw nuts are passed through a bath of hot CNSL at 180-200°C, roasting method, are commonly used ones. Few reports are available on using steam distillation, solvent extraction, supercritical extraction using a mixture of CO₂ and isopropyl alcohol for extraction of CNSL.



Figure 3.1 Nut of Cashew

Industrial grade CNSL is reddish brown in color. CNSL constitutes about 20-25% of the weight of cashew. Naturally occurring CNSL contains mainly four compounds; cardanol, cardol, anacardic acid and 2-methyl cardol (**Figure 3.2**). Components of CNSL are themselves mixture of four constituents differing in side-chain unsaturation, namely, monoene, diene, triene and saturated one.

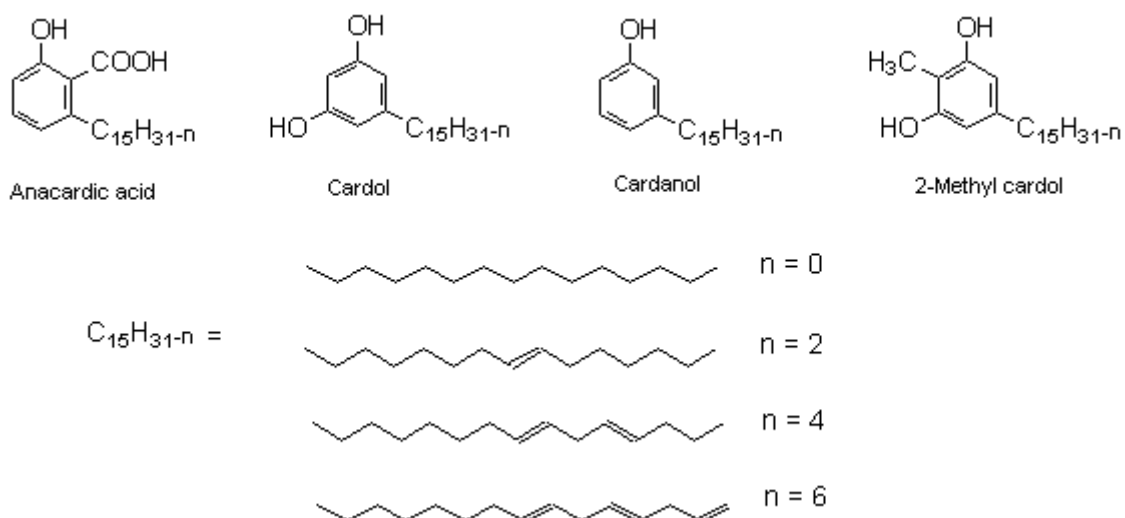


Figure 3.2 Constituents of CNSL

Commercial grade CNSL contains hardly any anacardic acid because of decarboxylation during roasting process, which converts anacardic acid to cardanol. Unsaturated 15-carbon chain and phenolic moiety in CNSL has offered a variety of possibilities for the synthetic chemist. Many reactions of CNSL such as, hydrogenation, polymerization, sulfonation, nitration, halogenation, etherification, esterification, epoxidation, phosphorylation, etc. have been documented in various patents and journal articles.⁷⁻¹⁰ Considerable attention from polymer scientists throughout the world is devoted to utilize CNSL's potential attributes as a substitute for petrochemical derivatives and has found use in phenolic resins in break lining, surface coatings, adhesives, foundry resins, laminates, rubber compounding, additives, etc. Of late, CNSL has been used in preparation of many specialty materials such as liquid crystalline polyesters, nanotubes, cross-linkable polyphenols, polyurethanes and range of other specialty polymers and additives⁸. Considering special structural features of cardanol and need for finding better opportunities for an appropriate utilization for this material, novel strategies can be developed to design specialty / high performance polymers from cardanol.

3.1.2 *p*-Cumylphenol

p-Cumylphenol or 4-(1-methyl-1-phenylethyl)phenol, an important member of alkylphenol family is produced by the alkylation of phenol with α -methyl styrene under acid catalysis. The principal by-products from the production of *p*-cumylphenol result from the dimerization and intramolecular alkylation of α -methyl styrene to yield substituted indanes. *p*-Cumylphenol is purified by either fractional distillation or crystallization from suitable solvent.

The major use of *p*-cumylphenol is as a chain terminator for polycarbonates. The other uses of *p*-cumylphenol include the production of phenolic resins and specialty surfactants.

Alkyl phenols undergo variety of chemical transformations, involving the hydroxyl group or the aromatic nucleus that convert them to value added products.

3.2 Experimental

3.2.1 Materials

p-Cumylphenol (Herdilia Chemicals Ltd., India), *p*-chloronitrobenzene, *p*-fluorocyanobenzene, 2,6-dimethylphenol, 10% Pd/C, 5% Ru/C, 3-mercaptopropionic acid (3-MPA) and CaH₂ (Aldrich Chemicals) were used as received. Aniline hydrochloride, calcium chloride, sodium sulfate, sodium bicarbonate, potassium carbonate, potassium hydroxide, sodium hydroxide, hydrazine hydrate, bromine, acetic acid, HCl, H₂SO₄ and HNO₃ (S.D. Fine Chem., India) were used as received. Cyclohexanone, *m*-cresol, *o*-cresol, tetrahydrofuran, methanol, ethanol, 2-propanol, dichloromethane, chloroform, ethyl acetate, hexane, toluene and N,N-dimethylformamide (DMF) (S.D. Fine Chem., India) were of reagent grade and were purified prior to use according to reported procedures¹². Pyridiniumchlorochromate (PCC) was prepared according to the procedure reported in the literature¹³.

Cardanol was obtained by the vacuum distillation of cashew nut shell liquid at 220°C/1mm Hg. (Lit. bp 230-235°C/3-4 mm Hg).¹⁴

3.2.2 Measurements

Melting points were determined by open capillary method and are uncorrected.

FTIR spectra were recorded on a Perkin-Elmer *Spectrum GX* spectrophotometer in KBr pellet or in chloroform.

HPLC analysis was performed on Waters Modular System consisting of three 515 pumps, 717 auto sampler, 996-photodiode array detector, 2410 RI detector controlled by *Millenium 32* software. Column used was *Zorbax RP-C8*.

All of the NMR spectra were recorded on a Bruker 200, 400 or 500 MHz spectrometer at resonance frequencies of 200, 400 or 500 MHz for ¹H and 50, 100 or 125 MHz for ¹³C measurements using CDCl₃ as a solvent.

Single crystal X-ray diffraction measurements were carried out on *Bruker SMART APEX* CCD diffractometer with Mo K_α radiation at room temperature and fine focus tube with 50kV and 30 mA. All the data were corrected for Lorentzian, polarization and absorption effects. SHELX-97 (ShelxTL)¹⁵ was used for structure solution and full matrix least

squares refinement on F². Hydrogen atoms were included in the refinement as per the riding model.

3.3 Synthesis

3.3.1 Synthesis of 1,1-bis(4-hydroxyphenyl)-3-pentadecylcyclohexane

3.3.1.1 Synthesis of 3-pentadecylphenol

Side chain of the cardanol was reduced according to following procedure.

Cardanol (500 g, 1.64 mol) obtained from cashew nut shell liquid was distilled twice under reduced pressure and hydrogenated in the presence of 5%Pd/C (1.5 g) catalyst at 70°C in a Parr autoclave under 600 psi hydrogen pressure. When no more hydrogen absorption was noticed, the hydrogenation was stopped. The product was filtered and recrystallized from hexane (40-60°C) to obtain 3-pentadecylphenol. Yield: 480 g (97%) m.p.: 50-51°C (Lit. m.p.: 50-51°C).¹⁶

3.3.1.2 Synthesis of 3-pentadecylcyclohexanol

3-Pentadecylphenol (80 g, 0.26 mol) dissolved in isopropanol (300 ml) was hydrogenated using 5% Ru/C (2.4 g) as the catalyst in a Parr reactor at 125°C and at hydrogen pressure of 1000 psi. At the end of the reduction, the catalyst was filtered off and isopropanol was distilled off to obtain 3-pentadecyl cyclohexanol. Yield, 79.90 g (98%), m.p. 46-49°C (Lit. m.p. 45-48°C)¹⁷

3.3.1.3 Synthesis of 3-pentadecylcyclohexanone

Into a 1 liter round bottom flask equipped with a mechanical stirrer was added a finely ground mixture of PCC (97 g, 0.45 mol) and silica gel (97 g, 100-200 mesh). To this mixture, dichloromethane (600 mL) was added, the suspension was stirred and 3-pentadecylcyclohexanol (50 g, 0.22 mol) was added in small portions at room temperature. The reaction mixture darkened (30 min) and the stirring was continued for 4 h. The

reaction mixture was filtered through a short column of celite and silica gel. The filtrate was concentrated under reduced pressure to obtain a solid. The solid was dissolved in ethyl acetate (300 mL) and washed with water (2 × 200 mL) followed by washing with saturated aqueous sodium chloride (2 × 200 mL). The organic layer was dried over anhydrous sodium sulfate, filtered and ethyl acetate was removed at a rotary evaporator. The residue obtained was recrystallized from methanol; yield, 46.68 g (94%), m.p. 44°C (Lit. m.p. 43°C)¹⁷

3.3.1.4 Synthesis of 1,1-bis(4-hydroxyphenyl)-3-pentadecylcyclohexane

Into a 250 ml three-necked round bottom flask fitted with a magnetic stirrer bar, a HCl dip tube and a reflux condenser connected to a scrubber were placed 3-pentadecylcyclohexanone (20 g, 0.06 mol), phenol (36.62 g, 0.38 mol) and 3-MPA (0.1 mL). Dry HCl was bubbled into the reaction mixture at room temperature. The reaction mixture became solid at the end of 1 h. The reaction mixture was dissolved in ethyl acetate (600 mL) and neutralized by washing with aqueous sodium bicarbonate solution (3 × 200 mL) followed by washing with water (2 × 200 mL). The organic layer was dried over sodium sulfate, filtered and ethyl acetate was distilled off. The product was crystallized two times from a mixture of hexane and toluene (9:1, v/v); yield, 21.72g (70%), m.p. 104°C (Lit. m.p. 104°C).¹⁰

3.3.2 Synthesis of 1,1-bis(4-hydroxyphenyl)cyclohexane

Into a 500 ml three-necked round bottom flask fitted with a magnetic stirrer bar, a HCl dip tube and a reflux condenser connected to a scrubber were placed cyclohexanone (10 g, 0.10 mol), phenol (57.52 g, 0.61 mol) and 3-MPA (0.2 mL). Dry HCl was bubbled into the reaction mixture at room temperature. The reaction mixture became solid at the end of 2 h. The reaction mixture was dissolved in ethyl acetate (1 lit) and neutralized by washing with aqueous sodium bicarbonate solution (3 × 300 mL) followed by washing with water (2 × 300 mL). The organic layer was dried over sodium sulfate, filtered and ethyl acetate was distilled off to obtain a viscous liquid. Upon addition of pet-ether (1 lit) white solid

separated out which was crystallized twice from a mixture of pet-ether and benzene (80:20, v/v). Yield 18.32 g (67%), m.p. 190°C (Lit. m.p. 186°C)¹⁸

3.3.3 Synthesis of 1,1-bis(4-hydroxyphenyl)-3-methylcyclohexane

3-Methylcyclohexanol was synthesized from by reduction of *m*-cresol which upon oxidation yielded 3-methylcyclohexanone following the procedure reported for 3-pentadecylcyclohexanone (**Section 3.3.1**). 3-Methylcyclohexanone was used for the synthesis of 1,1-bis(4-hydroxyphenyl)-3-methylcyclohexane.

Into a 250 ml three-necked round bottom flask fitted with a magnetic stirrer bar, a HCl dip tube and a reflux condenser connected to a scrubber were placed 3-methylcyclohexanone (11.2 g, 0.10 mol), phenol (56.4 g, 0.60 mol) and 3-MPA (0.2mL). Dry HCl was bubbled into the reaction mixture at room temperature. The reaction mixture became solid at the end of 2 h. The reaction mixture was dissolved in ethyl acetate (600 mL) and neutralized by washing with aqueous sodium bicarbonate solution (3× 200 mL) followed by washing with water (2× 200 mL). The organic layer was dried over sodium sulfate, filtered and ethyl acetate was distilled off. The product was recrystallized from toluene, yield 22.3 g (82%), m.p. 168°C.

3.3.4 Synthesis of 1,1-bis(4-aminophenyl)-3-pentadecylcyclohexane

Into a 250 mL round bottom flask equipped with a magnetic stirring bar and a reflux condenser were placed 3-pentadecylcyclohexanone (10 g, 0.032 mol), aniline hydrochloride (12.44 g, 0.096) and freshly distilled aniline (46 g, 0.48 mol). The reaction mixture was refluxed for 24 h. The reaction mixture was neutralized by adding 100 mL of 1 N aqueous sodium hydroxide. The organic layer was separated and washed with water (3× 20 mL) and excess aniline was distilled off. The resinous mass was crystallized from ethanol to yield colorless needles, yield 5.4 g (35%), m.p. 106-108°C.

3.3.5 Synthesis of 1,1-bis(4-hydroxyphenyl)-4-perhydrocumyl cyclohexane

3.3.5.1 Synthesis of 4-(1-cyclohexyl-1-methyl ethyl) cyclohexanol

p-Cumylphenol (40 g, 0.19 mol) dissolved in isopropanol (150 ml) was hydrogenated using 5 % Ru/C (1.2 g) as catalyst in a Parr reactor at 175°C and at hydrogen pressure of 1400 psi. At the end of the reduction the catalyst was filtered off and filtrate with bluish tinge was passed through a short column of silica gel (100-200 mesh) to obtain colorless solution. Isopropanol was distilled off and the residue was treated with 10% NaOH solution (100 ml) at reflux for 2 h. The reaction mixture was extracted with dichloromethane (400 mL). The dichloromethane solution was washed with water (3× 100 mL), separated, dried over anhydrous sodium sulfate and filtered. The dichloromethane was distilled off to obtain a viscous liquid, which solidified on prolonged standing; yield, 53.6 g (85%).

3.3.5.2 Synthesis of 4-(1-cyclohexyl-1-methyl ethyl) cyclohexanone

Into a 1 lit round bottom flask equipped with a mechanical stirrer was added a finely ground mixture of PCC (97 g, 0.45 mol) and silica gel (97 g, 100-200 mesh). To this, dichloromethane (600 mL) was added, the suspension was stirred and 4-(1-cyclohexyl-1-methyl ethyl)cyclohexanol (HPCP) (50 g, 0.22 mol) was added in small portions at room temperature. The reaction mixture darkened (30 min) and the stirring was continued for 4 h. The reaction mixture was filtered through a short silica gel column. The filtrate was concentrated under vacuum to obtain a solid. The solid was taken up in ethyl acetate (400 mL), washed with water (2× 100 mL) followed by washing with saturated aqueous sodium chloride (2× 100 mL) and water (1× 100 mL). The organic layer was dried over anhydrous sodium sulfate, filtered and ethyl acetate was removed on a rotary evaporator. The residue obtained was recrystallized from methanol; yield, 44.59 g (90%), m.p. 86°C.

3.3.5.3 Synthesis of 1,1-bis(4-hydroxyphenyl) -4-perhydrocumyl cyclohexane

Into a 100 ml three-necked round bottom flask fitted with a magnetic stirrer bar, a HCl dip tube and a reflux condenser connected to a scrubber were placed 4-(1-cyclohexyl-1-methyl ethyl) cyclohexanone (10 g, 0.05 mol), phenol (25.38 g, 0.27 mol) and 3-MPA (0.1 mL). Dry HCl was bubbled into the reaction mixture at room temperature. The reaction mixture became solid at the end of 2 h. The reaction mixture was dissolved in ethyl acetate (250 mL) and neutralized by washing with aqueous sodium bicarbonate solution (3× 50 mL) followed by washing with water (3× 50 mL). The organic layer was dried over sodium sulfate, filtered and ethyl acetate was distilled off. The product was recrystallized from toluene; yield, 12.71 g (72%), m.p. 197°C

3.3.6 Synthesis of 1,1-bis(4-hydroxy-3-methylphenyl) -4-perhydrocumyl cyclohexane

Into a 100 ml three-necked round bottom flask fitted with a magnetic stirrer bar, a HCl dip tube and a reflux condenser connected to a scrubber were placed cyclohexanone 4-(1-cyclohexyl-1-methyl ethyl) (10 g, 0.05 mol), *o*-cresol (29.16 g, 0.27 mol) and 3-MPA (0.1ml). Dry HCl was bubbled into the reaction mixture for 24 h at 45°C. The reaction mixture was dissolved in ethyl acetate (250 mL) and neutralized by washing with aqueous sodium bicarbonate solution (3× 50 mL) followed by washing with water (3× 50 mL). The organic layer was dried over sodium sulfate, filtered and ethyl acetate was distilled off. The product was recrystallized from a mixture of pet-ether and benzene (80/20, v/v); yield, 13.24 g (70%), m.p. 189°C

3.3.7 Synthesis of 1,1-bis(4-hydroxy-3,5-dimethylphenyl) -4-perhydrocumyl cyclohexane

Into a 100 ml round bottom flask containing 15 mL HCl/acetic acid mixture (2:1, v/v), 4-(1-cyclohexyl-1-methyl ethyl)cyclohexanone (10 g, 0.05 mol) and 2,6-dimethylphenol (10.98 g, 0.09 mol) were stirred for seven days at room temperature. The reaction mixture

was dissolved in ethyl acetate (150 mL) and neutralized by washing with aqueous sodium bicarbonate solution (3× 40 mL) followed by washing with water (2× 40 mL). The organic layer was dried over sodium sulfate, filtered and ethyl acetate was distilled off. The product was recrystallized from hexane, yield 12.1 g (60 %), m.p. 213°C

3.3.8 Synthesis of 1,1-bis(4-hydroxy-3,5-dibromophenyl) -4-perhydrocumyl cyclohexane

Into a 100 ml round bottom flask equipped with a magnetic stirring bar, were placed 1,1-bis(4-hydroxyphenyl) -4-perhydrocumyl cyclohexane (5.0 g, 0.012mol) and ethanol (20 mL). The reaction mixture was maintained at 10°C. To the reaction mixture bromine (7.99 g, 0.05 mol) was added dropwise over a period of 30 min and reaction mixture was stirred for additional 30 minutes. The reaction mixture was refluxed for 1 h and 10 ml of water was added and refluxion was continued for 30 min. The reaction mixture was cooled to room temperature and solid formed was separated by filtration. The crude product obtained was recrystallized from ethanol, yield 7.22 g (80 %), m.p. 220°C.

3.3.9 Synthesis of 1,1-bis(4-hydroxy-3-methyl-5-bromophenyl)-4-perhydro-cumyl cyclohexane

Into a 100 ml round bottom flask equipped with a magnetic stirring bar, were placed 1,1-bis(4-hydroxy-3-methylphenyl) -4-perhydrocumyl cyclohexane (5 g, 0.012mol) and methanol (20 mL). The reaction mixture was maintained at 10°C. To the reaction mixture, bromine (4.02 g, 0.025 mol) was added dropwise over a period of 30 min and reaction mixture was stirred for additional 30 minutes. The reaction mixture was refluxed for 1 h and 10 ml of water was added and refluxion was continued for 30 min. The reaction mixture was cooled to room temperature and solid formed was separated by filtration. The crude product was recrystallized from methanol, yield 5.50 g (80 %), m.p. 204°C.

3.3.10 Synthesis of 1,1-bis(4-aminophenyl) -4-perhydrocumyl cyclohexane

Into a 250 mL round bottom flask equipped with a magnetic stirring bar and a reflux condenser were placed cyclohexanone 4-(1-cyclohexyl-1-methyl ethyl) (10 g, 0.045 mol), aniline hydrochloride (17.51 g, 0.135) and freshly distilled aniline (62 mL, 0.675 mol). The mixture was refluxed for 24 h. The reaction mixture was neutralized by 1 N aqueous sodium hydroxide (100 ml). The organic layer was washed with water (3 x 20 mL) and excess aniline was distilled off. The crude product obtained was recrystallized from ethanol to yield colorless plates, yield 8.8 g (50%), m.p. 186-188°C.

3.3.11 Synthesis of 1,1-bis[4-(4-aminophenoxy)phenyl]-4-per-hydrocumyl cyclohexane

3.3.11.1 Synthesis of 1,1-bis[4-(4-nitrophenoxy)phenyl]-4-per-hydrocumyl cyclohexane

In a 250 mL round bottom flask equipped with a magnetic stirrer, a nitrogen inlet and a reflux condenser were placed 1,1-bis(4-hydroxyphenyl) -4-perhydrocumyl cyclohexane (10 g, 0.026 mol), *p*-chloronitrobenzene (8.19 g, 0.052 mol) and anhydrous DMF (90 mL). To the reaction mixture potassium carbonate (7.75g, 0.056 mol) was added and the reaction mixture was refluxed under the stream of nitrogen for 10 h. The reaction mixture was then cooled to room temperature and poured into 600 mL of water. The solid separated was filtered and washed with water. The crude product was recrystallized from DMF to give yellow crystals; yield, 15.20 g (94%), m.p. 189°C.

3.3.11.2 Synthesis of 1,1-bis[4-(4-aminophenoxy)phenyl]-4-per-hydrocumyl cyclohexane

Into a 250 mL three necked round bottom flask equipped with a magnetic stirrer, a nitrogen inlet and a reflux condenser were placed 1,1-bis[4-(4-nitrophenoxy)phenyl]-4-per-hydrocumyl cyclohexane (10.14 g, 0.016 mol), 10 wt% Pd/C (0.2 g) and ethanol (100 mL). To the reaction mixture hydrazine hydrate (6 mL) was added dropwise over a period of 1 h at reflux temperature under inert atmosphere. After completion of hydrazine hydrate

addition, the mixture was refluxed for additional 4 h. The solid separated out. To the reaction mixture 15 mL of THF was added to dissolve the solid and refluxion was continued for additional 2 h. The reaction mixture was filtered while hot to remove Pd/C and THF was removed at rotary evaporator. After cooling, colorless needles were isolated by filtration; yield, 7.24 g (80%), m.p. 165-166°C.

3.3.12 Synthesis of 1,1-bis[4-(4-carboxyphenoxy)phenyl]-4-per-hydrocumyl cyclohexane

3.3.12.1 Synthesis of 1,1-bis[4-(4-cyanophenoxy)phenyl]-4-per-hydrocumyl cyclohexane

Into a 250 mL round bottom flask equipped with a magnetic stirring bar, a Dean–Stark trap and a condenser were placed 1,1-bis(4-hydroxyphenyl) -4-perhydrocumyl cyclohexane (5g, 12.6 mmol), DMF (35 mL) and toluene (25 mL). To the reaction mixture anhydrous potassium carbonate (3.52 g, 25.2 mmol) was added . The suspension was heated to reflux and water was removed by azeotropic distillation with toluene. After complete removal of water, the residual toluene was distilled off. The reaction mixture was cooled to about 60°C and *p*-fluorobenzonitrile (3.09 g, 0.025 mol) was added. The reaction mixture was refluxed for 6 h and then cooled to room temperature and was poured into 500 mL of water. The precipitated white powder was collected by filtration, thoroughly washed with water and dried. The crude product was purified by recrystallization from acetonitrile; yield, 6.43 g (85%) m.p. 148-149°C.

3.3.12.2 Synthesis of 1,1-bis[4-(4-carboxyphenoxy)phenyl]-4-per-hydrocumyl cyclohexane

Into a 100 mL round bottom flask equipped with a magnetic stirring bar and a reflux condenser were placed 1,1-bis[4-(4-cyanophenoxy)phenyl]-4-per-hydrocumyl cyclohexane (5 g, 8.4 mmol), potassium hydroxide (4.41 g, 84 mmol), ethanol (30 mL), and water (30 mL). The reaction mixture was refluxed for 72h. The resulting clear solution was filtered while hot to remove any insoluble impurities and was cooled to room temperature. The filtrate was acidified with concentrated HCl to pH = 2. The precipitated

white powder was isolated by filtration, washed repeatedly with water, and dried under vacuum at 150°C for 12 h; yield, 5.1 g (96%), m. p. 245°C.

3.4 Results and Discussion

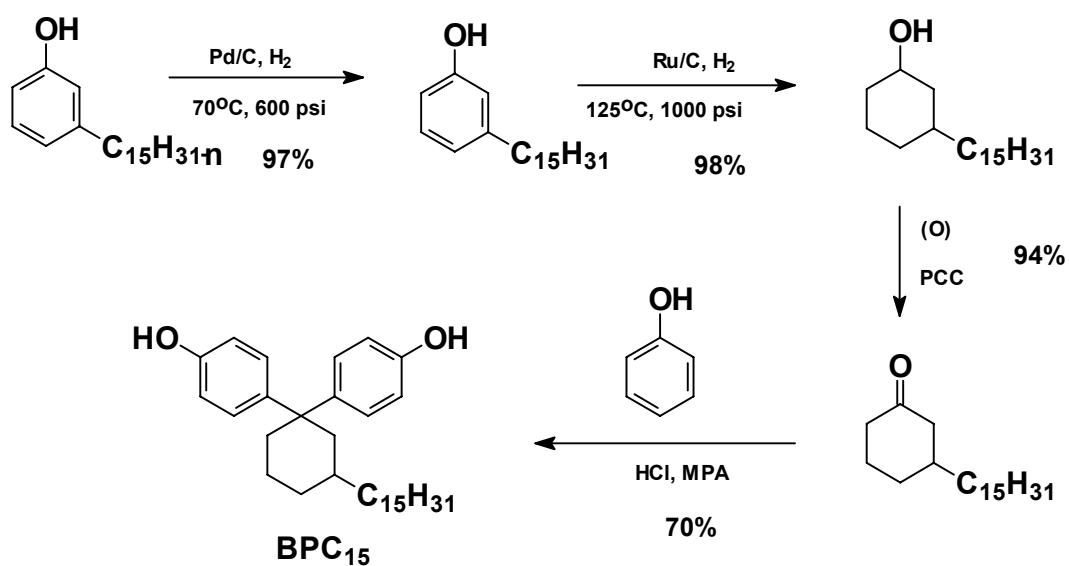
3.4.1 Synthesis and characterization of 1,1-bis(4-hydroxyphenyl)-3-pentadecylcyclohexane

Bisphenols are an important class of chemicals and/or intermediates for the preparation of industrially useful epoxy resins, polycarbonates, polyesters, polyether sulfones, polyetherketones, etc. Bisphenols are usually synthesized by the acid-catalyzed condensation of aldehydes or ketones with phenols. The properties of the end polymers depends on the structure of the bisphenol. There is a wide scope to design new bisphenol molecules by varying either aldehyde/ ketone or phenol. A variety of aldehydes/ or ketones have been used for synthesis of bisphenols. Bisphenols synthesized from cyclic ketones yielded polymers with improved thermal and mechanical properties. However, cyclohexanone derived bisphenols yielded polyesters with poor processability. The substitution on the cyclohexyl ring, is one of the approaches for achieving processable polymers.

The present work mainly deals with the substituted cyclohexylidene containing polymers. Cyclohexanone is synthesized by oxidation of cyclohexanol, which is obtained by the reduction of phenol. Alkyl substituted cyclohexanones can be derived from alkyl phenols. Cardanol, a renewable resource material obtained from cashew nut shell liquid, is a source of long chain alkenyl phenol which can take part in variety of reactions.

A new bisphenol monomer containing 3-pentadecylcyclohexylidene moiety was designed and synthesized from cardanol making use of simple organic transformations like hydrogenation, oxidation and acid-catalyzed condensation with phenol.

Scheme 3.1 depicts the route for the synthesis of 1,1-bis(4-hydroxyphenyl)-3-pentadecylcyclohexane (BPC₁₅). The synthesis of BPC₁₅ involved four steps.



Scheme 3.1 Synthesis of 1,1-bis(4-hydroxyphenyl)-3-pentadecylcyclohexane

In the first step, 3-pentadecylphenol was prepared by the catalytic hydrogenation of freshly distilled cardanol in the presence of 5% Pd/C catalyst. The product obtained was recrystallized from petroleum ether (60-80°C) and was characterized by FTIR and ^1H NMR spectroscopy. FTIR spectrum showed absorption band at 3342 cm^{-1} , corresponding to $-\text{OH}$ stretching.

Several researchers have studied the catalytic hydrogenation of cardanol at normal and elevated temperatures with different catalysts like nickel, Raney nickel, etc.^{16,17} Effect of hydrazine hydrate on the reduction of cardanol was studied by Bhole et al and the products were compared to those obtained by catalytic hydrogenation. It was observed that increase in the molar ratio of hydrazine hydrate to cardanol (more than 1:15) gave better reduction of cardanol.¹⁹ In the present study, Pd/C was used for high yields and reusability of the catalyst.

In the second step, 3-pentadecyl phenol was hydrogenated using 5% Ru/C to get 3-pentadecylcyclohexanol. Transition metal catalysts such as Ni, Pd, Co, Rh, Pt, Ru, etc can also be used for the hydrogenation of phenols.²⁰⁻²⁴ After complete reduction reaction mixture was filtered and the catalyst was recovered. The filtrate had slight blackish tinge, which could be mainly because of the fine carbon powder. The filtrate was passed through short column of silica gel (100-200 mesh) to obtain colorless solution. The evaporation of solvent under reduced pressure yielded 3-pentadecylcyclohexanol as white solid.

The reduction of 3-pentadecyl phenol gives *cis*- and *trans*-3-pentadecylcyclohexanols.¹⁷ 3-Pentadecylcyclohexanol was characterized by FTIR, ¹H NMR and ¹³C-NMR spectroscopy.

The disappearance of the band at 1600 cm⁻¹ corresponding to aromatic C=C stretching indicates the reduction of aromatic ring. The O-H stretching vibration was observed at 3334 cm⁻¹.

The complete reduction of aromatic ring was further indicated by the disappearance of peaks corresponding to aromatic protons in the region 6.65-7.18 ppm in ¹H NMR spectrum (**Figure 3.3**). The two isomers can be distinguished by ¹H-NMR spectroscopy as proton 'a' and 'e' appear at 3.35 and 4.04 ppm, respectively.

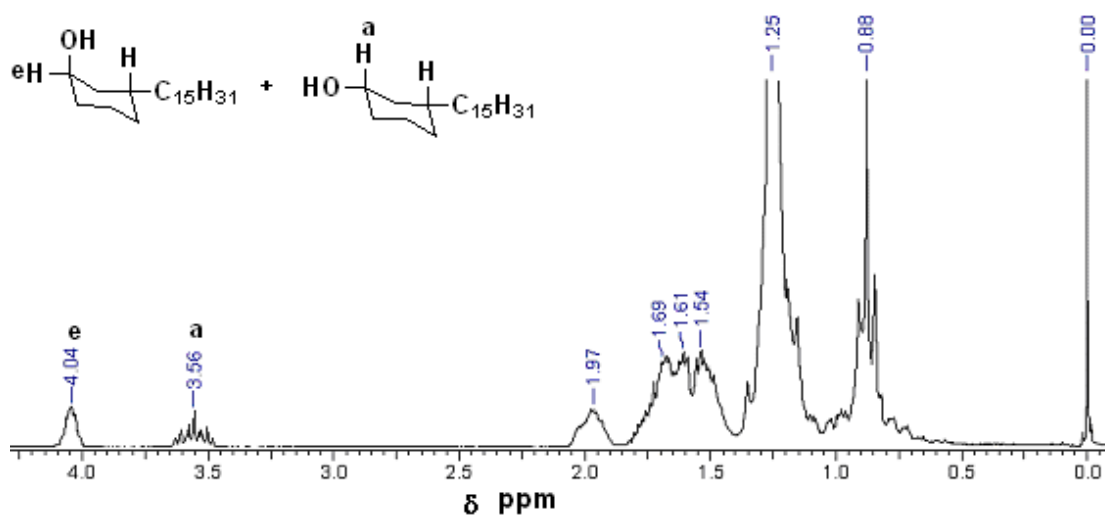


Figure 3.3 ¹H-NMR spectrum of 3-pentadecylcyclohexanol

¹³C-NMR spectrum of 3-pentadecylcyclohexanol with partial assignments is presented in **Figure 3.4**. The assignment for the pentadecyl chain is not given because of the complexity of the system. The spectrum indicates the presence of *cis* and *trans* isomers. The carbon number 1 from *cis* isomer was observed at 70.94 ppm, where as carbon 1' from *trans* isomer was observed at 66.90 ppm. Carbon 3 and 3' were observed at same chemical shift value (31.56 ppm). The terminal CH₃ from pentadecyl chain appeared at 14.05 ppm. However, isomer separation and detailed spectral analysis was not carried out as it was outside the scope of present work.

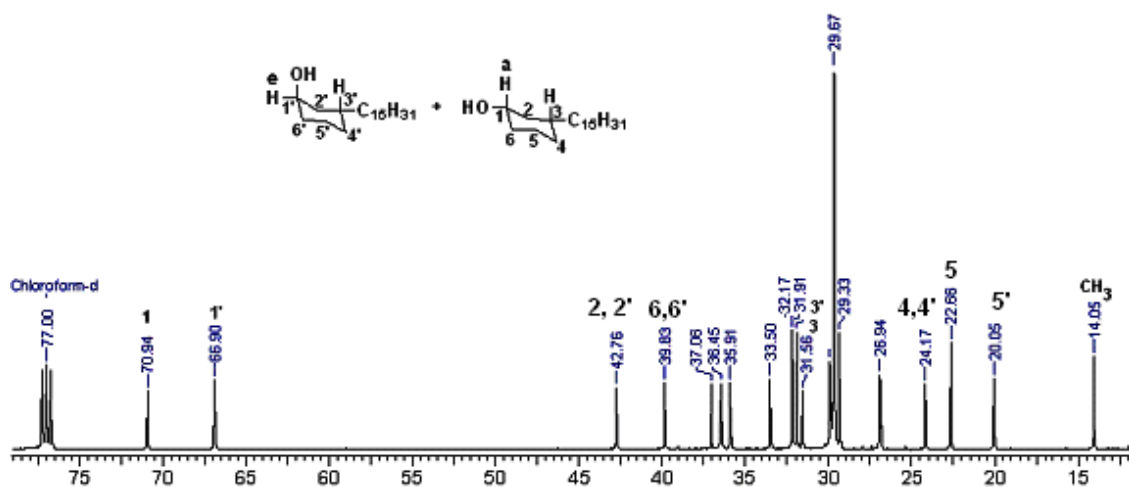


Figure 3.4 ^{13}C -NMR spectrum of 3-pentadecylcyclohexanol

The oxidation of alcohols to aldehydes and ketones is fundamental reaction in organic synthesis. Since the first experiment in 1820 by Davy who oxidized ethanol with air over a platinum catalyst, various reagents have been reported which include, high valent chromium, and manganese compounds²⁵, hypervalent iodine compounds²⁶, *m*-CPBA or sodium hypochlorite with TEMPO,²⁷ etc. From the standpoint of the green and sustainable chemistry cleaner catalytic systems for oxidations have been in demand.²⁸ Recently metal-catalyzed oxidations of alcohols using clean and cheap oxidants such as H_2O_2 , O_2 , and/air have been investigated.²⁹⁻³²

In the present study, pyridinium chlorochromate (PCC) was used for oxidation of 3-pentadecylcyclohexanol because of the easy and safe preparation as well as the its demonstrated utility for moderate to large scale oxidations.¹³

In the third step 3-pentadecyl cyclohexanol was oxidized to 3-pentadecyl cyclohexanone using PCC. The reaction mixture turned dark brown in color within 30 min. After the completion of reaction, the reaction mixture was filtered through short column of celite and silica gel to get colorless filtrate. The solvent was distilled off and solid was dissolved in ethyl acetate and washed with water followed by brine. It is known that the presence of metal impurities in the final polymer can lead to the degradation of polymer chain and deteriorate the mechanical properties of polymer. Therefore care was taken to eliminate the presence of metal residue. 3-Pentadecylcyclohexanone was crystallized from methanol to get white solid.

3-Pentadecylcyclohexanone was characterized by FTIR and ^1H -NMR spectroscopy. FTIR spectrum showed the absence of band at 3300 cm^{-1} corresponding to hydroxyl group and appearance of characteristic band for the carbonyl stretch at 1705 cm^{-1} .

^1H NMR spectrum of 3-pentadecylcyclohexanone is reproduced in **Figure 3.5**, which shows absence of peaks at 3.56 and 4.04 ppm, corresponding to 'a' and 'e' protons of 3-pentadecylcyclohexanol.

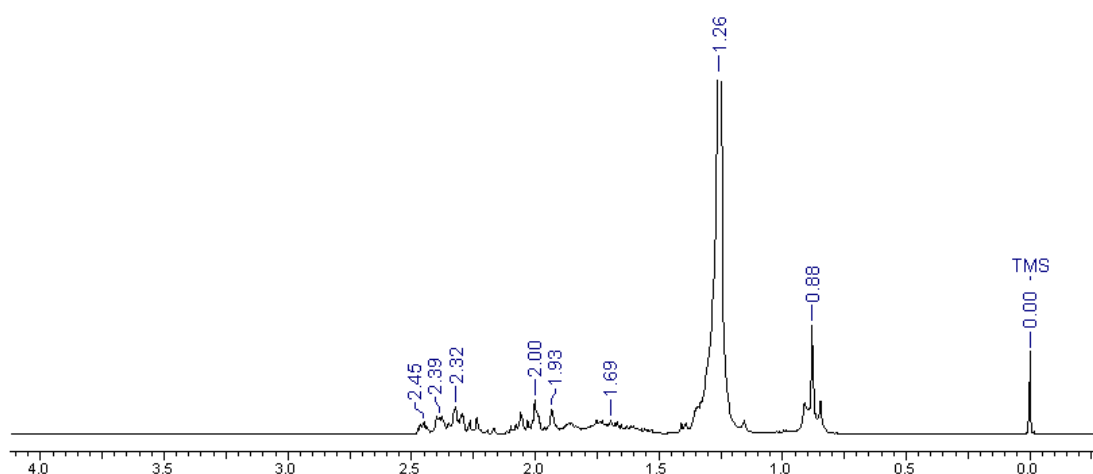


Figure 3.5 ^1H -NMR spectrum of 3-pentadecylcyclohexanone

In the fourth step, 1,1-bis(4-hydroxyphenyl)-3-pentadecylcyclohexane (BPC_{15}) was prepared by condensation of 3-pentadecyl cyclohexanone with phenol using hydrogen chloride/3-mercaptopropionic acid catalyst system. The role of 3-mercaptopropionic acid for this reaction has been investigated in detail by various researchers.^{33,34} When 3-mercaptopropionic acid is used in combination with other strong acids, for the condensation, the rate and the selectivity for the formation of desired bisphenol (p,p-isomer) is increased. Under these conditions the reaction was complete within one hour. The pink colored solid mass was dissolved in ethyl acetate and was washed with sodium bicarbonate solution and water. Ethyl acetate was removed under reduced pressure to get resinous mass. The excess phenol was removed by washing with hexane and crude BPC_{15} was crystallized two times from hexane toluene mixture (9:1 v/v). Unlike bisphenol-A, which forms a crystalline 1:1 adduct with phenol, BPC_{15} does not crystallize as 1:1 adduct with phenol. The purity of BPC_{15} was monitored by high performance liquid

chromatography. HPLC trace for BPC₁₅ is reproduced in **Figure 3.6**. The purity of BPC₁₅ was found to be >99.9 %.

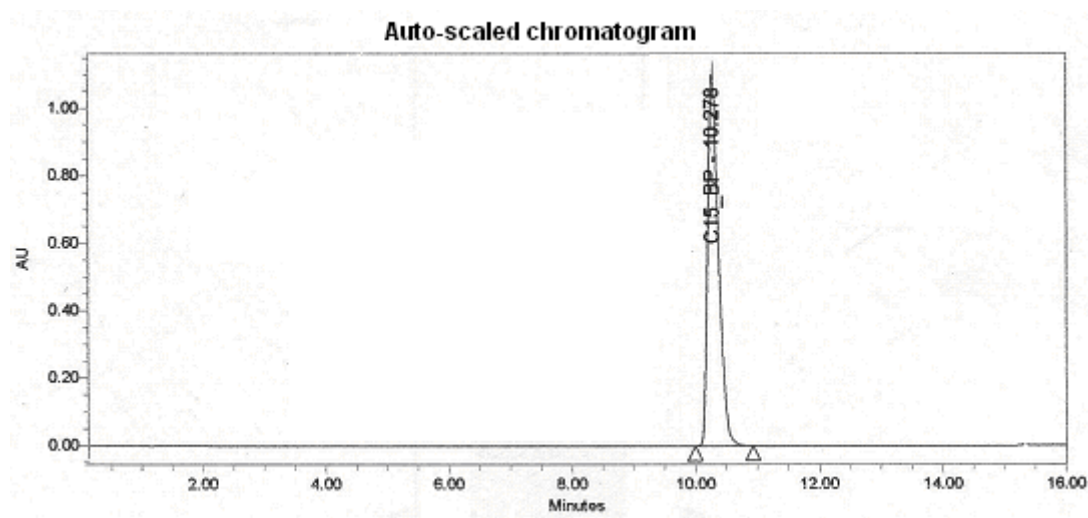


Figure 3.6 HPLC trace of 1,1-bis(4-hydroxyphenyl)-3-pentadecylcyclohexane

BPC₁₅ was characterized by FTIR, ¹H and ¹³C NMR spectroscopy.

FTIR spectrum of BPC₁₅ (**Figure 3.7**) showed broad band at 3291 cm⁻¹ corresponding to –OH group.

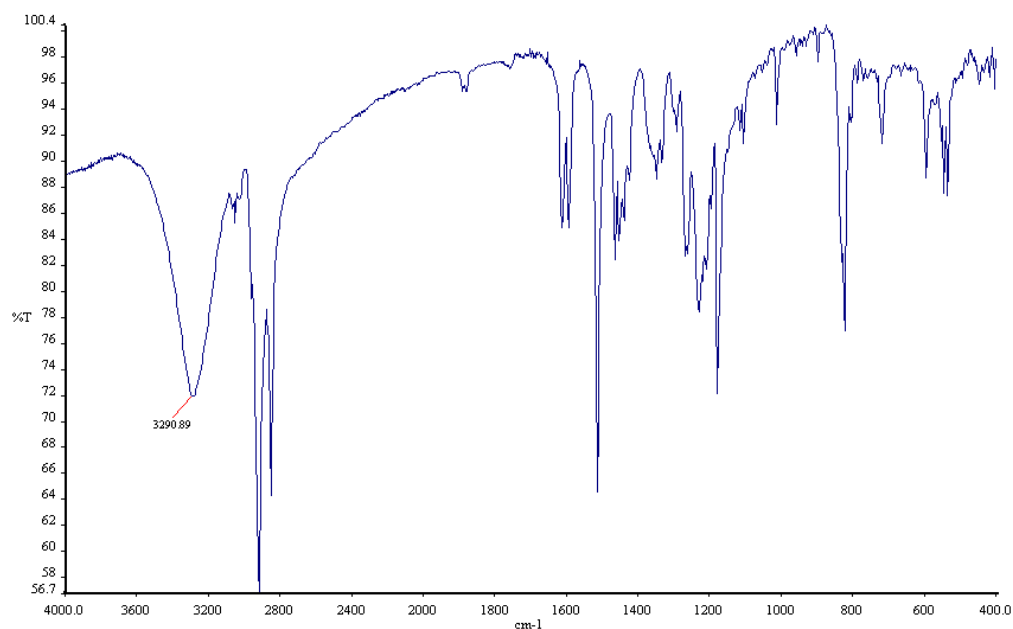


Figure 3.7 FTIR spectrum of 1,1-bis(4-hydroxyphenyl)-3-pentadecylcyclohexane

^1H NMR spectrum of BPC_{15} along with assignments is presented in **Figure 3.8**.

Detailed study of ^1H and ^{13}C NMR spectra showed the presence of distereotopic phenyl rings, which are magnetically non-equivalent. BPC_{15} is not symmetrical about a C_2 axis between the two phenyl rings and this results in different environments for two phenyl rings. Because of this, the aromatic rings showed four doublets in ^1H NMR spectrum and two sets of four aromatic shifts in ^{13}C spectrum as compared to only one set for symmetrical bis-phenols. The substituent on the cyclohexyl ring prevents the ring inversion of cyclohexyl ring and axial and equatorial phenyl groups can hence be distinguished.

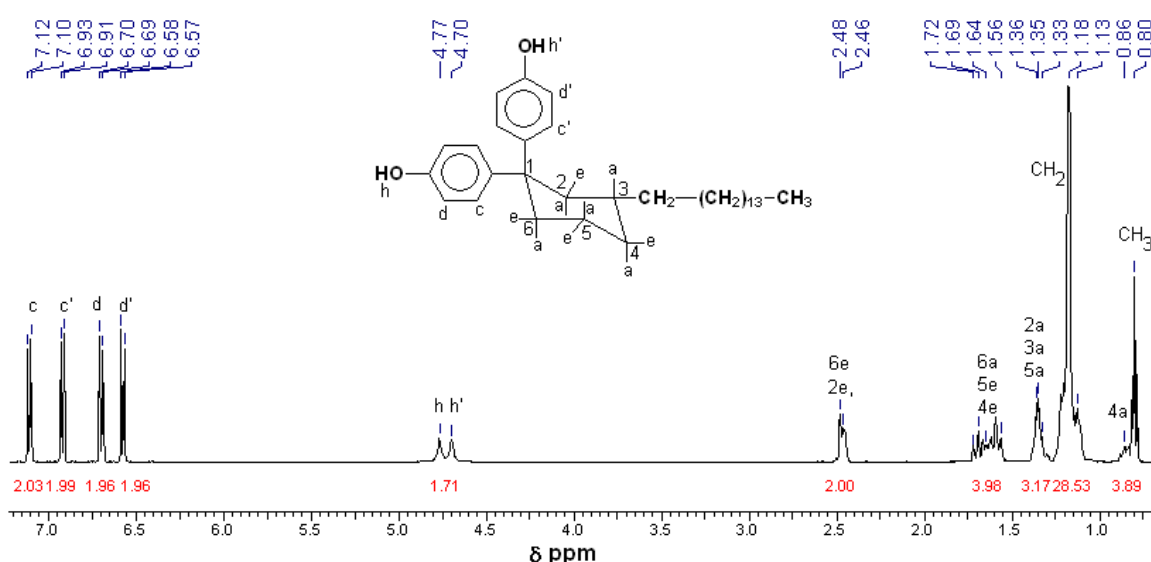


Figure 3.8 ^1H -NMR spectrum of 1,1-bis(4-hydroxyphenyl)-3-pentadecylcyclohexane

The protons of axial and equatorial phenyl rings can be distinguished. Two sets of doublets are observed in the region of 6.57 – 7.12 ppm. Protons *meta* to hydroxy of equatorial phenyl ring appeared at 7.11 ppm, while those for axial ring appeared at 6.92 ppm. Protons *ortho* to hydroxy of equatorial phenyl ring appeared at 6.70 ppm while those of axial ring appeared at 6.58 ppm. These assignments are based on the 2D NOESY experiment. The two hydroxyl protons appeared as two well resolved singlets at 4.77 and 4.70 ppm. Axial and equatorial protons of cyclohexyl rings appeared at different chemical shift values. Generally, the equatorial protons are found to appear at a lower field compared to the corresponding axial proton. A combination of COSY, NOESY and ^{13}C -

^1H HETCOR experiments have been used for the complete assignments of the protons. Two dimensional COSY, NOESY and ^{13}C - ^1H HETCOR spectra are reproduced in **Figure 3.9**, **3.10** and **3.11**, respectively.

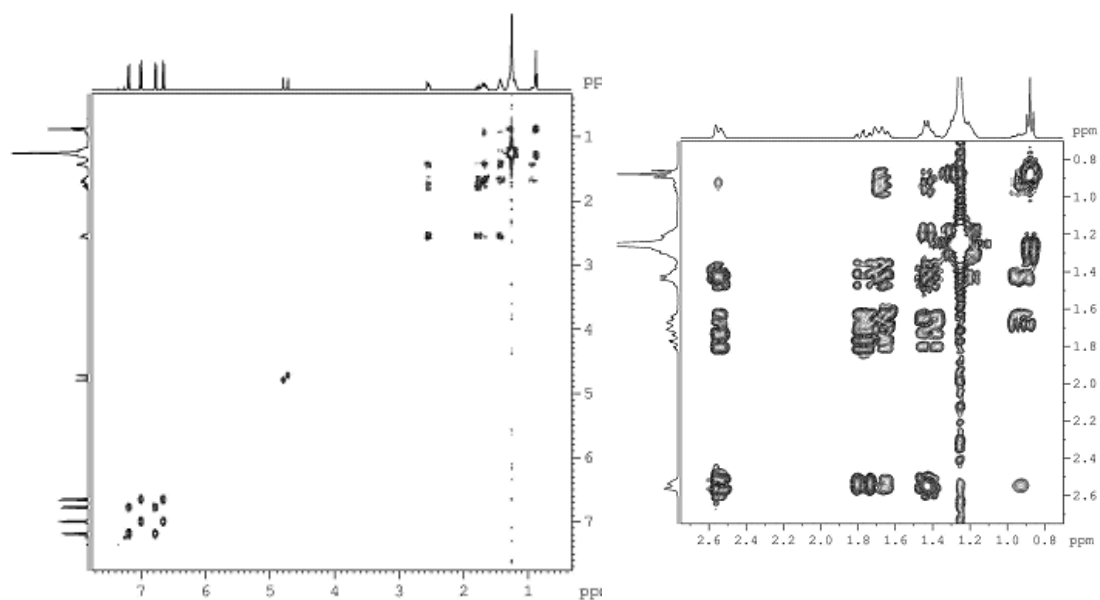


Figure 3.9 COSY spectrum of 1,1-bis(4-hydroxyphenyl)-3-pentadecylcyclohexane

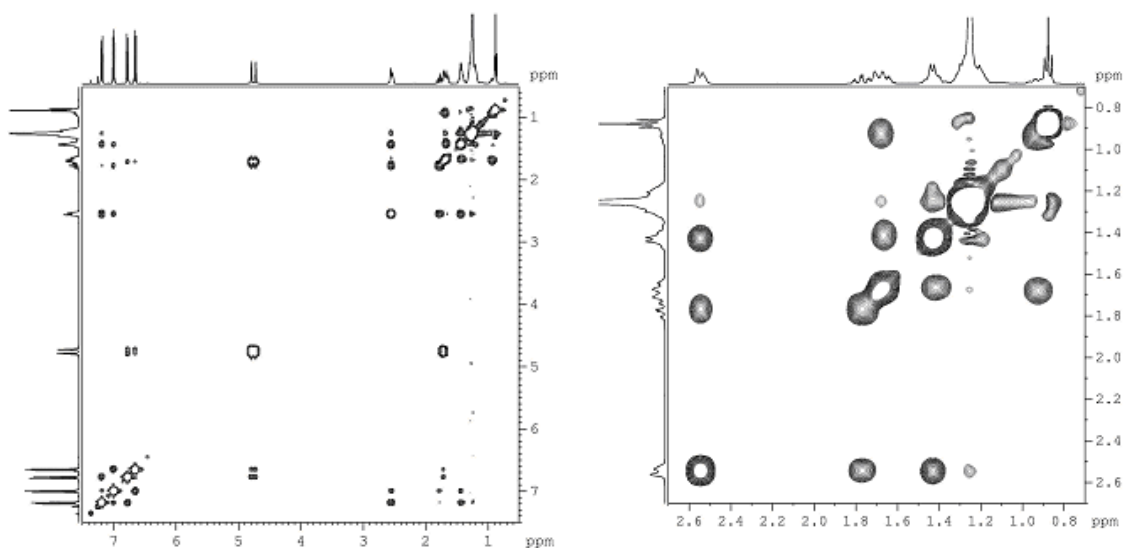


Figure 3.10 NOESY spectrum of 1,1-bis(4-hydroxyphenyl)-3-pentadecylcyclohexane

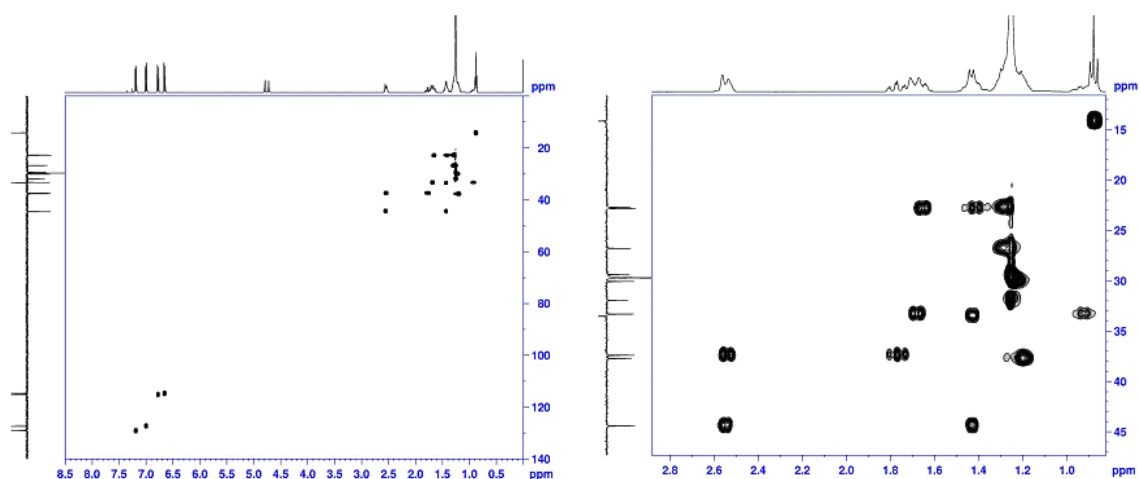


Figure 3.11 ^1H - ^{13}C HETCOR spectrum of 1,1-bis(4-hydroxyphenyl)-3-pentadecylcyclohexane

The protons of carbon 2 and 6 can be assigned unambiguously on the basis of their NOE's to the aromatic protons c and c'. The equatorial protons of carbon 2 and 6 are expected to be at a lower field compared to their axial counterparts.

Axial proton of carbon number 6 and equatorial protons of carbon number 4 and 5 appeared as multiplet in the region 1.69 – 1.59 ppm. Axial protons for carbon number 2, 3 and 4 appeared as multiplet in the region 1.36 – 1.32 ppm. Methylene protons of alkyl chain appeared in the region 1.21 – 1.12 ppm as broad multiplet. Axial proton of carbon number 4 and terminal methyl protons of alkyl chain appeared as distorted triplet and a multiplet in the region 0.90– 0.78 ppm.

The CH_2 group α to the terminal methyl group of alkyl chain and α to the cyclohexyl ring can be easily identified from the COSY spectrum and appear at 1.21 and 1.12 ppm respectively. The former one showed cross peak to the terminal CH_3 while the latter attached to the cyclohexyl ring shows cross peak to the axial proton of carbon 3, which made it possible to assign the axial proton of carbon 3. The multiplet centered at 0.9 ppm showed correlations to proton at \sim 1.59 ppm. The HETCOR experiment showed that these protons are attached to the same carbon at 33.09 ppm. These two protons also showed strong NOE. Moreover, a weak cross peak between equatorial proton of carbon 2 and equatorial proton of carbon 4 at \sim 1.59 ppm also confirms the assignment of carbon 4 and its protons.

A clear cut assignment of various protons and carbons can be made from the spectra recorded from C_6D_6 solution which gave better dispersion of the various cyclohexyl

protons except for axial proton attached to carbon 4 which was very close to the terminal CH₃ group. Partial ¹H NMR spectrum of BPC₁₅ in C₆D₆ is reproduced in **Figure 3.12**. Equatorial protons of carbon 2 and 6 have been resolved as two doublets and appear at 2.51 and 2.49 ppm, respectively.

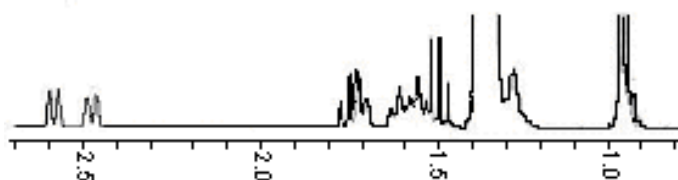


Figure 3.12 Partial ¹H-NMR spectrum of 1,1-bis(4-hydroxyphenyl)-3-pentadecylcyclohexane in C₆D₆

¹³C NMR spectrum of BPC₁₅ along with assignments is presented in **Figure 3.13**. Equatorial phenyl ring carbons appeared downfield compared to their axial phenyl ring partners. Carbons attached to hydroxyl group appeared as two peaks at 153.07 and 153.01 ppm for equatorial and axial phenyl rings, respectively. Carbons *para* to hydroxyl group appeared at 144.78 and 138.19 ppm. Carbons *meta* to hydroxyl group appeared at 129.15 and 127.35 ppm, whereas carbons *ortho* to hydroxyl group showed signal at 115.20 and 114.78 ppm. Aliphatic carbons were observed at higher field. Carbon 1, 2, 6, 3, 4 and 5 appeared at 45.59, 44.46, 37.73, 33.56, 33.35 and 22.85 ppm, respectively. Terminal CH₃ of alkyl chain showed signal at 14.07 ppm. All these assignments were made and confirmed with two dimensional NMR experiments.

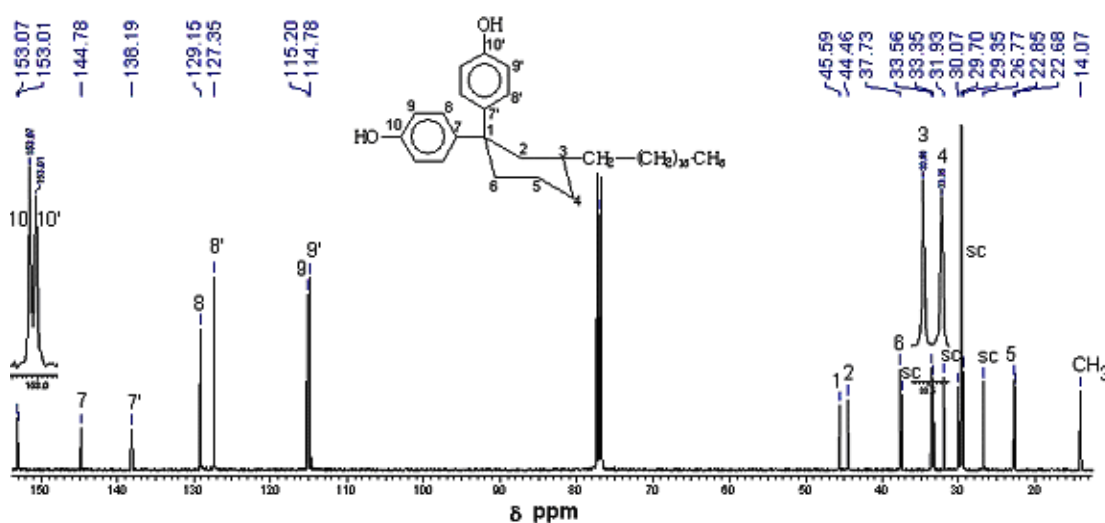


Figure 3.13 ¹³C-NMR spectrum of 1,1-bis(4-hydroxyphenyl)-3-pentadecylcyclohexane

X-ray crystallography provided unequivocal assignment of both chemical structure and configuration of cyclohexane ring.

Colorless single crystals of BPC₁₅ were grown from benzene solution. The X-ray crystal data for BPC₁₅ is given in **Table 3.1**.

Table 3.1. X-Ray crystal data for 1,1-bis(4-hydroxyphenyl)-3-pentadecyl-cyclohexane

Formula	C ₃₃ H ₅₀ O ₂
Formula weight	478.73
Crystal color	Colorless plates
Crystal size (mm ³)	0.70 x 0.62 x 0.23
Lattice parameters	
<i>a</i> (Å)	6.966(1)
<i>b</i> (Å)	9.927(2)
<i>c</i> (Å)	21.791(4)
α (deg)	87.897 (4)
β (deg)	83.038(4)
γ (deg)	84.867(4)
<i>V</i> (Å ³)	1489.1(5)
Crystal system	triclinic
Space group	P ⁻ 1
<i>Z</i>	2
Calculated density (mg m ⁻³)	1.068
μ (mm ⁻¹)	0.061
No. of measured reflections	14522
No. of observed reflections	5232
R	0.0480
R _w	0.0944

Table 3.2 Analysis of potential hydrogen bonds in 1,1-bis(4-hydroxyphenyl)-3-pentadecylcyclohexane crystals

Donor---H···Acceptor	H···A	D···A	D-H···A (°)
1 O(1) ---H(1) ··· O(2) ⁱ	1.9578	2.7457	160.87
1 O(2) ---H(2) ··· O(1) ⁱⁱ	1.9237	2.7020	158.12

Equivalent position code

i = 1-x,2-y,-z

ii = 1+x,-1+y,z

The ORTEP drawing of BPC₁₅ is shown in **Figure 3.14a**. Selected bond length and bond angle values are listed in **Appendix-1**. As is clearly seen from **Figure 3.14a**, the alkyl chain of the molecule is in all-*trans* conformation. The torsion angles observed for the alkyl chain region are all in the neighborhood of 180° and are fully in agreement with above observation. Packing diagram for BPC₁₅ is presented in **Figure 3.14b**. The BPC₁₅ molecules are packed head-to-head (and tail-to-tail) similar to arrangement in stacked bilayers. The O-H···O hydrogen bonds between the head groups (phenolic -OH) of opposite layers of the bilayer are most likely the driving force for this arrangement (**Table 3.2**). The alkyl chains of the adjacent molecules are in van der Waals contacts, with a distance of 6.592 Å. The hydrogen bonding pattern observed in the crystal lattice of BPC₁₅ is depicted in **Figure 3.14b**. **Figure 3.14b** gives a picture of molecular packing together with the hydrogen bonds between the hydroxyl groups in opposite layers. Each hydroxyl group is involved in two hydrogen bonds, one as hydrogen bond donor and other as hydrogen bond acceptor. From **Figure 3.14b**, it is clear that O-H···O hydrogen bonds form four-member ring structure.

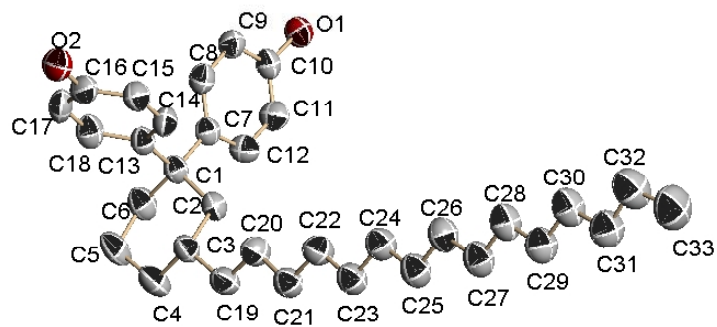


Figure 3.14a ORTEP diagram for 1,1-bis(4-hydroxyphenyl)-3-pentadecylcyclohexane. Ellipsoids are drawn at 50% probability level.

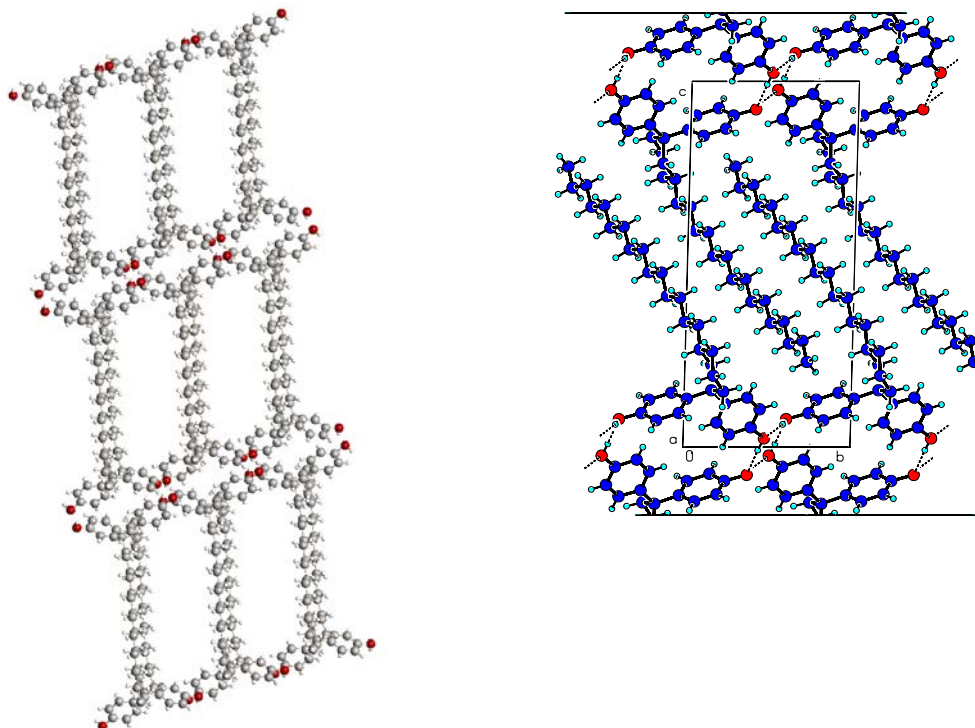
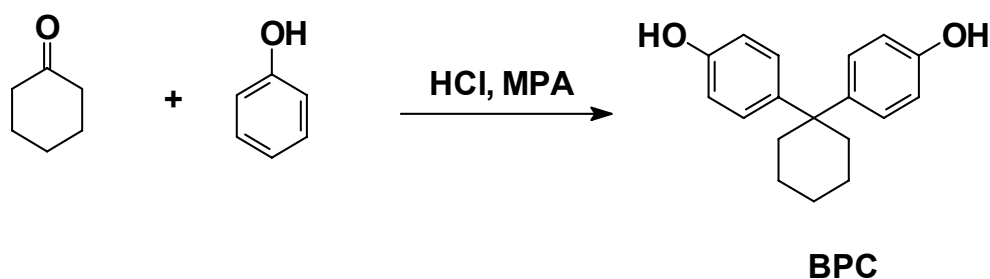


Figure 3.14b Packing diagram for 1,1-bis(4-hydroxyphenyl)-3-pentadecylcyclohexane molecules

3.4.2 Synthesis and characterization of 1,1-bis(4-hydroxyphenyl)cyclohexane

Cyclohexanone has been exploited for synthesis of various value added chemicals and polymers *via* various organic transformations. Cyclohexanone has been condensed with phenol and substituted phenols to get cyclohexylidene containing bisphenols. In the present, study bisphenol based on cyclohexanone was synthesized to compare the properties of polyesters derived from cyclohexylidene containing bisphenols and substituted cyclohexylidene containing bisphenols.

Scheme 3.2 outlines route for synthesis of 1,1-bis(4-hydroxyphenyl)cyclohexane (BPC).



Scheme 3.2 Synthesis of 1,1-bis(4-hydroxyphenyl)cyclohexane

Cyclohexanone was reacted with excess phenol in the presence of HCl and 3-MPA. The solid product obtained at the end of reaction was dissolved in ethyl acetate and neutralized by sodium bicarbonate solution followed by water wash. Ethyl acetate was distilled off under vacuum to obtain resinous mass. Upon addition of pet-ether white solid was separated out. The crude product was crystallized twice from mixture of pet-ether and benzene (8:2, v/v).

BPC was characterized by FTIR, ^1H and ^{13}C NMR spectroscopy.

FTIR spectrum exhibited a broad absorption band at 3282 cm^{-1} corresponding to $-\text{OH}$ stretching.

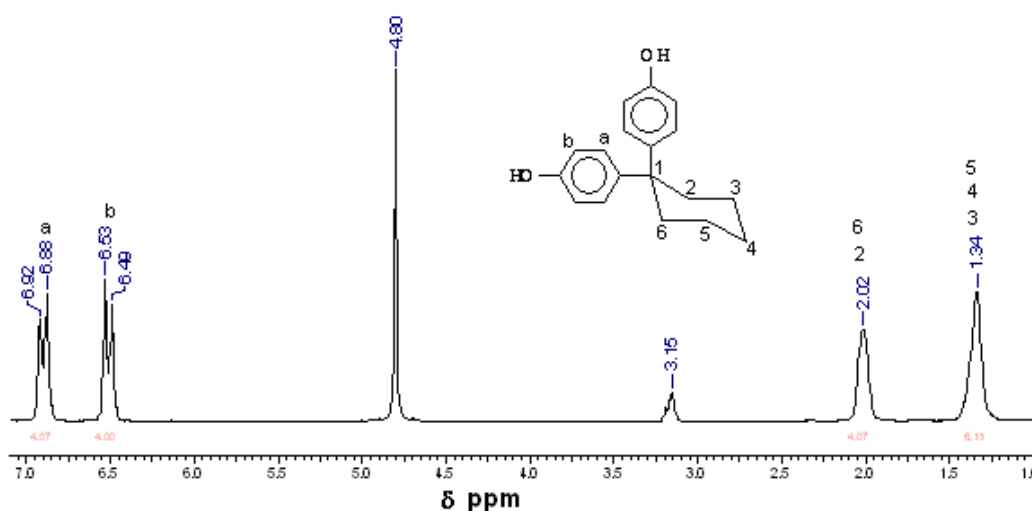


Figure 3.15 ^1H -NMR spectrum of 1,1-bis(4-hydroxyphenyl)cyclohexane in CD_3OD

^1H NMR spectrum of BPC (**Figure 3.15**) showed a set of doublets for aromatic protons. Since cyclohexyl rings undergoes ring inversion the axial and equatorial phenyl rings are in equilibrium and spectrum appears as that of symmetrical bisphenols. Doublet at 6.90 ppm corresponds to the protons *ortho* to hydroxyl group, whereas protons *meta* to hydroxyl group appears at 6.51 ppm. Unlike in case of substituted cyclohexanone derived bisphenol (BPC_{15}), aliphatic region showed only two broad peaks. Protons attached to carbon number 2 and 6 appeared as a broad peak at 2.02 ppm and those attached to carbon number 3, 4 and 5 appeared at 1.34 ppm.

^{13}C NMR spectrum of BPC along with individual carbon assignments is presented in **Figure 3.16**, which confirmed the symmetric nature of BPC molecule.

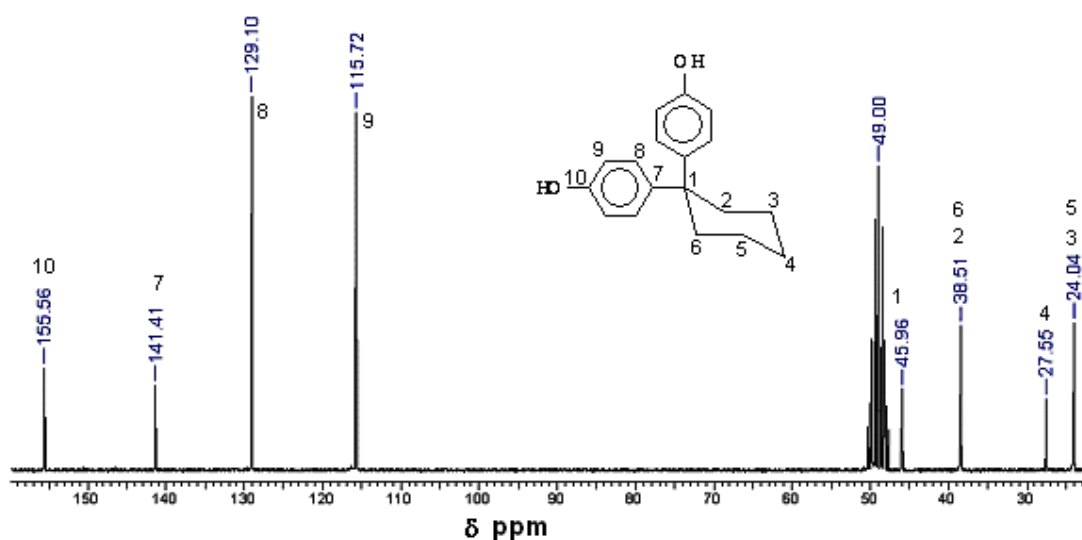
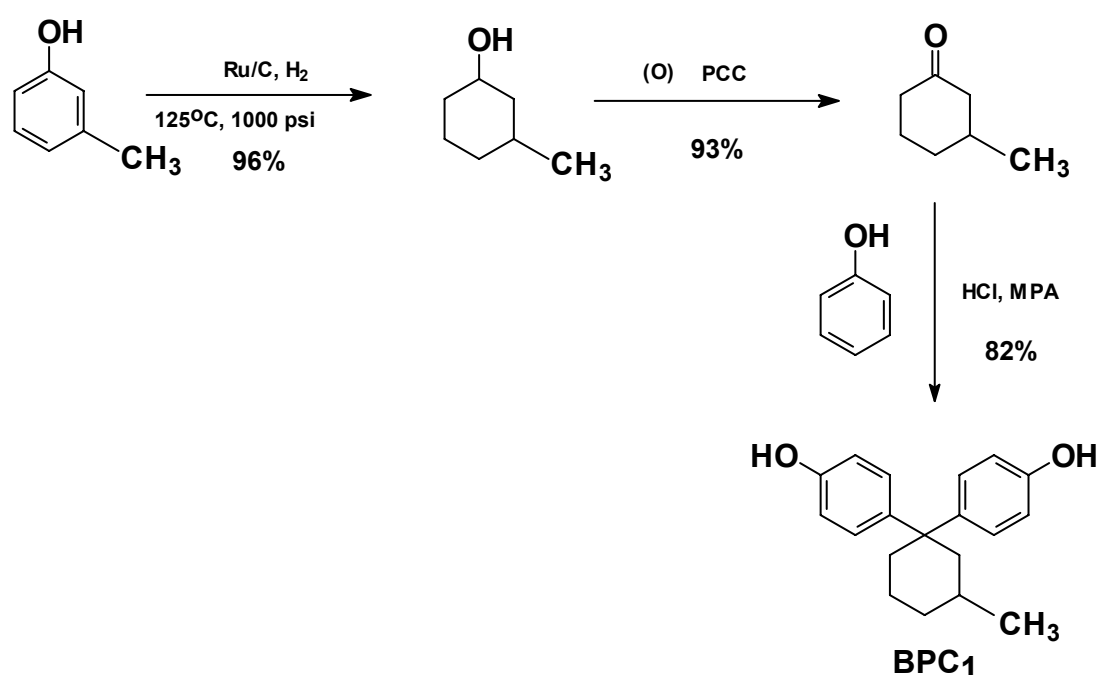


Figure 3.16 ^{13}C -NMR spectrum of 1,1-bis(4-hydroxyphenyl)cyclohexane in CD_3OD

3.4.3 Synthesis and characterization of 1,1-bis(4-hydroxyphenyl)-3-methylcyclohexane

The synthesis of 1,1-bis(4-hydroxyphenyl)-3-methylcyclohexane (BPC₁) was undertaken for two reasons. a) to understand the effect of alkyl substituent at position three of cyclohexyl ring on the ¹H-NMR spectral shifts of cyclohexylidene containing bisphenols and b) to check the effect of methyl substitution on the solubility of aromatic polyesters derived therefrom.

Scheme 3.3 outlines the route for synthesis of BPC₁.



Scheme 3.3 Synthesis of 1,1-bis(4-hydroxyphenyl)-3-methylcyclohexane

BPC₁ was synthesized starting from 3-methylphenol by the hydrogenation to get 3-methylcyclohexanol, which was oxidized to 3-methylcyclohexanone. 3-Methylcyclohexanone was condensed with excess phenol in presence of HCl and 3-MPA as discussed in **Section 3.4.1**.

BPC₁ was characterized by FTIR, ¹H and ¹³C-NMR spectroscopy.

FTIR spectrum showed a broad absorption band at 3275 cm⁻¹ corresponding to –OH stretching.

^1H -NMR spectrum exhibited upfield shift of the axial proton of carbon four of cyclohexyl ring as observed in case of BPC_{15} and was confirmed by the two dimensional NMR spectroscopy. Axial proton of carbon 4 of BPC_1 and BPC_{15} appeared at 0.89 and 0.86 ppm, respectively.

^1H and ^{13}C NMR spectra for BPC_1 along with assignment are presented in Figure 3.17 and 3.18, respectively.

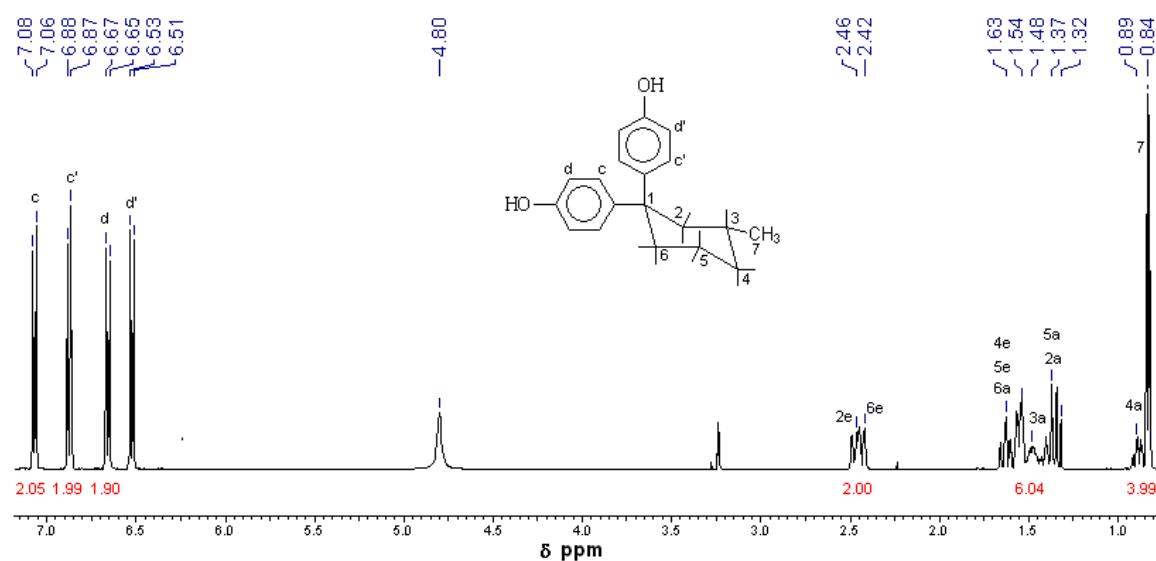


Figure 3.17 ^1H -NMR spectrum of 1,1-bis(4-hydroxyphenyl)-3-methylcyclohexane in CD_3OD

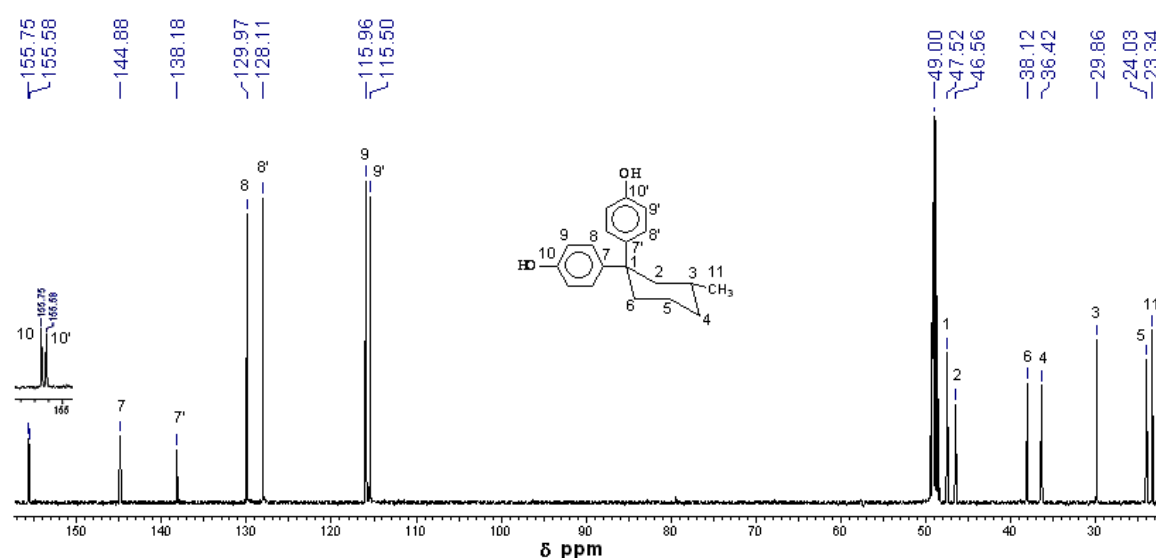


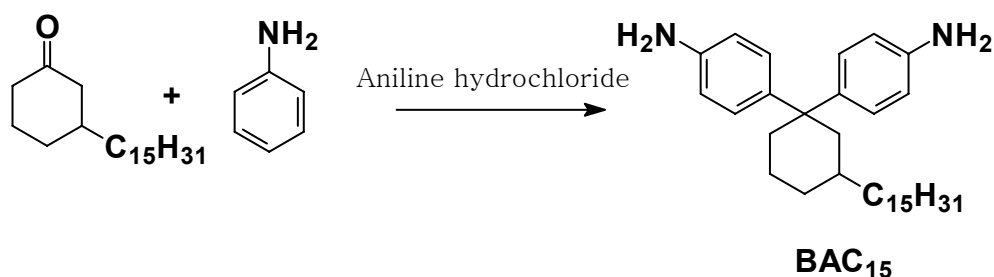
Figure 3.18 ^{13}C -NMR spectrum of 1,1-bis(4-hydroxyphenyl)-3-methylcyclohexane in CD_3OD

3.4.4 Synthesis and characterization of 1,1-bis(4-aminophenyl)-3-pentadecylcyclohexane

Diamines constitute a highly significant class of starting materials in the manufacture of a variety of polymers such as polyimides, polyamides, polyazomethines, polyurethanes, polyureas, etc. Various methods have been developed for the preparations of amines such as, replacement of halogen atom of alkyl or aryl halide by amino group, reduction of nitro compounds, alkaline hydrolysis of isocyanates, etc. Another method for the synthesis of diamines is to react aldehydes or ketones with aniline.³⁵⁻³⁷

Scheme 3.4 depicts route for synthesis of 1,1-bis(4-aminophenyl)-3-pentadecylcyclohexane (BAC₁₅)

The reaction of aniline with 3-pentadecyl cyclohexanone in the presence of aniline hydrochloride under reflux condition yielded BAC₁₅.



Scheme 3.4 Synthesis of 1,1-bis(4-aminophenyl)-3-pentadecylcyclohexane

The structure of the BAC₁₅ was confirmed by FTIR, ¹H and ¹³C-NMR spectroscopy. FTIR spectrum (**Figure 3.19**) of BAC₁₅ showed absorption bands at 3412 and 3338 cm⁻¹ indicating the presence of primary amino group.

¹H NMR spectrum (**Figure 3.20**) of BAC₁₅ showed the presence of four doublets in the aromatic region indicating the nonequivalent nature of the phenyl rings as in case of BPC₁₅. Aliphatic protons of BAC₁₅ exhibited similar pattern as that of BPC₁₅. Axial proton of carbon 4 of BAC₁₅ appeared at 0.88 ppm along with terminal CH₃ of pentadecyl chain. The equatorial protons of carbon 2 and 6 appeared down field at 2.51 and 2.53 ppm, respectively. The axial protons of carbon 6 and equatorial protons of carbon 4 and 5 appeared as multiplet in the region 1.74-1.61 ppm. Axial protons for carbon 2, 3 and 4 appeared as multiplet in the region 1.43-1.37 ppm. Methylene protons of alkyl chain

appeared as broad multiplet centered at 1.26 ppm. ^{13}C -NMR spectrum (Figure 3.21) showed two sets of four aromatic shifts.

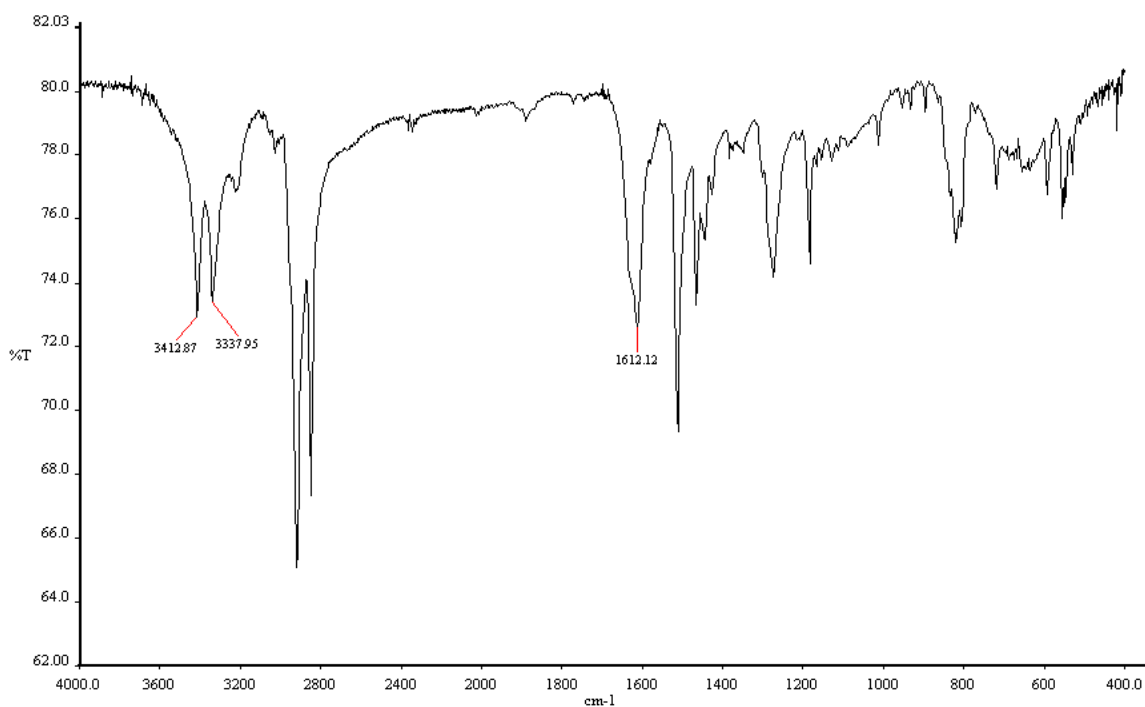


Figure 3.19 FTIR spectrum of 1,1-bis(4-aminophenyl)-3-pentadecylcyclohexane

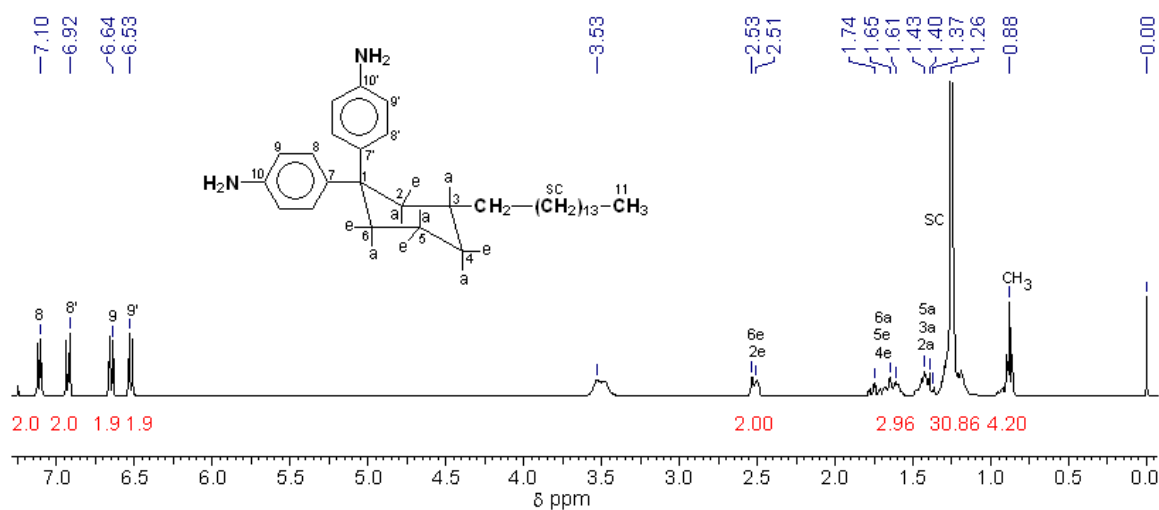


Figure 3.20 ^1H -NMR spectrum of 1,1-bis(4-aminophenyl)-3-pentadecylcyclohexane

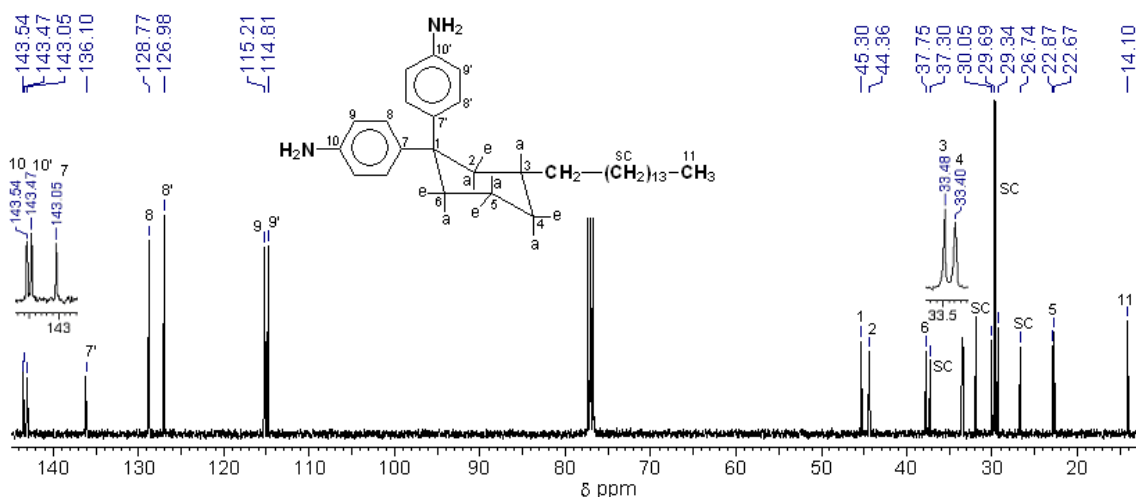


Figure 3.21 ¹³C-NMR spectrum of 1,1-bis(4-aminophenyl)-3-pentadecyl-cyclohexane

3.4.5 Synthesis and characterization of bisphenols derived from *p*-cumylphenol

Desired polymer properties can be achieved by careful design of the monomers. Introduction of the cardo groups into the polymer backbone has led to a valuable set of properties: the combination of increased thermal stability with an increased solubility in organic solvents because of specific contribution of the cardo group. *p*-Cumylphenol is commercially available raw material. Substituted cyclohexanone can be derived from *p*-cumylphenol through simple organic transformations and which can be used for the synthesis of various cardo monomers.

Five new bisphenol monomers with systematic variation in structure were designed and synthesized starting from *p*-cumylphenol to understand the structure property relationship of the polyesters. Following five bisphenols were designed and synthesized.

1,1-Bis(4-hydroxyphenyl) -4-perhydrocumyl cyclohexane

1,1-Bis(4-hydroxy-3-methylphenyl) -4-perhydrocumyl cyclohexane

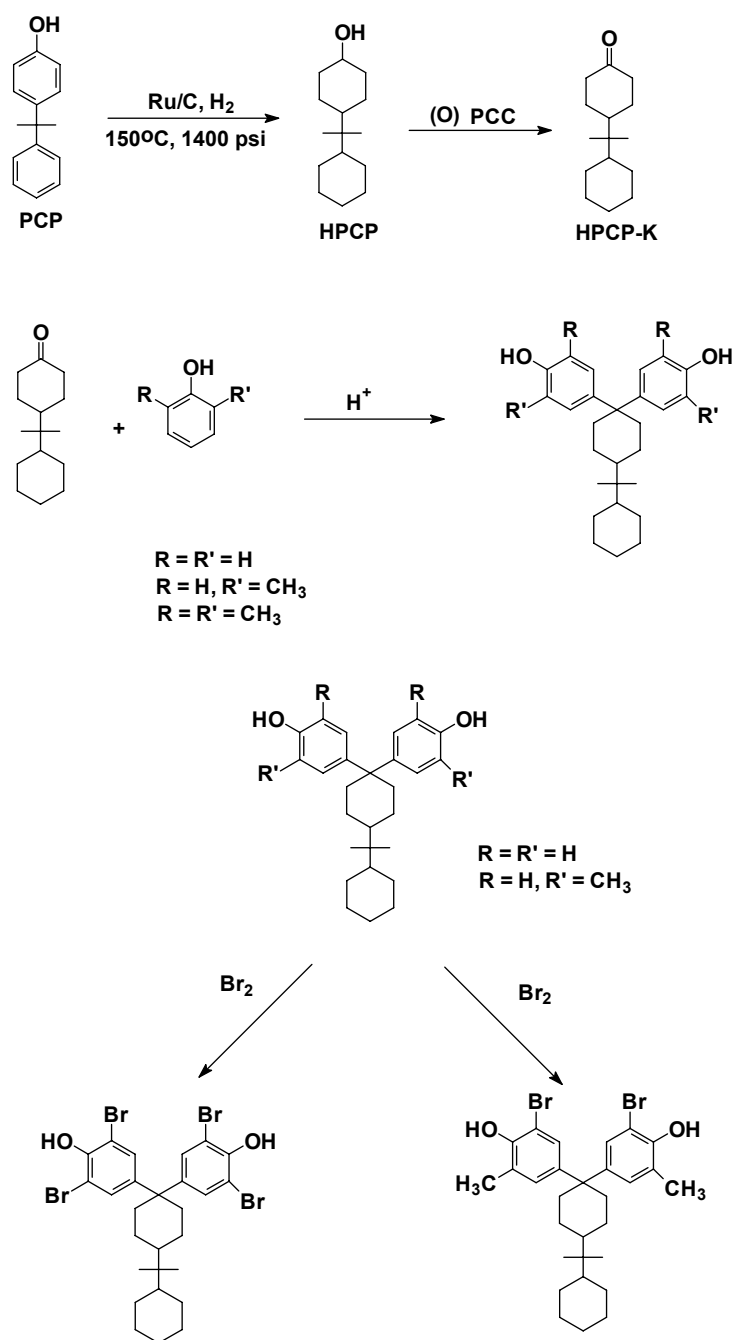
1,1-Bis(4-hydroxy-3,5-dimethylphenyl) -4-perhydrocumyl cyclohexane

1,1-Bis(4-hydroxy-3,5-dibromophenyl) -4-perhydrocumyl cyclohexane

1,1-Bis(4-hydroxy-3-methyl-5-bromophenyl) -4-perhydrocumyl cyclohexane

Systematic variation in the bisphenol molecule was achieved using simple organic reaction sequences.

Scheme 3.5 depicts route for the synthesis of five new bisphenols starting from *p*-cumylphenol.



Scheme 3.5 Synthesis of bisphenols starting from *p*-cumylphenol

p-Cumylphenol was used as a starting material for the synthesis of 4-(1-cyclohexyl-1-methylethyl)cyclohexanone, hereafter will be referred as perhydrocumylcyclohexanone.

In the first step *p*-cumylphenol was hydrogenated using Ru/C as a catalyst in Parr reactor using isopropanol as solvent. The reaction was stopped when hydrogen absorption had ceased. The catalyst was filtered off and filtrate with blackish tinge was passed through short column of silica gel (100-200 mesh) to obtain colorless solution. Solvent was

distilled off at reduced pressure and the residue was treated with 10% NaOH at reflux temperature for 2 hours. The reaction mixture was extracted in dichloromethane and washed with water to ensure the complete removal of any unreacted *p*-cumylphenol. Solvent was distilled off to obtain viscous liquid, which got partially crystallized on prolonged standing. Serijan et. al.³⁸ separated the solid and crystallized it from petroleum ether. The solid obtained melted over a temperature range of 80-90°C and inferred to be one of the geometric isomer of 4-(1-cyclohexyl-1-methylethyl)cyclohexanol, hereafter will be referred as perhydrocumylcyclohexanol. The product was characterized by FTIR and NMR spectroscopy. FTIR spectrum (**Figure 3.22**) showed the absence of C=C stretch corresponding to aromatic ring around 1600 cm⁻¹ and showed a band at 3275 cm⁻¹ corresponding to hydroxyl stretching.

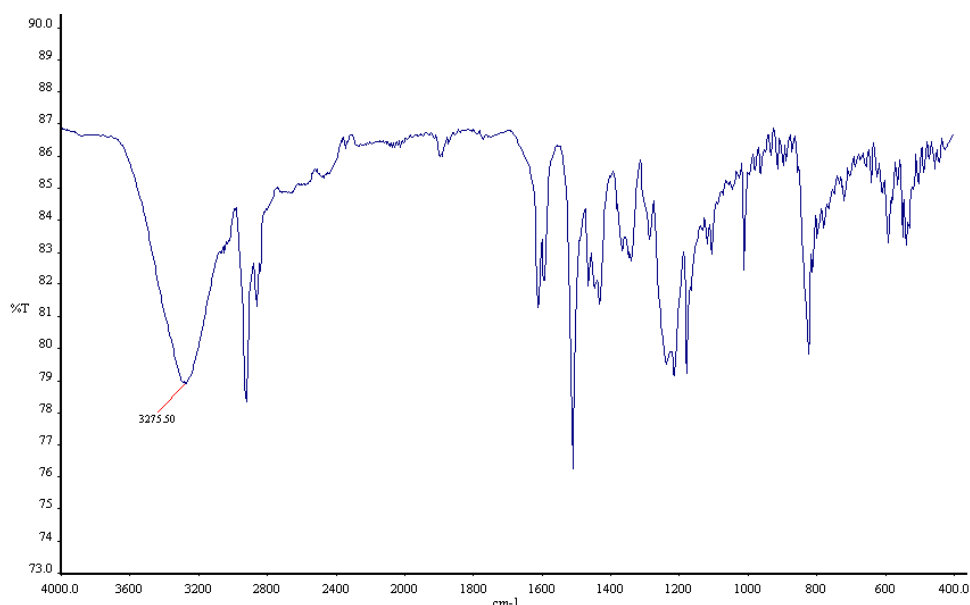


Figure 3.22 FTIR spectrum of perhydrocumylcyclohexanol

Two isomers can be distinguished by ¹H-NMR spectroscopy as proton ‘a’ and ‘e’ appear at 3.52 and 4.02 ppm, respectively (**Figure 3.26**). However, isomer separation and detailed analysis was not carried out as it was beyond the scope of work.

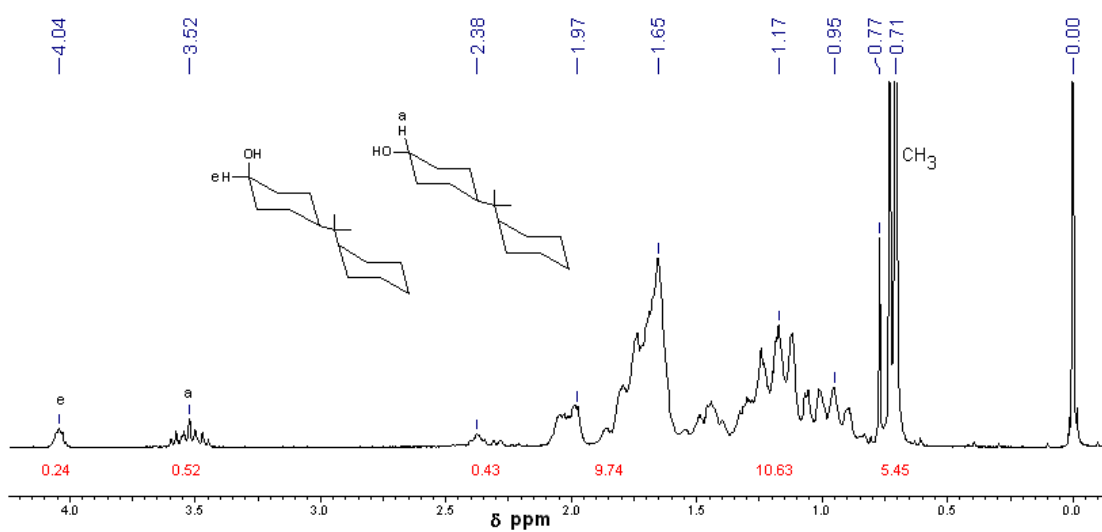


Figure 3.23 $^1\text{H-NMR}$ spectrum of perhydrocumylcyclohexanol

In the second step, perhydrocumylcyclohexanol was oxidized using PCC. The reaction could be monitored by FTIR spectroscopy. FTIR spectrum (**Figure 3.24**) showed the presence of C=O stretch at 1720 cm^{-1} and absence of hydroxyl band around 3300 cm^{-1} . $^1\text{H-NMR}$ spectrum (**Figure 3.25**) showed the absence of protons adjacent to hydroxyl at 3.52 and 4.04 ppm.

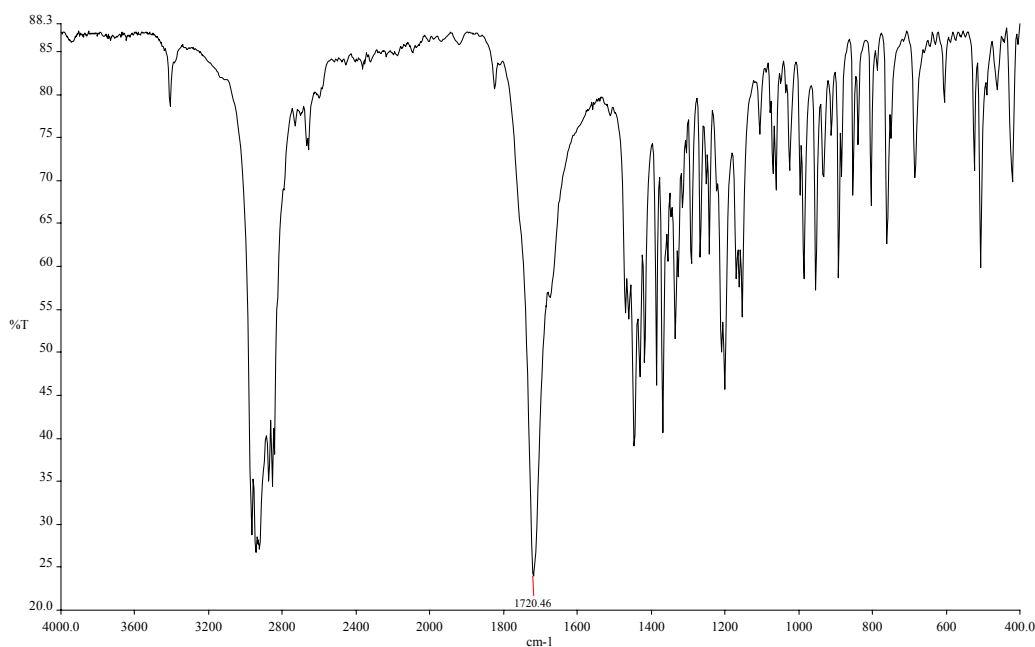


Figure 3.24 FTIR spectrum of perhydrocumylcyclohexanone

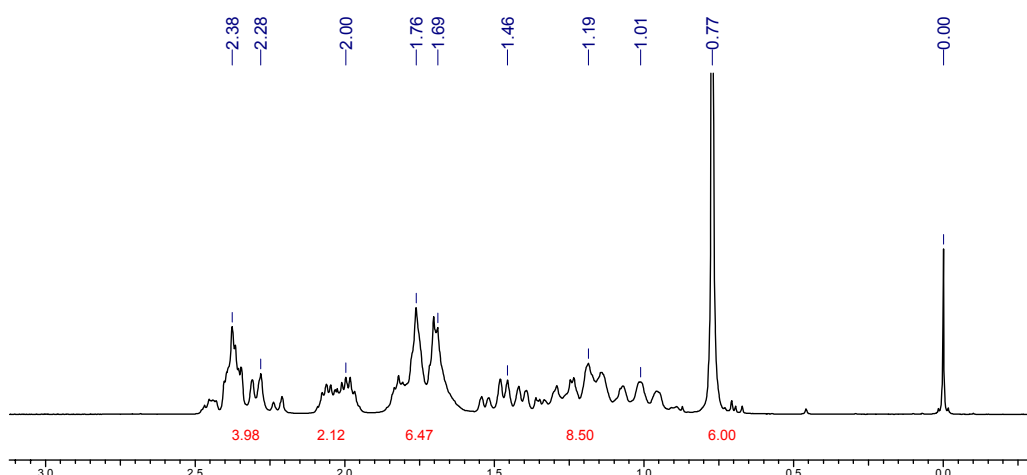


Figure 3.25 $^1\text{H-NMR}$ Spectrum of perhydrocumylcyclohexanone

3.4.5.1 Synthesis and characterization of 1,1-bis(4-hydroxyphenyl) -4-perhydrocumyl cyclohexane

1,1-Bis(4-hydroxyphenyl) -4-perhydrocumyl cyclohexane (BPPCP) was prepared by the hydrogen chloride-3MPA catalyzed condensation of perhydrocumylcyclohexanone with phenol. BPPCP was crystallized twice from toluene. Unlike bisphenol-A, which forms a crystalline 1:1 adduct with phenol, BPPCP does not crystallize as 1:1 adduct with phenol. The purity of BPPCP was confirmed by HPLC, and was found to be >99.9% (**Figure 3.26**).

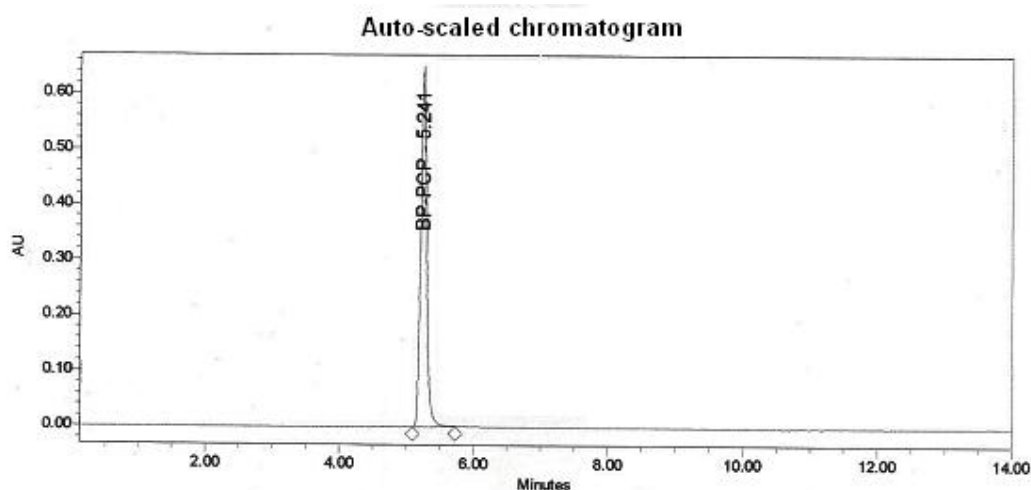


Figure 3.26 HPLC trace of 1,1-bis(4-hydroxyphenyl) -4-perhydrocumyl cyclohexane

BPPCP was characterized by FTIR, ^1H and ^{13}C NMR spectroscopy.

FTIR spectrum of BPPCP showed a broad band at 3296 cm^{-1} corresponding to $-\text{OH}$ stretching.

^1H NMR spectrum showed the presence of distereotopic phenyl rings, which are magnetically non-equivalent. BPPCP is not symmetrical about a C_2 axis between the two phenolic rings and this results in different environments for two phenyl rings. Because of this, the aromatic rings showed four doublets in ^1H NMR spectrum and two sets of four aromatic shifts in ^{13}C spectrum as compared to only one set for symmetrical bisphenols (eg., BPC **Figure 3.15** and **3.16**). The substituent on the cyclohexyl ring prevents the ring inversion of cyclohexyl ring and making possible the distinction between axial and equatorial phenyl rings.

^1H NMR and ^{13}C NMR spectra along with the assignments are presented in **Figure 3.27** and **3.28**, respectively. Assignments for aromatic protons were easy and straightforward as compared to aliphatic protons. The presence of two substituted cyclohexyl rings complicate the assignment of the spectrum. Two dimensional NMR experiments were designed and the assignments to each proton could be made possible. These proton assignments were used for assigning individual carbons. COSY, NOESY and ^1H - ^{13}C HETCOR spectra for BPPCP are reproduced in **Figure 3.29**, **3.30** and **3.31**, respectively. TOCSY Spectrum (**Figure 3.32**) made it possible to identify protons of two cyclohexyl rings.

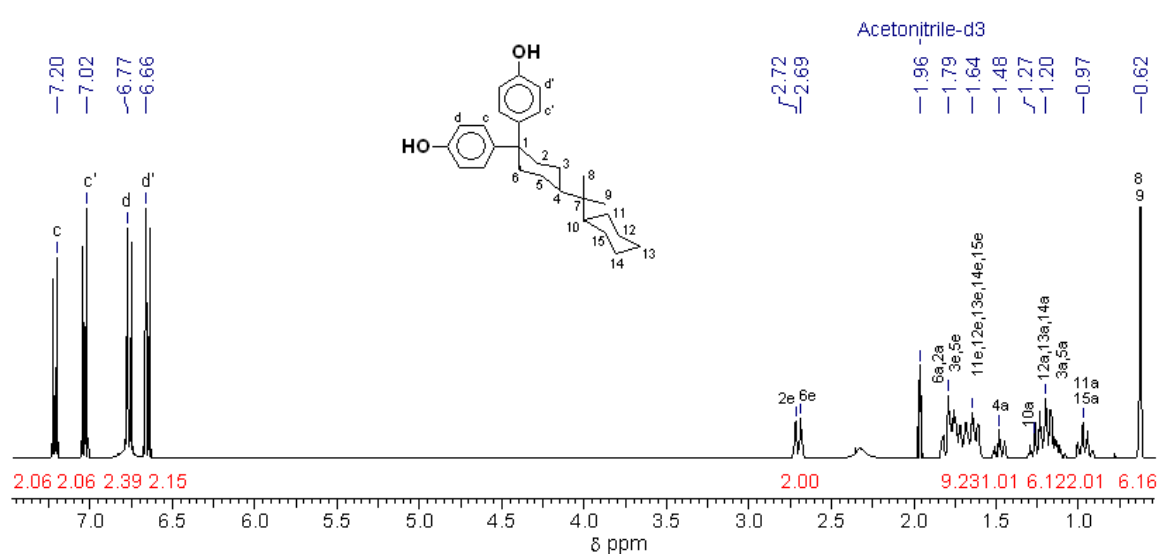


Figure 3.27 ^1H NMR spectrum of 1,1-bis(4-hydroxyphenyl)-4-perhydrocumyl cyclohexane in CD_3CN

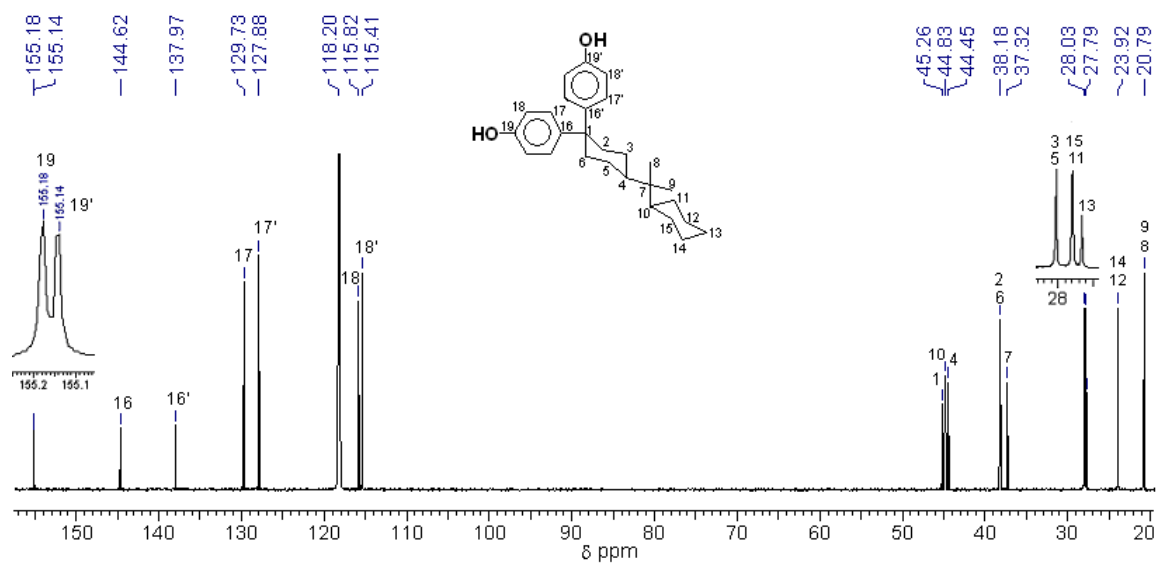


Figure 3.28 ^{13}C NMR spectrum of 1,1-bis(4-hydroxyphenyl)-4-perhydrocumyl cyclohexane

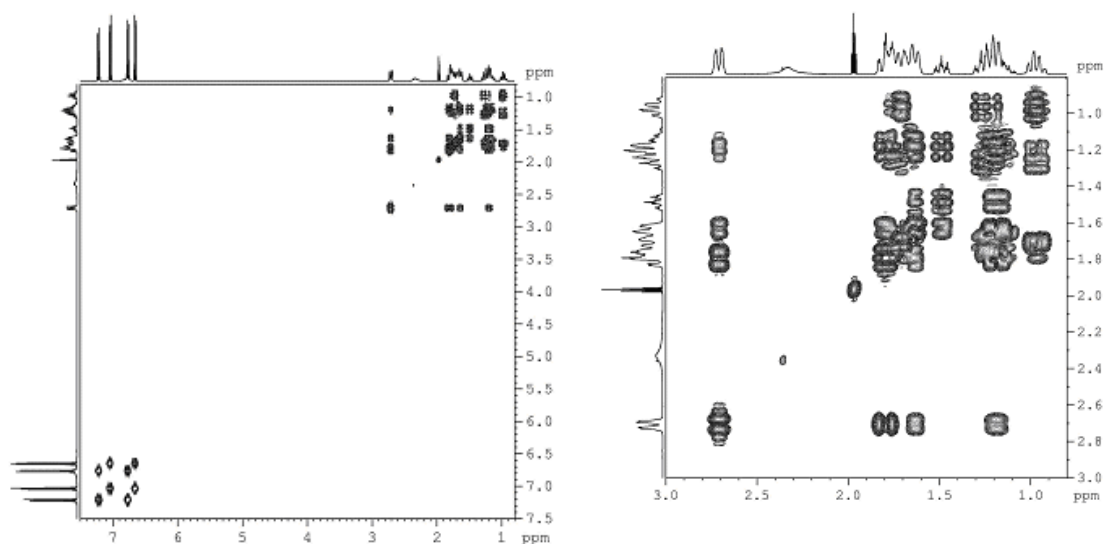


Figure 3.29 COSY spectrum of 1,1-bis(4-hydroxyphenyl)-4-perhydrocumyl cyclohexane

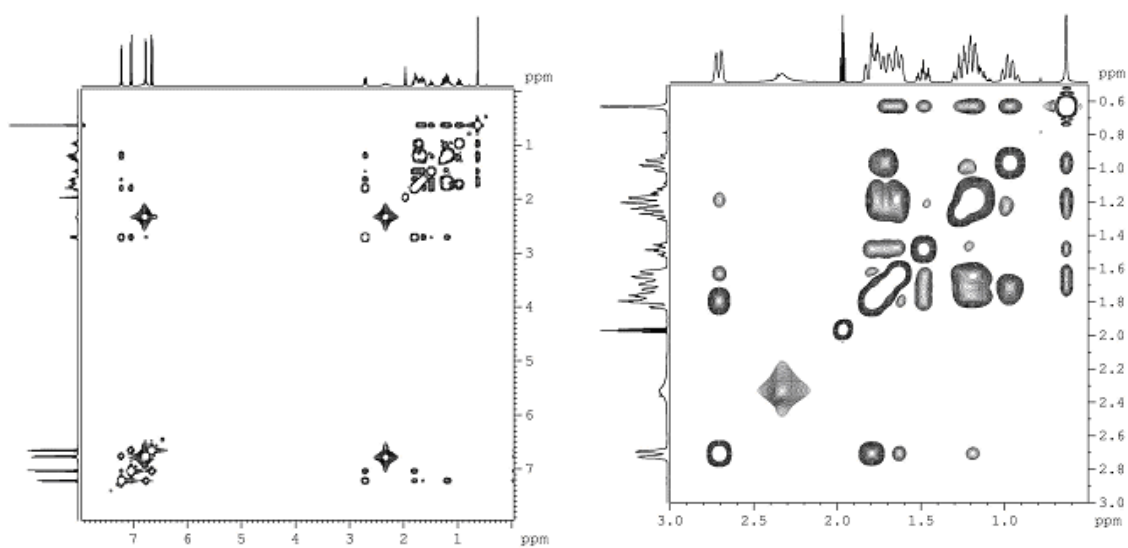


Figure 3.30 NOESY spectrum of 1,1-bis(4-hydroxyphenyl) -4-perhydrocumyl cyclohexane

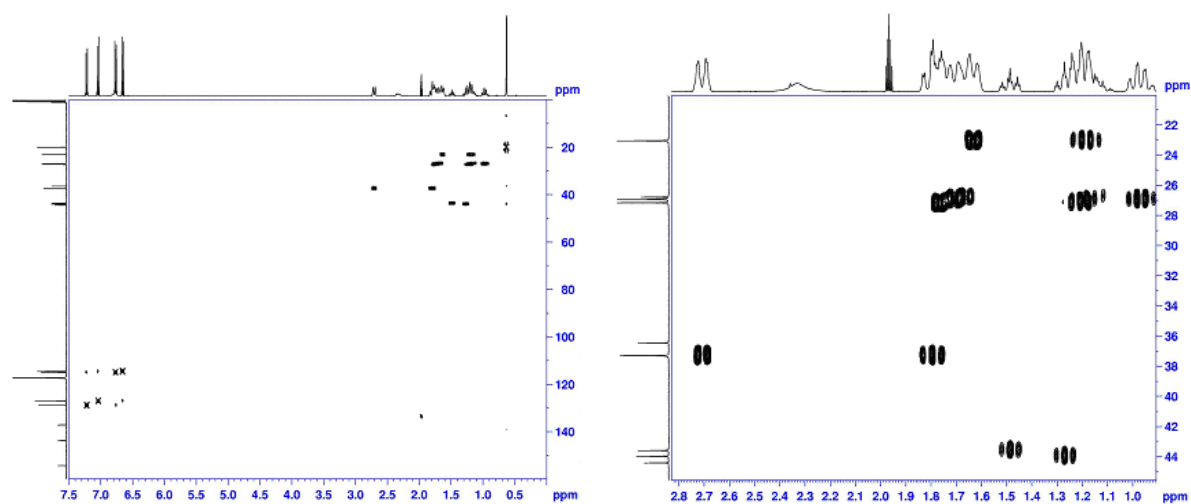


Figure 3.31 ^1H - ^{13}C -HETCOR spectrum of 1,1-bis(4-hydroxyphenyl) -4-perhydrocumyl cyclohexane

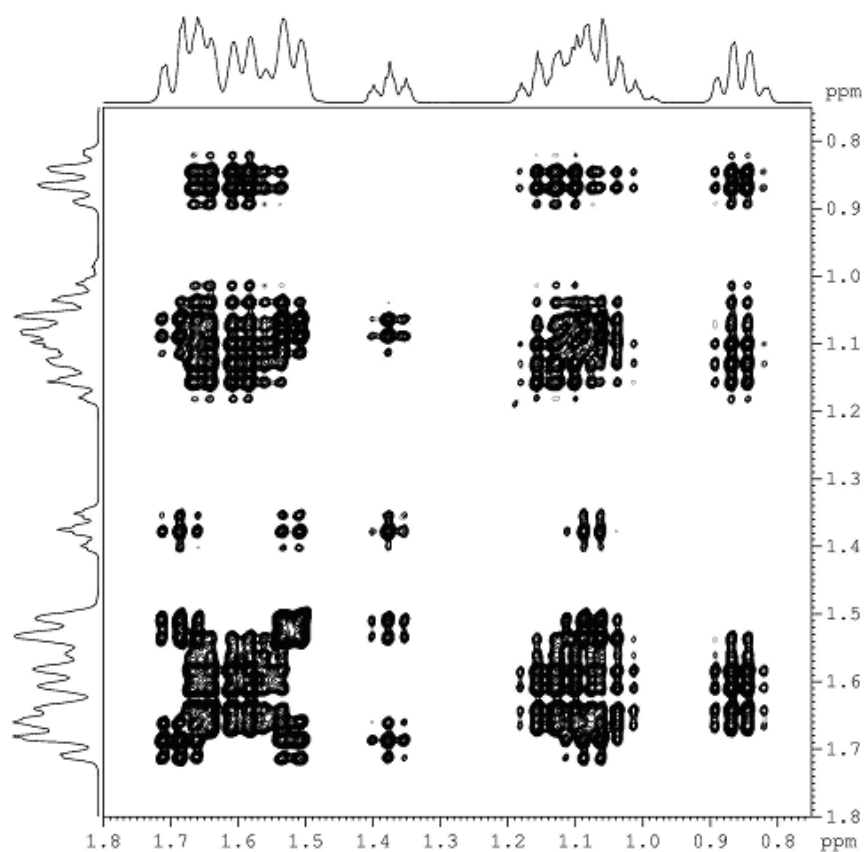


Figure 3.32 Partial TOCSY spectrum of 1,1-bis(4-hydroxyphenyl)-4-perhydrocumyl cyclohexane

The structure of BPPCP was further detailed by single-crystal X-ray analysis.

Single crystals of BPPCP were grown from ethanol solution. The X-ray crystal data for BPPCP is given in **Table 3.3**.

Table 3.3 X-Ray crystal data for 1,1-bis(4-hydroxyphenyl) -4-perhydrocumyl cyclohexane

Formula	(C ₂₇ H ₃₆ O ₂).CH ₃ CH ₂ OH
Formula weight	438.63
Crystal color	Colorless
Crystal size (mm ³)	0.38 x 0.27 x 0.05
Crystal system	Monoclinic
Lattice parameters	
<i>a</i> (Å)	6.4260(8)
<i>b</i> (Å)	36.529(5)
<i>c</i> (Å)	12.247(1)
β (°)	115.974(2)
<i>V</i> (Å ³)	2584.4(5)
Space group	P2 ₁ /c
Z	4
Calculated density (mg m ⁻³)	1.127
No. of measured reflections	15815
No. of observed reflections	3713
R	0.0563
R _w	0.1396
Theta range for data collection	2.16 to 23.28 °
Completeness to theta = 23.28	99.7%

Table 3.4 Analysis of potential hydrogen bonds in 1,1-bis(4-hydroxyphenyl) -4-perhydrocumyl cyclohexane

Donor---H···Acceptor	H···A	D···A	D-H···A (°)
1 O(1) ---H(1) ··· O(2) ⁱ	1.92	2.739	176
1 O(2) ---H(2) ··· O(3) ⁱⁱ	1.80	2.604	168
2 O(3) ---H(3) ··· O(1) ⁱⁱⁱ	2.01	2.791	159

Equivalent position code
i = 1-x,y,1+z
ii= 1-x,2-y,1-z
iii= 1-x,2-y,2-z

The ORTEP drawing of BPPCP is shown in **Figure 3.33a** and packing diagram is presented in **Figure 3.33b**. Selected bond length and bond angle values are listed in

Appendix-2. As can be seen from crystal data in **Table 3.3** and **Figure 3.33**, ethanol molecule has been crystallized along with BPPCP. Generally, crystallization begins with solute-solvent aggregates that contain solute-solute, solute-solvent and solvent-solvent interactions. The entropic gain in eliminating solvent molecules from these aggregates into the bulk solution, and the simultaneous enthalpic gain in forming stable solute species that contain robust supramolecular synthons, provides adequate driving force for nucleation and crystallization with the result that most (85%) organic crystals are unsolvated. However, when solvent molecules are attached to solute molecules in a multi-point manner via either strong (O/N-H...O) or weak (C-H...O) hydrogen bonds, the extrusion of solvent from aggregates into the bulk may become sufficiently disadvantageous from an enthalpic viewpoint with the result that the solvent remains an integral part of nucleating crystal.³⁹ Multi-point recognition with strong hydrogen bonds between ethanol and BPPCP molecules might have facilitated the retention of ethanol molecule in BPPCP crystals (**Table 3.4**).

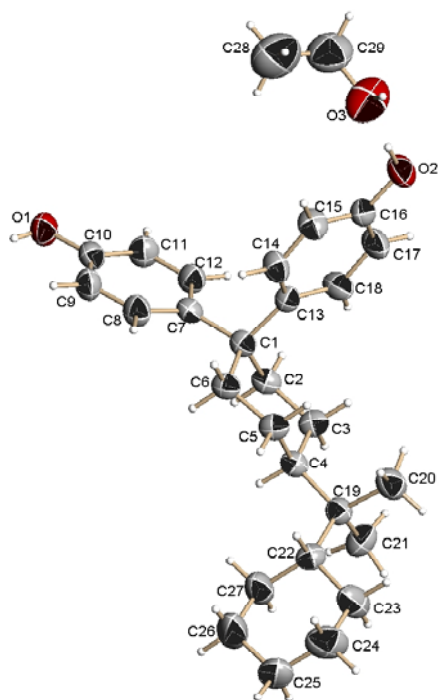


Figure 3.33a ORTEP diagram for 1,1-bis(4-hydroxyphenyl) -4-perhydrocumyl cyclohexane along with solvent molecule (ethanol). Ellipsoids are drawn at 50% probability level.

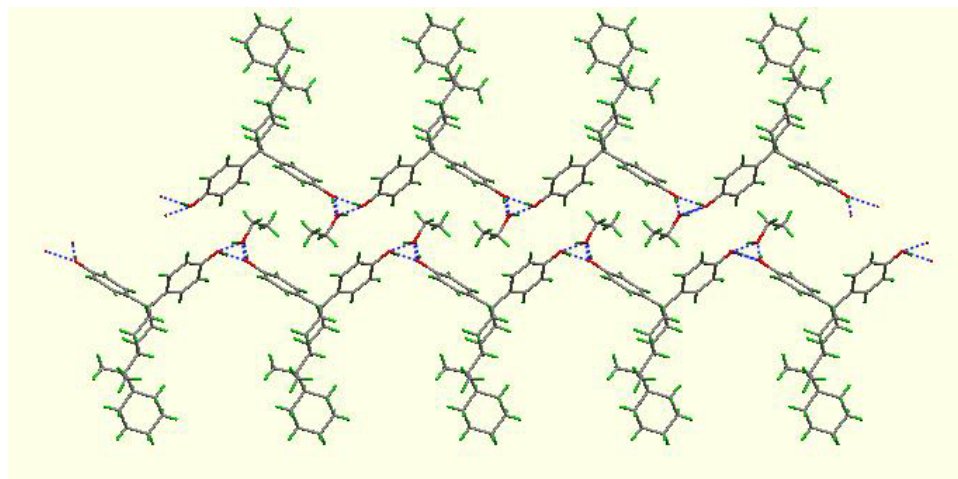


Figure 3.33b Packing diagram for 1,1-bis(4-hydroxyphenyl) -4-perhydrocumyl cyclohexane.

The nature of solvated crystal was further confirmed by DSC and TGA. The DSC measurement of the BPPCP crystals grown from ethanol solution shows endothermic transition at 132°C and this can be accounted for the loss of ethanol molecule, which was further quantified with thermogravimetric analysis. DSC curve (**Figure 3.34**) of BPPCP exhibits two endothermic transitions, one at 132°C (loss of ethanol molecule) and second at 198°C (melting).

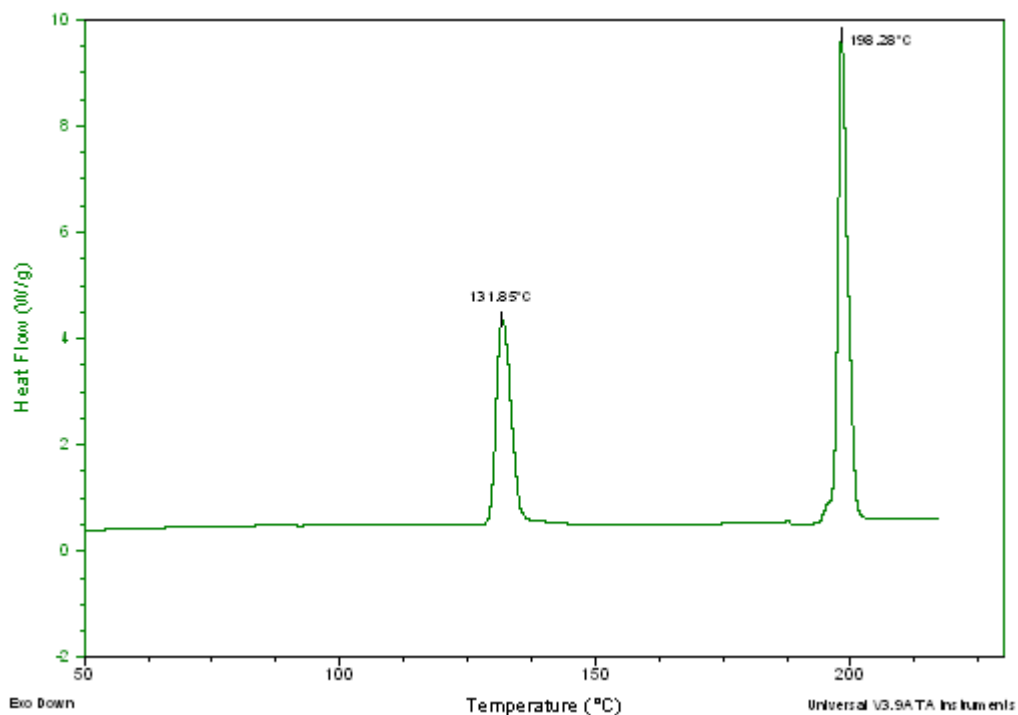


Figure 3.34 DSC curve for 1,1-bis(4-hydroxyphenyl) -4-perhydrocumyl cyclohexane

3.4.5.2 Synthesis and characterization of 1,1-bis(4-hydroxy-3-methylphenyl) -4-perhydrocumyl cyclohexane

1,1-Bis(4-hydroxy-3-methylphenyl) -4-perhydrocumyl cyclohexane (DMBPPCP) was synthesized by hydrogen chloride/3-MPA-catalyzed condensation of perhydrocumylcyclohexanone with *o*-cresol as reported in **Section 3.4.6a**. The purity of monomer was checked by HPLC, and was found to be >99.9% (**Figure 3.35**).

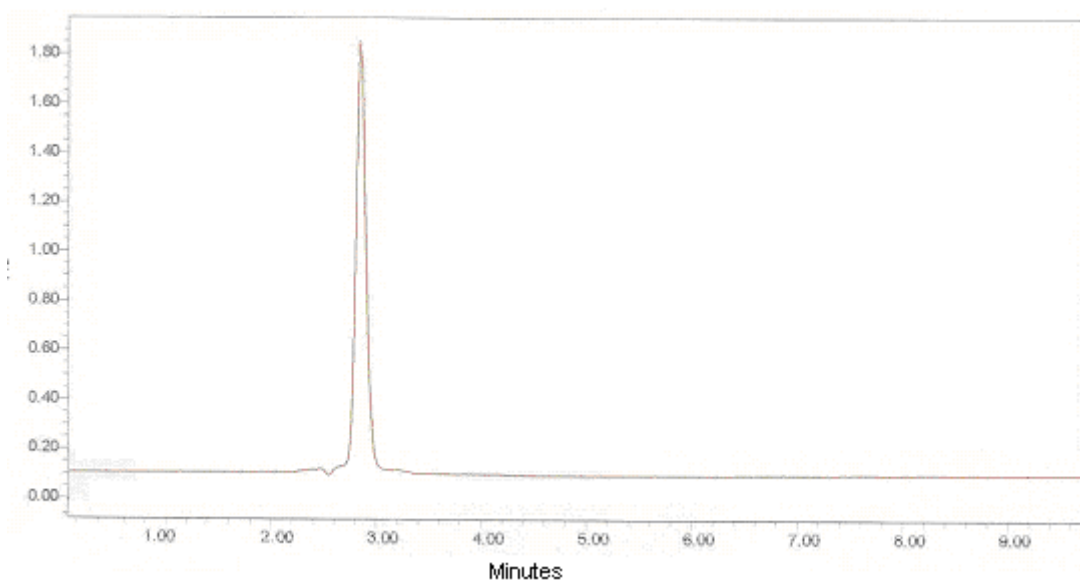


Figure 3.35 HPLC trace of 1,1-bis(4-hydroxy-3-methylphenyl) -4-perhydrocumyl cyclohexane

BPPCP was characterized by FTIR, ^1H and ^{13}C NMR spectroscopy.

FTIR spectrum of DMBPPCP showed a broad band at 3388 cm^{-1} corresponding to $-\text{OH}$ stretching.

^1H and ^{13}C NMR spectra of DMBPPCP along with assignments are presented in **Figure 3.36** and **3.37**, respectively.

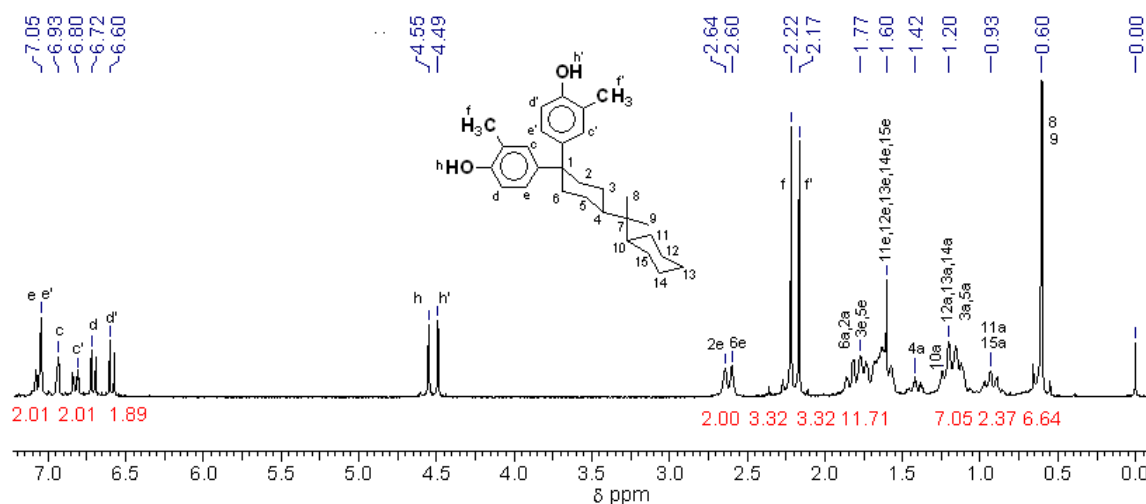


Figure 3.36 ^1H NMR spectrum of 1,1-bis(4-hydroxy-3-methylphenyl) -4-perhydrocumyl cyclohexane

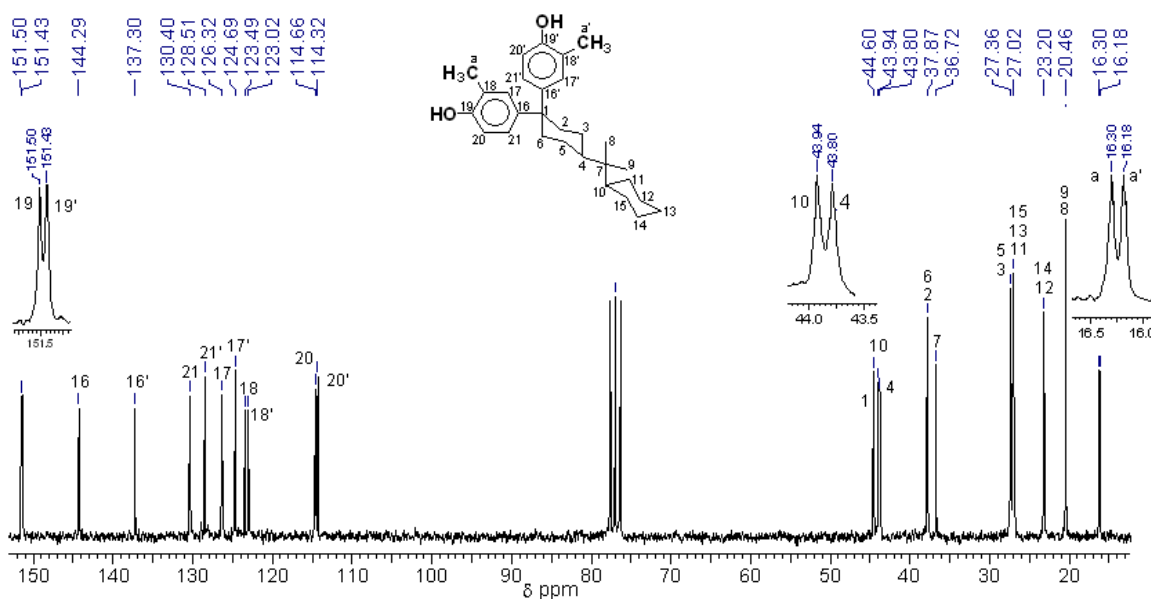


Figure 3.37 ^{13}C NMR spectrum of 1,1-bis(4-hydroxy-3-methylphenyl) -4-perhydrocumyl cyclohexane

3.4.5.3 Synthesis of 1,1-bis(4-hydroxy-3,5-dimethylphenyl) -4-perhydrocumyl cyclohexane

1,1-Bis(4-hydroxy-3,5-dimethylphenyl) -4-perhydrocumyl cyclohexane (TMBPPCP) was synthesized by hydrogen chloride-catalyzed condensation of perhydrocumylcyclohexanone with 2,6-dimethyl phenol in HCl/acetic acid mixture (2:1, v/v). The solid mass formed at the end of reaction was dissolved in ethyl acetate and was washed with aqueous sodium bicarbonate followed by water. Ethyl acetate was removed under reduced pressure and crude product was crystallized from hexane to yield white crystals of TMBPPCP. The purity of monomer was checked by HPLC and was found to be >99.9 % (Figure 3.38).

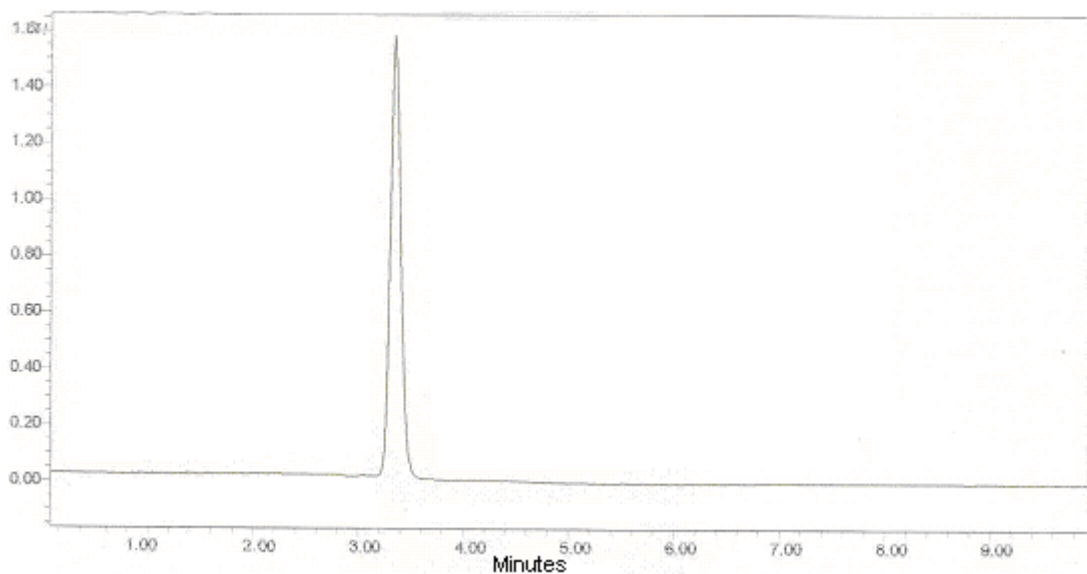


Figure 3.38 HPLC trace of 1,1-bis(4-hydroxy-3,5-dimethylphenyl) -4-perhydrocumyl cyclohexane

TMBPPCP was characterized by FTIR, ^1H and ^{13}C NMR spectroscopy.

FTIR spectrum of TMBPPCP showed broad band at 3389 cm^{-1} corresponding to $-\text{OH}$ stretching.

^1H and ^{13}C NMR spectra of TMBPPCP along with assignments are presented in **Figure 3.39** and **3.40**, respectively.

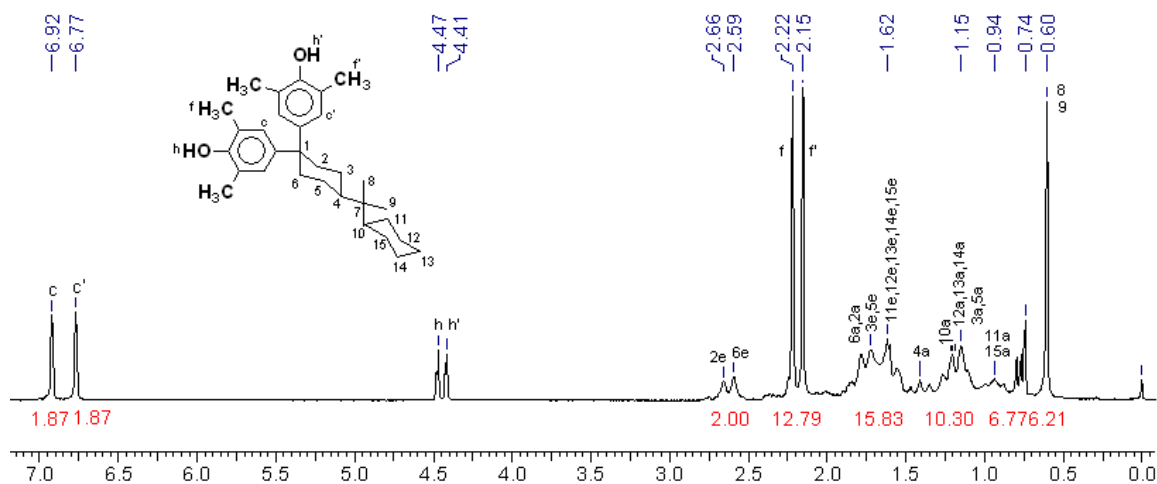


Figure 3.39 ^1H NMR spectrum of 1,1-bis(4-hydroxy-3,5-dimethylphenyl) -4-perhydrocumyl cyclohexane

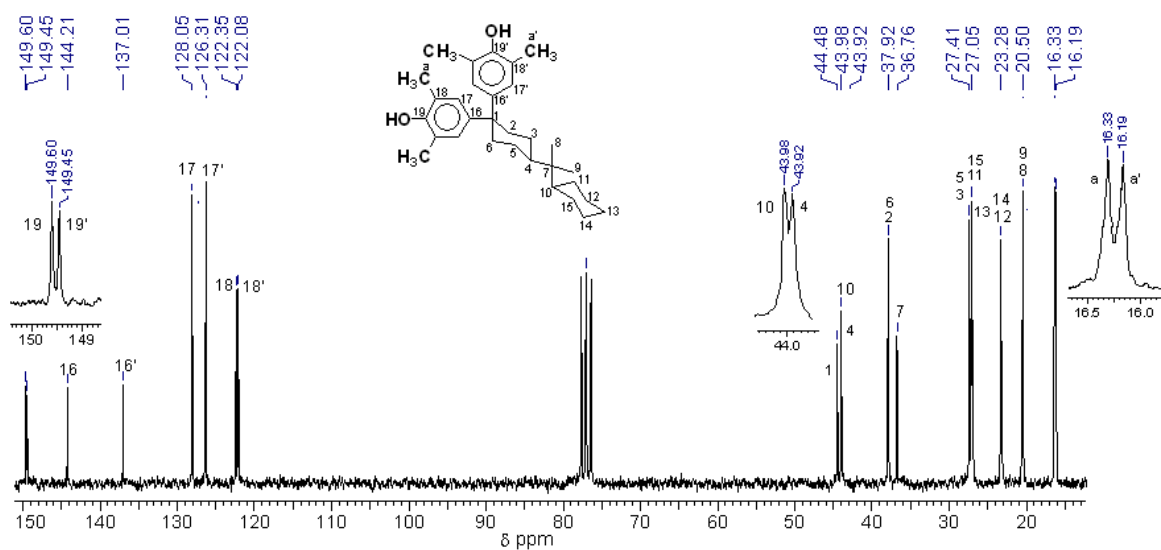


Figure 3.40 ¹³C NMR spectrum of 1,1-bis(4-hydroxy-3,5-dimethylphenyl)-4-perhydrocumyl cyclohexane

The structure of TMBPPCP was further detailed by single-crystal X-ray analysis.

Single crystals of TMBPPCP were grown from slow cooling of hexane solution. The X-ray crystal data for TMBPPCP is given in **Table 3.5**.

Table 3.5 X-Ray crystal data for 1,1-bis(4-hydroxy-3,5-dimethylphenyl) -4-perhydrocumyl cyclohexane

Formula	C ₃₁ H ₄₄ O ₂
Formula weight	448.66
Crystal color	Colorless
Crystal size (mm ³)	0.55 x 0.24 x 0.06
Lattice parameters	
<i>a</i> (Å)	7.082(2)
<i>b</i> (Å)	11.467(3)
<i>c</i> (Å)	17.163(4)
α (deg)	91.024(4)
β (deg)	96.414(4)
γ (deg)	101.090(4)
<i>V</i> (Å ³)	1358.1(6)
Crystal system	Triclinic
Space group	P $\bar{1}$
<i>Z</i>	2
Calculated density (mg m ⁻³)	1.097
No. of measured reflections	13076
No. of observed reflections	4791
<i>R</i>	0.0575
<i>R</i> _w	0.1554
Theta range for data collection	1.81 to 25 deg
Completeness to theta = 23.28	99.7%

Table 3.6 Analysis of potential hydrogen bonds in 1,1-bis(4-hydroxy-3,5-dimethylphenyl) -4-perhydrocumyl cyclohexane

Donor---H···Acceptor	H···A	D···A	D-H···A (deg)
1 O(1) ---H(1)···O(2) ⁱ	2.25	2.93	140
1 O(2) ---H(2)···O(1) ⁱⁱ	1.98	2.79	169

Equivalent position code
i = 1-x, 1-y, -z
ii = x, 1+y, z

Selected bond length and bond angle values are listed in **Appendix-3**. The ORTEP drawing of TMBPPCP is shown in **Figure 3.41a** and packing diagram is presented in **Figure 3.41b**. As can be seen from **Figure 3.41b**, TMBPPCP forms intermolecular

hydrogen bonds (**Table 3.6**). Molecules of TMBPPCP are arranged in head-to-head fashion forming one dimensional tapes, which are arranged in translation modes in two dimensions.

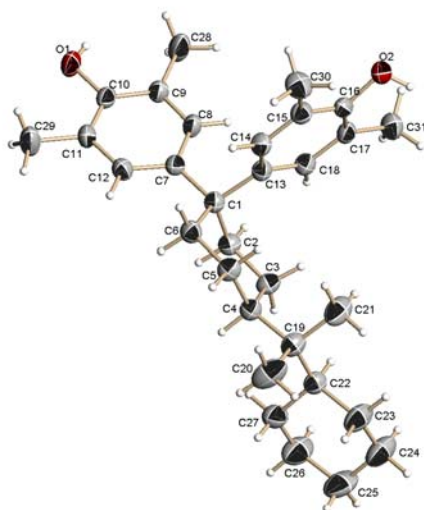


Figure 3.41a ORTEP diagram for 1,1-bis(4-hydroxy-3,5-dimethylphenyl) -4-perhydrocumyl cyclohexane. Ellipsoids are drawn at 50% probability level

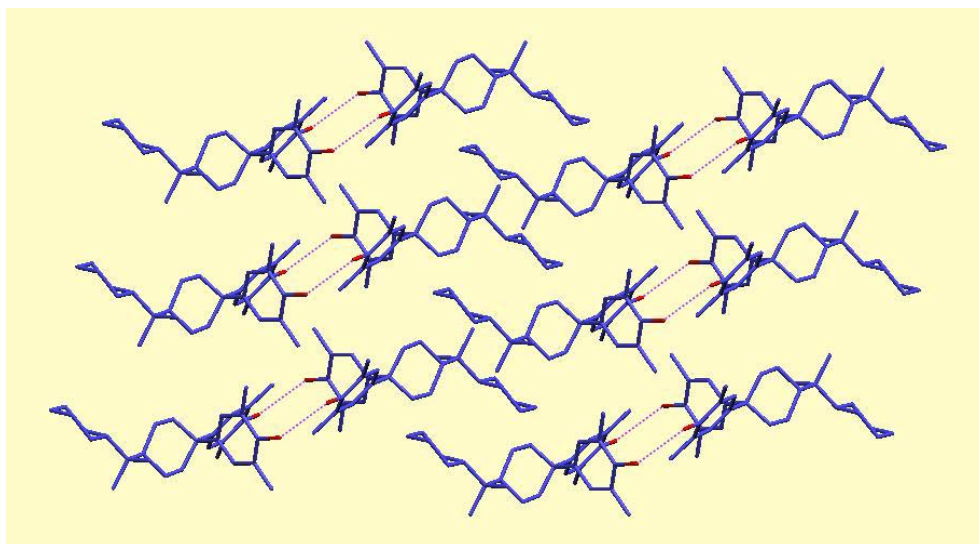


Figure 3.41b Packing diagram for 1,1-bis(4-hydroxy-3,5-dimethylphenyl) -4-perhydrocumyl cyclohexane.

3.4.5.4 Synthesis and characterization of 1,1-bis(4-hydroxy-3,5-dibromophenyl) -4-perhydrocumyl cyclohexane and 1,1-bis(4-hydroxy-3-methyl-5-bromophenyl) -4-perhydrocumyl cyclohexane

Bromo-substituted bisphenols, namely, 1,1-bis(4-hydroxy-3-methyl-5-bromophenyl) -4-perhydrocumyl cyclohexane (DDBPPCP) and 1,1-bis(4-hydroxy-3,5-dibromophenyl) -4-perhydrocumyl cyclohexane (TBrBPPCP) were synthesized by reacting DMBPPCP and BPPCP, respectively with bromine. Higher electron density at the two o-positions with respect to the phenolic –OH group of the phenyl ring provides the favorable condition for electrophilic substitution.

DDBPPCP and TBrBPPCP were characterized by FTIR, ^1H and ^{13}C NMR spectroscopy.

FTIR spectra of DDBPPCP and TBrBPPCP exhibited a broad band at 3507 and 3493 cm^{-1} respectively, corresponding to –OH stretching.

^1H and ^{13}C NMR spectra of DDBPPCP along with assignments are presented in **Figure 3.42** and **3.43**, respectively.

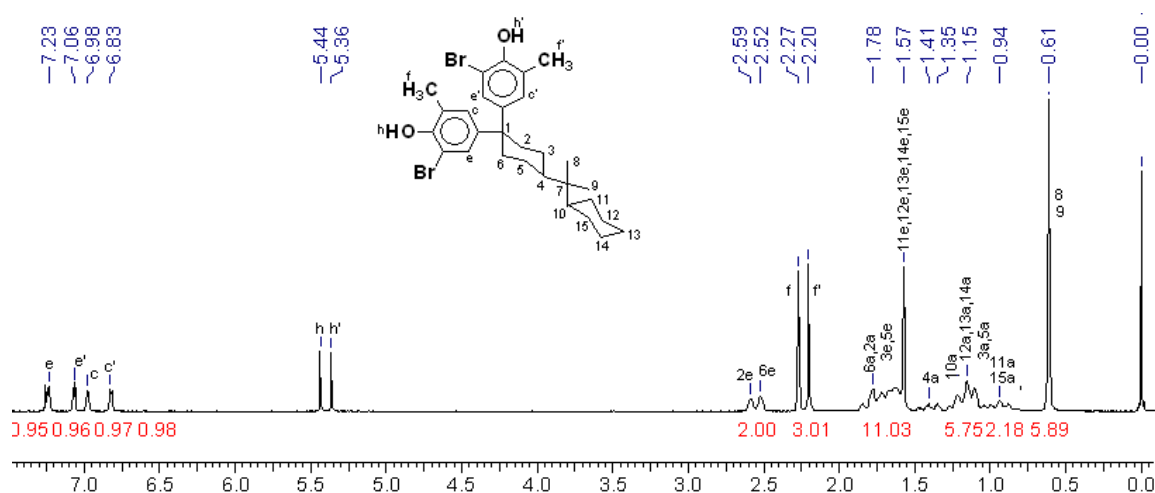


Figure 3.42 ¹H NMR spectrum of 1,1-bis(4-hydroxy-3-methyl-5-bromophenyl) 4-perhydrocumyl cyclohexane

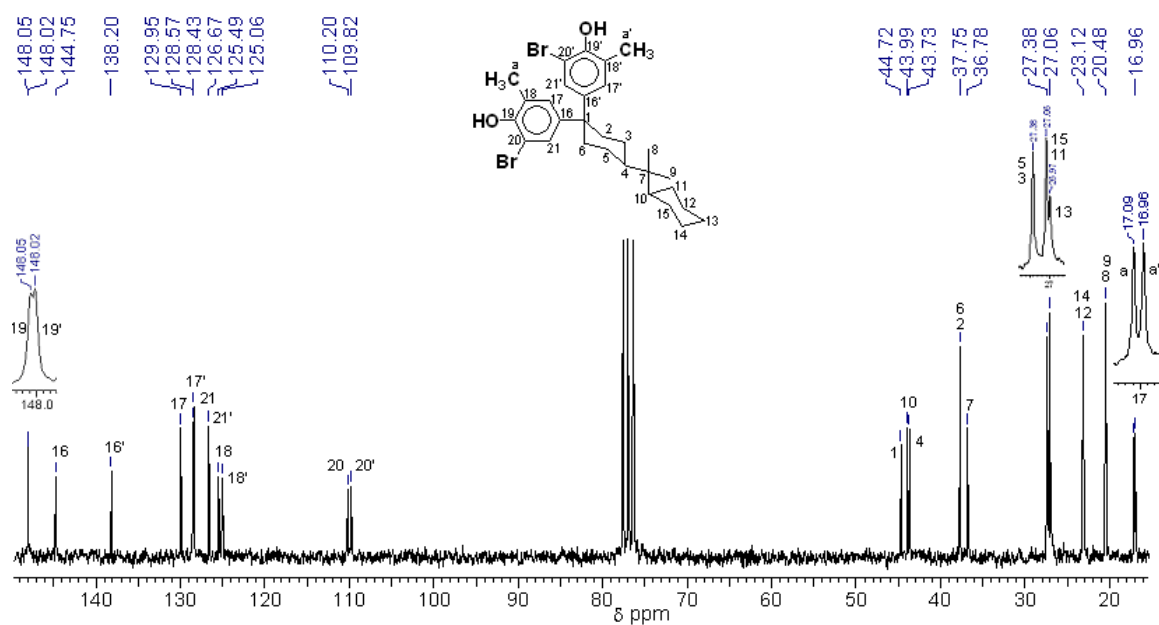


Figure 3.43 ¹³C NMR spectrum of 1,1-bis(4-hydroxy-3-methyl-5-bromophenyl) 4-perhydrocumyl cyclohexane

^1H and ^{13}C NMR spectra of TBrBPPCP along with assignments are presented in **Figure 3.44** and **3.45**, respectively.

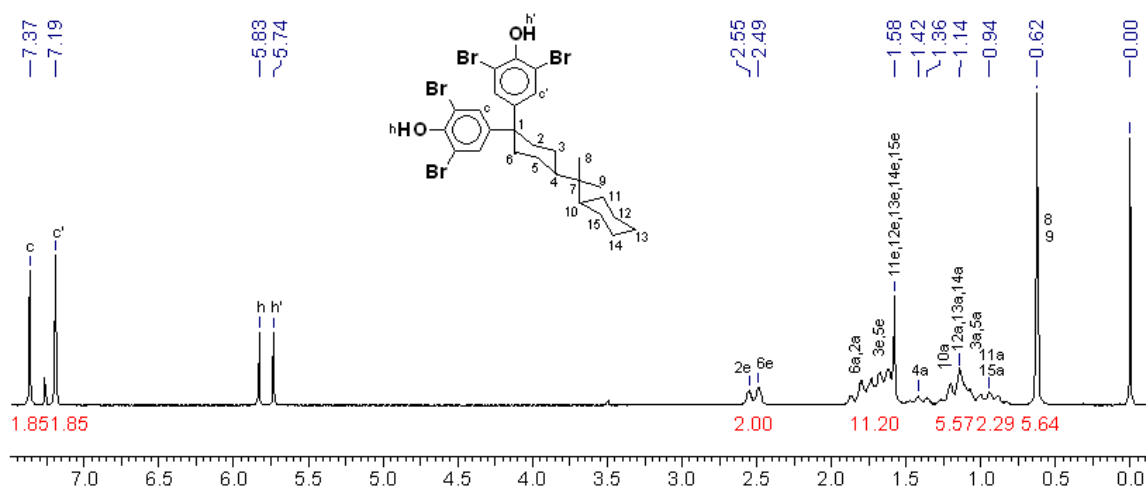


Figure 3.44 ^1H NMR spectrum of 1,1-bis(4-hydroxy-3,5-dibromophenyl) -4-perhydrocumyl cyclohexane

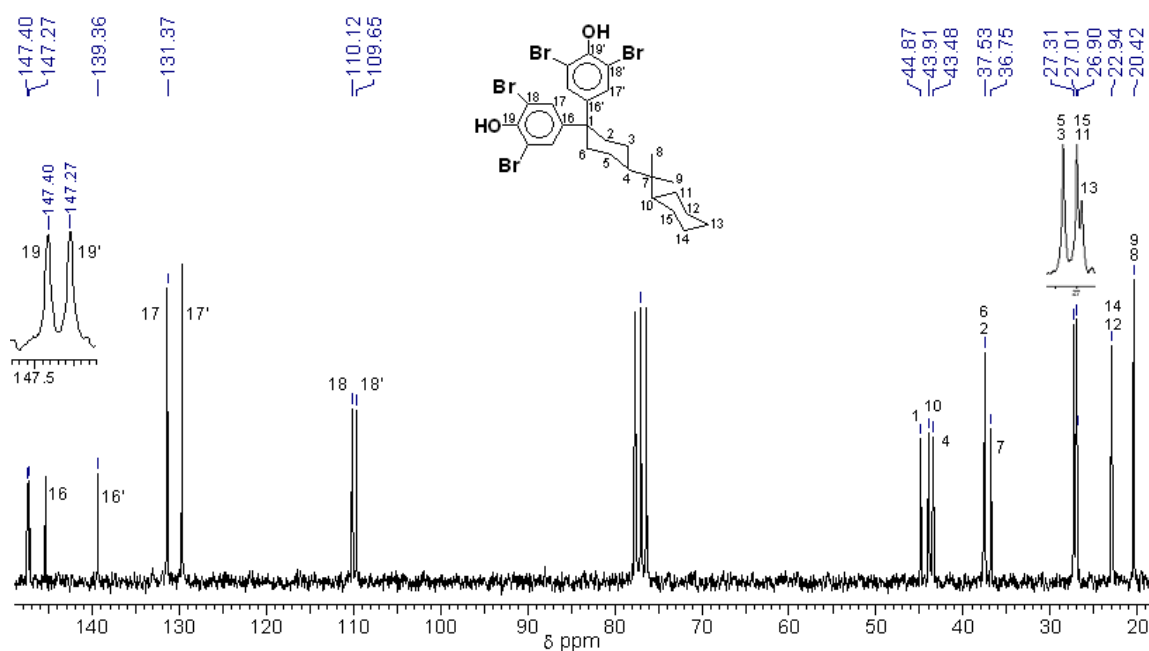


Figure 3.45 ^{13}C NMR spectrum of 1,1-bis(4-hydroxy-3,5-dibromophenyl) -4-perhydrocumyl cyclohexane

Structure of TBrBPPCP was further detailed by single-crystal X-ray analysis.

Single crystals of TBrBPPCP were grown from chloroform solution. The X-ray data and ORTEP diagram for TBrBPPCP is given in **Table 3.7** and **Figure 3.46**, respectively.

Table 3.7 X-Ray crystal data for 1,1-bis(4-hydroxy-3,5-dibromophenyl) -4-perhydrocumyl cyclohexane

Formula	C ₂₇ H ₃₂ Br ₄ O ₂
Formula weight	708.17
Crystal color	Colorless
Crystal size (mm ³)	0.38 x 0.27 x 0.05
Lattice parameters	
<i>a</i> (Å)	9.5008(12)
<i>b</i> (Å)	11.1074(14)
<i>c</i> (Å)	14.4104(18)
α (deg)	69.656(2)
β (deg)	76.670(2)
γ (deg)	76.803(2)
<i>V</i> (Å ³)	1369.0(3)
Crystal system	Triclinic
Space group	P ⁻ 1
<i>Z</i>	2
Calculated density (mg m ⁻³)	1.718
No. of measured reflections	11162
No. of observed reflections	3941
<i>R</i>	0.0389
<i>R</i> _w	0.0969
Theta range for data collection	1.98to 23.32 deg
Completeness to theta = 23.28	99.2%

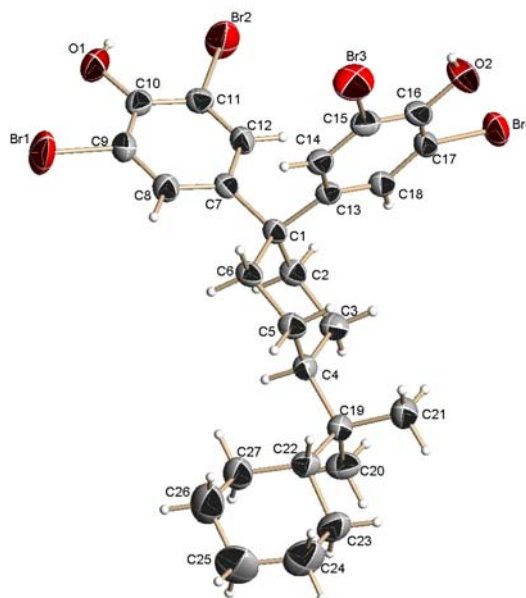


Figure 3.46 ORTEP diagram for 1,1-bis(4-hydroxy-3,5-dibromophenyl) -4-perhydrocumyl cyclohexane. Ellipsoids are drawn at 50% probability level

3.4.5.5 Conformational analysis of 1,1-bis(4-hydroxy-3,5-dibromophenyl) -4-perhydrocumyl cyclohexane

Three possible conformations of TBrBPPCP were investigated by the B3LYP nonlocal density functional with extended 6-31G(d,p) basis set for studying the conformational energies. The Gaussian 98 A.11.1 program suit was used for all quantum chemical computations. The three possible conformations of TBrBPPCP were optimized using density functional theory (DFT).

Three conformers, equatorial-equatorial (**1a**), equatorial-axial (**1b**) and axial-equatorial (**1c**) based on the orientations of two cyclohexyl rings in TBrBPPCP were studied (**Figure 3.47**)

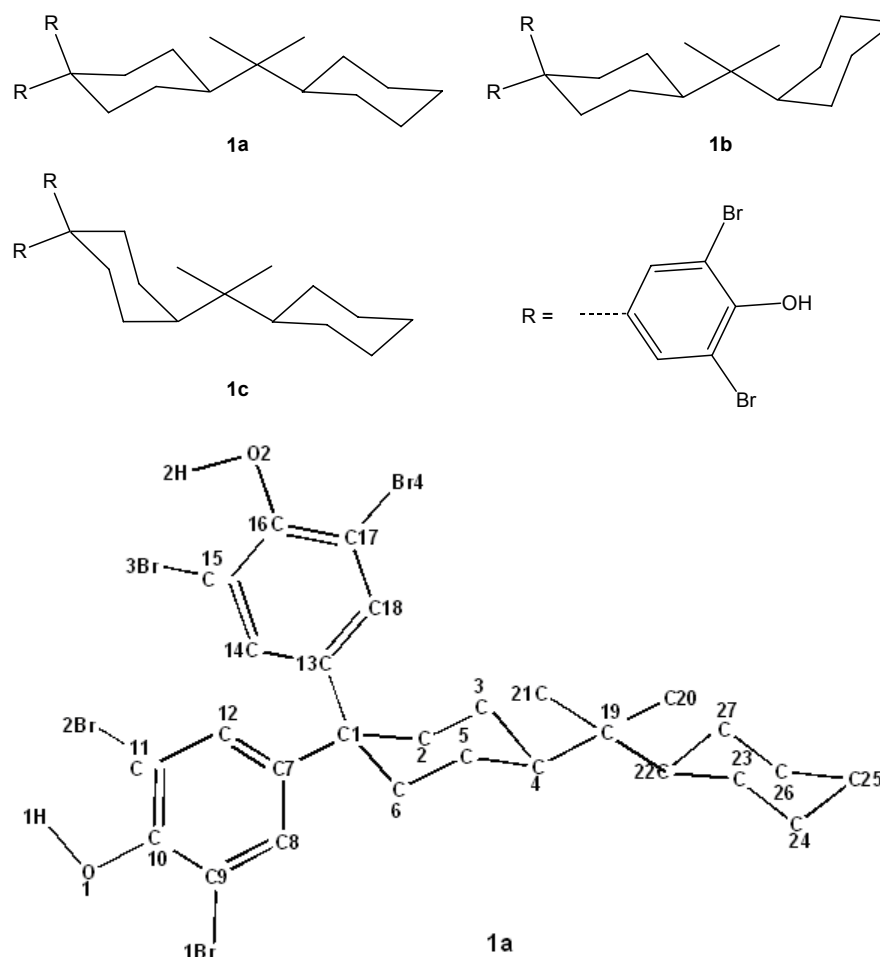


Figure 3.47 Conformers of 1,1-bis(4-hydroxy-3,5-dibromophenyl) -4-perhydrocumyl cyclohexane

The geometry optimized parameters of **1a** were in excellent agreement with the single crystal X-ray data of TBrBPPCP. Some small differences were observed in the geometry of the bonds connecting two cyclohexyl rings. The data is presented in **Table 3.5** along with X-ray data. The bond lengths and bond angles with marginal deviation are highlighted in table.

Table 3.8 Bond lengths and bond angles for 1,1-bis(4-hydroxy-3,5-dibromophenyl) -4-perhydrocumyl cyclohexane and its B3LYP/6-31G level geometry optimized structure 1a**

Bond length	TBrBPPCP	1a	Bond angle	TBrBPPCP	1a
Br1-C9	1.894	1.904	Br1-C9-C8	119.3	119.4
Br2-C11	1.896	1.919	Br1-C9-C10	118.0	118.9
Br3-C15	1.905	1.919	Br2-C11-C10	117.4	117.6
Br4-C17	1.901	1.904	Br2-C11-C12	120.0	119.9
O1-C10	1.351	1.349	Br3-C15-C14	118.7	119.8
O2-C16	1.364	1.349	Br3-C15-C16	118.6	117.6
C1-C2	1.544	1.557	Br4-C17-C16	119.1	119.0
C1-C6	1.541	1.552	Br4-C17-C18	119.2	119.4
C1-C7	1.545	1.547	O1-C10-C9	119.2	119.9
C1-C13	1.549	1.547	O1-C10-C11	124.9	123.8
C2-C3	1.532	1.541	O2-C16-C15	123.4	123.9
C3-C4	1.532	1.544	O2-C16-C17	119.6	119.9
C4-C5	1.538	1.543	C2-C1-C6	106.4	106.0
C4-C19	1.565	1.576	C2-C1-C7	108.4	108.2
C5-C6	1.523	1.535	C2-C1-C13	113.3	113.3
C7-C8	1.391	1.399	C1-C2-C3	114.6	115.4
C7-C12	1.397	1.403	C6-C1-C7	111.3	111.8
C8-C9	1.379	1.393	C6-C1-C13	110.8	110.4
C9-C10	1.379	1.400	C1-C6-C5	113.7	113.1
C10-C11	1.394	1.404	C7-C1-C13	106.7	107.2
C11-C12	1.371	1.386	C1-C7-C8	123.2	123.3
C13-C14	1.397	1.403	C1-C7-C12	119.6	119.3
C13-C18	1.381	1.400	C1-C13-C14	118.4	119.5
C14-C15	1.388	1.387	C1-C13-C18	123.1	123.3
C15-C16	1.375	1.404	C2-C3-C4	111.6	112.6
C16-C17	1.379	1.400	C3-C4-C5	107.1	108.1
C17-C18	1.389	1.393	C3-C4-C19	115.4	114.5
C19-C20	1.536	1.546	C5-C4-C19	115.2	114.1
C19-C21	1.531	1.546	C4-C5-C6	110.4	111.8
C19-C22	1.566	1.578	C4-C19-C20	108.0	109.7
C22-C23	1.540	1.548	C4-C19-C21	109.7	109.9
C22-C27	1.525	1.547	C4-C19-C22	110.2	109.6
C23-C24	1.529	1.538	C8-C7-C12	117.1	117.4
C24-C25	1.506	1.533	C7-C8-C9	120.8	121.4

C25-C26	1.516	1.533	C7-C12-C11	120.8	120.7
C26-C27	1.531	1.537	C8-C9-C10	122.7	121.7
			C9-C10-C11	115.9	116.3
			C10-C11-C12	122.6	122.5
			C14-C13-C18	118.2	117.2
			C13-C14-C15	119.5	120.8
			C13-C18-C17	120.9	121.6
			C14-C15-C16	122.8	122.6
			C15-C16-C17	117.0	116.2
			C16-C17-C18	121.6	121.6
			C20-C19-C21	109.7	107.7
			C20-C19-C22	110.2	110.1
			C21-C19-C22	109.0	109.8
			C19-C22-C23	113.9	114.4
			C19-C22-C27	115.8	114.2
			C23-C22-C27	107.6	108.7
			C22-C23-C24	112.3	112.0
			C22-C27-C26	112.2	112.3
			C23-C24-C25	111.2	112.1
			C24-C25-C26	111.2	110.8
			C25-C26-C27	110.9	111.5

Fully optimized structures **1a**, **1b** and **1c** were used for the energy comparison. As shown in **Figure 3.48**, the geometry optimized conformation **1a** (equatorial-equatorial) is the lowest energy structure. The equatorial-axial conformation **1b** is higher by 5.7 kcal/mol, whereas, the axial-equatorial conformation **1c** is higher by 6.1 Kcal/mol relative to that of **1a**. The observed differences between energies of the conformers 1b and 1c are marginal. There exists a possibility of equilibrium between all these conformers in solution. The axial-axial conformation, which was not feasible to calculate in B3LYP/6-31G** basis level, presumably is the highest energy conformation.

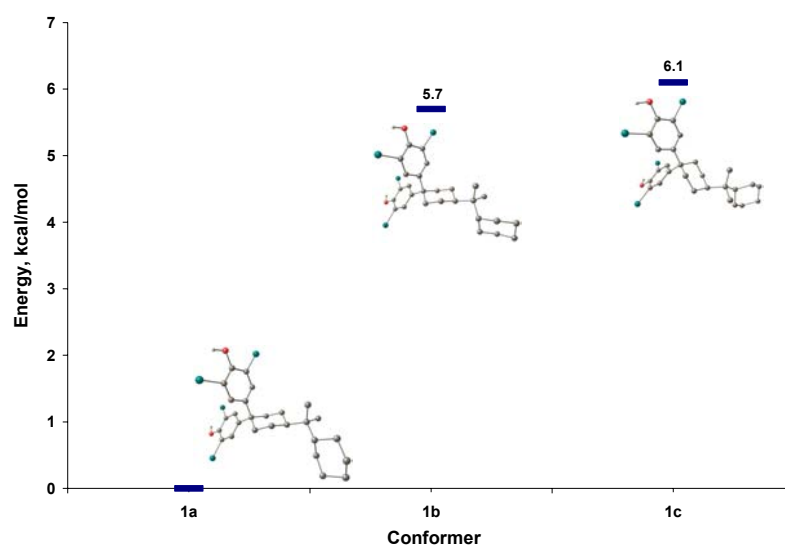
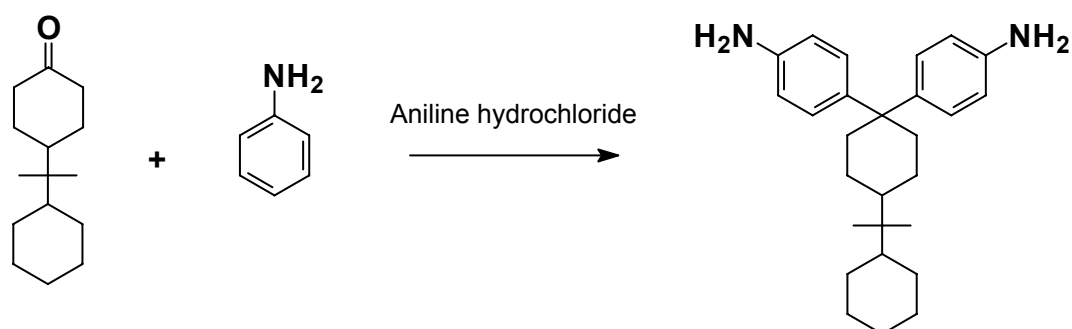


Figure 3.48 Energy comparison graph for conformers of 1,1-bis(4-hydroxy-3,5-dibromophenyl) -4-perhydrocumyl cyclohexane

3.4.6 Synthesis and characterization of 1,1-bis(4-aminophenyl) -4-perhydrocumyl cyclohexane

1,1-Bis(4-aminophenyl) -4-perhydrocumyl cyclohexane (BAPCP) was synthesized according to the procedure reported in **Section 3.4.4**.

Scheme 3.6 depicts the route for synthesis of BAPCP.



Scheme 3.6 Synthesis of 1,1-bis(4-aminophenyl) -4-perhydrocumyl cyclohexane

BAPCP was characterized by FTIR, ¹H and ¹³C NMR spectroscopy.

FTIR spectrum showed absorption bands at 3445 and 3361 cm⁻¹ indicating the presence of primary amino group.

^1H and ^{13}C NMR spectra of BAPCP along with assignments are reproduced in **Figure 3.49** and **3.50**, respectively.

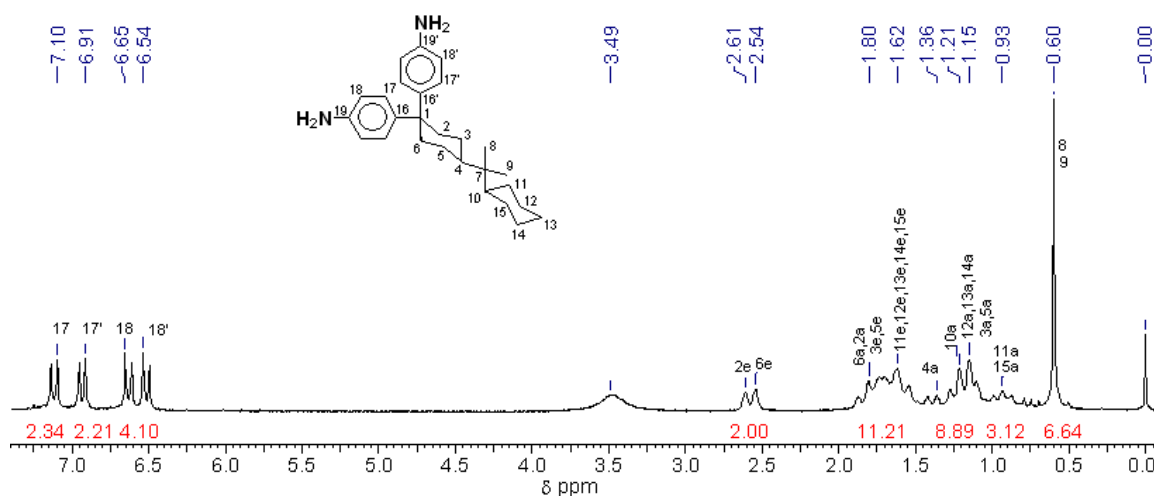


Figure 3.49 ^1H -NMR spectrum of 1,1-bis(4-aminophenyl)-4-perhydrocumyl cyclohexane

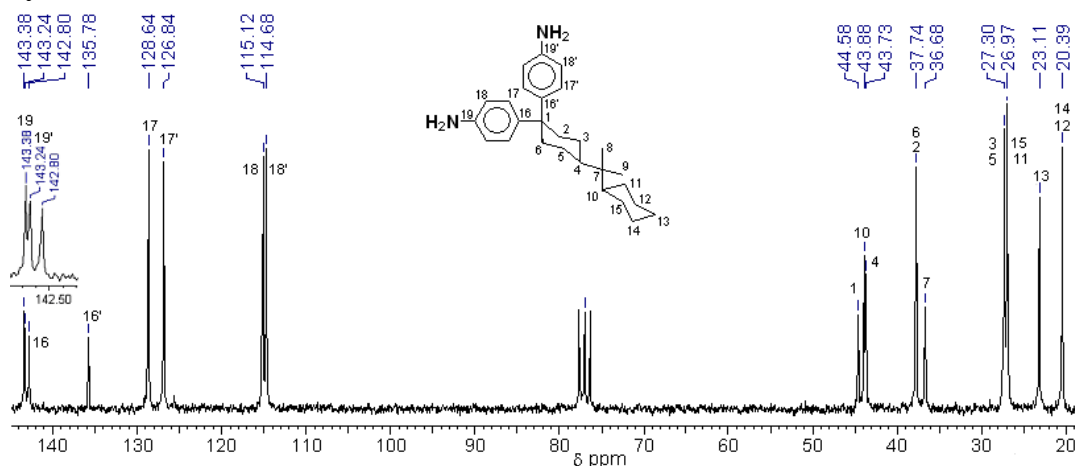


Figure 3.50 ^{13}C -NMR spectrum of 1,1-bis(4-aminophenyl)-4-perhydrocumyl cyclohexane

The structure of BAPCP was further detailed by single crystal X-ray analysis. Single crystals of BAPCP were grown from ethanol solution. The X-ray crystal data and ORTEP diagram for BAPCP is given in **Table 3.9** and **Figure 3.51**, respectively.

Table 3.9 X-ray crystal data for 1,1-bis(4-aminophenyl) -4-perhydrocumyl cyclohexane

Formula	C ₂₇ H ₃₈ N ₂
Formula weight	390.59
Crystal color	Colorless
Crystal size (mm ³)	0.55 x 0.24 x 0.06
Lattice parameters	
<i>a</i> (Å)	6.387(8)
<i>b</i> (Å)	11.159(1)
<i>c</i> (Å)	15.781(2)
β (deg)	97.921(2)
<i>V</i> (Å ³)	1114.0(2)
Crystal system	Monoclinic
Space group	P2 ₁
<i>Z</i>	2
Calculated density (mg m ⁻³)	1.164
No. of measured reflections	111548
No. of observed reflections	3221
<i>R</i>	0.0309
<i>R</i> _w	0.0796
Theta range for data collection	1.30 to 23.33 deg
Completeness to theta = 23.28	99.8%

Selected bond length and bond angle values are listed in **Appendix-4**.

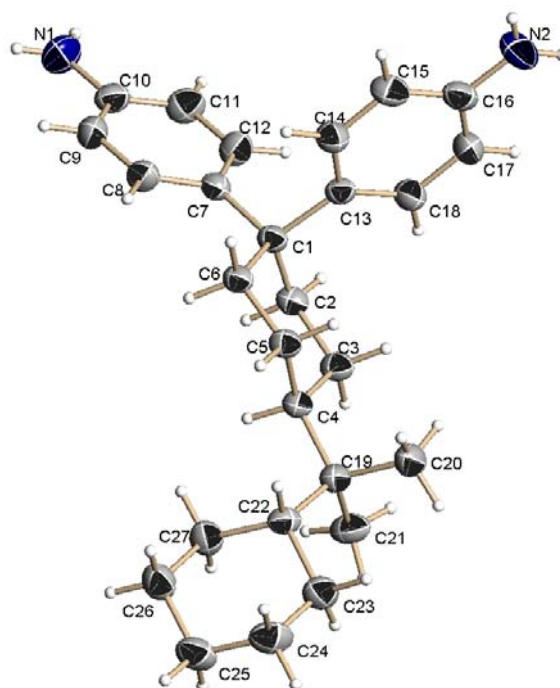
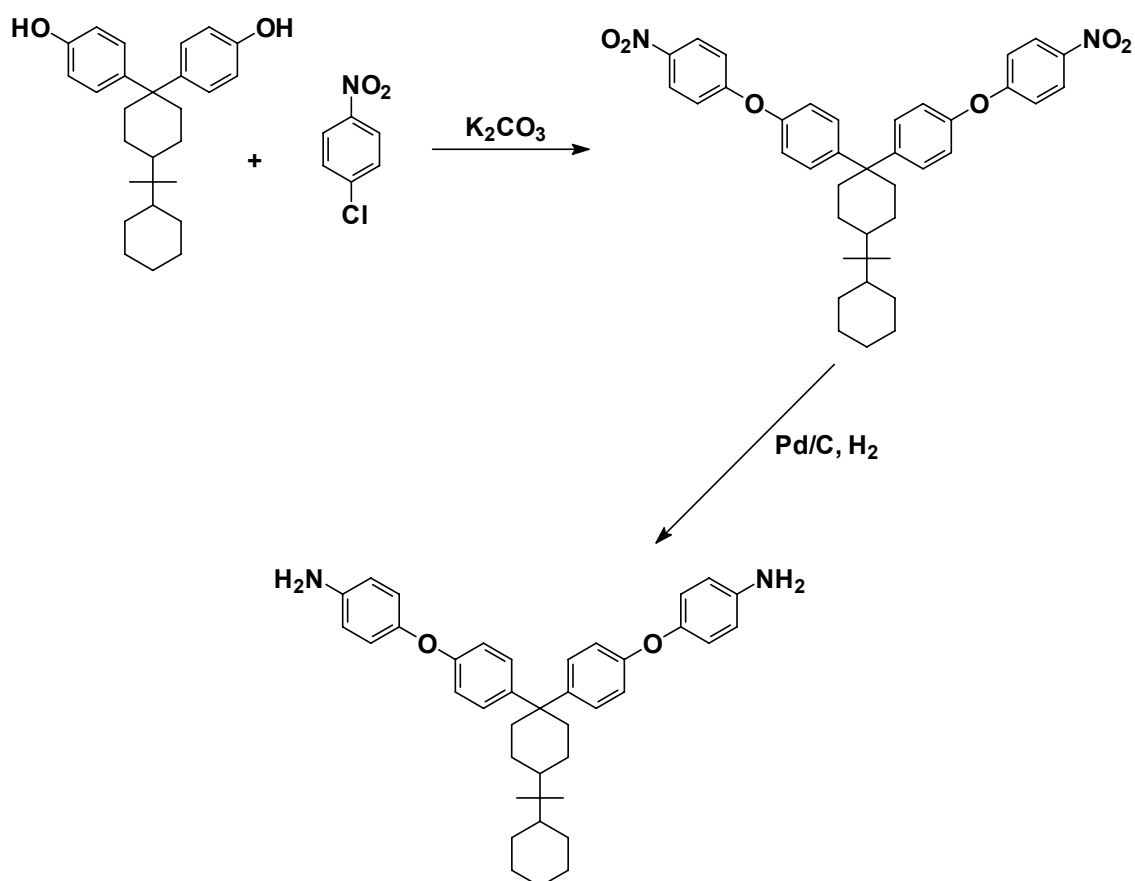


Figure 3.51 ORTEP diagram for 1,1-bis(4-aminophenyl) -4-perhydrocumyl cyclohexane. Ellipsoids are drawn at 50% probability level

3.4.7 Synthesis and characterization of 1,1-bis[4-(4-aminophenoxy)phenyl]-4-per-hydrocumyl cyclohexane

Scheme 3.7 outlines the route for synthesis of 1,1-bis[4-(4-aminophenoxy)phenyl]-4-per-hydrocumyl cyclohexane (BAPPHC). The intermediate 1,1-bis[4-(4-nitrophenoxy)phenyl]-4-per-hydrocumyl cyclohexane (BNPPHC), was prepared by nucleophilic chloro displacement of *p*-chloro nitrobenzene with BPPCP in the presence of K_2CO_3 . The reaction was carried out in DMF at reflux temperature for 10 h. At the end of reaction, the reaction mixture was cooled to room temperature and was poured in excess water. Yellow solid obtained was collected by filtration and was crystallized from DMF to get yellow crystals of BNPPHC. The diamine, BAPPHC was obtained in high purity and high yield by reduction of BNPPHC using hydrazine hydrate and Pd/C catalyst in refluxing ethanol.



Scheme 3.7 Synthesis of 1,1-bis[4-(4-aminophenoxy)phenyl]-4-per-hydrocumyl cyclohexane

Both, BNPPHC and BAPPHC were characterized by FTIR, ^1H and ^{13}C NMR spectroscopy.

Figure 3.52 shows FTIR spectrum of BNPPHC and BAPPHC. BNPPHC showed absorption bands at 1515 and 1343 cm^{-1} corresponding to asymmetrical and symmetrical stretching of nitro group. BAPPHC exhibited absorption bands at 3448, 3369 cm^{-1} (N-H stretching) and 1619 cm^{-1} (N-H deformation) corresponding to primary amine. Both BNPPHC and BAPPHC showed absorption band at 1236 and 1245 cm^{-1} , respectively corresponding to C-O-C stretching.

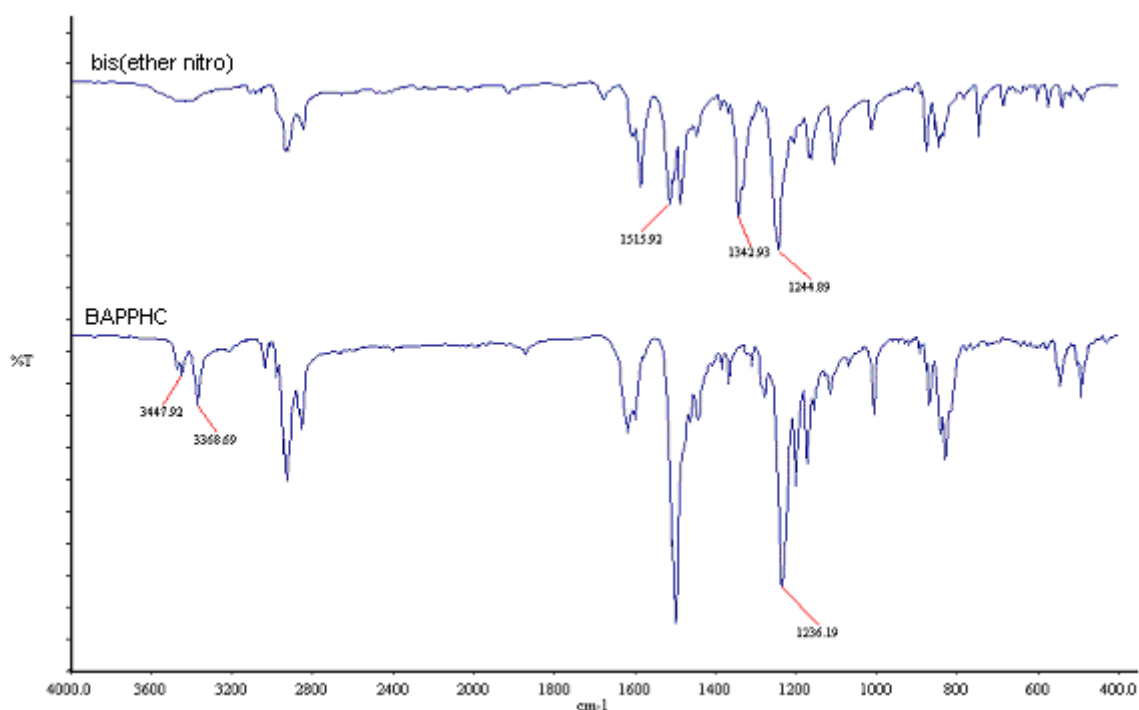


Figure 3.52 FTIR spectrum of 1,1-bis[4-(4-nitrophenoxy)phenyl]-4-per hydrocumyl cyclohexane and 1,1-bis[4-(4-aminophenoxy)phenyl]-4-per hydrocumyl cyclohexane

^1H NMR spectrum of BNPPHC and BAPPHC along with assignments are presented in **Figure 3.53**

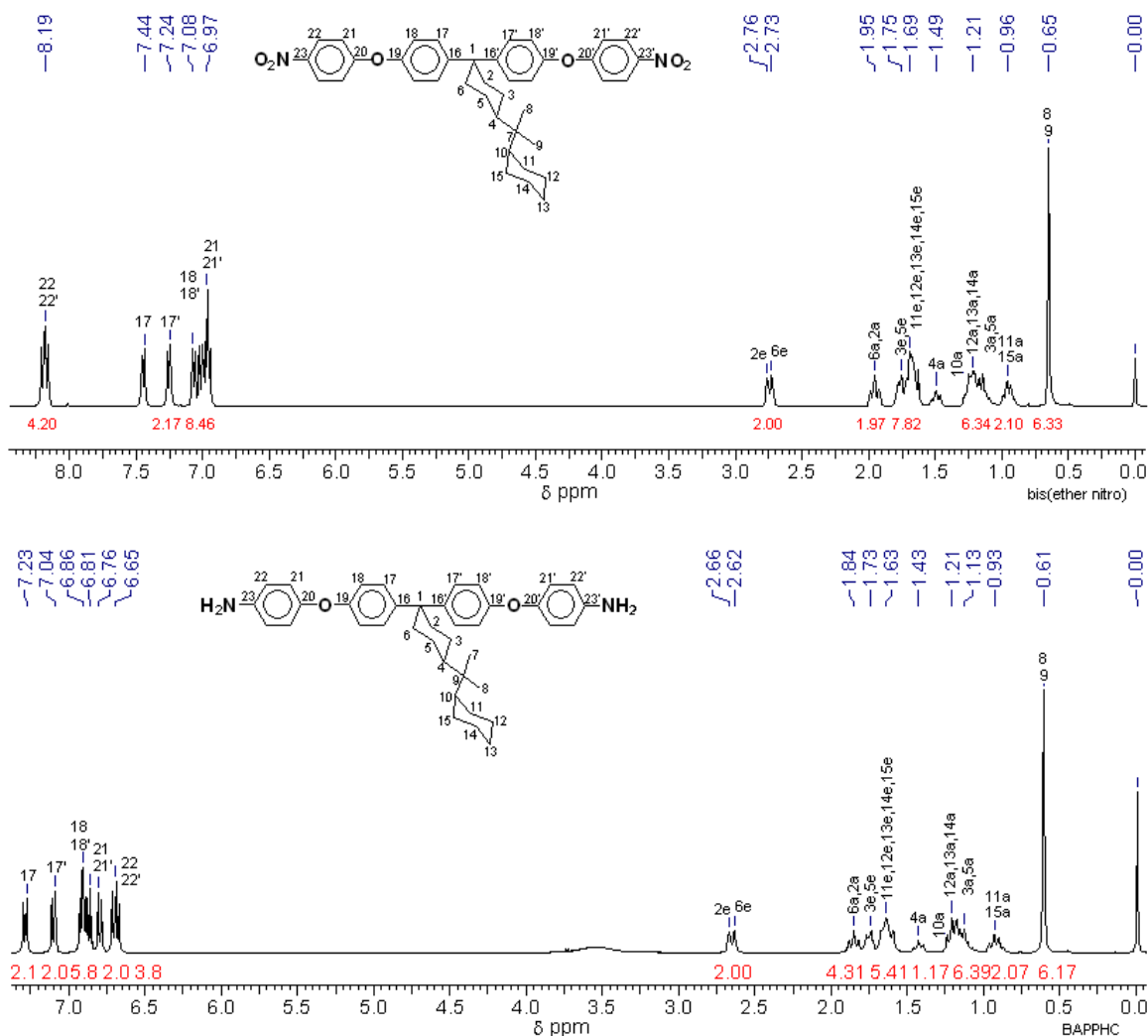


Figure 3.53 ^1H NMR spectra of 1,1-bis[4-(4-nitrophenyl)phenyl]-4-per hydrocumyl cyclohexane and 1,1-bis[4-(4-aminophenyl)phenyl]-4-per hydrocumyl cyclohexane

Peaks corresponding to aromatic protons 22, 22'ortho to nitro and amino group appeared at 8.19 and 6.65 ppm, respectively. The upfield shift of protons 22 and 22' in case of BAPPHC because of shielding effect of amino group confirms the complete reduction of BNPPHC.

^{13}C NMR spectrum of BNPPHC and BAPPHC along with assignments are presented in **Figure 3.54**

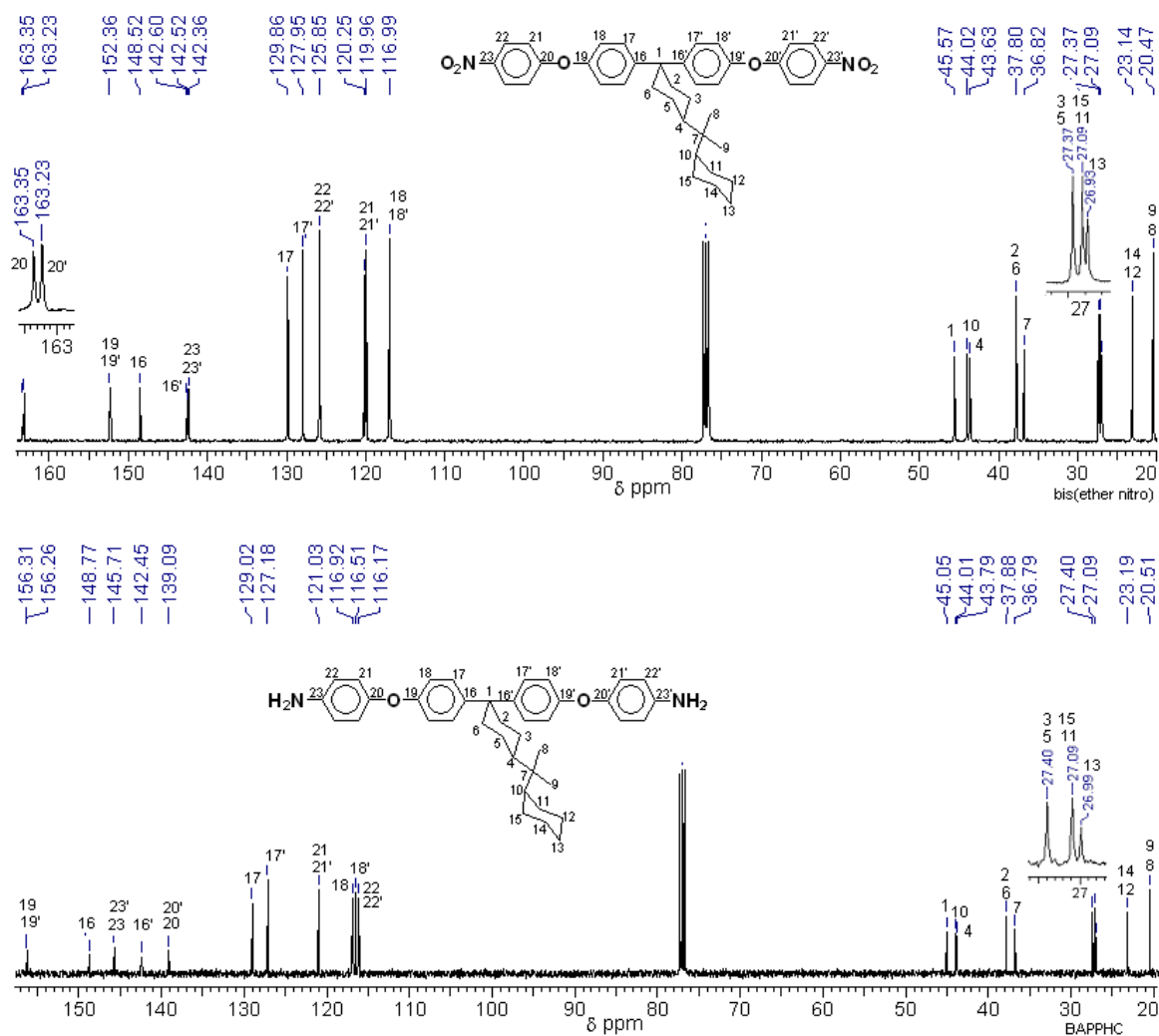


Figure 3.54 ^{13}C NMR spectra of 1,1-bis[4-(4-nitrophenoxy)phenyl]-4-per hydrocumyl cyclohexane and 1,1-bis[4-(4-aminophenoxy)phenyl]-4-per hydrocumyl cyclohexane

Carbons, 22 and 20 of BAPPHC showed signal at 116.17 and 139.09 ppm, respectively, where as those of BNPPHC showed signal at 125.85 and 163.35 and 163.23 ppm respectively. The upfield shift of the aromatic carbon resonances, especially for the carbons *ortho* and *para* to the amino groups were observed in BAPPHC because the resonance effect caused by the electron donating amino groups. All the spectroscopic data agreed with the proposed structure.

The structure of the diamine was further detailed by single-crystal X-ray analysis. The X-ray crystal data for BAPPHC is given in **Table 3.10**.

Table 3.10 X-Ray crystal data for 1,1-bis[4-(4-aminophenoxy)phenyl]-4-per hydrocumyl cyclohexane

Formula	C ₃₉ H ₄₆ N ₂ O ₂
Formula weight	574.78
Crystal color	Colorless, needles
Crystal size (mm ³)	0.27 x 0.17 x 0.08
Lattice parameters	
<i>a</i> (Å)	6.5665(6)
<i>b</i> (Å)	12.415(1)
<i>c</i> (Å)	21.193(2)
α (°)	104.513(2)
β (°)	93.657(2)
γ (°)	102.196(2)
<i>V</i> (Å ³)	1622.3(3)
Crystal system	Triclinic
Space group	P ⁻ 1
<i>Z</i>	2
Calculated density (mg m ⁻³)	1.177
No. of measured reflections	15370
No. of observed reflections	5676
<i>R</i>	0.0773
<i>R</i> _w	0.1529
Theta range for data collection	1.74 to 25 °
Completeness to theta = 23.28	99.3%

Table 3.11 Analysis of potential hydrogen bonds in 1,1-bis[4-(4-aminophenoxy)phenyl]-4-per hydrocumyl cyclohexane

Donor---H···Acceptor	H···A	D···A	D-H···A (°)
1 N(1) ---H(1B)···O(2) ⁱ	2.28	3.07	152

Equivalent position code
i = -x,-y,1-z

Selected bond distances and bond angles are listed in **Appendix-5**. The ORTEP drawing of BAPPHC is shown in **Figure 3.55a** and packing diagram is presented in **Figure 3.55b**. As can be seen from **Figure 3.55b**, BAPPHC forms intermolecular hydrogen bonding between symmetry related molecules with primary amine and ether group. (**Table 3.11**)

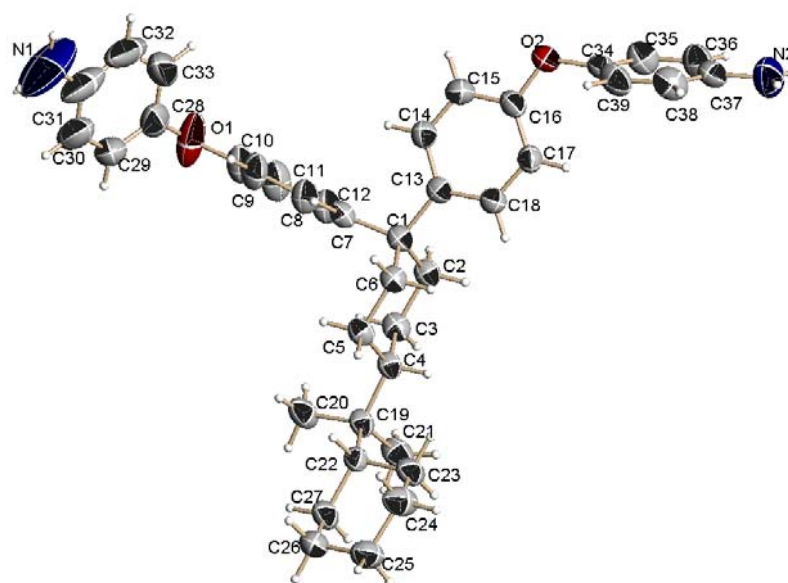


Figure 3.55a ORTEP diagram for 1,1-bis[4-(4-aminophenoxy)phenyl]-4-perhydrocumyl cyclohexane. Ellipsoids are drawn at 50% probability level

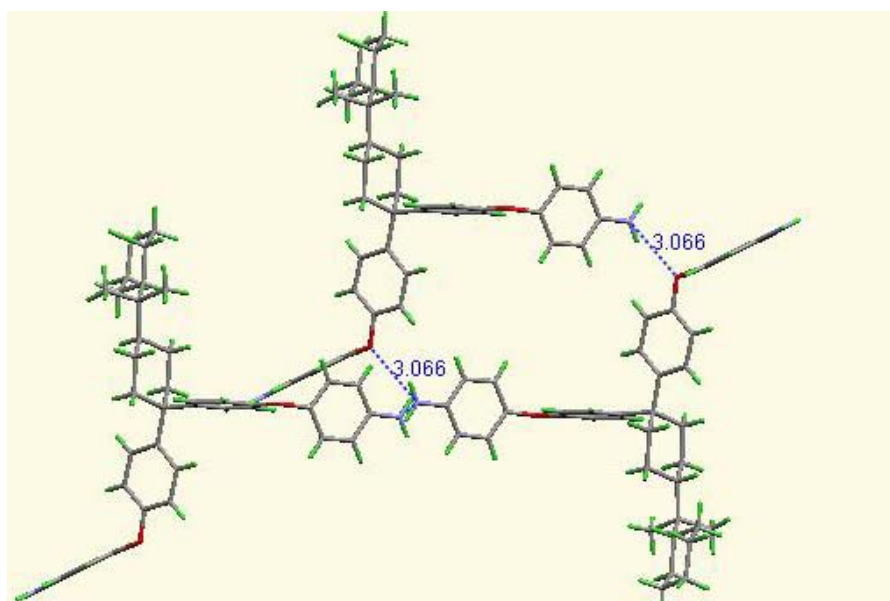
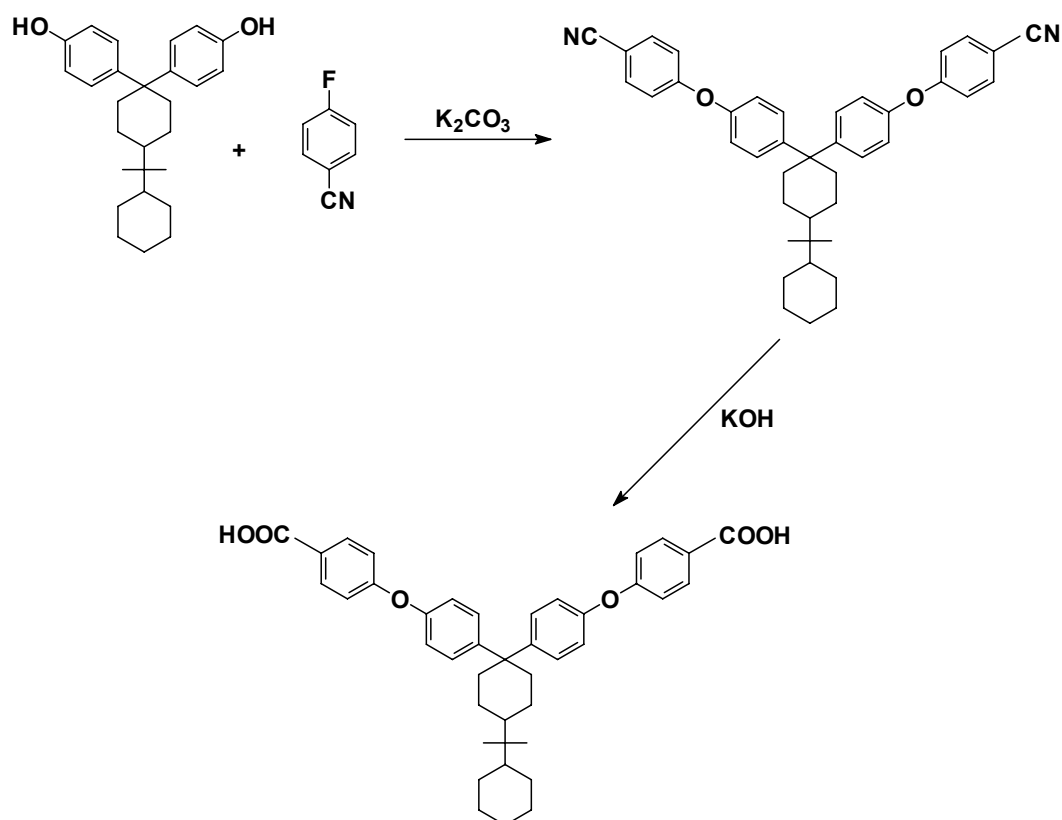


Figure 3.55b Packing diagram for 1,1-bis[4-(4-aminophenoxy)phenyl]-4-perhydrocumyl cyclohexane.

3.4.8 Synthesis and characterization of 1,1-bis[4-(4-carboxyphenoxy)phenyl]-4-per-hydrocumyl cyclohexane

Scheme 3.8 depicts the route for synthesis of 1,1-bis[4-(4-carboxyphenoxy)phenyl]-4-per hydrocumyl cyclohexane (BCPPHC). The intermediate 1,1-bis[4-(4-cyanophenoxy)phenyl]-4-per-hydrocumyl cyclohexane (BCyPHC), was obtained from nucleophilic fluoro displacement of *p*-fluorobenzonitrile with potassium salt of BPPCP. In a typical procedure potassium salt of BPPCP was prepared *in situ* by reaction of BPPCP with K_2CO_3 in refluxing DMF. *p*-Fluorobenzonitrile was added to the reaction mixture and refluxion was continued for 6 h. At the end of reaction, the reaction mixture was cooled to room temperature and was poured in excess water. White solid obtained was collected by filtration and was crystallized from acetonitrile to get colorless needles. The intermediate BCyPHC was then readily converted into BCPPHC by alkaline hydrolysis.



Scheme 3.8 Synthesis of 1,1-bis[4-(4-carboxyphenoxy)phenyl]-4-per-hydrocumyl cyclohexane

Both, BCyPHC and BCPPHC were characterized by FTIR, ^1H and ^{13}C NMR spectroscopy.

Figure 3.56 shows FTIR spectrum of intermediate BCyPHC and BCPPHC. BCyPHC showed absorption band at 2228 cm^{-1} corresponding to $\text{C}\equiv\text{N}$ stretching, which was not observed in BCPPHC, indicating complete hydrolysis of nitrile group. BCPPHC showed strong absorption at 1689 cm^{-1} corresponding to $\text{C}=\text{O}$ stretching. Both BCyPHC and BCPPHC exhibited absorption band at 1245 and 1244 cm^{-1} , respectively corresponding to C-O-C stretching.

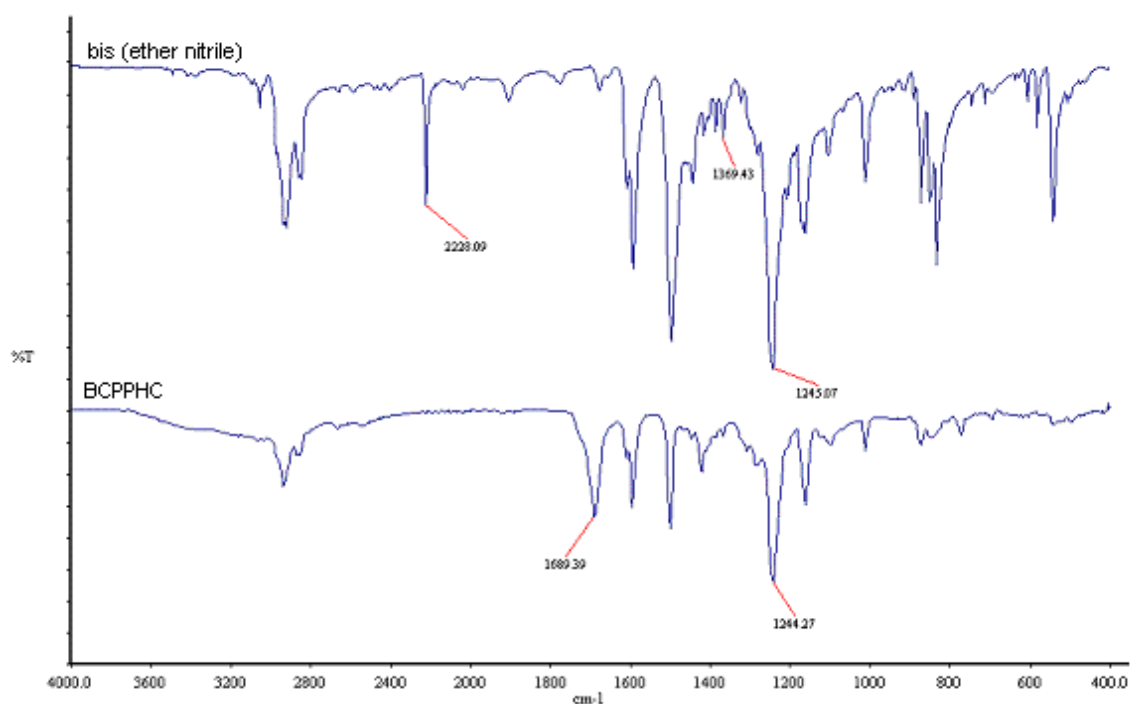


Figure 3.56 FTIR spectra of 1,1-bis[4-(4-cyanophenoxy)phenyl]-4-per hydrocumyl cyclohexane and 1,1-bis[4-(4-carboxyphenoxy)phenyl]-4-per hydrocumyl cyclohexane

^1H NMR spectra of BCyPHC and BCPPHC along with assignments are presented in **Figure 3.57**

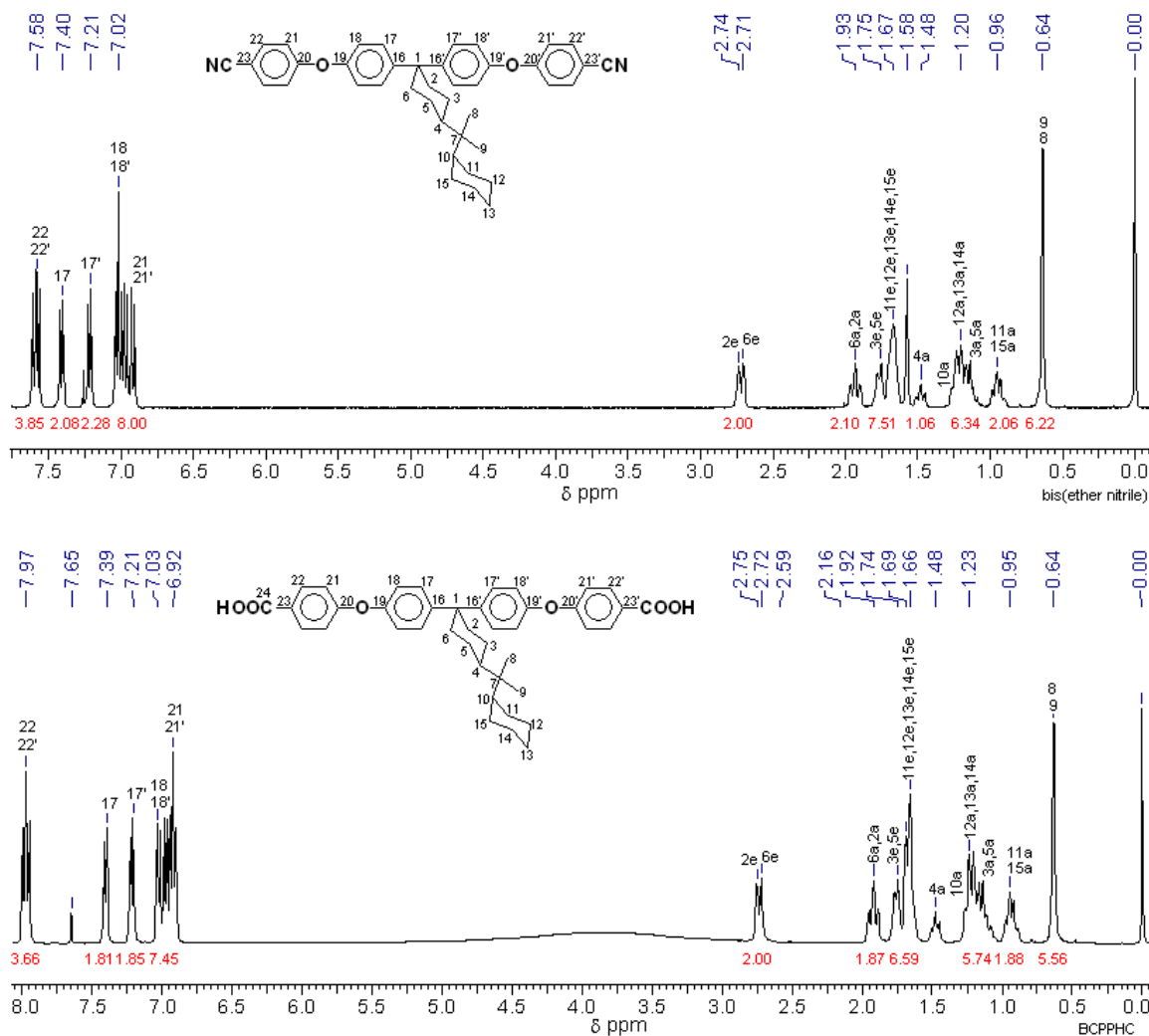


Figure 3.57 ¹H NMR spectra of 1,1-bis[4-(4-cyanophenoxy)phenyl]-4-perhydrocumyl cyclohexane and 1,1-bis[4-(4-carboxyphenoxy)phenyl]-4-perhydrocumyl cyclohexane

Peaks corresponding to the aromatic protons 22 and 22' *ortho* to nitrile and carboxylic group appeared at 7.58 and 7.97 ppm, respectively. The down field shift of protons 22 and 22' in case of BCPPHC because of stronger inductive effect of carboxylic groups confirms the complete hydrolysis of BCyPHC.

¹³C NMR spectra of BCyPHC and BCPPHC along with assignments are presented in **Figure 3.58**

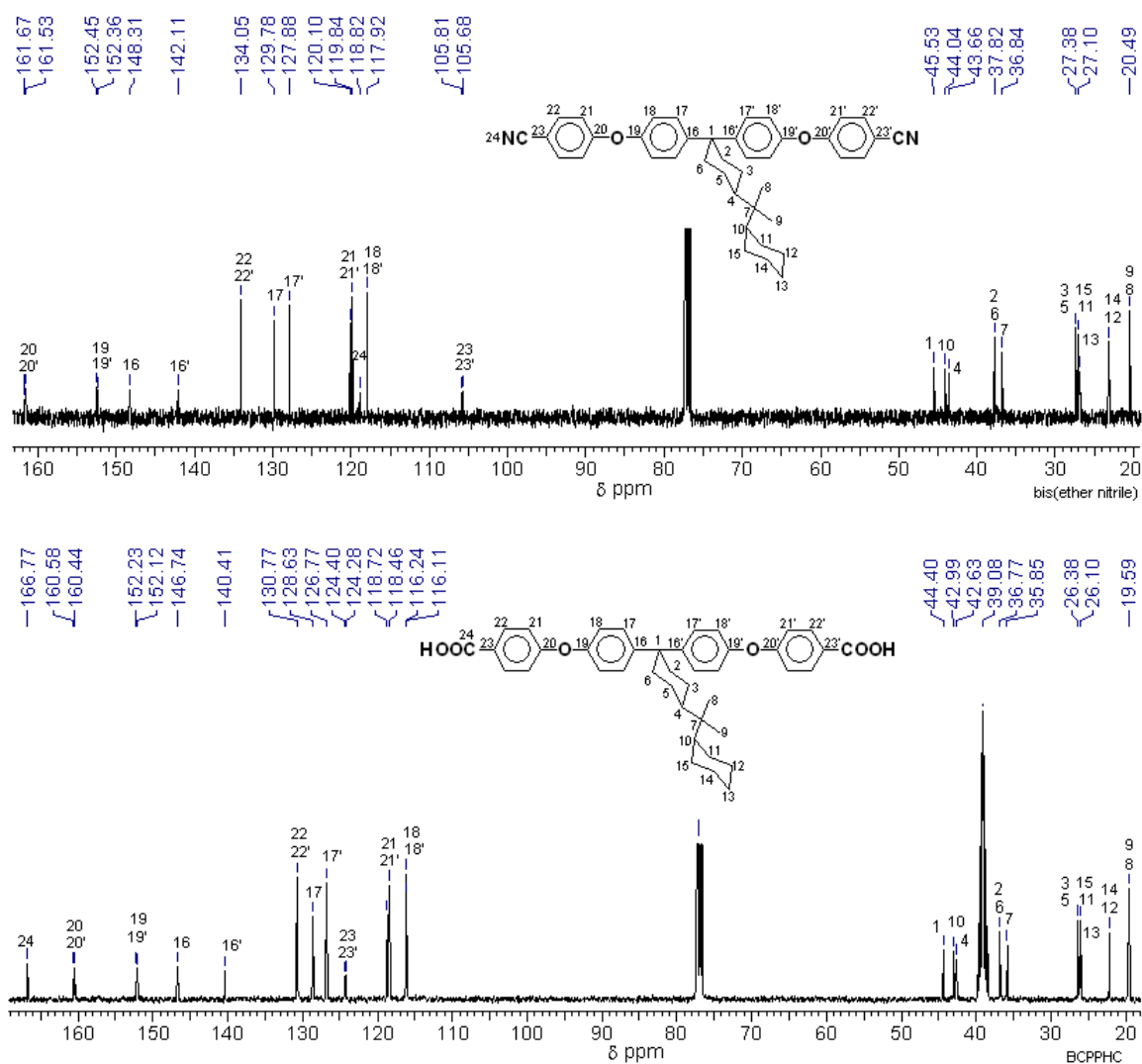


Figure 3.58 ^{13}C NMR spectra of 1,1-bis[4-(4-cyanophenoxy)phenyl]-4-perhydrocumyl cyclohexane and 1,1-bis[4-(4-carboxyphenoxy)phenyl]-4-perhydrocumyl cyclohexane

Peaks corresponding to carbons 23 and 23', adjacent to nitrile and carboxylic group, appeared at 105.81, 105.68 and 124.40, 124.28 ppm, respectively. The up field shift of carbons 23 and 23' in case of BCyPHC was mainly because of the anisotropic shielding by the π electrons of $\text{C}\equiv\text{N}$ group. A peak corresponding to carbon of $\text{C}\equiv\text{N}$ group appeared at 118.82 ppm, where as carbonyl carbon appeared at the farthest downfield at the frequency of 167.55 ppm. All the spectroscopic data agreed with the proposed structure.

3.5 Conclusions

1. Cashew nut shell liquid and *p*-cumylphenol were successfully utilized for the synthesis of value added monomers *via* simple organic reaction sequences.
2. Two new difunctional monomers viz., 1,1-bis(4-hydroxyphenyl)-3-pentadecylcyclohexane and 1,1-bis(4-aminophenyl)-3-pentadecylcyclohexane were synthesized from CNSL.
3. Five new bisphenols and 1,1-bis(4-aminophenyl) -4-perhydrocumyl cyclohexane were synthesized from *p*-cumylphenol.
4. Two new ether containing difunctional monomers viz., 1,1-bis[4-(4-aminophenoxy)phenyl]-4-per-hydrocumyl cyclohexane and 1,1-bis[4-(4-carboxyphenoxy)phenyl]-4-per-hydrocumyl cyclohexane were synthesized starting from *p*-cumylphenol.
5. All the monomers were characterized by spectral techniques and were of high purity.
6. Whenever suitable crystals could be obtained, X-ray crystallography provided unequivocal assignment of chemical structure.
7. All the monomers containing substituted cyclohexylidene moiety showed the presence of distereotopic phenyl rings, which are magnetically non-equivalent.
8. New difunctional monomers are potentially useful for the synthesis of host of processable high performance polymers.

References

1. *Relating Materials Properties to Structure: Handbook and Software for Polymer Calculations and Material Properties*; David, D.J.; Misra, A.; Eds.; Technomic Publishing Company Inc.: Lancaster, 1999.
2. Ulmer II, C. W.; Smith, D.A.; Sumpter, B.G.; Noid, D.I. *Computational and Theoretical Polymer Science* **1998**, *8*, 311.
3. *Prediction of Polymer Properties*; Bicerano, J., Marcel Dekker Inc.: New York, 1996.
4. *Synthetic Methods in Step Growth Polymers*, Rogers, M.E.; Long, T.E.; Eds.; John Wiley and Sons : New York , 2003.
5. *Polyimides and Other High Temperature Polymers, Vol. I*, Mittal, H.K., Ed.; VSP BV, The Netherlands, 2001.
6. Harvey, M.T.; Caplan, C. *Ind. Eng. Chem.* **1940**, *10*, 1306.
7. Lubi, M.C.; Thachil, E.T. *Designed monomers and polymers* **2000**, *3*, 123.
8. Suresh, K.I.; Kishanprasad, V.S. *Ind. Eng. Chem. Res.* **2005**, *44*, 4504
9. Shingte, R.D.; Wadgaonkar, P.P. U.S. Patent Number 6,790,993, **2004**.
10. Avadhani, C.V.; Wadgaonkar, P.P.; Sivaram, S. U.S. Patent Number 6,255,439, **2001**
11. *Kirk-Othmer Encyclopedia of Chemical Technology, Vol. 2*, Kroschwitz, J.I.; Seidel, A.; Backford, M.; Eds.; Wiley Interscience : Hoboken, 2004.
12. *Purification of Laboratory Chemicals*; Perrin, D.D.; Armarego, W.L.F. Pergamon Press: NewYork, 1989.
13. Corey, E.J.; Suggs, J.W. *Tetrahedron Lett.* **1975**, *31*, 2647
14. Murthy, B.G.; Menon, M.C.; Aggarwal, J.S.; Zaheer, S.H. *Paint Manuf.* **1961** *31*, 47
15. Sheldrick, G. M. SHELX-97 program for crystal structure solution and refinement, University of Gottingen, Germany, 1997
16. Madhusudhan, V; Ramaiah M.S.; Naidu, N.B.; Sivasamban, M.A. *Indian J. Technol.* **1973**, *11*, 347.
17. Sethi, S.C.; Subba Rao, B.C. *Indian J. Chem.* **1964**, *2*, 178.
18. Rao, M.V.; Rojivadiya, A.J.; Parsania, P.H.; Parekh, H.H. *J. Indian Chem. Soc.* **1987**, 758
19. Bhople, R.D.; Rao, B.Y.; Rao, C.V.N. *J. Oil. Technol. Ass. India.* **1969**, 15.
20. Tobicik, J.; Cerveny, L. *J. Mol. Catal. A: Chemical* **2003**, *194*, 249
21. Silberova, B.; Cerveny, L. *React. Kinet. Catal. Lett.* **1999**, *67*, 29

22. Murzin, D.Y.; Allachverdiev, A.I.; Kulkova, N.V. in *Heterogeneous Catalysis and Fine Chemical III*, Guisnet, M. (Eds.), Elsevier Science Publishers, **1993**
23. Srinivas, S. T.; Jhansi Lakshmi L.; Kanta Rao P. *Appl. Cata. A* **1994**, *110*, 167.
24. Kut, O.M.; Datwyler, U.R.; Gut, G. *Ind. Eng. Chem. Res.* **1988**, *27*, 219.
25. *Organic Synthesis by Oxidation with Metal Compounds*, Mijs, W.J.; de Jonge, C.R.H.I. Eds, Plenum Press, New York, **1986**
26. Dess, D.B.; Martin, J.C. *J.Org. Chem.* **1983**, *48*, 4155.
27. de Nooy, A.E.J.; Besemer, A.C.; van Bekkum, H. *Synthesis*, **1996**, 1153.
28. Satov, K.; Aoki, M.; Takagi, J.; Zimmermann, K.; Noyori, R. *Bull. Chem. Soc. Jpn.* **1999**, *72*, 2287
29. Markao, I.E.; Gautier, A.; Chelle-Regnaut, I.; Giles, P.R.; Tsukazaki, M.; Urch, C.J.; Brown, S.M. *J. Org. Chem.* **1998**, *63*, 7576.
30. Kakiuchi, N.; Maeda, Y.; Nishimura, T.; Uemura, S. *J. Org. Chem.* **2001**, *66*, 6620.
31. Vocanson, F.; Guo, Y.P.; Namy, J.L.; Kagan, H.B. *Synth. Commun.* **1998**, *28*, 2577.
32. Nishimura, T.; Onoue, T.; Ohe, K.; Uemura, S. *J. Org. Chem.* **1999**, *64*, 6750.
33. Yamada, M.; Sun, J.; Suda, Y.; Nakaya, T. *Chem. Lett.* **1998**, 1055.
34. Wehmeyer, R.; Walters, M.; Tasset, E.; Brewster, S. US Patent Number 5,463,140, **1995** issued to Dow Chemical.
35. Ghatge, N.D.; Khune, G.D. *Indian Chem. J.* **1978**, 23
36. Srinivasan, P.R.; Mahadevan, V.; Srinivasan, M. *J. Polym. Sci. Polym. Chem.* **1981**, *19*, 2277.
37. Yi, M.H.; Huang, W.; Jin, M.Y.; Choi, K.-Y. *Macromolecules*, **1997**, *30*, 5606.
38. Serijan, K.T.; Wise, P.H. *J. Am. Chem. Soc.* **1951**, *73*, 4766.
39. Nangia, A.; Desuraju, G.R. *Chem. Commun.* **1999**, 605.

Chapter 4. Synthesis and Characterization of Processable High Performance Polymers Containing Cyclohexylidene Moiety with Flexible Pentadecyl Substituent

4.1 Introduction

Aromatic polyimides and polyesters are important examples of high performance polymers. High thermal stabilities, solvent resistance and good mechanical properties of these polymers makes them possible to meet the demands of the modern industry in the areas of aviation, automobile, electronics, etc. However, high regularity and rigidity of the backbone of these polymers poses a challenge for their processing. Several approaches have been adapted to improve the processability of polyimides and polyesters.¹⁻⁵ Of the many approaches attempted to improve processability of high performance polymers, introduction of “cardo” groups (pendant loops) into rigid polymer backbone has resulted in greater success.⁶⁻¹¹

Another approach of interest is introduction of flexibilizing linkages either in the backbone or as pendant group, both of which lead to improved solubility/processability.¹²⁻¹⁴ When the flexibilizing group is appended to the polymer chains it is referred to as an “internal plasticizer” which can also act as a bound solvent. The pendant flexibilizing groups affect the polymer properties leading to reduction in melt viscosity, lowering the temperature of second order transition (T_g) and elastic modulus.

The methylene units in the side chains cause lowering in the glass transition temperature by providing more number of rotational degrees of freedom and relative ease of rotational mobility.¹² Pentadecyl-substituted cyclohexylidene containing monomers were designed and synthesized starting from cashew nut shell liquid (CNSL), a renewable resource material *via* simple organic transformations (**Chapter 3**). It was of interest to study the effect of pentadecyl chain on the polymer solubility/processability.

A series of (co)polyesters and (co)polyimides was synthesized by reacting bisphenol and diamine containing pentadecyl cyclohexylidene moiety with diacid chlorides and commercial dianhydrides, respectively.

Polyesters and polyimides were characterized by inherent viscosity measurements, solubility tests, FTIR, $^1\text{H-NMR}$, $^{13}\text{C-NMR}$ spectroscopy, X-ray diffraction, thermogravimetric analysis (TGA), and differential scanning calorimetry (DSC). Polyimides were studied by UV-visible spectroscopy. Copolyimides were evaluated for pretilt angle measurements.

4.2 Experimental

4.2.1 Materials

1,1-Bis(4-hydroxyphenyl)-3-pentadecylcyclohexane (BPC_{15}), 1,1-bis(4-hydroxyphenyl)cyclohexane (BPC), 1,1-bis(4-hydroxyphenyl)-3-methylcyclohexane (BPC_1) and 1,1-bis(4-aminophenyl)-3-pentadecylcyclohexane (BAC_{15}) were synthesized as described in **Chapter 3**. The dianhydrides, pyromellitic dianhydride (PMDA), 3,3',4,4'-biphenyl tetracarboxylic dianhydride (BPDA), 3,3',4,4'-benzophenonetetracarboxylic dianhydride (BTDA), 3,3',4,4'-oxydiphthalic anhydride (ODPA) and 4,4'-(hexafluoro isopropylidene)diphthalic anhydride (6-FDA), all received from Aldrich, USA, were sublimed before use. 4,4'-Oxydianiline (ODA) (Aldrich, USA) was sublimed before use. Bisphenol-A and benzyltriethylammonium chloride (BTEAC), both received from Aldrich, USA were used as received. Dichloromethane and *m*-cresol, both from S. D. Fine Chem., India were dried and distilled according to the reported procedure.¹⁵

Isophthalic acid chloride and terephthalic acid chloride were synthesized from isophthalic acid and terephthalic acid, respectively using excess thionyl chloride in the presence of pyridine as a catalyst and were purified by distillation under reduced pressure.

4.2.2 Measurements

Inherent viscosity of polymers was measured with 0.5 % (w/v) solution of polymer in either chloroform or phenol/tetrachloroethane (60/40, w/w) at $30\pm 0.1^\circ\text{C}$ using an Ubbelohde suspended level viscometer.

Molecular weight of polyesters were measured on Thermofinnigan make gel permeation chromatograph (GPC), using the following conditions: Column - polystyrene-divinylbenzene (10^5 \AA to 50 \AA), Detector - RI, room temperature. Polystyrene was used as the calibration standard. Polymer sample (5 mg) was dissolved in 5 ml chloroform and filtered through $0.2 \mu\text{m}$ SS-filter.

FTIR spectra were recorded using polymer films on a Perkin-Elmer *Spectrum GX* spectrophotometer.

NMR spectra were recorded on a Bruker 200, 400 or 500 MHz spectrometer at resonance frequencies of 200, 400 or 500 MHz for ^1H and 50, 100 or 125 MHz for ^{13}C measurements using CDCl_3 as a solvent.

Thermogravimetric analysis was performed on Perkin-Elmer TGA-7 system at a heating rate of $10^\circ\text{C} / \text{minute}$ under nitrogen atmosphere. Sample weight taken was ~ 5 mg.

DSC was carried out on TA Instruments *DSC Q10*, at a heating rate of $10^\circ\text{C} / \text{minute}$ in nitrogen atmosphere.

X-Ray diffraction patterns of polymers were obtained on a Rigaku Dmax 2500 X-ray diffractometer at a tilting rate of $2^\circ / \text{minute}$. Dried polymer films or powder was used for X-ray measurements.

4.2.3 Cell preparation for pretilt angle measurement

Indium tin oxide (ITO) coated glass (25 mm x 25 mm) was obtained from M/s Merck, Germany. The ITO coated glass substrate was thoroughly washed successively with soap solution, deionised water and ethanol followed by drying. A 1 wt. % solution of copolyimide derived 1,1-bis(4-aminophenyl)-3-pentadecylcyclohexane, 4,4'-oxydianiline and BPDA was prepared in tetrachloroethane. Spin coating of polyimide was performed using a Karl Süss CT-62 spin coater (5 s at 1000 rpm, 40 s at 5000 rpm) on the ITO side. After spin coating, the substrate was heated at 100°C for 10 minutes.

The liquid crystal E7, a mixture consisting of 50.6 % 4'-pentylcyanobiphenyl (5CB), 25.2 % 4'-heptylcyanobiphenyl (7CB), 17.8 % 4'-octyloxycyanobiphenyl (8OCB), and 6.4 % 4'-pentylcyanoterphenyl (5CT), ($T_{NI} = 60^\circ\text{C}$, $\rho = 1.06\text{ g/cm}^3$, $\epsilon_{//} = 19$ and $\epsilon_{\perp} = 5.2$, and $\Delta n = 0.225$) was obtained from M/s Merck Ltd., Germany.

Electro-optical cells were constructed using ITO-coated glass coated with the polyimide substrate. Polyimide surface was rubbed uniformly with a velvet cloth. A twisted nematic cell was constructed by placing the two substrates orthogonal to each other with respect to their rubbing direction. The cells were secured with UV curable glue (Norland UV Sealant 91) having $18\ \mu\text{m}$ spacers. The cells were filled with liquid crystal material E7, by capillary action at 80°C , which is 20°C above the nematic-isotropic transition temperature of the liquid crystal.

Electro-optical characteristics were investigated using DMS 703 display measuring system (Autronic-Melchers GmbH). A square wave was used to drive the cells for the dynamic response measurements at 1000 Hz. The pretilt angle was measured directly using the crystal rotation method (Autronic, TBA 107).¹⁶

4.3 Synthesis of (co)polyesters and (co)polyimides containing pentadecylcyclohexylidene moiety

4.3.1 Synthesis of polyesters from 1,1-bis(4-hydroxyphenyl)-3-pentadecylcyclohexane and terephthalic acid chloride / isophthalic acid chloride

A representative procedure for synthesis of polyesters is described below.

Into a 100 ml two-necked round bottom flask equipped with a high-speed mechanical stirrer and an addition funnel, were placed 1,1-bis(4-hydroxyphenyl)-3-pentadecylcyclohexane (BPC₁₅) (2.39 g, 5 mmol) and 1M NaOH (10.2 mL). Thereafter, BTEAC (30 mg) was added to the reaction mixture and the flask was cooled to 10 °C. A solution of terephthalic acid chloride (1.02 g, 5 mmol) dissolved in dichloromethane (12 mL) was added in one lot to the reaction mixture and the mixture was stirred vigorously at 2000 rpm for 1 h. The aqueous layer was decanted and the organic layer was diluted with additional 15 mL of dichloromethane. The polymer solution was precipitated in excess methanol and the precipitated polymer was filtered and washed several times with water and then with methanol. The polymer was dried at 60°C under reduced pressure for two days.

A similar procedure was followed for the synthesis of other polyester.

4.3.2 Synthesis of copolyesters from 1,1-bis(4-hydroxyphenyl)-3-pentadecylcyclohexane and BPA with terephthalic acid chloride

A representative procedure for synthesis of copolyesters is described below.

Into a 100 ml two-necked round bottom flask equipped with a high-speed mechanical stirrer and an addition funnel, were placed BPA (1.08 g, 4.75 mmol), BP-C₁₅ (0.12 g, 0.25 mmol) and 1M NaOH (10.2 mL). Thereafter, BTEAC (30 mg) was added to the reaction mixture and flask was cooled to 10 °C. A solution of terephthalic acid chloride (1.02 g, 5 mmol) dissolved in dichloromethane (12 mL) was added in one lot to the reaction mixture

and the mixture was stirred vigorously at 2000 rpm for 1 h. The aqueous layer was decanted and the organic layer was diluted with additional 15 mL of dichloromethane. The polymer solution was precipitated in excess methanol, the precipitated polymer was filtered and washed several times with water and then with methanol and dried at 80°C under reduced pressure for two days.

A similar procedure was followed for the synthesis of other copolyesters.

4.3.3 Synthesis of polyimides from 1,1-bis(4-aminophenyl)-3-pentadecylcyclohexane and commercial dianhydrides

Polyimides were synthesized by one-step high temperature solution polymerization in *m*-cresol. A representative procedure for the synthesis of polyimides is described below.

Into a 50 mL three-necked round bottom flask equipped with a magnetic stirring bar, nitrogen inlet and a guard tube, 1,1-bis(4-aminophenyl)-3-pentadecylcyclohexane (0.48 g, 1 mmol) was added and dissolved in 6 mL of freshly distilled *m*-cresol. To the homogeneous solution, PMDA (0.22 g, 1 mmol) was added in portions at room temperature. The reaction mixture was heated to 80°C and was stirred for 1 h. The temperature was then raised to 200°C and reaction mixture was stirred for 6 h at that temperature. The polymerization reaction was performed under gentle stream of nitrogen and the water formed during imidization was continuously removed with a stream of nitrogen. After 6 h, reaction mixture was cooled to room temperature and was added to excess methanol. The precipitated polymer was washed with methanol to remove *m*-cresol and was dried at 100°C for 24 h under reduced pressure.

4.3.4 Synthesis of copolyimides from 1,1-bis(4-aminophenyl)-3-pentadecylcyclohexane and 4,4'-oxydianiline with biphenyltetracarboxylic dianhydride

Copolyimides were synthesized by one-step high temperature solution polymerization in *m*-cresol. A representative procedure for the synthesis of copolyimides is described below.

Into a 50 mL three-necked round bottom flask equipped with a magnetic stirring bar, nitrogen inlet and a guard tube, 1,1-bis(4-aminophenyl)-3-pentadecylcyclohexane (0.24 g, 0.5 mmol) and 4,4'-oxydianiline (0.10 g, 0.5 mmol) were added and dissolved in 6 mL of freshly distilled *m*-cresol. To the homogeneous solution, BPDA (0.29 g, 1 mmol) was

added in portions at room temperature. The reaction mixture was heated to 80°C and was stirred for 1 h. The temperature was raised to 200°C and the reaction mixture was stirred for 6 h at that temperature. The polymerization reaction was performed under gentle stream of nitrogen and the water formed during imidization was continuously removed with a stream of nitrogen. After 6 h, reaction mixture was cooled to room temperature and was added to excess methanol. The precipitated polymer was washed with methanol to remove *m*-cresol and was dried at 100°C for 24 h under reduced pressure.

4.4 Results and Discussion

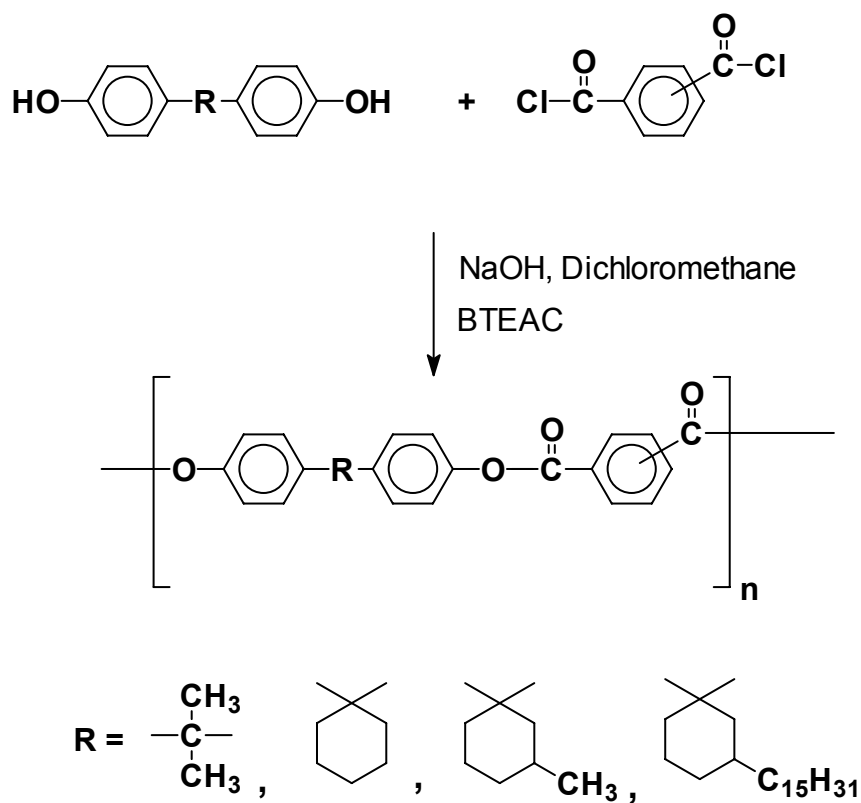
4.4.1 Synthesis and characterization of polyesters from 1,1-bis(4-hydroxyphenyl)-3-pentadecylcyclohexane and terephthalic acid chloride / isophthalic acid chloride

Aromatic polyesters are well known for their high thermal stabilities and mechanical properties.^{1,4,7} Different kinds of polyesters have been synthesized over the past decades from various types of diacid chlorides and diols. Polyester derived from isophthalic acid and terephthalic acid with bisphenol-A have been commercialized. However, they are difficult to process because of the rigid polymer backbone. Much attention has been paid to improve the processability of polyesters by design of new monomers.

In the present study, 3-pentadecylcyclohexylidene containing polyesters were synthesized to study the effect of incorporation of flexible pentadecyl chain on the polymer properties. Polyesters containing unsubstituted cyclohexylidene and methyl-substituted cyclohexylidene were synthesized for comparison purpose.

The interfacial polycondensation using phase transfer catalyst is a very effective method for the synthesis of aromatic polyesters.¹⁷⁻²⁰ In the present work, polyesters were synthesized by interfacial polycondensation with a solution of diacid chloride in dichloromethane and aqueous solution of sodium salt of bisphenols using BTEAC as the phase transfer catalyst.

Scheme 4.1 illustrates the synthesis of polyesters from diacid chlorides and bisphenols.



Scheme 4.1 Synthesis of polyesters from bisphenols and terephthalic acid chloride / isophthalic acid chloride

The results of polymerizations are summarized in **Table 4.1** and **4.2**. Polymerization reactions based of BPC₁₅ proceeded in a homogeneous manner and polyesters did not phase out of the reaction medium. However, polyesters derived form BPA, BPC and BPC₁ phased out of the reaction medium.

Table 4.1 Synthesis of polyesters from 1,1-bis(4-hydroxyphenyl)-3-pentadecylcyclohexane and terephthalic acid chloride / isophthalic acid chloride

Polyester	Bisphenol	Diacid chloride	Yield (%)	η_{inh} (dL/g) ^a
P-1	BPC ₁₅	TPC	97	1.45
P-2	BPC ₁₅	IPC	96	0.66

a: η_{inh} was measured with 0.5% (w/v) solution of polyester in chloroform at 30±0.1°C.

Table 4.2 Synthesis of polyesters from BPA, BPC and BPC₁ with terephthalic acid chloride / isophthalic acid chloride

Polyester	Bisphenol	Diacid chloride	Yield (%)	η_{inh} (dL/g) ^a
P-3	BPA	TPC	95	1.23
P-4	BPA	IPC	95	0.90
P-5	BPC	TPC	96	0.60
P-6	BPC ₁	TPC	97	0.35
P-7	BPC ₁	IPC	96	0.35

a: η_{inh} was measured with 0.5% (w/v) solution of polyester in phenol/tetrachloroethane (60/40, w/w) at 30±0.1°C.

The inherent viscosities of polyesters were in the range 0.35 – 1.45 dL/g.

BPC₁₅ derived polyesters were soluble in chloroform and the results of GPC measurements on polyesters are presented in **Table 4.3**.

Table 4.3 GPC data for polyesters derived from 1,1-bis(4-hydroxyphenyl)-3-pentadecylcyclohexane and terephthalic acid chloride / isophthalic acid chloride

Polyester	Bisphenol	Diacid chloride	Molecular weight ^a		Polydispersity index
			M _n	M _w	M _w /M _n
P-1	BPC ₁₅	TPC	58,350	200,000	3.4
P-2	BPC ₁₅	IPC	53,380	111,340	2.1

a measured by GPC in chloroform, polystyrene was used as a calibration standard.

Number average molecular weights (M_n) for terephthalic acid chloride and isophthalic acid chloride- based polyesters were 58,350 and 53,380 with polydispersity index of 3.4 and 2.1, respectively. Inherent viscosity and GPC data indicated the formation of reasonably high molecular weight polymers. However, the molecular weight values provided by GPC should not be taken as absolute as the calibration of GPC was carried out using polystyrene standards.

Tough, transparent and flexible films of polyesters derived from BPC₁₅ could be cast from chloroform solutions.

4.4.1.1 Structural characterization

The formation of polyesters was confirmed by FTIR, ¹H-NMR and ¹³C-NMR spectroscopy.

FTIR spectrum of polyester derived from BPC₁₅ and terephthalic acid chloride is reproduced in **Figure 4.1**. Ester carbonyl band was observed at 1741 cm⁻¹

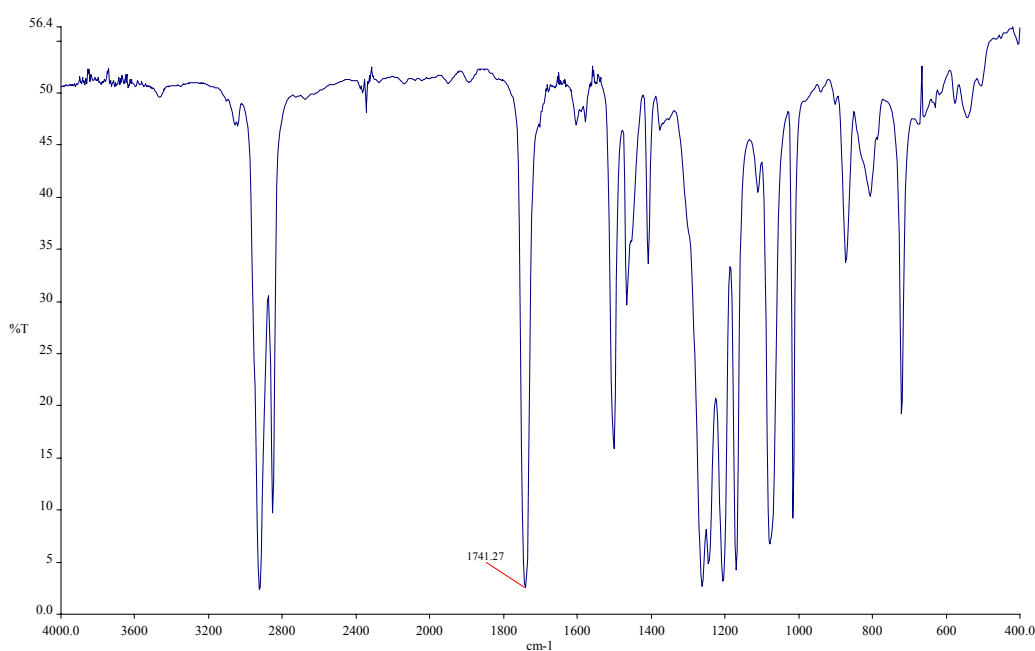
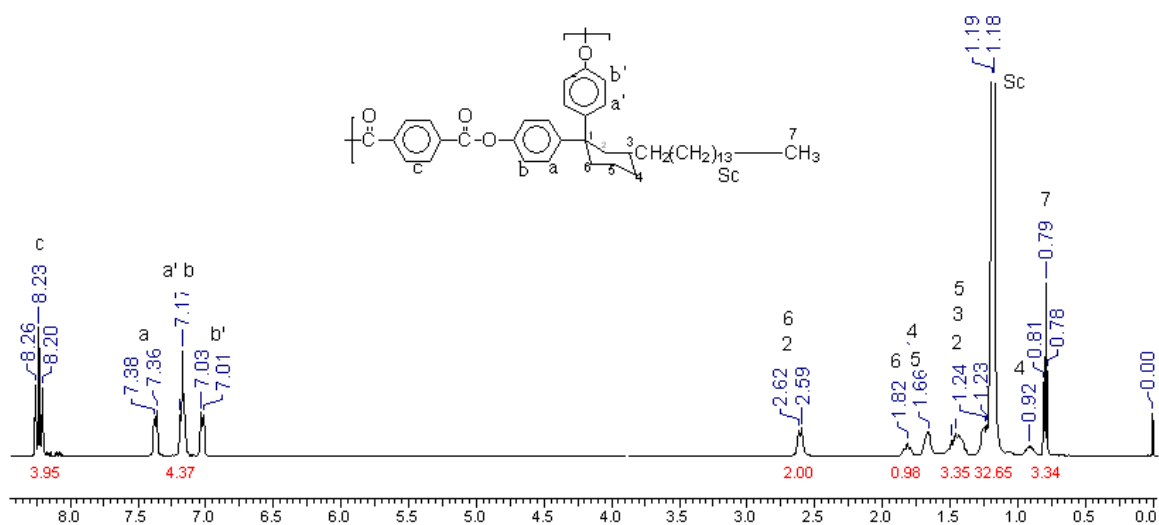
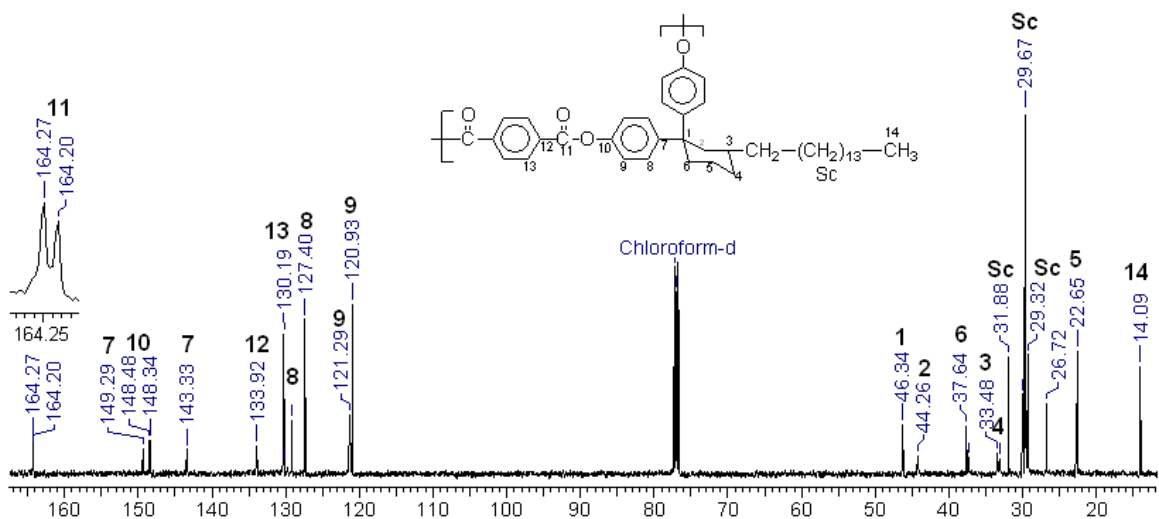


Figure 4.1 FTIR spectrum of polyester derived from 1,1-bis(4-hydroxyphenyl)-3-pentadecylcyclohexane and terephthalic acid chloride

¹H and ¹³C-NMR spectra of polyester derived from BPC₁₅ and terephthalic acid chloride along with assignments are shown in **Figure 4.2**.



¹H-NMR spectrum of polyester (P-4)



¹³C-NMR spectrum of polyester (P-4)

Figure 4.2 ¹H and ¹³C-NMR spectra of polyester derived from BPC₁₅ and terephthalic acid chloride

¹H-NMR spectrum of polyester derived from BPC₁₅ and terephthalic acid chloride (P-4) showed the presence of three peaks at 8.26, 8.23 and 8.20 ppm for terephthalic acid ring protons. Terephthalic acid ring protons in 4-cumylphenyl terephthalate (a model compound for polyester derived from BPA terephthalic acid), exhibited a singlet at 8.31 ppm as studied by the ¹H-NMR (300 MHz) spectroscopy indicating that all the four protons of terephthalic acid moiety are magnetically equivalent. (Figure 4.3).²¹

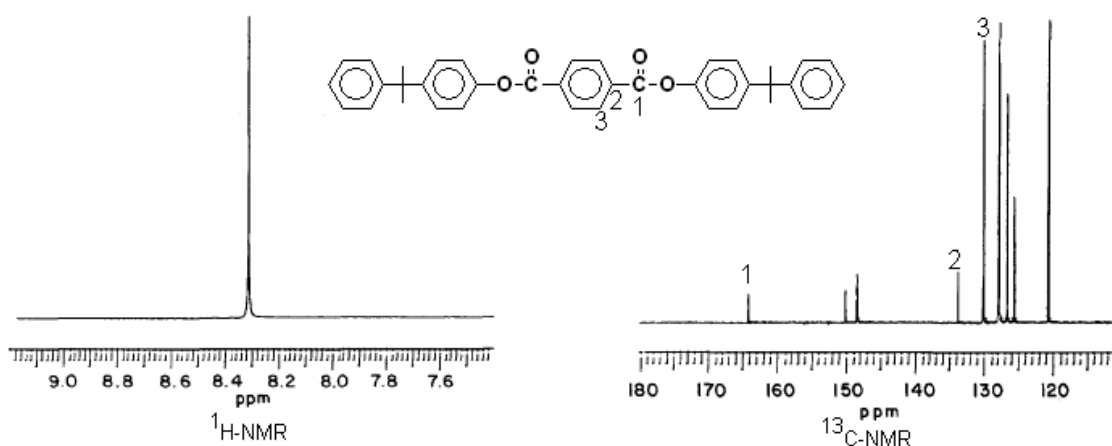
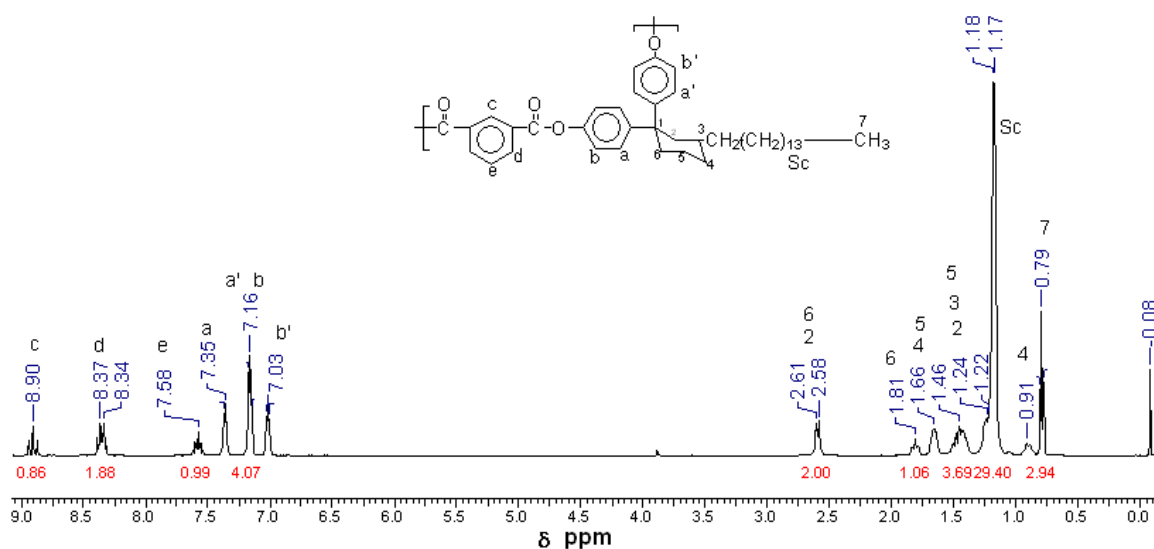


Figure 4.3 Partial $^1\text{H-NMR}$ and ^{13}C NMR spectra of 4-cumylphenyl terephthalate at 300 MHz²¹

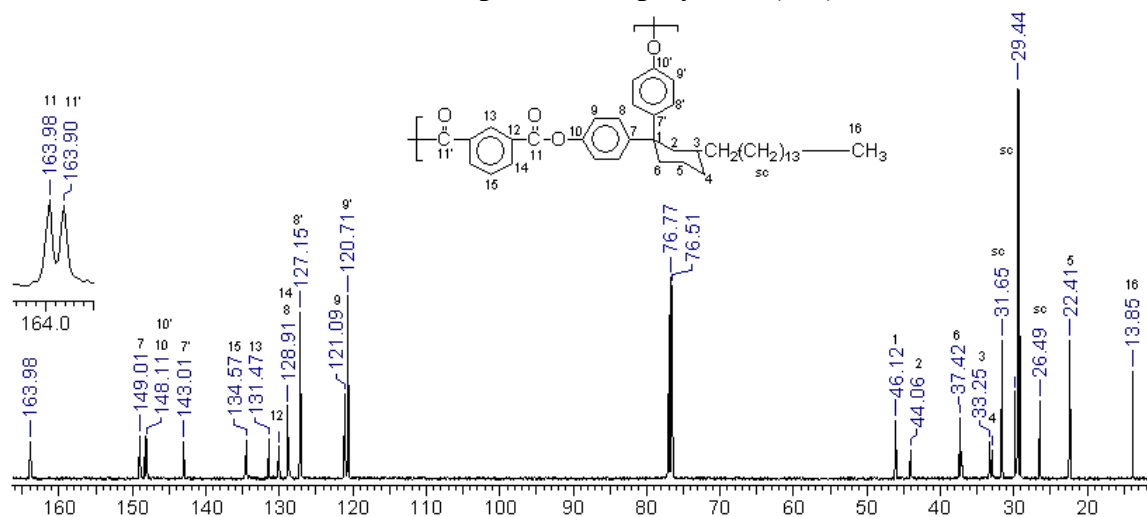
$^{13}\text{C-NMR}$ spectrum for polyester derived from BPC₁₅ and terephthalic acid chloride showed two ester carbonyl peaks at 164.25 and 164.20 δ ppm indicating the two different environments for the carbonyl carbons. 4-Cumyl phenyl terephthalate exhibited only one peak at 163.37 ppm corresponding to carbonyl carbon.

It was observed that, all the polyesters derived from terephthalic acid chloride and substituted cyclohexylidene containing bisphenols, discussed in this thesis showed the similar pattern of proton and carbon NMR signals. A detailed discussion on the origin of three peaks for terephthalic protons is presented in **Chapter 5**.

$^1\text{H-NMR}$ and $^{13}\text{C-NMR}$ spectra of polyester derived from BPC₁₅ and isophthalic acid chloride along with assignments is reproduced in **Figure 4.4**.



¹H-NMR spectrum of polyester (P-5)



¹³C-NMR spectrum of polyester (P-5)

Figure 4.4 ¹H and ¹³C-NMR spectra of polyester derived from 1,1-bis(4-hydroxyphenyl)-3-pentadecylcyclohexane and isophthalic acid chloride

Three different types of protons c, d and e can be distinguished for isophthalic moiety in ¹H-NMR spectrum of polyester derived from BPC₁₅ and isophthalic acid chloride. The most deshielded proton 'c' is located at 8.98 ppm as a split triplet. The magnetically equivalent protons 'd' exhibited multiplet in the region 8.46-8.40 ppm as compared to doublet of doublet in case of 4-cumylphenyl isophthalate. Multiplet in the region 7.69-7.61 ppm was observed for proton 'e' as compared to the triplet in case of 4-cumylphenyl isophthalate. Comparison of ¹H-NMR spectra of isophthalate parts for polyester derived from isophthalic acid chloride and BPC₁₅ with 4-cumylphenyl isophthalate is given in **Figure 4.5**. The origin of the multiplicity of the peaks centered around 8.43 and 7.65

ppm might be in the different magnetic environment experienced by these protons because of the axial equatorial phenyl rings of the bisphenol unit.

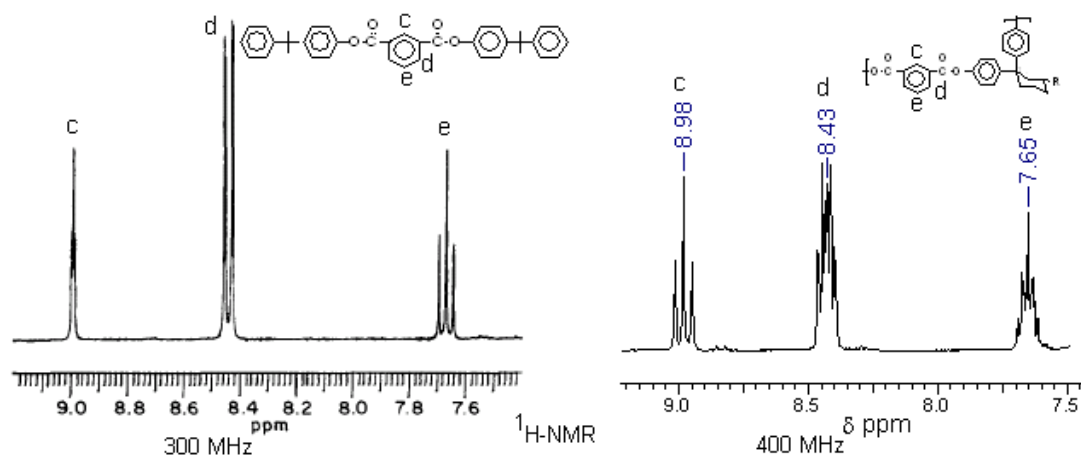


Figure 4.5 Comparison of partial $^1\text{H-NMR}$ spectra of 4-cumylphenyl isophthalate with polyester derived from isophthalic acid chloride and BPC_{15}

As in case of polyester derived from BPC_{15} and terephthalic acid chloride, $^{13}\text{C-NMR}$ spectrum of the polyester derived from BPC_{15} and isophthalic acid chloride showed two signals for carbonyl of ester linkage at 163.98 and 163.90 δ ppm, indicating the two different environments for carbonyl carbons.

All the above observations suggest the presence of constitutional isomers for the substituted cyclohexylidene containing polyesters. The different constitutional isomers can be formed by the way bisphenol and diacid chloride monomers condense with each other. It can be predicted that axial and equatorial phenyl rings in the bisphenol molecule can enchain with isophthalic acid chloride or terephthalic acid chloride in the following manner resulting in the observed NMR splitting patterns.

Axial---- Diacid----- Axial

Equatorial-----Diacid-----Equatorial

Axial-----Diacid-----Equatorial

Equatorial-----Diacid-----Axial

4.4.1.2 Solubility measurements

Solubility of polyesters was tested in various organic solvents at 3 wt % concentration and the data is summarized in **Table 4.4**.

Table 4.4 Solubility data of polyesters derived from bisphenols and terephthalic acid chloride / isophthalic acid chloride

Polyester	Bisphenol	Diacid chloride	DCM	CHCl ₃	TCE	THF	DMF	DMAC	NMP	<i>m</i> -Cresol
P 1	BPC ₁₅	TPC	++	++	++	++	-	-	-	++
P 2	BPC ₁₅	IPC	++	++	++	+	-	-	-	++
P 3	BPA	TPC	-	-	-	-	-	-	-	-
P 4	BPA	IPC	-	-	-	-	-	-	-	-
P 5	BPC	TPC	-	-	-	-	-	-	-	-
P 6	BPC ₁	TPC	-	-	-	-	-	-	-	-
P 7	BPC ₁	IPC	-	-	-	-	-	-	-	-

++ soluble at room temperature, + soluble on heating, - insoluble

Polyesters derived from BPA and terephthalic acid chloride / isophthalic acid chloride were insoluble in all the solvents tested. BPC₁₅-based polyesters were soluble in all the organic solvents tested except for amide solvents. The insolubility of BPC₁₅-based polyesters in amide solvents could be due to presence of long aliphatic chain. It is well known that amides are not good solvents for polyolefins. One of the approaches for improving the solubility is introduction of bulky cardo group along the polymer backbone. However, polyester derived from BPC and terephthalic acid chloride (P-5) was insoluble in all the organic solvents tested. The cyclohexyl ring is conformationally flexible and undergoes chair-boat transformation, allowing polymer chains to pack better.²² Consequently, cyclohexyl-containing polymers have lower free volume, as demonstrated by gas transport properties,²³ and reduces their solubility.

Polyesters were synthesized from BPC₁ to check the effect of methyl substitution on the solubility. Both the polyesters derived from terephthalic acid chloride and isophthalic acid chloride with BPC₁ were insoluble in all the organic solvents tested. This demonstrated that the methyl substitution is not large enough to impart solubility in common organic solvents. On the other hand, the presence of C₁₅ alkyl chain disrupted the packing of polymer chains, as well as provided the additional 'handle' for interaction with solvents.

4.4.1.3 X-Ray diffraction studies

Wide-angle X-ray diffraction patterns of polyesters are reproduced in **Figure 4.6**.

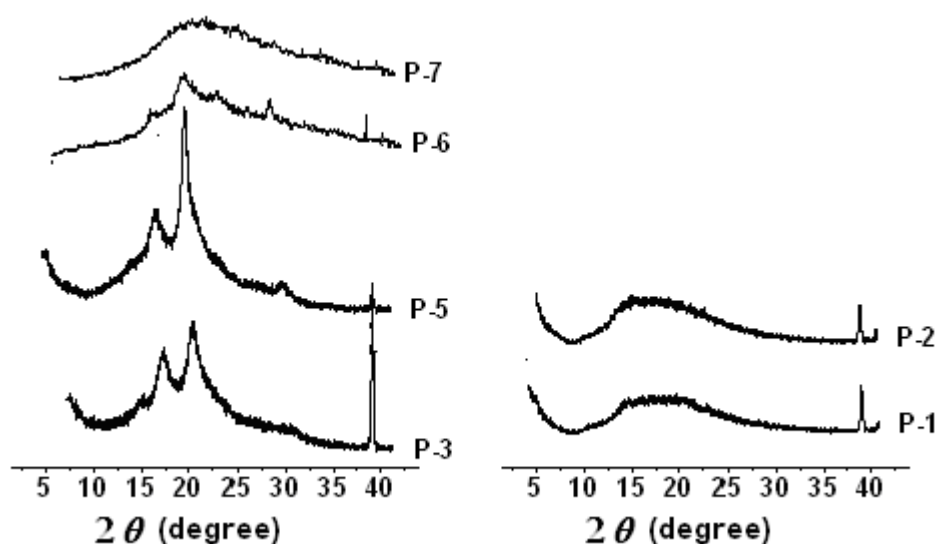


Figure 4.6 X-Ray diffraction patterns of polyesters derived from bisphenols and terephthalic acid chloride / isophthalic acid chloride

Polyesters derived from BPA, BPC and BPC₁ with terephthalic acid chloride (P-3, P-5 and P-6, respectively) showed sharp peaks, which could be attributed to their partially crystalline nature. This was reflected in their poor solubility behavior. However polyester derived from BPC₁ and isophthalic acid chloride showed only amorphous hollow. X-Ray diffraction patterns for polyesters derived from BPC₁₅ and terephthalic acid chloride / isophthalic acid chloride (P-1 and P-2) showed absence of sharp peaks. The broad amorphous hollow was observed for these polyesters, which could be mainly because of the presence of long pentadecyl chain, which hinders the packing of the polymer chains

making them amorphous. This was reflected in their improved solubility in common organic solvents.

4.4.1.4 Thermal properties

In the present study, thermal stability of polyesters was determined by thermogravimetric analysis (TGA) at a heating rate of 10°C /minute under nitrogen. TG curves of polyesters containing cyclohexylidene and substituted cyclohexylidene moiety are shown in **Figure 4.7**.

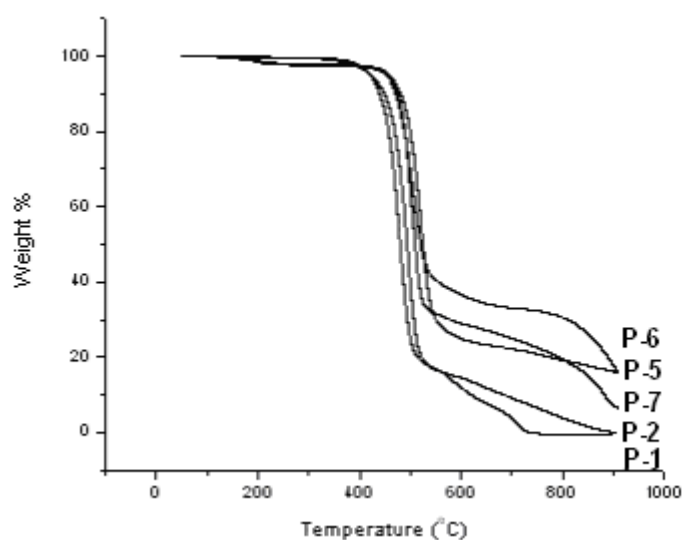


Figure 4.7 TG curves of polyesters derived from bisphenols and terephthalic acid chloride / isophthalic acid chloride

The initial decomposition temperature (IDT) and the decomposition temperature at 10% weight loss (T_{10}) for polyesters are given in **Table 4.5**. T_{10} for polyesters derived from BPA and terephthalic acid chloride and isophthalic acid chloride was 495 and 490°C, respectively. T_{10} for polyesters derived from BPC and BPC₁ with that of terephthalic acid chloride was 480 and 471°C, respectively. T_{10} for polyesters derived from BPC₁₅ and terephthalic acid chloride and isophthalic acid chloride were 451 and 439°C, respectively. An examination of the data for polyesters indicates that there was a marginal decrease in the thermal stability of polyesters containing pentadecyl chain (**Figure 4.7**).

Table 4.5 Thermal properties of the polyesters derived from bisphenols and terephthalic acid chloride / isophthalic acid chloride

Polyester	Bisphenol	Diacid chloride	IDT (°C)	T ₁₀ (°C)	T _g (°C)
P-1	BPC ₁₅	TPC	438	451	94
P-2	BPC ₁₅	IPC	428	439	74
P-3	BPA	TPC	487	495	234
P-4	BPA	IPC	475	490	190
P-5	BPC	TPC	475	480	N.D.
P-6	BPC ₁	TPC	460	471	263
P-7	BPC ₁	IPC	476	478	218

N.D. = not detected

Glass transition (T_g) temperature of polyesters was evaluated by differential scanning calorimetry (DSC). T_g values were obtained from second heating scans of polyester samples at a heating rate of 10°C / minute. DSC curves for polyesters are shown in **Figure 4.8** and T_g values are given in **Table 4.5**. T_g values of polyesters derived from BPC₁₅ with that of terephthalic acid chloride and isophthalic acid chloride were 94 and 74°C, respectively. T_g values of polyesters derived from BPC₁ with terephthalic acid chloride and isophthalic acid chloride were 263 and 218°C, respectively. Glass transition temperature of polyester derived from BPC and terephthalic acid chloride could not be detected under the present experimental conditions. All these observations clearly indicate that there is remarkable drop in glass transition temperature of polyesters by the incorporation of long pentadecyl chain. The incorporation of long pentadecyl chain as a pendant group could act as an “internal plasticizer” which can help in reduction of T_g of polyesters.

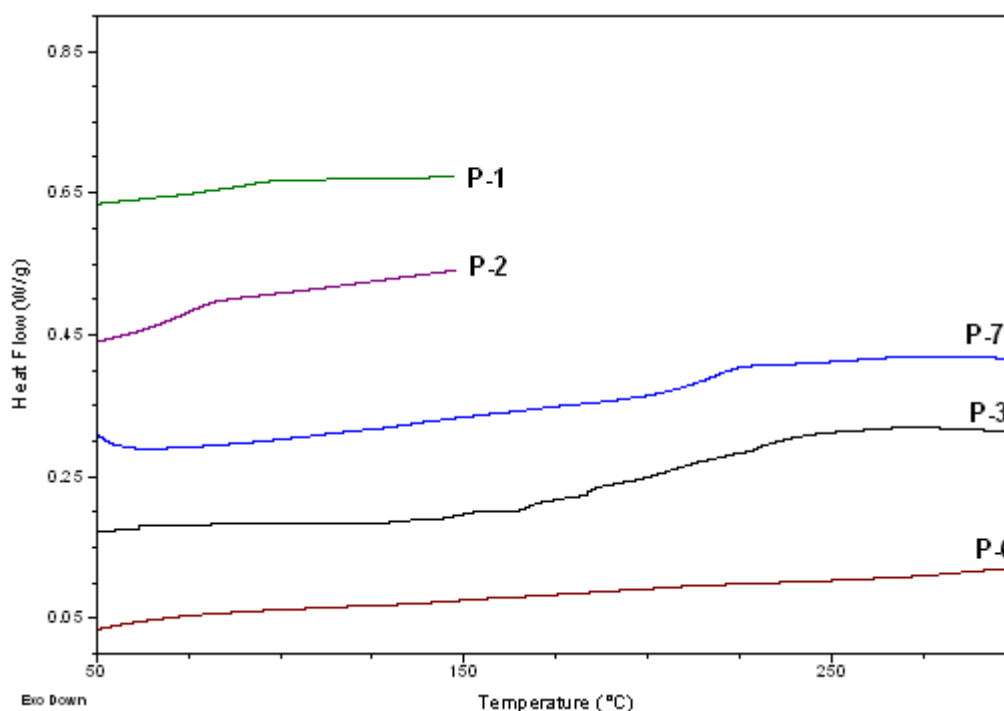
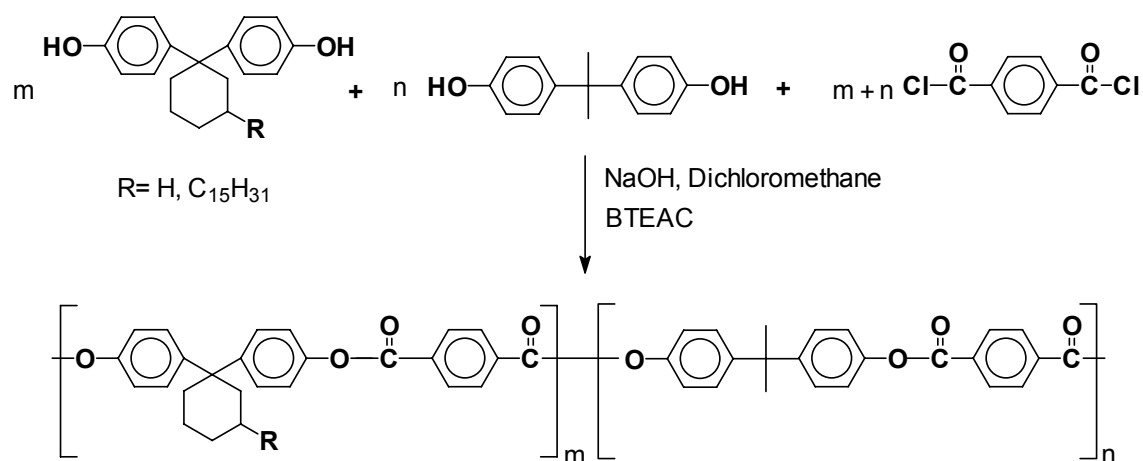


Figure 4.8 DSC curves of the polyesters derived from bisphenols and terephthalic acid chloride / isophthalic acid chloride

4.4.2 Synthesis and characterization of copolyesters from 1,1-bis(4-hydroxyphenyl)-3-pentadecylcyclohexane and BPA with terephthalic acid chloride

Copolymerization is one of the approaches for improving the solubility and in-turn processability of polymers.¹ Polyester derived from BPA and terephthalic acid chloride is insoluble in common organic solvents. It was of interest to study the effect of incorporation of varying mol% of BPC₁₅ on the properties of polyesters derived from BPA and terephthalic acid chloride.

High molecular weight copolyesters were synthesized from combination of BPA, BPC₁₅ and terephthalic acid chloride by phase transfer-catalyzed interfacial polycondensation (**Scheme 4.2**) in the presence of BTEAC as the phase transfer catalyst. The results of copolyester synthesis are summarized in **Table 4.6**



Scheme 4.2 Synthesis of aromatic copolyesters based on BPC₁₅ and BPA with terephthalic acid chloride

The synthesis of polyester P-1, P-9 and P-10 proceeded in homogeneous manner, whereas polyester P-3, P-8 and P-11 phased out of reaction mixture. Homopolyesters P-1 and P-3 synthesized in Section 4.3.1, were used for comparison.

Table 4.6 Synthesis of copolyesters from BPC₁₅ and BPA with terephthalic acid chloride

Polyester	BPA mol%	BPC ₁₅ mol%	BPC mol%	Yield (%)	η_{inh} (dL/g) ^a
P-1	0	100	0	97	1.07
P-3	100	0	0	95	1.23
P-8	95	5	0	96	1.74
P-9	90	10	0	95	2.40
P-10	85	15	0	96	1.50
P-11	85	0	15	97	0.62

a: η_{inh} was measured with 0.5% (w/v) solution of polyester in phenol/tetrachloroethane (60/40, w/w) at 30±0.1°C

Inherent viscosities of the copolyesters were in the range 0.62 to 2.40 dL/g indicating the formation of medium to high molecular weight copolyesters. The number average and weight average molecular weight for copolyester P-10 containing 15 mol % of BPC₁₅

were, 25,870 and 99,150 respectively with polydispersity index of 3.8, as determined by GPC.

Tough, transparent and flexible film of copolyester containing 15 mol % of BPC₁₅ could be cast from chloroform solution.

4.4.2.1 Structural characterization

The formation of copolyesters was confirmed by FTIR, ¹H-NMR and ¹³C-NMR spectroscopy.

FTIR spectrum of polyester (P-10) derived from BPC₁₅ and BPA with terephthalic acid chloride is shown in **Figure 4.9**. Ester carbonyl band was observed at 1741 cm⁻¹.

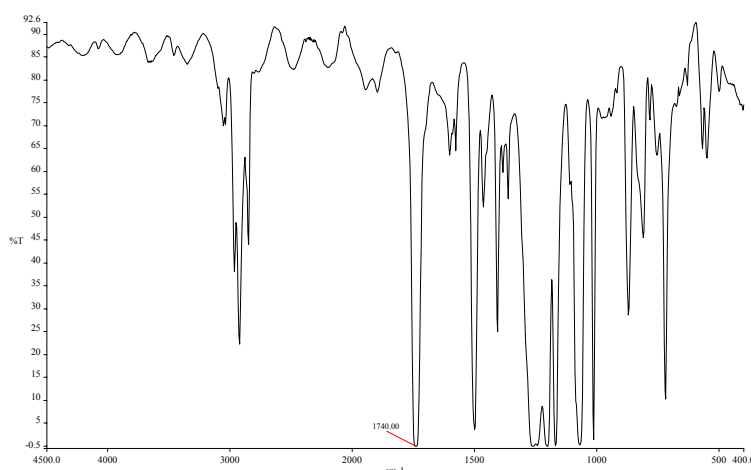


Figure 4.9 FT-IR spectrum of copolyester derived from BPC₁₅ and BPA with terephthalic acid chloride (P-10)

Composition of copolyester P-10 containing 15 mole % of BPC₁₅ was determined from ¹H-NMR spectrum (**Figure 4.10**) and it matches with the monomer feed ratio. For calculating the composition of copolyester the integration of terephthalic ring protons were compared with that of the two cyclohexyl ring protons at 2.4 ppm.

¹³C-NMR spectrum of copolyester P-10 along with assignments is reproduced in **Figure 4.11**

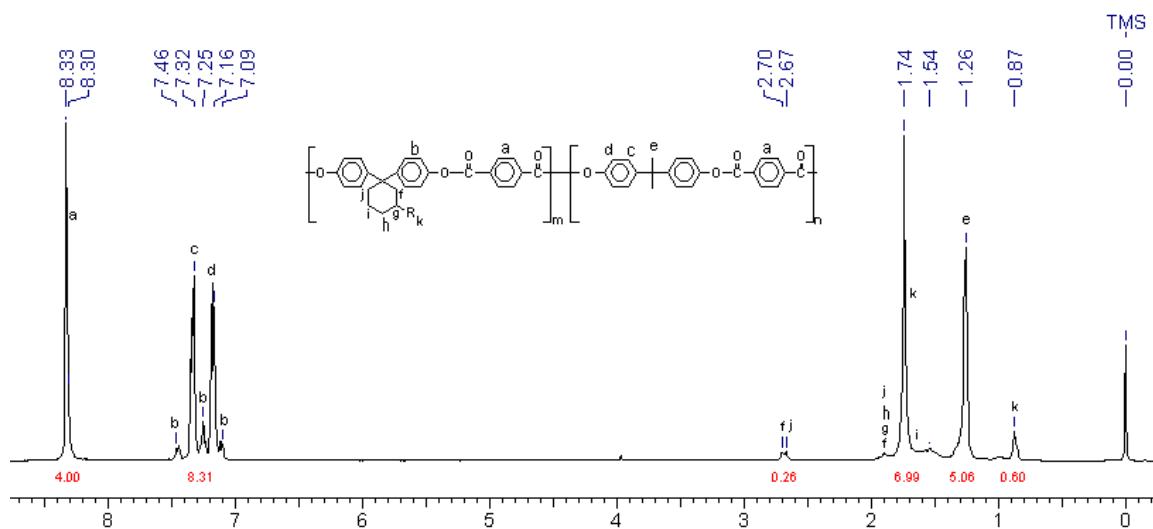


Figure 4.10 $^1\text{H-NMR}$ spectrum of copolyester derived from BPC_{15} and BPA with terephthalic acid chloride (P-10)

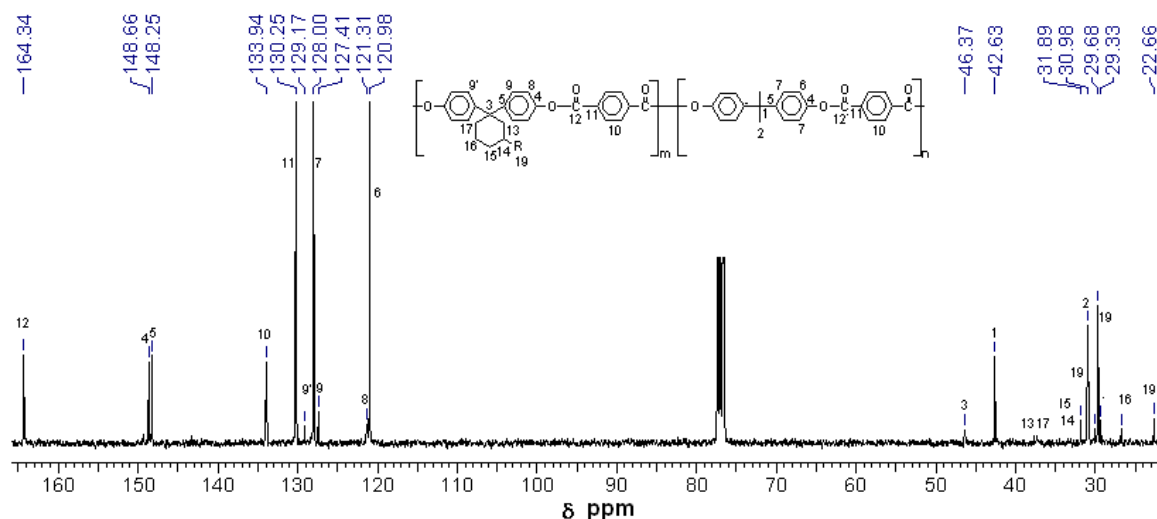


Figure 4.11 $^{13}\text{C-NMR}$ spectrum of copolyester derived from BPC_{15} and BPA with terephthalic acid chloride (P-10)

4.4.2.2 Solubility measurements

Solubility of copolyesters was tested in various organic solvents at 3 wt % concentration and data is summarized in **Table 4.7**

Table 4.7 Solubility data of copolyesters derived from BPA and BPC₁₅ with terephthalic acid chloride

Polyester	BPA mol%	BPC ₁₅ mol%	BPC mol%	DCM	CHCl ₃	TCE	THF	<i>m</i> -Cresol	ODCB	NMP	DMF
P-3	100	0	0	-	-	-	-	-	-	-	-
P-8	95	5	0	+-	+-	++	+-	++	-	-	-
P-9	90	10	0	++	++	++	+-	++	++	-	-
P-10	85	15	0	++	++	++	++	++	++	-	-
P-1	0	100	0	++	++	++	++	++	++	-	-
P-11	85	0	15	-	-	-	-	-	-	-	-

++ soluble, + soluble on heating, +- swelling, - insoluble

The systematic increment in the mol % of BPC₁₅ showed that 10 mol % of BPC₁₅ was sufficient to impart solubility to copolyester in common organic solvents. Copolyester containing 15 mol % of BPC₁₅ was soluble in all the solvents tested except amide solvents. Copolyester of BPA with terephthalic acid chloride containing 15 mol % of BPC was synthesized to compare its solubility behavior with that of BPC₁₅ derived copolyesters. However, copolyester containing BPC was not soluble in any of the organic solvents tested.

4.4.2.3 X-Ray diffraction studies

X-Ray diffraction patterns of copolyesters derived from BPA and BPC₁₅ with terephthalic acid chloride are shown in **Figure 4.12**. As is reported in literature, polyester derived from BPA and terephthalic acid chloride (P-3) is partially crystalline in nature. Copolyesters containing 5 and 10 mol % of BPC₁₅ showed presence of crystalline peaks whereas, copolyester containing 15 mol % of BPC₁₅ showed no sharp peaks, indicating the amorphous nature. However, copolyester containing 15 mol% BPC exhibited crystalline peaks (**Figure 4.12**). This clearly indicates that the pentadecyl chain is responsible for disrupting chain regularity and packing in case of copolyester containing 15 mol% BPC₁₅

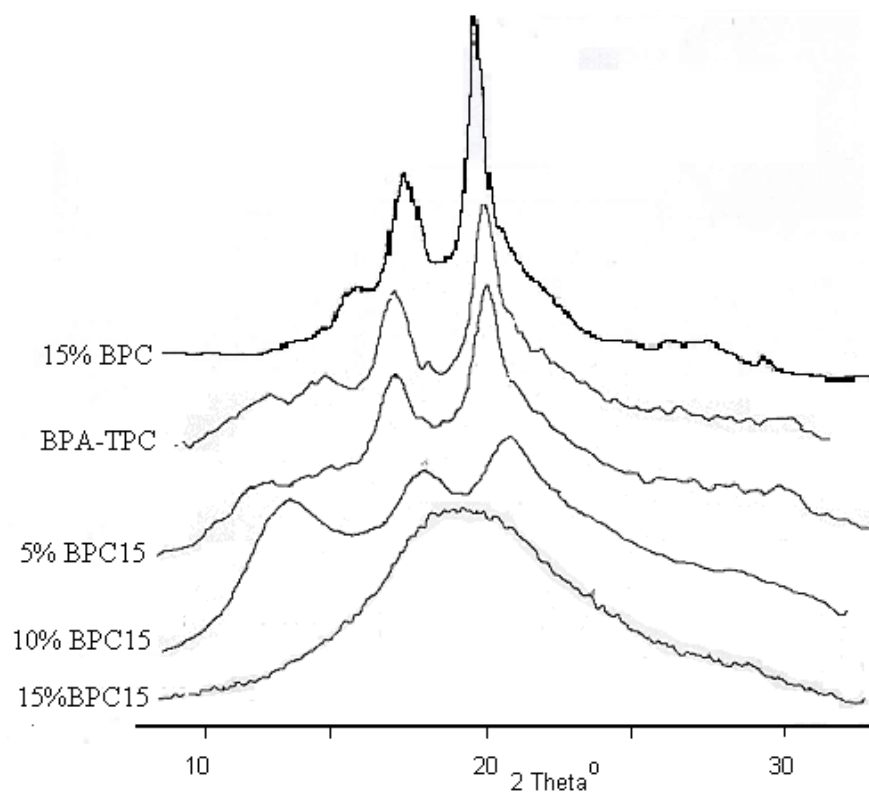


Figure 4.12 X-ray diffraction patterns of copolyesters derived from BPC₁₅ and BPC with terephthalic acid chloride.

4.4.2.4 Thermal properties

Thermal stability of the copolyesters was determined by thermogravimetric analysis (TGA) at a heating rate of 10°C /minute under nitrogen. TG curves of copolyesters are shown in **Figure 4.13**.

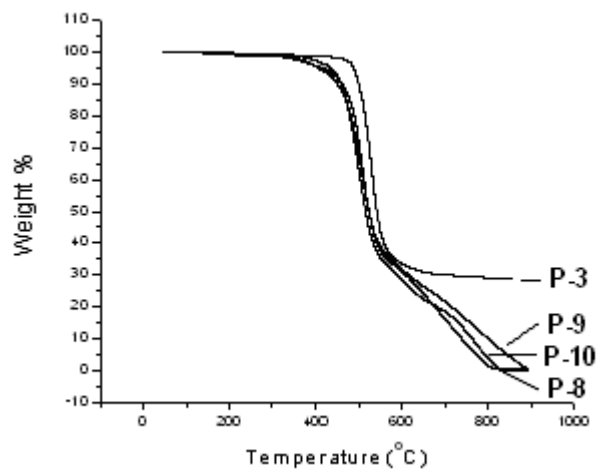


Figure 4.13 TG curves of copolyesters derived from BPA and BPC₁₅ with terephthalic acid chloride

The initial decomposition temperature (IDT) and the decomposition temperature at 10% weight loss (T_{10}) for copolyesters are given in **Table 4.8**. IDT for copolyesters containing BPC₁₅ were in the range 441-466°C while T_{10} values were in the range 451-465 °C. Observation of data indicated that there is a marginal decrease in the thermal stability of copolyesters compared to that of polyester derived from BPA and terephthalic acid chloride.

Table 4.8 Thermal properties of the copolyesters derived from BPA and BPC₁₅ with terephthalic acid chloride

Polyester	BPA mol %	BPC ₁₅ mol %	BPC mol %	IDT (°C)	T ₁₀ (°C)	T _g (°C)
P-1	0	100	0	439	451	94
P-3	100	0	0	485	498	234
P-8	95	5	0	466	465	212
P-9	90	10	0	451	450	206
P-10	85	15	0	441	451	188
P-11	85	0	15	428	439	N.D

N.D. – not detected

Glass transition (T_g) temperature of copolyesters was determined by differential scanning calorimetry (DSC). T_g values were obtained from second heating scans of polyester samples at a heating rate of 10°C / minute. DSC curves are shown in **Figure 4.14** and T_g values are given in **Table 4.8**.

T_g of copolyesters decreases with the increase in the BPC₁₅ content. This is mainly due to the presence of pentadecyl chain, which could act as an “internal plasticizer” and increases the chain mobility thus decreasing T_g of copolyesters.

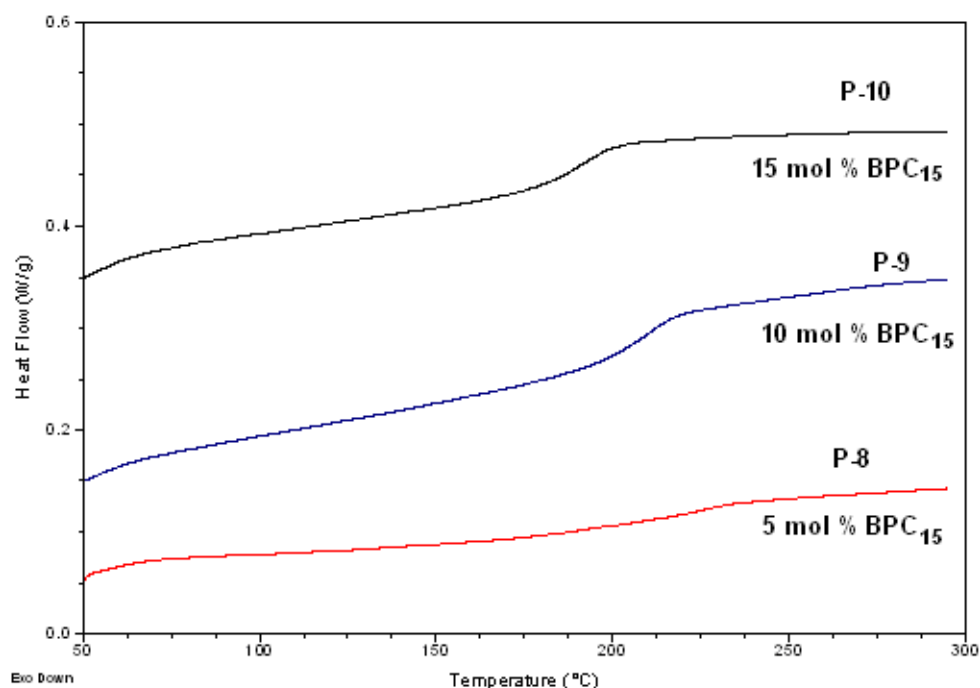


Figure 4.14 DSC curves of copolyesters derived from the BPA and BPC₁₅ with terephthalic acid chloride

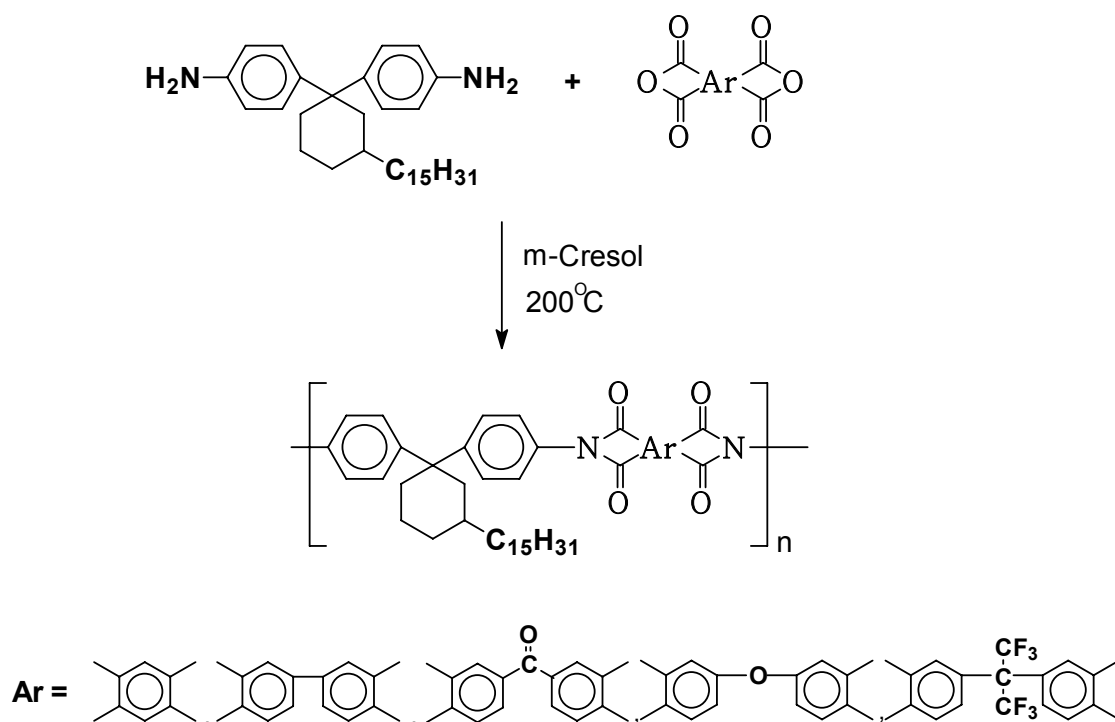
4.4.3 Synthesis of polyimides from 1,1-bis(4-aminophenyl)-3-pentadecylcyclohexane and commercial dianhydrides

Polyimides exhibit outstanding mechanical and electrical properties, exceptional thermal and thermooxidative stability, and excellent solvent resistance. These properties make them highly desirable for high-performance applications. However, their use in some applications is hampered due to their poor processability. Considerable research has been carried out aimed at developing polyimides that are processable in their imide form. Earlier polyimide research concentrated on modifying the dianhydride or diamine moiety to either increase solubility or to reduce glass transition temperature. The approach varied from phenylating the dianhydride for improved solubility, to changing backbone catenation to lower the T_g.

The goal of this present study was to improve polyimide processability *via* “internal plasticization”. Plasticization normally involves the incorporation of a low-molecular-weight plasticizer, which improves polymer flow and processability. In internal plasticization, the plasticizer is chemically attached to or incorporated in the polymer

backbone. It was postulated that the introduction of long alkyl chains along the polymer backbone would disrupt intermolecular interactions and allow the backbone more freedom for flow during processing.

New diamine containing alkyl chain, 1,1-bis(4-aminophenyl)-3-pentadecylcyclohexane (BAC_{15}), was synthesized starting from cashew nut shell liquid as described in **Chapter 3**. Alkyl chain containing monomers are known to reduce glass transition temperature *via* “internal plasticization”. Five new polyimides were synthesized by one-step high temperature solution polycondensation of BAC_{15} with five commercial dianhydrides in *m*-cresol at 200°C (**Scheme 4.3**). Boiling *m*-cresol is known to be excellent reaction medium allowing for rather clean polycondensations.²⁴⁻²⁶ All the polymerization reactions proceeded in a homogeneous manner. The results of synthesis of polyimides are summarized in **Table 4.9**.



Scheme 4.3 Synthesis of polyimides from 1,1-bis(4-aminophenyl)-3-pentadecylcyclohexane and commercial dianhydrides

Table 4.9 Synthesis of polyimides from 1,1-bis(4-aminophenyl)-3-pentadecylcyclohexane and commercial dianhydrides

Polymer	Dianhydride	Yield, %	η_{inh} , dL/g	Molecular Weight ^b		Polydispersity index ^b
				Mn	Mw	Mw/Mn
PI-1	PMDA	95	0.33	16,500	34,500	2.1
PI-2	BPDA	97	0.40	31,900	81,700	2.5
PI-3	BTDA	95	0.40	18,000	56,000	3.1
PI-4	ODPA	94	0.33	14,700	28,500	1.9
PI-5	FDA	94	0.30	17,100	35700	2.5

a: η_{inh} was measured with 0.5% (w/v) solution of polyimide in chloroform at $30 \pm 0.1^\circ\text{C}$.

^b: measured by GPC in chloroform, polystyrene was used as the calibration standard.

The inherent viscosity values were in the range 0.30-0.40 dL/g. The results of GPC measurements on polyimides in chloroform are presented in **Table 4.7**. Number average molecular weights were in the range 14,700 to 31,900 with polydispersity index in the range 1.9-3.1. Inherent viscosity values and GPC data indicates the formation of medium to high molecular weight polymers. However, the molecular weight values provided by GPC should not be taken as absolute as the calibration of GPC was carried out using polystyrene standards.

Tough, transparent, and flexible films of polyimides could be cast from their chloroform solutions.

4.4.3.1 Structural characterization

The formation of polyimides was confirmed by FTIR, $^1\text{H-NMR}$ and $^{13}\text{C-NMR}$ spectroscopy. FTIR spectrum of polyimide derived from BAC₁₅ and BPDA is shown in Figure 4.15. The complete imidization was confirmed by the absorption bands at approximately 1775, 1721, 1371 and 739 cm^{-1} due to symmetric C=O, asymmetric C=O, C-N stretching and imide ring deformation, respectively. These wavelengths corresponded

to previously reported imide ring absorptions.²⁷⁻³⁰ Complete cyclization was also evident by the lack of amide C=O (1640 cm⁻¹) and N-H (1550 cm⁻¹) absorption bands.^{31,32} Representative ¹H-NMR and ¹³C-NMR spectra of BAC₁₅ based- polyimide along with assignments are given in **Figure 4.16** and **4.17** respectively. As in case of BPC₁₅ derived polyesters, phenyl rings of BAC₁₅ retained their axial and equatorial identity. However, complex nature of the spectrum made detailed spectral analysis difficult.

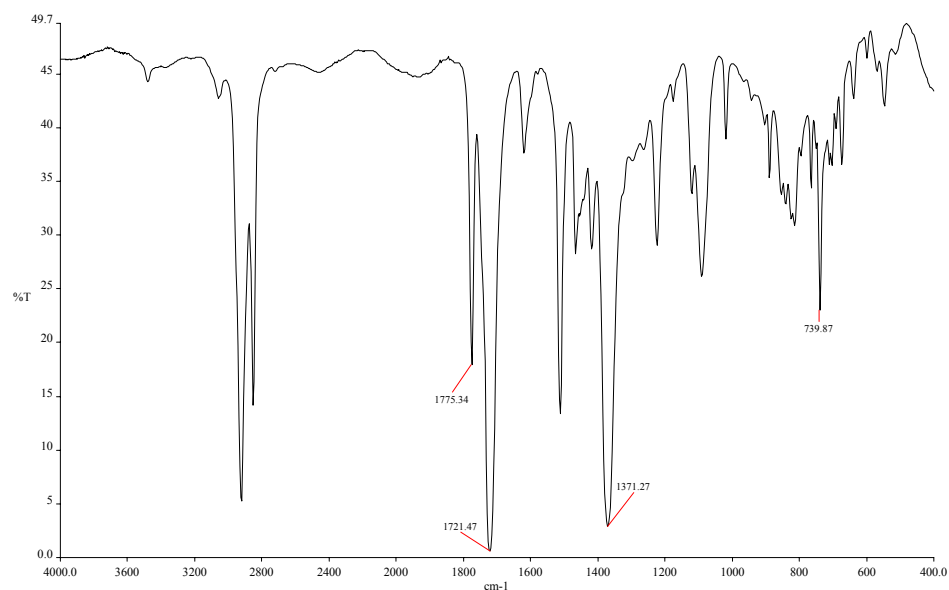


Figure 4.15 FT-IR spectrum of polyimide derived from BAC₁₅ and BPDA (PI-2)

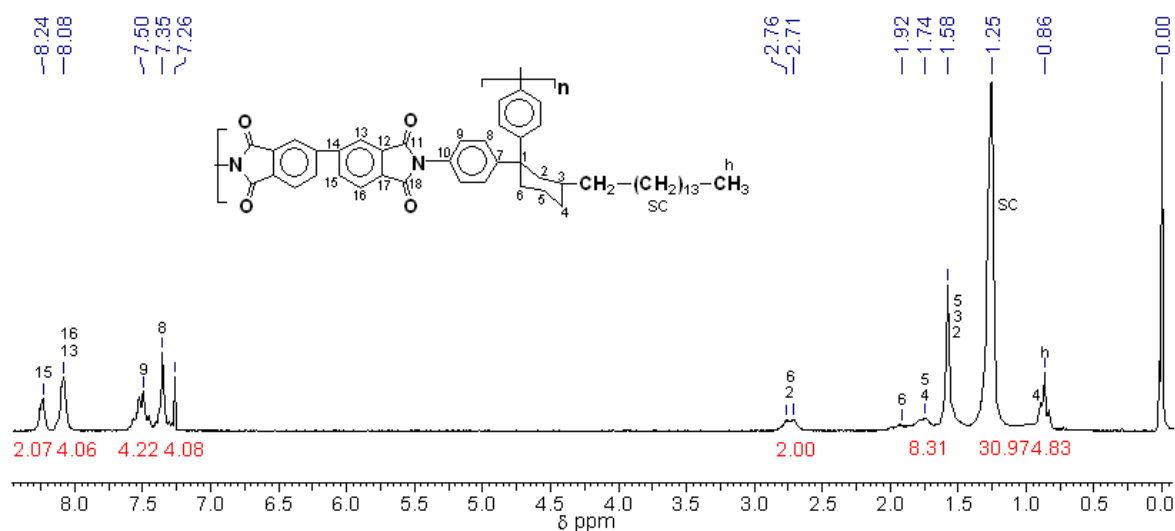


Figure 4.16 ¹H-NMR spectrum of polyimide derived from 1-bis(4-aminophenyl)-3-pentadecylcyclohexane and BPDA (PI-2)

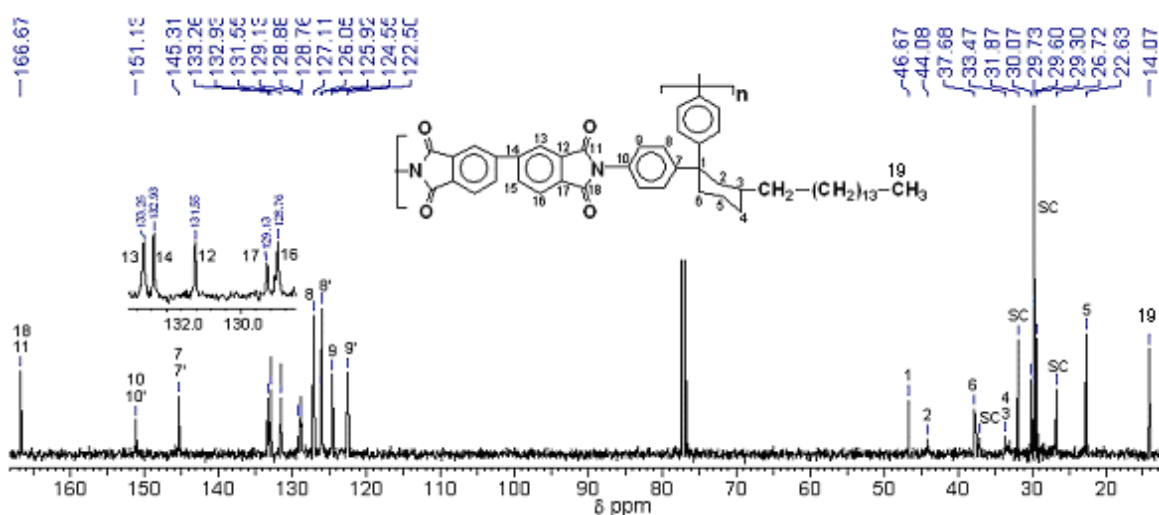


Figure 4.17 ^{13}C -NMR spectrum of polyimide derived from 1-bis(4-aminophenyl)-3-pentadecylcyclohexane and BPDA (PI-2)

4.4.3.2 Solubility measurements

Solubility of polyimides was tested in various organic solvents at 3 wt % concentration and data is summarized in **Table 4.10**.

Table 4.10 Solubility data of polyimides synthesized from 1-bis(4-aminophenyl)-3-pentadecylcyclohexane and commercial dianhydrides

Polymer	CHCl_3	TCE	ODCB	THF	<i>m</i> -Cresol	NMP	DMAC
PI-1	++	++	++	++	++	++	+ -
PI-2	++	++	++	++	++	++	+ -
PI-3	++	++	++	++	++	++	+ -
PI-4	++	++	++	++	++	++	+ -
PI-5	++	++	++	++	++	++	+ -

++ soluble, + - swelling

BAC₁₅-based polyimides were soluble in all the organic solvents tested. The good solubility in a number of solvents is attributed to the “cardo” cyclohexyl group along with long pentadecyl chain. In case of DMAC, polyimides showed swelling and this could be due to the presence of hydrophobic alkyl group. It is reported in literature that polyimides

derived from 1,1-bis(4-aminophenyl)cyclohexane were insoluble in almost all the solvents tested except tetrachloroethane.³³ The presence of C₁₅ alkyl chain disrupted the packing of polymer chains, as well as provided the additional ‘handle’ for interaction with solvents resulting into improved solubility behavior of BAC₁₅ derived polyimides.

4.4.3.3 X-Ray diffraction studies

X-Ray diffraction patterns of polyimides are shown in **Figure 4.18**. All polyimides were amorphous in nature. The presence of pentadecyl chain along with cyclohexyl “cardo” group hindered the packing of the polyimide chains. The amorphous nature of these polyimides was also reflected in their excellent solubilities in common organic solvents.

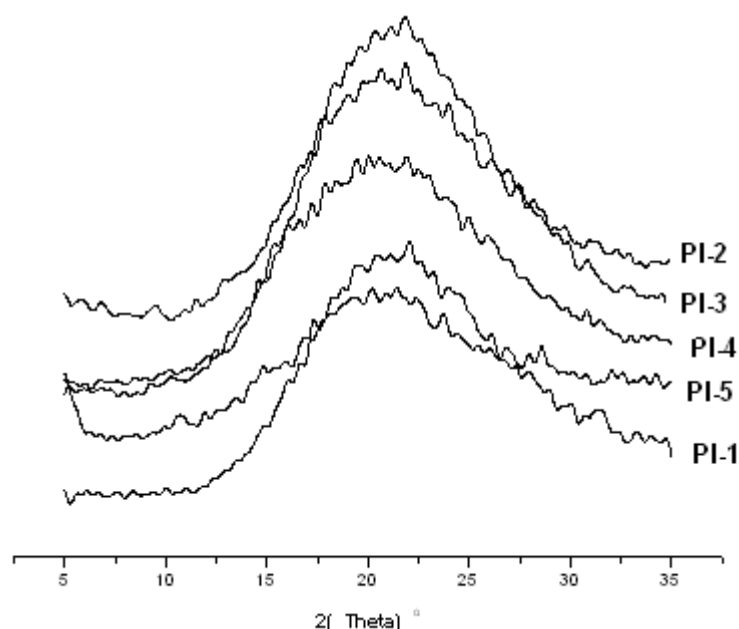


Figure 4.18 Wide-angle X-ray diffraction patterns of polyimides derived from 1-bis(4-aminophenyl)-3-pentadecylcyclohexane and commercial dianhydrides

4.4.3.4 Thermal properties

In the present study, thermal stability of polyimides was determined by thermogravimetric analysis (TGA) at a heating rate of 10°C /minute under nitrogen. TG curves for polyimides are shown in **Figure 4.19**. The initial decomposition temperature (IDT) and the decomposition temperature at 10% weight loss (T₁₀) for polyimides are given in **Table 4.11**. IDT for polyimides was in the range 487-499°C. T₁₀ values for polyimides were in

the range 493-513°C indicating their high thermal stabilities. Despite the presence of aliphatic chain along the polymer backbone, these polyimides exhibited high thermal stability with the advantage of being soluble.

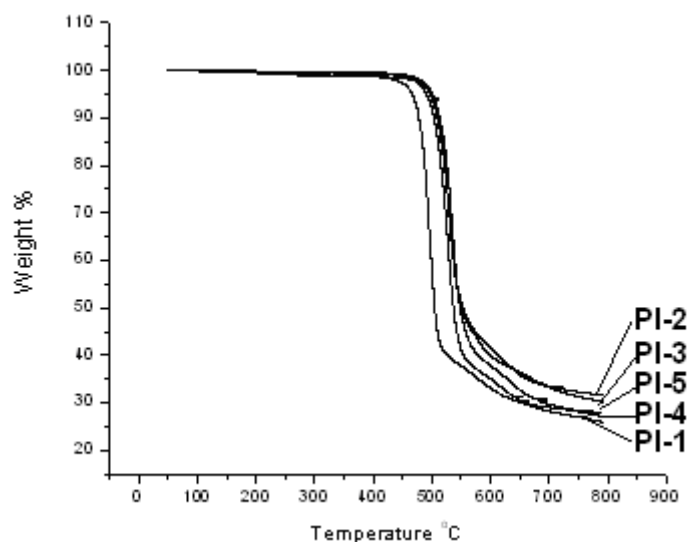


Figure 4.19 TG curves of polyimides derived from 1-bis(4-aminophenyl)-3-pentadecylcyclohexane and commercial dianhydrides

Table 4.11 Thermal properties of polyimides derived from 1-bis(4-aminophenyl)-3-pentadecylcyclohexane and commercial dianhydrides

Polyimide	Dianhydride	IDT (°C)	T ₁₀ (°C)	T _g (°C)
P-1	PMDA	487	493	191
P-2	BPDA	498	513	209
P-3	BTDA	499	512	178
P-4	ODPA	495	503	161
P-5	FDA	499	509	165

DSC curves of polyimides are reproduced in **Figure 4.20**. The T_g values of polyimides were in the range 161-209 °C. The T_g values decreased in the following order. BPDA > PMDA > BTDA > FDA > ODPA. Polyimide derived from BPDA and BAC₁₅ showed highest T_g in the series, which could be attributed to the rigid nature of BPDA. The lowest T_g value observed for ODPA containing polyimide could be attributed to the presence of

flexible ether linkage along the polymer backbone. Like in case of polyesters (Section 4.3.1.4), presence of long pentadecyl chain is responsible for the reduction of polyimide glass transition temperature substantially. Pentadecyl chain acts as an “internal plasticizer” aiding the processability to the polyimides.

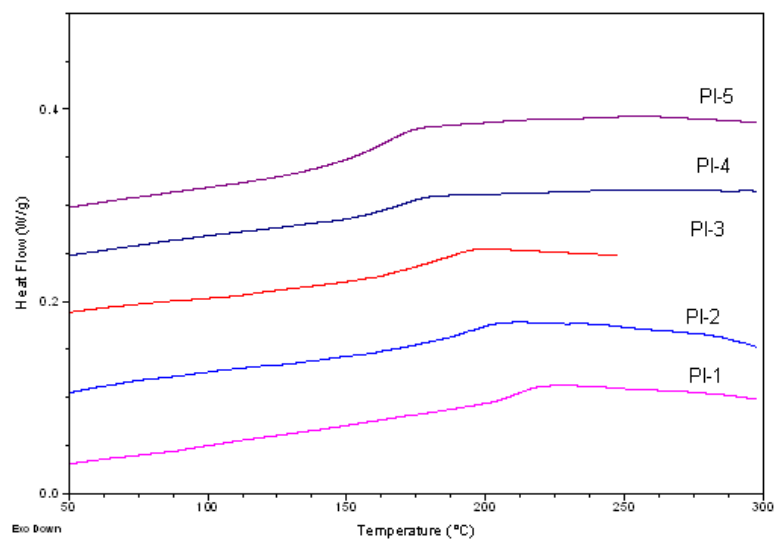


Figure 4.20 DSC curves of polyimides derived from the 1,1-bis(4-aminophenyl)-3-pentadecylcyclohexane and commercial dianhydrides

Polyimides derived from 1,1-bis(4-aminophenyl)cyclohexane (BAC) and commercial dianhydrides exhibited glass transition temperature in the range 293-305 °C. Comparison of glass transition temperatures of polyimides derived from BAC₁₅ and 1,1-bis(4-aminophenyl)cyclohexane shows that there is a depression in Tg by introduction of flexible pentadecyl chain along the polymer backbone indicating its plasticizing effect. Polyimides were stable up to 493-513 °C in nitrogen atmosphere. A large window between glass transition and degradation temperature was observed. This gives an opportunity for these polyimides to be melt processed or compression molded.

4.4.3.5 Optical properties

Strong absorption of wholly aromatic polyimides in the ultraviolet to visible range, sometimes becomes a serious obstacle in practical uses. For example, the visible absorption of polyimide films is unfavorable in some applications such as flexible solar radiation protectors, alignment layers in liquid crystal display devices, optical wave-guides for communication interconnectors and optical half-wave plates for planar light wave

circuits. However, most of the conventional polyimides show considerable coloration due to charge-transfer complexation between alternating electron-donor (diamine) and electron acceptor (dianhydride) moieties.³⁴ St. Clair et al.^{35,36} investigated the structure-coloration relationship in a number of polyimides and have shown that the modifications that result in a lowering of charge-transfer complexation generally lead to polyimides with a low color intensity. The fluorine containing monomers have gained particular importance in the synthesis of optically transparent polyimides since polyimides synthesized from them are highly soluble, colorless and thermally stable.^{36a} Some alicyclic monomers have also been investigated for the synthesis of optically transparent polyimides.^{36b-c} But the polyimides synthesized from them exhibit lower thermal stability. An effective approach for lowering the color of polyimides has been to use diamines and dianhydrides having pendant alkyl groups which minimize electronic interactions between polymer chains.^{36d-e} In the present study, the optical transparencies of polyimide films having thickness of ~ 10 μm were determined by transmission UV-visible spectroscopy. **Figure 4.21** shows UV-visible spectra of BPC₁₅-based polyimides.

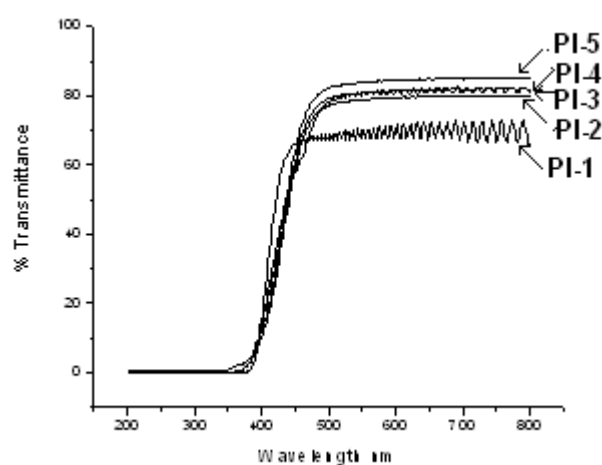
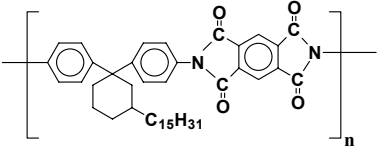
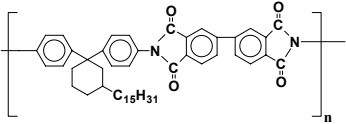
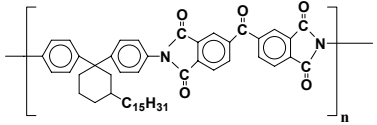
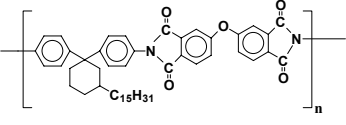
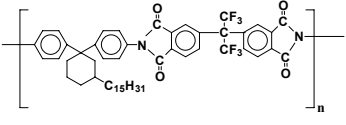


Figure 4.21 UV-vis absorption spectra of polyimide films derived from 1,1-bis(4-aminophenyl)-3-pentadecylcyclohexane and commercial dianhydrides

The cut off wavelength (absorption edge, λ_0), and % transmittance at 500 nm (the solar maximum) are given in **Table 4.12**. Polyimide derived from BAC₁₅ and 6-FDA showed the maximum transparency. In the case of all polyimides, the transmissions of light started below 400 nm and were found to be optically transparent. Polyimides showed cut off wavelength (λ_0) between 344 and 379 nm which were lower than the commercially available polyimide Kapton with λ_0 of 414 nm.

The % transmittance for the polyimides was in the range of 67-82 %. The order of the transparency based on % transmittance at 500 nm is PMDA < BPDA < BTDA < ODPA < 6-FDA. The high optical transparency could be attributed to the pentadecyl substituted cyclohexylidene moiety along the polymer backbone, which might hinder the packing of polymer chain and thus minimize the formation of charge transfer complexes. The highest transmittance of the 6-FDA based polyimide is because of the bulky CF₃, which minimizes the CTC formation between the polymer chains through steric hindrance. The low polarizability of the fluorine and fluorinated groups also weakens the intermolecular interactions leading to high optical transmittance.^{36f}

Table 4.12 Optical properties of polyimides derived from 1,1-bis(4-aminophenyl)-3-pentadecylcyclohexane and commercial dianhydrides

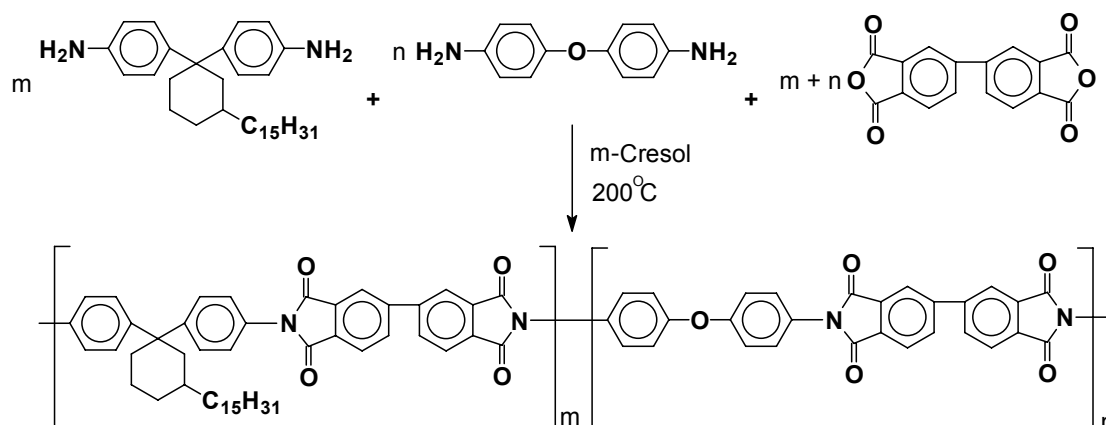
Polyimide	λ_0 , nm	% Transmittance at 500 nm
 <p>PI-1</p>	379	67
 <p>PI-2</p>	344	77
 <p>PI-3</p>	348	78
 <p>PI-4</p>	350	79
 <p>PI-5</p>	348	82

4.4.4 Synthesis of copolyimides from 1,1-bis(4-aminophenyl)-3-pentadecylcyclohexane and 4,4'-oxydianiline with biphenyltetracarboxylic dianhydride

One of the approaches used in the modification of polyimides in order to achieve a combination of desired properties such as, solubility, thermal stability and mechanical properties is to merge the properties of different polyimides into one system. Such a modification in properties can be achieved through copolymerization or blending. Copolymerization is particularly attractive since tailoring properties of the resulting polymers is possible even on molecular levels. Random copolyimides are synthesized by the reaction of a single dianhydride with two or more diamines or by the reaction of a single diamine with two or more dianhydrides.^{37,38} Copolymerization is the most general and powerful tool used for systematically modifying the properties of commercial polymers.³⁹

Encouraged by the results on the improvement of processability of homopolyimides derived from BAC₁₅ and rigid dianhydrides (**Section 4.4.3**), a study was undertaken to improve the processability of polyimide derived from 4,4'-oxydianiline (ODA) and BPDA, which is known to be insoluble in its imide form.

Three different copolyimides from BAC₁₅ and ODA were synthesized with BPDA (**Scheme 4.4**) in order to determine the effect of different amounts of the BAC₁₅ on solubility and thermal properties. The results of copolyimide synthesis are summarized in **Table 4.13**. All polymerization reactions proceeded in a homogeneous manner. Inherent viscosities of copolyimides were in the range 0.56 – 1.4 dL/g.



Scheme 4.4 Synthesis of copolyimides from BAC₁₅ and ODA with BPDA

Table 4.13: Synthesis of copolyimides from BAC₁₅ and ODA with BPDA

Polymer	BAC ₁₅ ,	ODA,	Yield, %	η_{inh}^a dL/g	Molecular Weight		PDI Mw/Mn
	mol %	mol %			Mn	Mw	
PI-2	100	0	97	0.40	31,900	81,700	2.5
PI-6	0	100	93	-	- ^c	- ^c	-
PI-7	25	75	94	1.4 ^b	- ^c	- ^c	-
PI-8	50	50	96	1.03	130320	232210	1.8
PI-9	75	25	95	0.56	79540	158070	2.0

^a: η_{inh} was measured with 0.5% (w/v) solution of copolyimide in chloroform at $30 \pm 0.1^\circ\text{C}$.

^b: η_{inh} was measured with 0.5% (w/v) solution of copolyimide in tetrachloroethane at $30 \pm 0.1^\circ\text{C}$

^c: (co)polyimides were not soluble in chloroform.

Copolyimides with the composition 25/75 and 50/50 mol % (ODA:BAC₁₅) were soluble in CHCl₃ and were used for GPC analysis. The results of GPC measurements are presented in **Table 4.13**. Number average molecular weights of PI-8 and PI-9 were 130320 and 79,540 with polydispersity index 1.8 and 2.0, respectively. Inherent viscosity and GPC data indicates the formation of reasonably high molecular weight polymers. However, the molecular weight values provided by GPC should not be taken as absolute as the calibration of GPC was carried out using polystyrene standards.

Tough, transparent, and flexible films of the copolyimides could be cast from their chloroform solutions.

4.4.4.1 Structural characterization

The formation of copolyimides was confirmed by FTIR, ¹H-NMR and ¹³C-NMR spectroscopy.

A representative FTIR spectrum of copolyimide derived from BAC₁₅ with ODA and BPDA is represented in **Figure 4.22**. The complete imidization was confirmed by the absorption bands at approximately 1775, 1721, 1373 and 739 cm⁻¹ due to symmetric C=O, asymmetric C=O, C-N stretching and imide ring deformation, respectively. These wavelengths corresponded to previously reported imide ring absorptions.²⁷⁻³⁰ In

addition to the imide bands C–O–C absorption band was observed at 1241 cm^{-1} indicating the presence of ODA moiety along the polymer backbone.

Representative ^1H and ^{13}C -NMR spectrum of copolyimide along with assignments are reproduced in **Figure 4.23** and **4.24**, respectively.

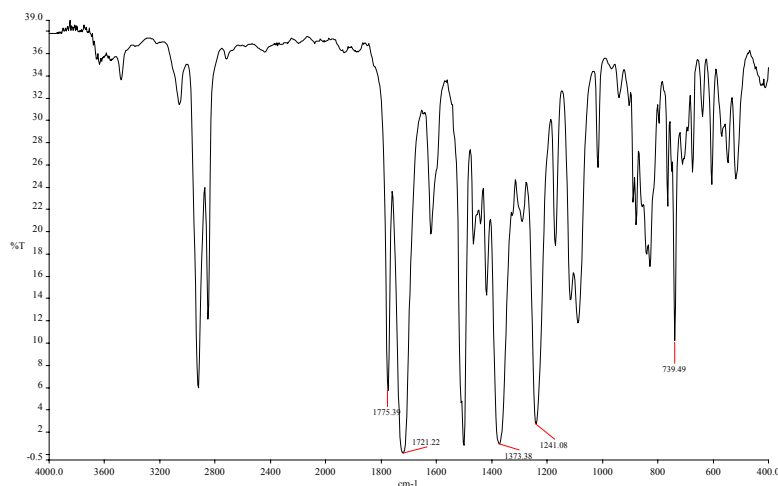


Figure 4.22 FT-IR spectrum of copolyimide derived from BAC_{15} and ODA with BPDA (PI-9)

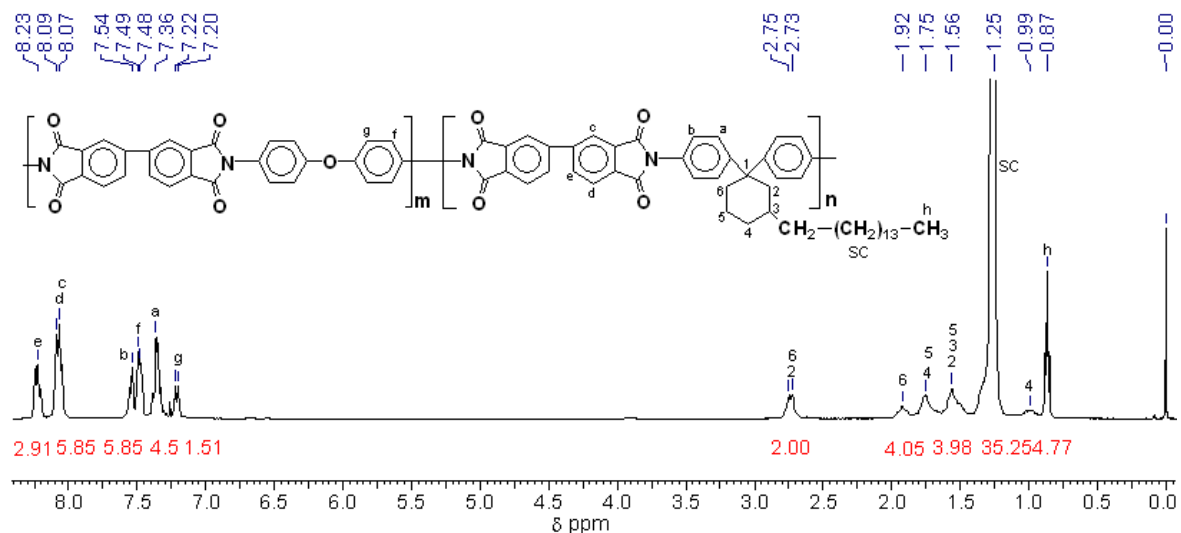


Figure 4.23 ^1H -NMR spectrum of the copolyimide derived from BAC_{15} and ODA with BPDA (PI-9)

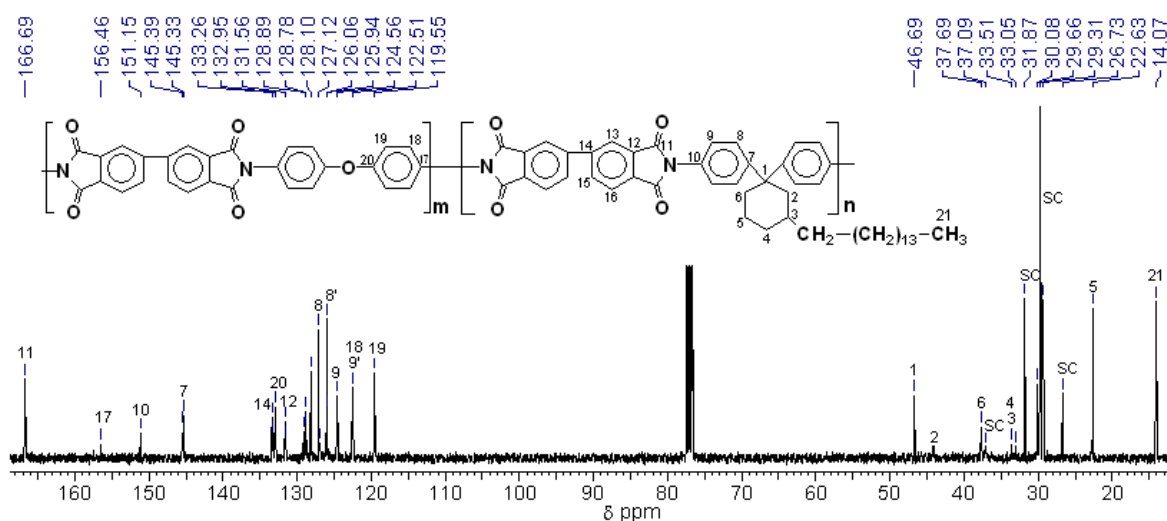


Figure 4.24 ^{13}C -NMR spectrum of the copolyimide derived from BAC_{15} and ODA with BPDA (PI-9)

4.4.4.2 Solubility measurements

Solubility of copolyimides was tested in various organic solvents at 3 wt% concentration and data is summarized in **Table 4.12**. All the copolyimides were soluble in the range of solvents tested.

Table 4.14 Solubility data of the polyimides derived from BAC_{15} and ODA with BPDA

Polymer	DCM	CHCl_3	TCE	ODCB	THF	<i>m</i> -Cresol	NMP	DMAC
PI-6	--	--	--	--	--	--	--	--
PI-7	+ -	+ -	++	++	+ -	+	+ -	+ -
PI-8	++	++	++	++	+ -	++	++	+ -
PI-9	++	++	++	++	++	++	++	+ -
PI-2	++	++	++	++	++	++	++	+ -

++ soluble, + soluble on heating, + - swelling, - insoluble

The base polyimide PI-6, synthesized from BPDA and ODA was insoluble in all the solvents tested. The presence of pentadecyl chain provided the “handle” for interaction with solvent and thus aided the solubility to the resultant copolyimides.

4.4.4.3 X-Ray diffraction studies

X-Ray diffraction patterns of copolyimides along with homopolyimide (PI-6) are reproduced in **Figure 4.25**. Polyimide derived from BPDA and ODA (PI-6) exhibited crystalline-like diffraction peaks seated on an amorphous halo over an angle range of 10-30°. This indicates that BPDA-ODA polymer has good molecular chain orientation and packing order. This might result from the high packing efficiency of rotational planer dianhydride phenyl rings in the BPDA-ODA main chain.⁴⁰ In contrast to this WAXD patterns of copolyimides exhibited only featureless amorphous halos and this might be due to the presence of BAC₁₅ molecule with “cardo” cyclohexyl group along with long pentadecyl chain which might hinder the packing of polyimide chains.

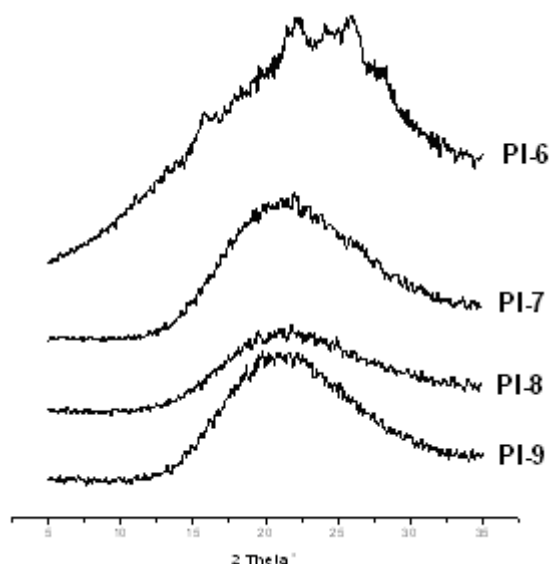


Figure 4.25 Wide angle X-ray diffraction patterns for copolyimides derived from 1,1-bis(4-aminophenyl)-3-pentadecylcyclohexane and BPDA

4.4.4.4 Thermal properties

In the present study, thermal stability of copolyimides was determined by thermogravimetric analysis (TGA) at a heating rate of 10°C /minute under nitrogen. TG curves for copolyimides are reproduced in **Figure 4.26**. Initial decomposition temperature (IDT) and the decomposition temperature at 10% weight loss (T_{10}) for copolyimides are given in **Table 4.15**. The 10% weight loss occurred in the range 475-500°C indicating high thermal stability. Incorporation of long pentadecyl chain reduced the thermal

stability, but the values are still acceptable for the applications in the areas such as microelectronics, displays devices, etc.

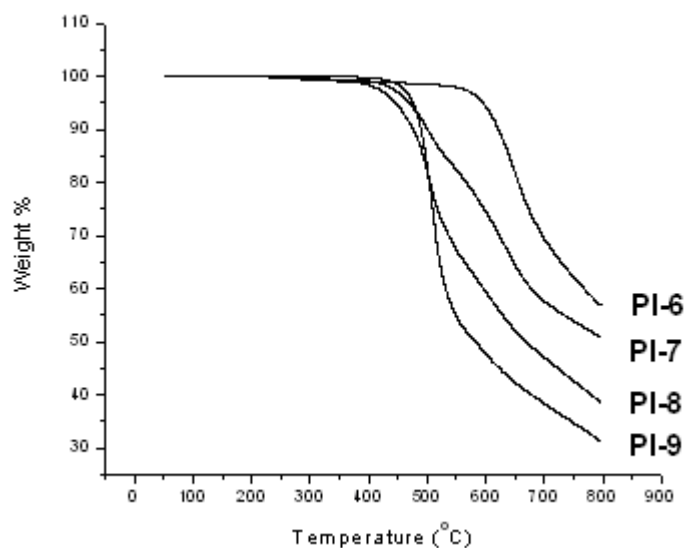


Figure 4.26 TG curves of copolyimides derived from BAC₁₅ and ODA with BPDA

Table 4.15 Thermal properties of copolyimides derived from BAC₁₅ and ODA with BPDA

Polyimide	BAC ₁₅ , mol %	ODA, mol %	IDT, (°C)	T ₁₀ , (°C)	T _g , (°C)
PI-6	0	100	584	621	320 ^a
PI-7	25	75	431	500	254
PI-8	50	50	440	475	237
PI-9	75	25	463	489	216
PI-2	100	0	498	513	209

a: value taken from reference 41

Glass transition (T_g) temperature of copolyimides was determined by differential scanning calorimetry (DSC). T_g values were obtained from second heating scans of copolyimide samples at a heating rate of 10°C / minute. Although the DSC thermogram of control polyimide, PI-6 did not contain any noticeable baseline shifts, the polymer was previously reported to have a T_g of 320°C. The T_gs of copolyimides, which could be detected, with DSC, decreased as their BAC₁₅ content increased. (**Figure 4.27**). Lower glass transition

temperatures of and polyimides demonstrated the plasticization effect of the pentadecyl chain. It has been reported that as the plasticizer content increases the free volume of the polymer increases which eventually decreases the glass transition temperature.⁴² This has resulted in substantial decrease in the glass transition temperature as seen in **Figure 4.28**.

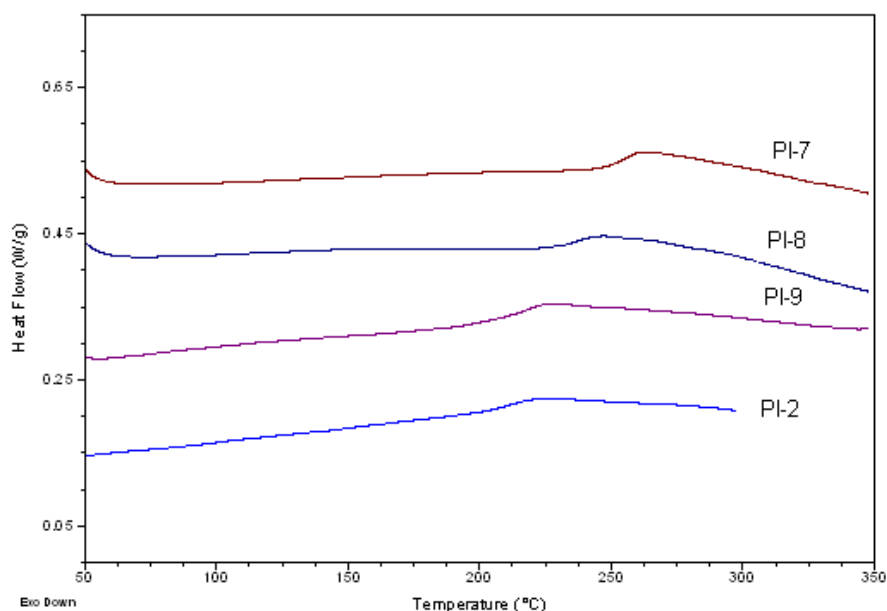


Figure 4.27 DSC curves of copolyimides derived from BAC₁₅ and ODA with BPDA

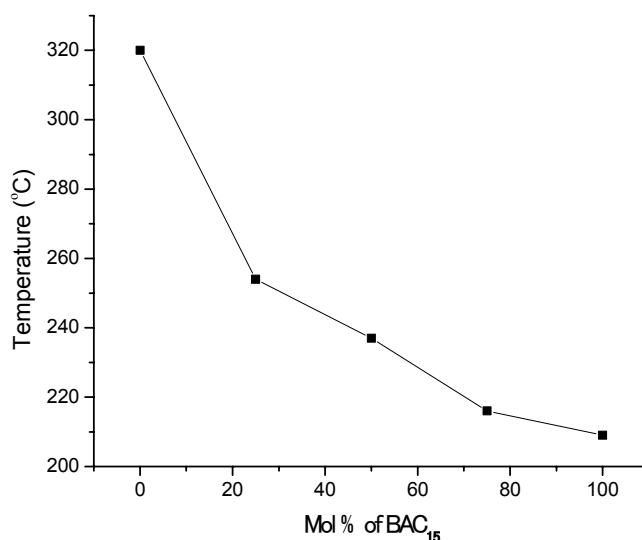


Figure 4.28 Glass transition temperature vs mol% of BAC₁₅ for copolyimides derived from BPDA with ODA and BAC₁₅

4.4.4.5 Optical properties

In the present study, optical transparencies of copolyimide films having thickness of ~ 14 μm were determined by transmission UV-visible spectroscopy. **Figure 4.29** shows UV-visible spectra of BPC₁₅ derived copolyimides. The cut off wavelength (absorption edge, λ_0), and % transmittance at 500 nm (the solar maximum) are given in **Table 4.16**. The cut off wavelength and % transmission at 500 nm was in the range 380-391 and 74-82 %, respectively. The presence of pentadecyl chain in BAC₁₅ derived copolyimides might hinder the packing of polymer chains thus minimizing the formation of charge transfer complexes.

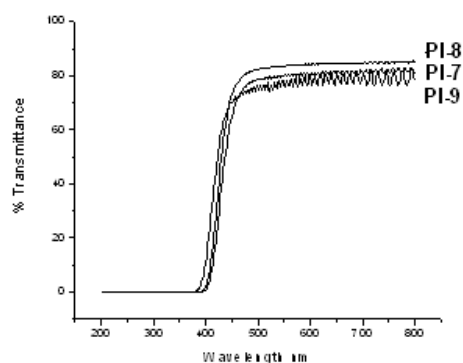


Figure 4.29 UV-vis absorption spectra of copolyimide films derived from BAC₁₅ and ODA with BPDA

Table 4.16 Optical properties of the copolyimides derived from BAC₁₅ and ODA with BPDA

Polyimide	λ_0 , nm	% Transmittance, at 500 nm
PI-7	380	74
PI-8	391	82
PI-9	391	79

4.5 Pretilt angle and electro-optical characteristics of copolyimide derived from 1,1-bis(4-aminophenyl)-3-pentadecylcyclohexane and 4,4'-oxydianiline with biphenyltetracarboxylic dianhydride

One of the objectives of the present study was to use pentadecyl chain containing polyimides as the alignment layers for liquid crystal displays. All (co)polyimides synthesized were used for testing pretilt angles.

The liquid crystal cells were prepared as described in **section 4a.2.3** and the measurements were done by crystal rotation method.¹⁶ The pretilt angle was then calculated from the obtained incident angle.

However, measurements could not be carried out with homopolyimide samples as swelling of the polyimides was observed in liquid crystals. Taking into consideration the excellent solubilities of polyimides (**Table 4.8**), alkylcyano biphenyls (liquid crystal used in the present study) in their isotropic state can act as a solvent for polyimides. A similar observation was reported by Lee, et. al.⁴³ in case of polyimides containing pendant octadecyloxy chain.

Figure 4.30 shows photographs of the twisted nematic cell between crossed and parallel polarizers made from copolyimide derived from BAC₁₅ and ODA (50:50 mol%) with BPDA (PI-8). Uniform alignment of liquid crystals was observed. This opens the route for these polyimide to be used as an alignment layer for liquid crystal displays. The pretilt angles were in the range 2.51-2.75°, which is adequate for display applications. Low LC pretilt angle is particularly attractive for In-Plane-Switching or twisted-nematic LCD modes. Organo-soluble polyimides are desirable as their processing temperature is low – a feature particularly important for low temperature poly-silicon-thin-film transistor-liquid crystal display (TFT-LCD) processes.^{43,44}

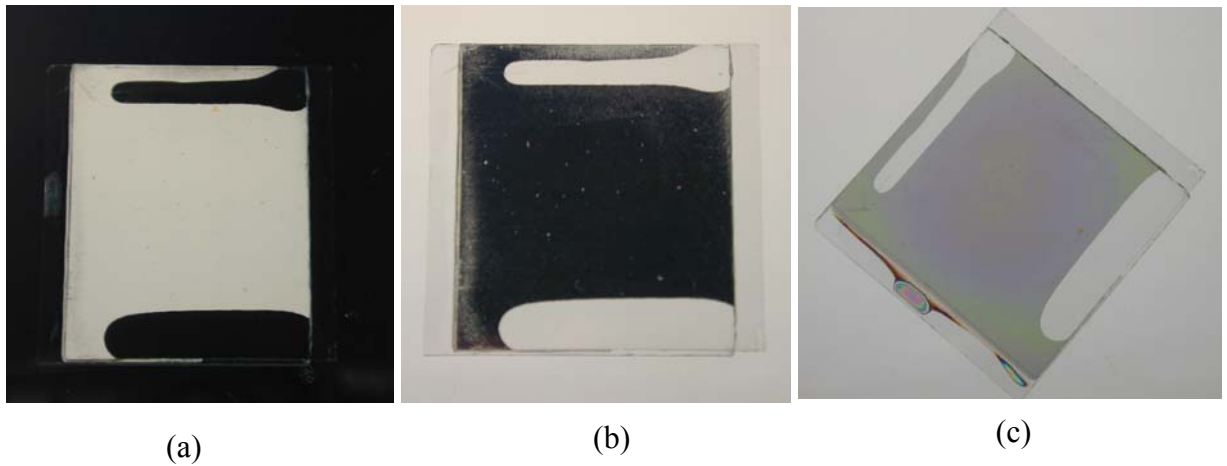


Figure 4.30: Twisted nematic cell made from polyimide PI-8. (a) cell between crossed polarizers (b) cell between parallel polarizers (c) cell at 45° between crossed polarizers.

Figure 4.31 (a) shows a typical transmittance-voltage curve for normal incidence of the twisted nematic cell. A typical switching curve is observed, with a switching voltage of nearly 3 V. Response and relaxation time of the twisted nematic cell is shown in **Figure 4.31b**, a switching time of 65 ms was observed at 5 V. In the OFF state, due to the $18\ \mu\text{m}$ cell thickness black flow effect is visible in the graph.

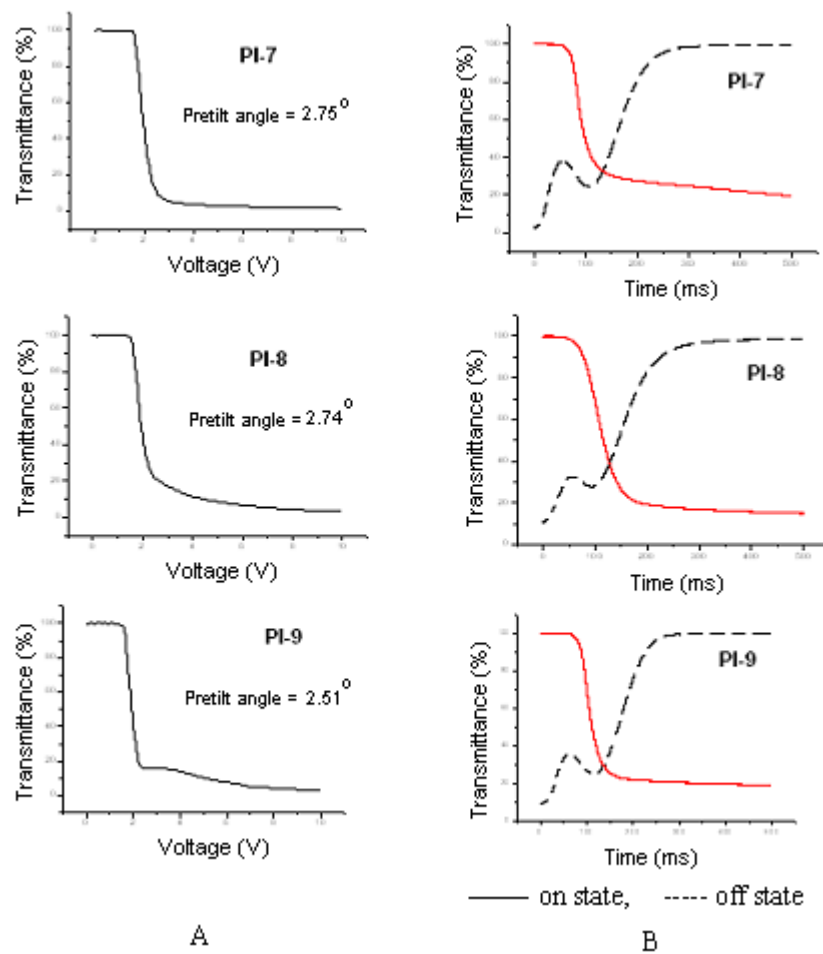


Figure 4.31 A) Electro-optical characteristics of copolyimide orientation layer
 B) Response and relaxation times for copolyimide orientation layer from the non-select to the select state (5V) at a frequency of 1000 Hz

4.6 Conclusions

1. A series of new polyesters and polyimides containing pendant pentadecyl chain were synthesized from BPC₁₅ and BAC₁₅, respectively.
2. Moderate to high molecular weight polyesters and polyimides with excellent solubilities in organic solvents were obtained.
3. A detailed NMR analysis of the polyesters derived from BPC₁₅ and terephthalic acid chloride / isophthalic acid chloride exhibited presence of constitutional isomerism owing to different enchainment of axial and equatorial phenyl rings of BPC₁₅ with that of acid chloride.
4. Wide angle X-ray diffraction patterns exhibited that polyesters and polyimides containing pendant pentadecyl chain were amorphous in nature.
5. The pentadecyl side chain along the polymer backbone was effective in lowering the T_g values of polyesters and polyimides.
6. T₁₀ values of the polyesters and polyimides were above 439°C, indicating their high thermal stabilities.
7. Copolyesters and copolyimides were synthesized from various amounts of pentadecyl cyclohexylidene containing monomers and commercially available monomers. The incorporation of 10-15 mol % of BPC₁₅ was sufficient to impart solubility to copolyester in common organic solvents.
8. Copolyester containing 15 mol % of BPC₁₅ and all the copolyimides were amorphous in nature as indicated by their wide angle X-ray diffraction patterns.
9. The T_g of copolyesters and copolyimides decreased with the increasing content of BPC₁₅ and BAC₁₅, respectively.
10. Copolyimides exhibited pretilt angles in the range 2.51-2.75°, which opens the route for these organo-soluble copolyimides to be used as alignment layers for liquid crystal displays.
11. Overall, internal plasticization effect of the pentadecyl chain was shown to be effective in achieving processable polyimides and polyesters.

References

1. *Synthetic Methods in Step Growth Polymers*, Rogers, M.E.; Long, T.E.; Eds. John Wiley and Sons : New York , 2003.
2. *Polyimides and Other High Temperature Polymers, Vol. I*, Mittal, H.K., Ed.; VSP BV: The Netherlands, 2001.
3. *Polyimides: Fundamentals and Applications*, Ghosh, M. K.; Mittal, K. L., Eds.; Marcel Dekker: New York, 1996.
4. *Heat Resistant Polymers: Technologically Useful Materials*, Critchley, J. P.; Knight, G. J.; Wright, W. W. Plenum Press: New York, 1983.
5. *Structure-Solubility Relationships in Polymers*, Harris, F.W.; Seymour, R.B., Eds.; Academic Press: New York, 1977.
6. Korshak, V. V.; Vinogradova, S. V.; Vygodskii, Y. S. *J. Macromol .Sci. Rev. Macromol. Chem.* **1974**, C11, 45.
7. Bier, G.; *Polymer* **1974**, 15, 127.
8. Sillion, B. *High Perform. Polym.* **1999**, 11, 417.
9. de Abajo, J.; de la Campa, J. G. *Adv. Polym. Sci.* **1999**, 140, 23.
10. Vinogradova, S.V.; Vasnev, V.A.; Valetskii, P.M. *Russ. Chem. Rev.* **1994**, 63, 833.
11. Morgan, P.W. *Macromolecules* **1970**, 3, 536.
12. *Prediction of Polymer Properties*; Bicerano, J., Marcel Dekker Inc.: New York, 1996.
13. *The Behavior of Plasticizers*; Mellan, I, Pergamon Press: New York, 1961.
14. *The Technology of Plasticizers*; Sears, J.K.; Darby, J.R., John Wiley and Sons : New York, 1981.
15. *Purification of Laboratory Chemicals*; Perrin, D.D.; Armarego, W.L.F. Pergamon Press: New York, 1989.
16. Scheffer, T.J.; Nehring, J. *J. Appl. Phys.* **1977**, 48, 1783
17. *Condensation Polymers by Interfacial and Solution Methods*; Morgan, P.W., Interscience: New York, 1965.
18. Iami, Y.; Tassavori, S. *J. Polym. Sci. Polym. Chem.* **1984**, 22, 1319.
19. Hsiao, S.H.; Chang H.Y. *J. Poly. Res.* **1995**, 2, 99.
20. Villegas-Coss, I.; ruiz-Trevino, F.A.; Hernandez-Lopez, S. *J. Polym. Sci. Polym. Phys.* **2006**, 44, 256
21. Eli Espinosa, M.J.; Fernandez-Berridi, I.M.; Miguel, V. *Polymer* **1993**, 34, 382.

22. Zhao, J.; Jones, A.A.; Inglefield, P.T.; Bendler, J.T. *Polymer* **1998**, *39*, 1339.
23. McHattie, J.S.; Koros, W.J., Paul, D.R. *J. Polym. Sci. Polym. Phys.* **1991**, *29*, 731.
24. Kricheldorf, H.R.; Fan, S.H.; Vakhtangishvili, L.; Schwarz, G.; Fritsch, D. *J. Polym. Sci. Polym. Chem.* **2005**, *43*, 6272.
25. Inoue, H.; sasaki, Y.; Ogawa, T. *J. Appl. Polym. Sci.* **1996**, *60*, 123.
26. Vinogradova, S.V.; Vygodskii, Y.S.; Korshak, V.V. *Vysokomol. Soyed.* **1970**, *A12*, 1987.
27. Arnold, C. A.; Summers, J. D.; Chen, Y. P.; McGrath, J. E. *Polymer* , **1989**, *30*, 986.
28. Summers, J. D.; Arnold, C. A.; McGrath, J. E. *Polym. Prepr.* **1986**, *27*, 403.
29. Summers, J. D.; Arnold, C. A.; McGrath, J. E. *Polym. Eng. Sci.* **1989**, *29*, 1413.
30. Farr, I.V. *Ph.D. Dissertation*, Virginia Polytechnic Institute, USA, 1999.
31. Saini, A. K.; Carlin, C. M.; Patterson, H. H., *J. Polym. Sci. Polym. Chem.* **1993**, *31*, 2751.
32. Ishida, H.; Wellingoff, S.T.; Baer, E.; Koenig, J.L. *Macromolecules*, **1980**, *13*, 826.
33. Yi, M.H.; Huang, W.; Jin, M.Y.; Choi, K.Y. *Macromolecules* **1997**, *30*, 5606.
34. Dine-Hart, R.A.; Wright, W.W. *Makromol. Chem.* **1971**, *143*, 189.
35. a) St. Clair, A.K.; St. Clair, T.L. U.S. Patent Number 4595548, **1985**. b) St. Clair, A.K.; Slep, W.S. *SAMPE J.* **1985**, *21*, 28.
36. a) Omote, T.; Koseki, K.; Yamaoka, T. *Macromolecules* **1990**, *23*, 4788. b) Lee, K.W.; Peak, S.; Lien, A.; Durning, C.; Fukuro, H. *Macromolecules*, **1996**, *29*, 8894. c) Moore, J.A.; Dasheff, A.N. *Chem. Mater.* **1989**, *1*, 163. d) Itamura, S.; Yamada, M.; Tamura, S.; Matsumoto, T.; Kurosaki, T. *Macromolecules*, **1993**, *26*, 3490. e) Chun, B. *Polymer* **1994**, *35*, 4203. f) *Polym. J.* **1997**, *29*, 69.
37. Varma, I.K.; Geol, R.N.; Varma, D.S. *J. Polym. Sci. Polym. Chem.* **1979**, *17*, 703.
38. Yang, C.P.; Hsiao, S.H. *J. Appl. Polym. Sci.* **1986**, *31*, 979.
39. Overberger, C.G. *J. Polym. Sci. Polym. Symp.* **1985**, *72*, 67.
40. Lee, C.; shul, Y.; Han, H. *J. Polym. Sci. Polym. Phys.* **2002**, *40*, 2190.
41. Laius, L.A.; DerGacheva, Y.N.; Zhukova, T.I.; Bessonov, M.I. *Polym. Sci. U.S.S.R.* **1986**, *28*, 2674.
42. Sasthav, J.R.; Harris, F.W. *Polymer*, **1995**, *26*, 4911.
43. Lee, W.C.; Chen, J.T.; Hsu, C.S.; Wu, S.T. *Liquid Crystals*, **2002**, *29*, 907.
44. Zhang, W.; Xu, H.J.; Yin, J.; Guo, X.X.; Ye, Y.F.; Fang, J.H.; Sui, Y.; Zhu, Z.K.; Wang, Z.G. *J. Appl. Polym. Sci.* **2001**, *81*, 2814.

Chapter 5 Synthesis and Characterization of Processable High Performance Polymers Containing Cyclohexylidene Moiety with Bulky Perhydrocumyl- Substituent

5.1 Introduction

One of the prominent approaches to address the processability issue of high performance polymers is the incorporation of “cardo” groups along the polymer backbone,¹⁻¹⁶ which not only improves the processability but also retains the high thermal properties of polymers. However, in many instances the incorporation of cyclohexylidene “cardo” group alone is not sufficient for improving the processability of these polymers. The substitution of bulky groups such as *t*-butyl or phenyl on cyclohexylidene group has resulted into improved solubility of high performance polymers.^{15,17}

In view of the above, monomers containing perhydrocumyl-substituted cyclohexylidene moiety were synthesized starting from *p*-cumylphenol, a cheap commercial raw material using simple organic reactions (**Chapter 3**).

The objective of the present work was to synthesize a series of polyesters, polyimides and polyetherimides containing perhydrocumyl substituted cyclohexylidene moiety and to study the effect of its incorporation on the polymer properties.

Polyesters, polyimides and polyetherimides were characterized by inherent viscosity measurements, gel permeation chromatography (GPC) solubility tests, FTIR, ¹H-NMR, ¹³C-NMR spectroscopy, X-ray diffraction, thermogravimetric analysis (TGA) and differential scanning calorimetry (DSC). Polyimides and polyetherimides were studied by UV-visible spectroscopy.

Polyesters containing perhydrocumyl substituted cyclohexylidene moiety were tested for gas permeability measurements. The effect of substituents (CH₃, Br) on all positions *ortho* to both hydroxyl groups in the bisphenol and the influence of diacid structure on the gas separation properties is discussed.

Polyimides were evaluated for pretilt angle measurements.

5.2 Experimental

5.2.1 Materials

1,1-Bis(4-hydroxyphenyl)-4-perhydrocumyl cyclohexane (BPPCP), 1,1-bis(4-hydroxy-3-methylphenyl)-4-perhydrocumyl cyclohexane (DMBPPCP), 1,1-bis(4-hydroxy-3,5-dimethylphenyl)-4-perhydrocumyl cyclohexane (TMBPPCP), 1,1-bis(4-hydroxy-3,5-dibromophenyl)-4-perhydrocumyl cyclohexane (TBrBPPCP), 1,1-bis(4-hydroxy-3-methyl-5-bromophenyl)-4-perhydrocumyl cyclohexane (DDBPPCP), 1,1-bis(4-aminophenyl)-4-perhydrocumyl cyclohexane (BAPCP) and 1,1-bis[4-(4-aminophenoxy)phenyl]-4-perhydrocumyl cyclohexane (BAPPHC), were synthesized as described in **Chapter 3**. The dianhydrides, pyromellitic dianhydride (PMDA), 3,3',4,4'-biphenyl tetracarboxylic dianhydride (BPDA), 3,3',4,4'-benzophenonetetracarboxylic dianhydride (BTDA), 3,3',4,4'-oxydiphthalic anhydride (ODPA) and 4,4'-(hexafluoroisopropylidene)diphthalic anhydride (6-FDA), all received from Aldrich, USA, were sublimed before use. Benzyltriethylammonium chloride (BTEAC), received from Aldrich, USA was used as received. Dichloromethane and *m*-cresol, both from S. D. Fine Chem., India were dried and distilled according to the reported procedure.¹⁸

Terephthalic acid chloride and isophthalic acid chloride were synthesized from terephthalic acid and isophthalic acid, respectively using excess thionyl chloride in the presence of pyridine as a catalyst and were purified by distillation under reduced pressure.

5.2.2 Measurements

Inherent viscosity of polymers was measured with 0.5 % (w/v) solution of polymer in CHCl₃ or tetrachloroethane at 30 ± 0.1°C using an Ubbelohde suspended level viscometer. Molecular weight of polyesters were measured on Thermofinnigan make gel permeation chromatograph (GPC), using the following conditions: Column - polystyrene-divinylbenzene (10⁵ Å to 50 Å), Detector - RI, room temperature. Polystyrene was used as the calibration standard. The polyester sample (5 mg) was dissolved in 5 ml chloroform and filtered through 0.2 μ SS-filter.

FTIR spectra were recorded using polymer films on a Perkin-Elmer *Spectrum GX* spectrophotometer.

NMR spectra were recorded on a Bruker 200, 400 or 500 MHz spectrometer at resonance frequencies of 200, 400 or 500 MHz for ^1H and at 50, 100 or 125 MHz for ^{13}C measurements using CDCl_3 as a solvent.

Thermogravimetric analysis was performed on Perkin-Elmer TGA-7 system at a heating rate of $10^\circ\text{C} / \text{minute}$ under nitrogen atmosphere. Sample weight taken was ~ 5 mg.

DSC was carried out on TA Instruments DSC Q10, at a heating rate of $10^\circ\text{C} / \text{minute}$ in nitrogen atmosphere.

X-Ray diffractograms of polymers were obtained on a Rigaku Dmax 2500 X-ray diffractometer at a tilting rate of $2^\circ / \text{minute}$. The measurements were carried on solution cast films.

Cells for pretilt angle measurements were prepared according to the procedure described in **Chapter 4, Section 4.2.3**.

5.2.2.1 Film preparation for gas permeability measurement

Polyester films of 30-40 μm thickness, used for permeability studies were obtained by casting from chloroform solution for each polymer. Three percent solution of polymer was prepared in chloroform and the solution was filtered through a 10 μm filter to remove any particulates. The clear polymer solution was poured into a clean glass disc (diameter 7.5 cm). The chloroform was evaporated slowly at room temperature. The films were removed and were subsequently dried at 100°C for seven days under reduced pressure.

The density of polyester films of thickness 100 μm was determined by floatation method at $40 \pm 0.1^\circ\text{C}$ using aqueous potassium carbonate solution. Minimum six samples of each polyester were used for density determinations and the obtained values were averaged. With the density, specific free volume and fractional free volume (FFV) was calculated by Van Krevelen's method.²⁷

5.2.2.2 Measurement of gas permeability

In the present work, the variable volume method was used to determine permeability of He, N_2 and O_2 .²⁸ The purity of the gases used was minimum 99 %. The permeability measurements were carried out at $35 \pm 0.1^\circ\text{C}$ and upstream pressures of 10 Kg/cm^2 while

maintaining permeate side at ambient pressure. The schematic diagram of the permeation apparatus is given in **Figure 5.1**

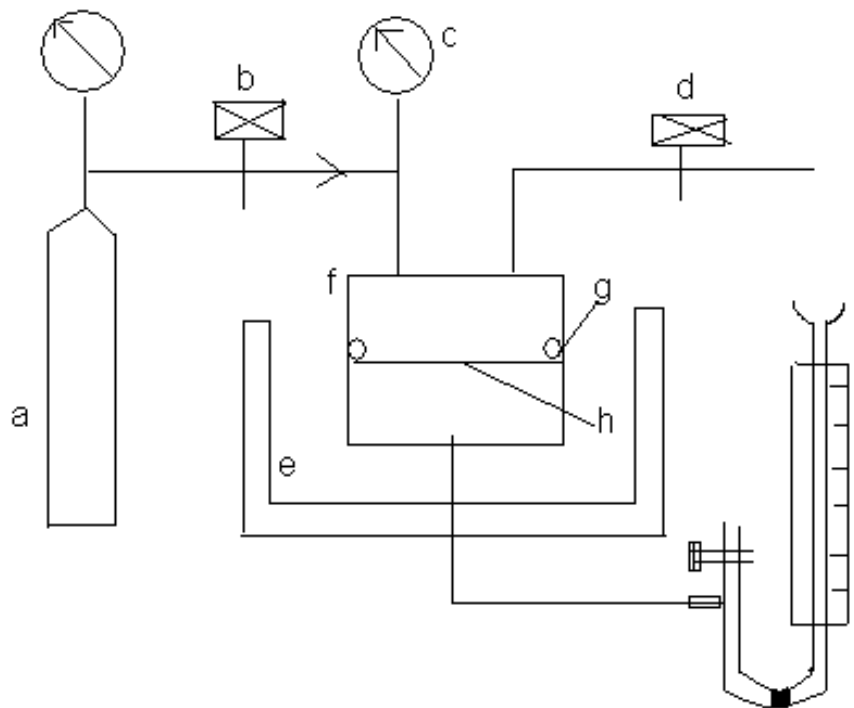


Figure 5.1: Schematic diagram for gas permeability measurement

(a: Gas cylinder; b: Inlet valve; c: Pressure gauge; d: Outlet valve; e: Thermostat; f: Permeation cell; g: 'O' ring; h: Membrane; i: Calibrated flow meter).

The permeation cell was opened and circular coupon (size: 49 mm) of membrane was mounted in the cell. An O-ring was placed on the top of membrane (vacuum grease was applied to the O-ring to ensure the leak-proof assembly). The cell was fixed with inlet (connected to the gas cylinder and a pressure gauge) and outlet tubing and tightened.

Using the regulator knob and the inlet valve, the pressure was adjusted in the cell while keeping the exhaust closed. Gas was flushed through the outlet valve seven to eight times in the system to ensure the removal of earlier gas to the maximum possible extent. The flow meter was attached to the permeate side through a flexible pipe. A desired pressure was applied to the upstream side of the cell while outlet valves were kept closed.

The amount of gas permeated per unit time was recorded after a certain period of time. The readings were continued till enough data generated to ensure the equilibrium had

reached (depends on the gas used and membrane mounted in the cell). The initial and final pressure on the gauge was also recorded while taking the readings. The gas permeability was calculated for each reading using the equation given below and the consistent data was averaged.

At the end of the experiment, cell was depressurized and disconnected from the cylinder.

$$p_{avg} = (p_{int} + p_{final}) / 2$$

$$\Delta p = p_{avg} - p_{ambient}$$

$$Permeability(P) = \frac{14.7 \bullet distance \bullet flow\ meter\ constant \bullet thickness}{76 \bullet area\ of\ the\ membrane \bullet \Delta p \bullet time} \dots\dots(1)$$

$$selectivity\alpha_{(A/B)} = P_A / P_B$$

Δp was recorded in psi, P is the gas permeability in barrer

From the permeability coefficients obtained by the **equation (1)**, the ideal separation factor for different pairs of gases was calculated.

5.3 Synthesis of polyesters, polyimides and polyetherimides containing bulky perhydrocumyl substituted cyclohexylidene group

5.3.1 Synthesis of polyesters from bisphenols containing perhydrocumyl cyclohexylidene and terephthalic acid chloride / isophthalic acid chloride

A representative procedure for synthesis of polyesters is described below.

Into a 100 ml two-necked round bottom flask equipped with a high-speed mechanical stirrer and an addition funnel were placed 1,1-bis(4-hydroxyphenyl) -4-perhydrocumyl cyclohexane (1.96 g, 5 mmol) and 1M NaOH solution (10.2 mL). Thereafter, BTEAC (30 mg) was added to the reaction mixture and the flask was cooled to 10°C. A solution of terephthalic acid chloride (1.02 g, 5 mmol) in dichloromethane (12 mL) was added in one lot to the reaction mixture and the mixture was stirred vigorously at 2000 rpm for 1 h. The aqueous layer was decanted and the organic layer was diluted with additional 15 mL of dichloromethane. The polymer solution was precipitated in excess methanol. The precipitated polymer was filtered and washed several times with water and then with methanol and dried at 80°C for 24 h under reduced pressure.

A similar procedure was followed for the synthesis of other polyesters.

5.3.2 Synthesis of polyimides from 1,1-bis(4-aminophenyl)-4-perhydrocumyl cyclohexane and commercial dianhydrides

Polyimides were synthesized by one-step high temperature solution polymerization in *m*-cresol. A representative procedure for the synthesis of polyimides is described below.

Into a 50 mL three-necked round bottom flask equipped with a magnetic stirring bar, a nitrogen inlet and a guard tube, 1,1-bis(4-aminophenyl)-4-perhydrocumyl cyclohexane (0.39 g, 1 mmol) was added and dissolved in freshly distilled *m*-cresol (6 mL). To the homogeneous solution, PMDA (0.22 g, 1 mmol) was added in portions at room temperature. The reaction mixture was heated to 80°C and was stirred for 1 h. The temperature was then raised to 200°C and the reaction mixture was stirred for 6 h at that temperature. The polymerization reaction was performed under gentle stream of nitrogen and the water formed during imidization was continuously removed with a stream of nitrogen. After 6 h, reaction mixture was cooled to room temperature and was added to excess methanol. The precipitated polymer was washed with methanol to remove *m*-cresol and was dried at 100°C for 24 h under reduced pressure.

5.3.3 Synthesis of polyetherimides from 1,1-bis[4-(4-aminophenoxy)phenyl]-4-perhydrocumyl cyclohexane and commercial dianhydrides

Polyetherimides were synthesized by one-step high temperature solution polymerization in *m*-cresol. A representative procedure for synthesis of polyetherimides is described below.

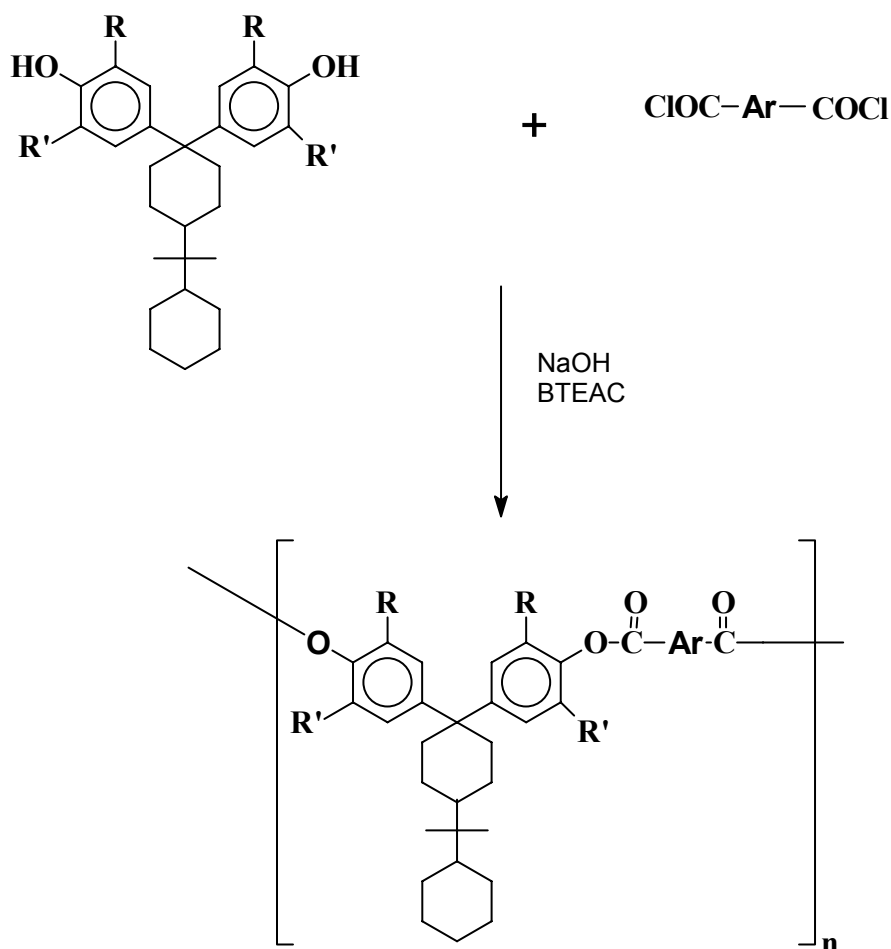
Into a 50 mL three-necked round bottom flask equipped with a magnetic stirring bar, a nitrogen inlet and a guard tube, 1,1-bis[4-(4-aminophenoxy)phenyl]-4-perhydrocumyl cyclohexane (0.58 g, 1 mmol) was added and dissolved in freshly distilled *m*-cresol (6 mL). To the homogeneous solution, BPDA (0.29 g, 1 mmol) was added in portions at room temperature. The reaction mixture was heated to 80°C and was stirred for 1 h. The temperature was then raised to 200°C and the reaction mixture was stirred for 6 h at that temperature. The polymerization reaction was performed under gentle stream of nitrogen and the water formed during imidization was continuously removed with a stream of nitrogen. After 6 h, reaction mixture was cooled to room temperature and was added to excess methanol. The precipitated polymer was washed with methanol to remove *m*-cresol and was dried at 100°C for 24 h under reduced pressure.

5.4 Results and Discussion

5.4.1 Synthesis and characterization of polyesters from perhydrocumyl cyclohexylidene containing bisphenols and terephthalic acid chloride / isophthalic acid chloride

Scheme 5.1 illustrates the synthesis of polyesters from diacid chlorides and bisphenols.

In the present study, polyesters were prepared by interfacial polycondensation with a solution of diacid chloride in dichloromethane and aqueous solution of sodium salt of bisphenols using BTEAC as the phase transfer catalyst. The results of polymerization are summarized in **Table 5.1**.



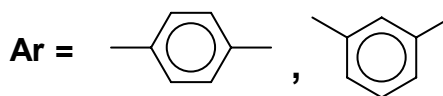
$R = R' = H$

$R = \text{CH}_3, R' = H$

$R = R' = \text{CH}_3$

$R = R' = \text{Br}$

$R = \text{CH}_3, R' = \text{Br}$



Scheme 5.1 Synthesis of polyesters from perhydrocumyl cyclohexylidene containing bisphenols and terephthalic acid chloride / isophthalic acid chloride.

All the polymerizations proceeded in a homogeneous manner. The inherent viscosities of the polyesters were in the range 0.51 – 0.86 dL/g.

The results of GPC measurements on polyesters are presented in **Table 5.2**. Number average molecular weights (M_n) were in the range 17,390 to 141,400 with polydispersity index in the range 1.7-3.7. Inherent viscosity and GPC data indicates the formation of reasonably high molecular weight polymers. However, the molecular weight values

provided by GPC should not be taken as absolute as the calibration of GPC was carried out using polystyrene standards.

Tough, transparent and flexible films of polyesters could be cast from chloroform solutions of polyesters.

Table 5.1: Synthesis of polyesters from perhydrocumyl cyclohexylidene containing bisphenols and terephthalic acid chloride / isophthalic acid chloride

Polyester	Diacid chloride	Bisphenol	Yield (%)	η_{inh} (dL/g)
P-1	TPC	BPPCP	95	0.62
P-2	TPC	DMBPPCP	95	0.60
P-3	TPC	TMBPPCP	96	0.57
P-4	TPC	TBrBPPCP	97	0.62
P-5	TPC	DMDBrBPPCP	96	0.60
P-6	IPC	BPPCP	97	0.51
P-7	IPC	DMBPPCP	98	0.52
P-8	IPC	TMBPPCP	97	0.64
P-9	IPC	TBrBPPCP	97	0.51
P-10	IPC	DMDBrBPPCP	96	0.86

a: η_{inh} was measured with 0.5% (w/v) solution of polyester in chloroform at $30 \pm 0.1^\circ\text{C}$.

Table 5.2: GPC data of polyesters derived from perhydrocumyl cyclohexylidene containing bisphenols and terephthalic acid chloride / isophthalic acid chloride

Polyester	Diacid chloride	Bisphenol	Molecular weight		PDI Mw/Mn
			Mn	Mw	
P-1	TPC	BPPCP	26450	93060	3.4
P-2	TPC	DMBPPCP	17390	42050	2.4
P-3	TPC	TMBPPCP	23780	42615	1.8
P-4	TPC	TBrBPPCP	23760	41140	1.7
P-5	TPC	DMDBrBPPCP	37610	100000	2.6
P-6	IPC	BPPCP	21300	45400	2.1
P-7	IPC	DMBPPCP	28300	58250	2.1
P-8	IPC	TMBPPCP	41430	154700	3.7
P-9	IPC	TBrBPPCP	40100	92890	2.3
P-10	IPC	DMDBrBPPCP	141400	291400	2.1

a : measured by GPC in chloroform, polystyrene was used as the calibration standard.

5.4.1.1 Structural characterization

The formation of polyesters was confirmed by FTIR, ¹H-NMR and ¹³C-NMR spectroscopy. FTIR spectra of polyesters derived from BPPCP and terephthalic acid chloride and isophthalic acid chloride are reproduced in **Figure 5.2**. The C=O absorption was observed at 1743.37 and 1743.80 cm⁻¹ for polyesters derived from BPPCP and terephthalic acid chloride and isophthalic acid chloride, respectively. The effect of substituents on the bisphenol molecule has been reflected in the shift of C=O absorption frequencies. The C=O stretching frequencies are given in **Table 5.3**. In case of the dimethyl and tetramethyl substitution, +I effect was more pronounced which decreased the force constant of the carbonyl group and hence there was decrease in the wave-number of

the absorption band. The presence of tetrabromo substitution displayed –I effect and the C=O absorption was observed at higher wave-number. In case of dibromo dimethyl-substituted polyesters, absorption shifted to the lower wave-number as compared to that of tetrabromo-substituted polyesters. This can be attributed to the +I effect of methyl group. In general, polyesters derived from isophthalic acid chloride showed C=O absorption at slightly higher wave-number than corresponding polyesters derived from that of terephthalic acid chloride.

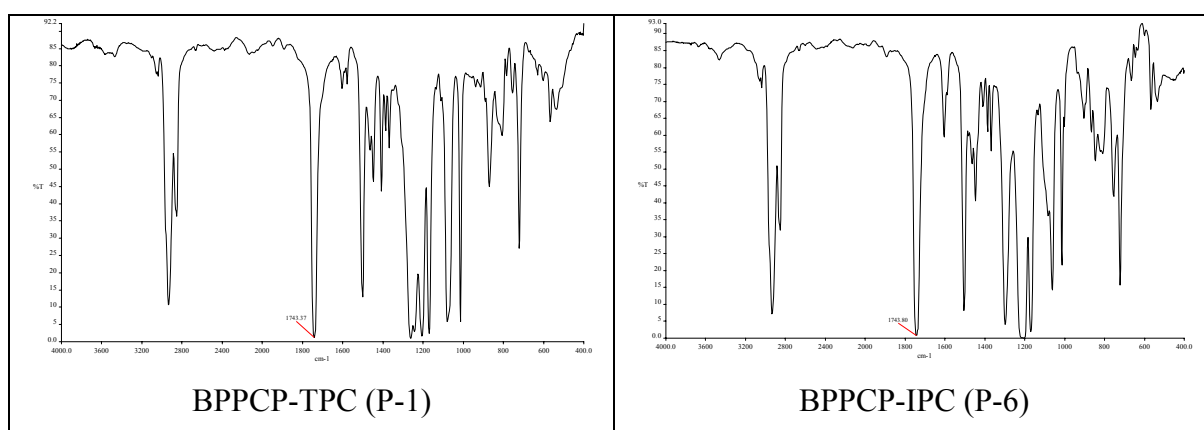
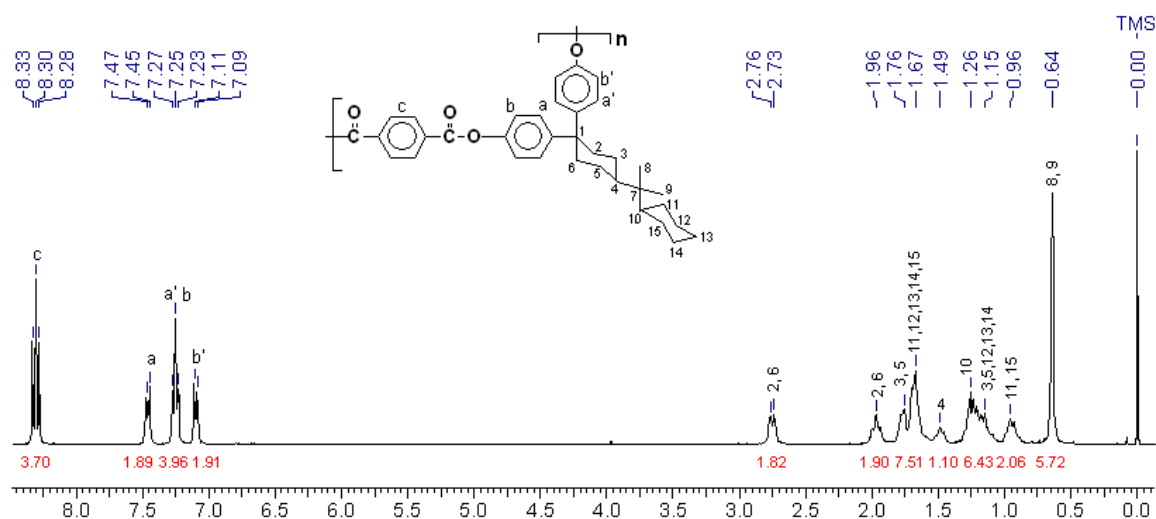


Figure 5.2: IR spectra (Film) of polyesters derived from BPPCP and terephthalic acid chloride / isophthalic acid chloride

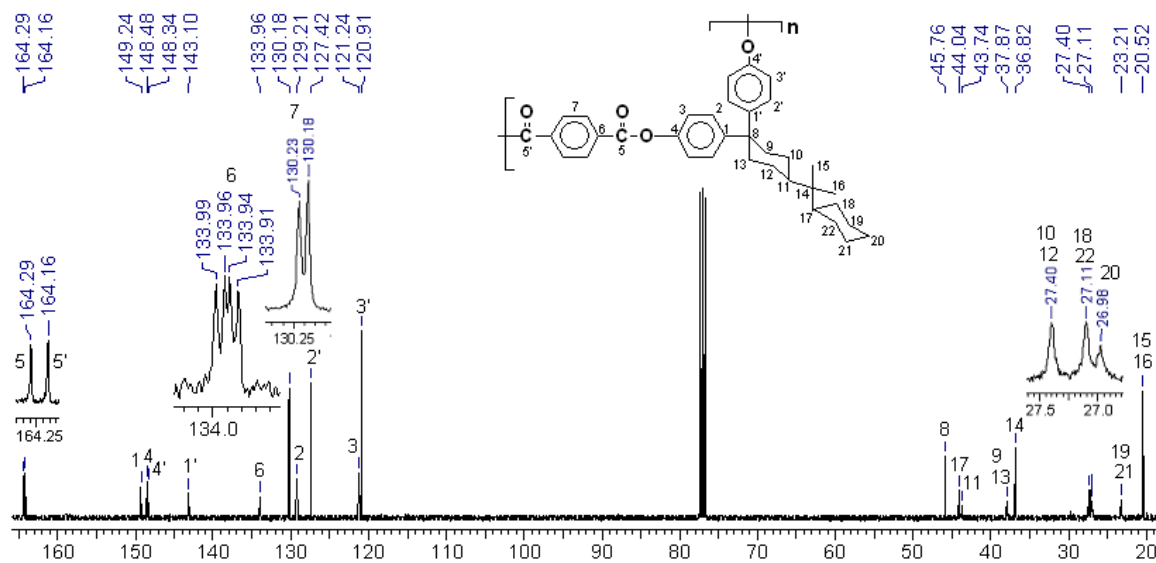
Table 5.3 C=O Absorption frequencies for polyesters derived from perhydrocumyl cyclohexylidene containing bisphenols and terephthalic acid chloride / isophthalic acid chloride

Polyester	C=O stretch cm ⁻¹	Polyester	C=O stretch cm ⁻¹
P-1	1743	P-6	1744
P-2	1740	P-7	1743
P-3	1740	P-8	1744
P-4	1759	P-9	1760
P-5	1750	P-10	1751

^1H -NMR and ^{13}C -NMR spectra of polyesters derived from perhydrocumyl cyclohexylidene containing bisphenol (BPPCP) and terephthalic acid chloride and isophthalic acid chloride are reproduced in **Figure 5.3** and **5.6**, respectively.



(a) ^1H NMR Spectrum of Polyester P-1



(b) ^{13}C NMR Spectrum of polyester P-1

Figure 5.3: ^1H -NMR and ^{13}C -NMR spectra of polyester derived from BPPCP and terephthalic acid chloride

^1H -NMR spectrum of polyester derived from BPPCP and terephthalic acid chloride (**Figure 5.3**), exhibited three peaks in the region 8.33-8.28 ppm for terephthalic acid protons. In case of symmetrical diols terephthalic acid protons gives a single peak. To check whether it was a due to spin-spin coupling (J coupling) or three independent singlets, ^1H -NMR spectrum was recorded at three different magnetic field strengths viz, 200, 400 and 500 MHz. It was observed that as the field strength increased the separation between terephthalic ring signals increased, whereas, the doublet for protons “a” of bisphenol phenyl ring (J coupling) remained unchanged (**Figure 5.4**). This indicates that the terephthalic moiety experiences different environments based on the way BPPCP has condensed with diacid chloride. There is a possibility of four types of constitutional isomerism

- Axial-----Diacid-----Axial
- Axial-----Diacid-----Equatorial
- Equatorial-----Diacid-----Axial
- Equatorial-----Diacid-----Equatorial.

As there is not much change in chemical shift difference between axial-equatorial and equatorial-axial isomers the protons of these terephthalic rings are undistinguishable under the recording conditions. At higher magnetic field strengths these protons might give separate signals.

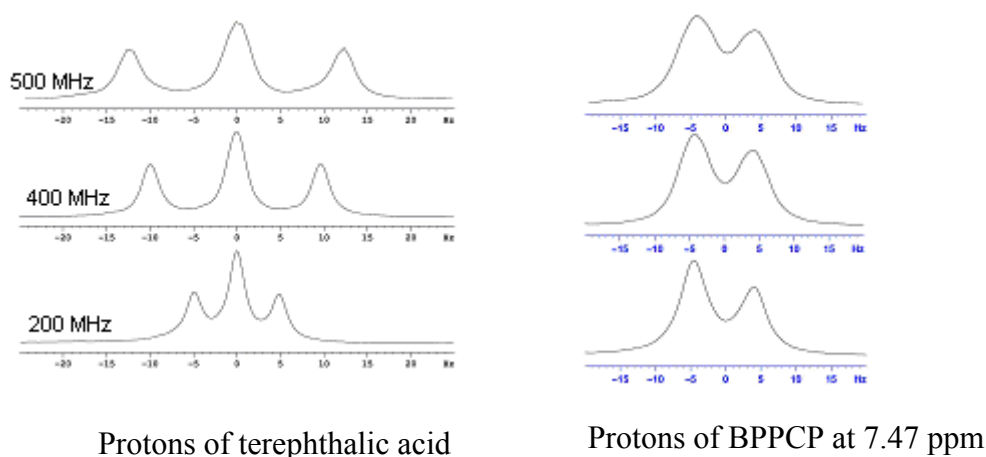


Figure 5.4: Partial ^1H -NMR spectrum of polyester P-1 at three different magnetic field strengths viz, 200, 400 and 500 MHz

The high-resolution ^{13}C NMR spectrum of P-1 showed two sets of four aromatic shifts for bisphenol phenyl ring carbons as that in case of monomer (BPPCP) (**Chapter 3, Figure 3.27**), which indicates that the axial and equatorial identity of the phenyl rings is retained

in polymer. This was expected to show some effect on the terephthalic acid carbons. The quaternary carbon of the terephthalic acid ring, carbon no. 6 in **Figure 5.3b** showed four peaks at 133.91, 133.94, 133.96 and 133.99 ppm. Terephthalic acid carbons experience four different environments arising from constitutional isomerism. Carbon no. 7 of terephthalic acid ring appears as two closely separated peaks, which indicates that these carbons are also experiencing different environments.

Based on the ^1H and ^{13}C NMR analysis polyester derived from BPPCP and terephthalic acid chloride following microstructure could be proposed. **Figure 5.5** shows the microstructure for polyester derived from BPPCP and terephthalic acid chloride, where terephthalic carbonyl is attached to either to axial-axial, equatorial-equatorial, axial-equatorial or equatorial-axial phenyl rings of BPPCP.

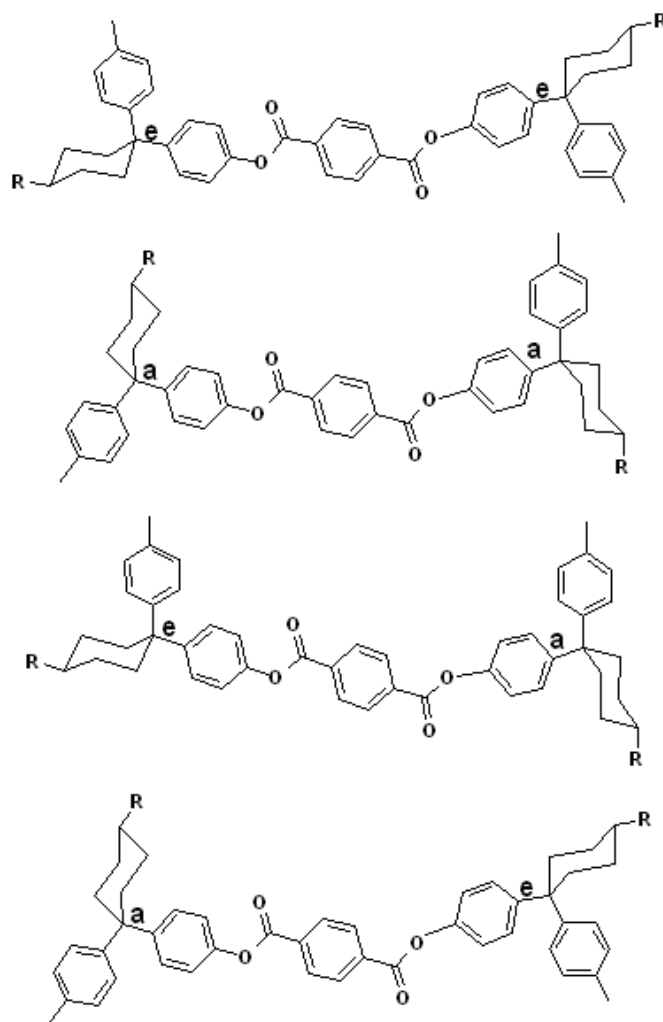
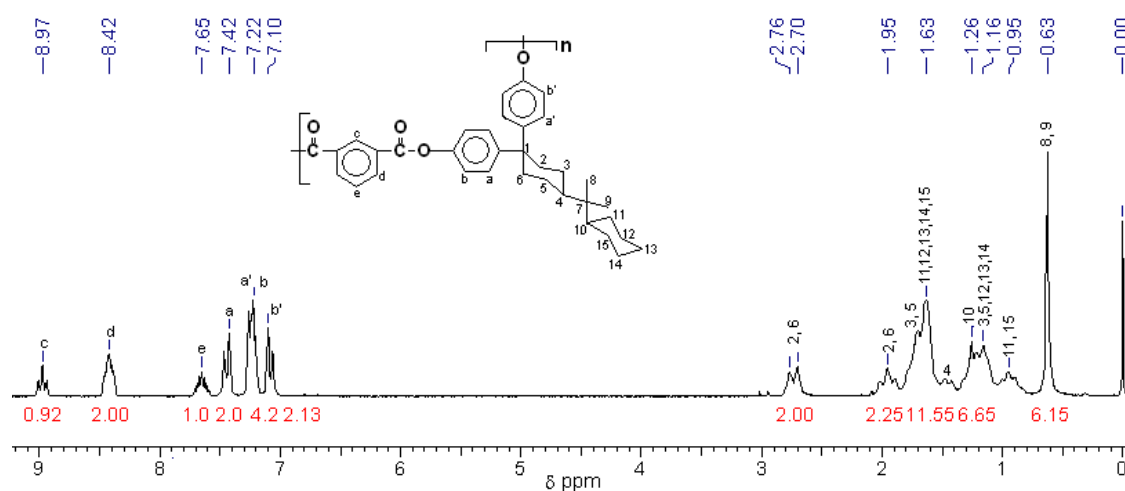
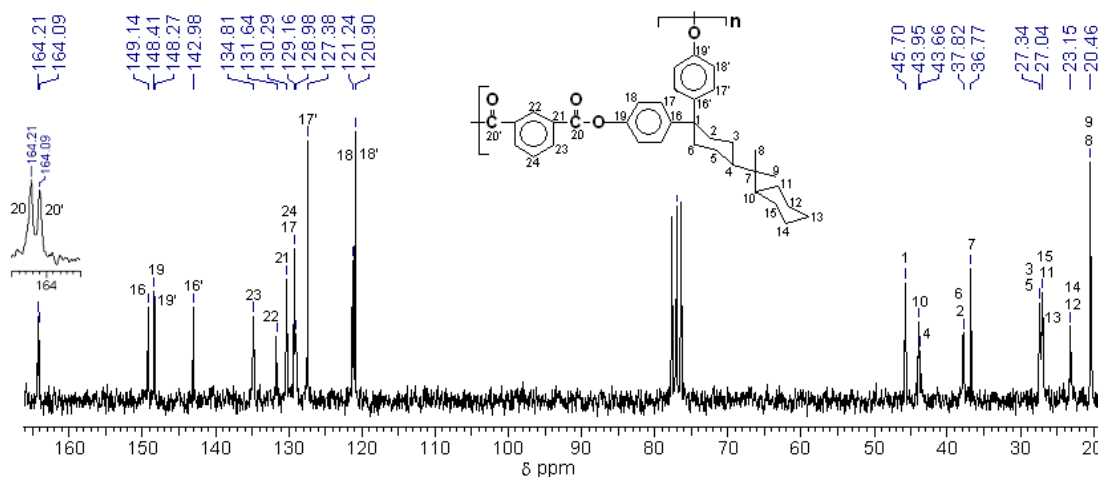


Figure 5.5: Microstructure of polyester derived from BPPCP and terephthalic acid chloride



(a) $^1\text{H-NMR}$ spectrum of polyester P-6



(b) $^{13}\text{C-NMR}$ spectrum of polyester P-6

Figure 5.6: $^1\text{H-NMR}$ and $^{13}\text{C-NMR}$ spectra of polyester derived from BPPCP and isophthalic acid chloride

NMR analysis of all the polyesters synthesized exhibited the retention of axial and equatorial identity of phenyl rings of bisphenol monomer. Partial ^{13}C NMR spectra along with the assignment for polyesters are reproduced in **Figure 5.7**.

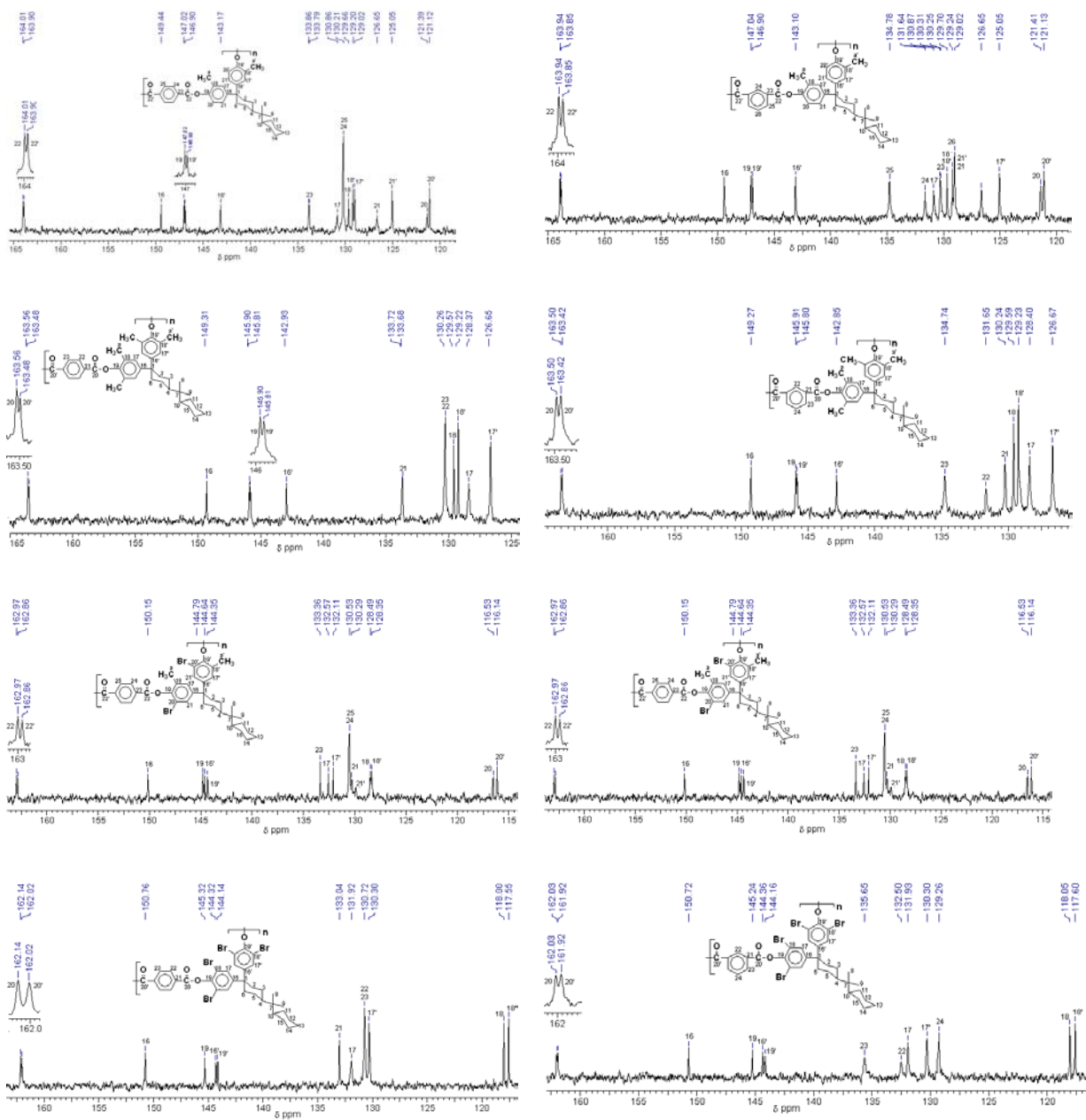


Figure 5.7 Partial ^{13}C -NMR spectra of polyesters synthesized from bisphenols containing perhydrocumyl cyclohexylidene group with terephthalic acid chloride / isophthalic acid chloride

5.4.1.2 Solubility measurements

Solubility of polyesters was tested in various organic solvents at a 3 wt % concentration and data is summarized in **Table 5.4**. All the polyesters were readily soluble in chlorinated hydrocarbons such as dichloromethane, chloroform and tetrachloroethane, as well as in *m*-

cresol and THF. These are typical solvents for amorphous polyarylates.¹⁹ Polyesters derived from perhydrocumyl cyclohexylidene containing bisphenols generally had better solubility than polyesters derived from bisphenol-A and cyclohexylidene bisphenol (**Chapter 4, section 4.4.1**). The solubility of these polyesters is attributed to the reduction in both polymer chain packing and regularity by the introduction of bulky pendant perhydrocumyl cyclohexylidene group. Like other common polyesters, the perhydrocumyl cyclohexylidene containing polyesters were practically insoluble in polar aprotic solvents like DMF, DMSO, etc.

Table 5.4: Solubility data of polyesters derived from perhydrocumyl cyclohexylidene containing bisphenols containing and terephthalic acid chloride / isophthalic acid chloride

Polyester	Diacid chloride	Bisphenol	DCM	CHCl ₃	TCE	ODCB	THF	DMF	DMSO
P-1	TPC	BPPCP	++	++	++	++	++	-	-
P-2	TPC	DMBPPCP	++	++	++	++	++	-	-
P-3	TPC	TMBPPCP	++	++	++	++	++	-	-
P-4	TPC	TBrBPPCP	++	++	++	++	++	-	-
P-5	TPC	DMDBrBPPCP	++	++	++	++	++	-	-
P-6	IPC	BPPCP	++	++	++	++	++	-	-
P-7	IPC	DMBPPCP	++	++	++	++	++	-	-
P-8	IPC	TMBPPCP	++	++	++	++	++	-	-
P-9	IPC	TBrBPPCP	++	++	++	++	++	-	-
P-10	IPC	DMDBrBPPCP	++	++	++	++	++	-	-

++: soluble ; -: insoluble

5.4.1.3 X-Ray diffraction studies

X-Ray diffractograms of polyesters derived from perhydrocumyl cyclohexylidene containing bisphenols and terephthalic acid chloride and isophthalic acid chloride are shown in **Figures 5.8**. X-Ray diffraction patterns showed that polyesters were predominantly amorphous in nature. All polyesters exhibited two broad but distinct diffraction peaks. Two distinct WAXD peaks have been reported for the polymers with pendant phenyl rings or aromatic connector groups such as polystyrene,^{20,21} fluorene bisphenol and phenolphthalein isophthalates,²² and poly(2,6-diphenyl-1,4-phenylene oxide)^{23,24} and have been attributed to pendant or connector group “stacking”. Since such “stacking” is impossible in the current polyesters, the secondary diffraction peaks must have some other origin. A similar observation was made by Paul et al.²⁵

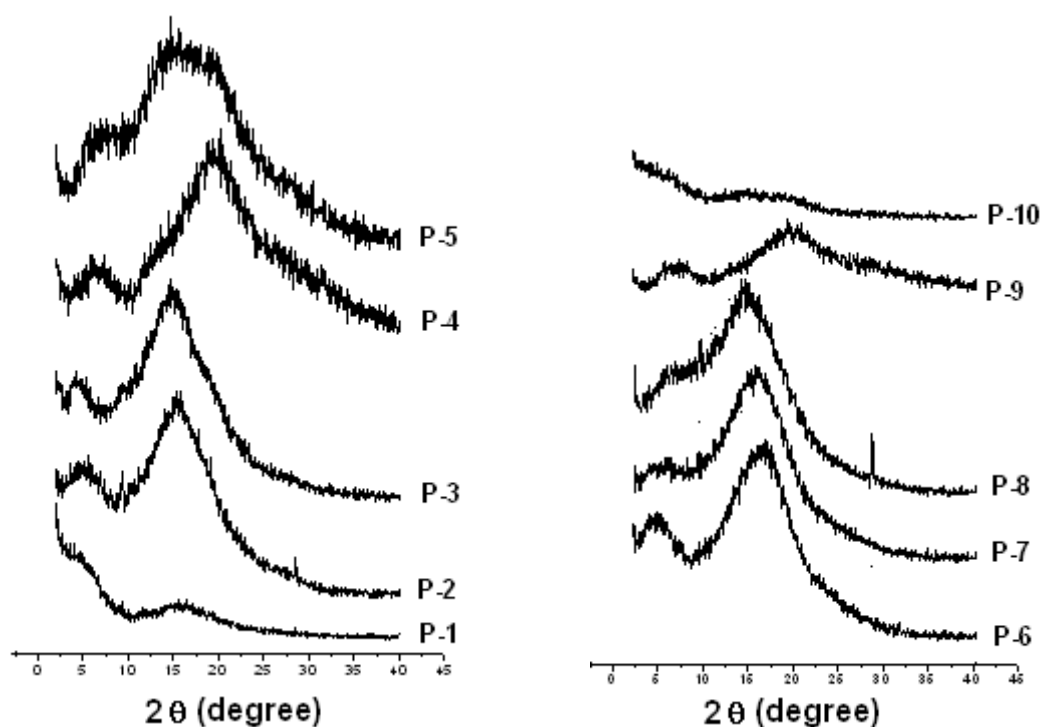


Figure 5.8: X-Ray diffraction patterns of polyesters derived from perhydrocumyl cyclohexylidene containing bisphenols and terephthalic acid chloride / isophthalic acid chloride

5.4.1.4 Thermal properties

In the present study, thermal stability of the polyesters was determined by thermogravimetric analysis (TGA) at a heating rate of 10°C /minute under nitrogen. TG curves of polyesters are shown in **Figure 5.9**. The initial decomposition temperature (IDT) and the decomposition temperature at 10% weight loss (T_{10}) for polyesters are given in **Table 5.5**. IDT for polyesters derived from terephthalic acid chloride and isophthalic acid chloride were in the range of 434-477°C. The temperature for 10% weight loss for these polyesters was in the range 435-485°C. T_{10} for polyester derived from BPC and terephthalic acid chloride was 480°C (**Chapter 4, Table 4.4**) and the examination of data in **Table 5.5** shows that the introduction of bulky perhydrocumyl cyclohexylidene group into polyester backbone retained their desirable high thermal stability.

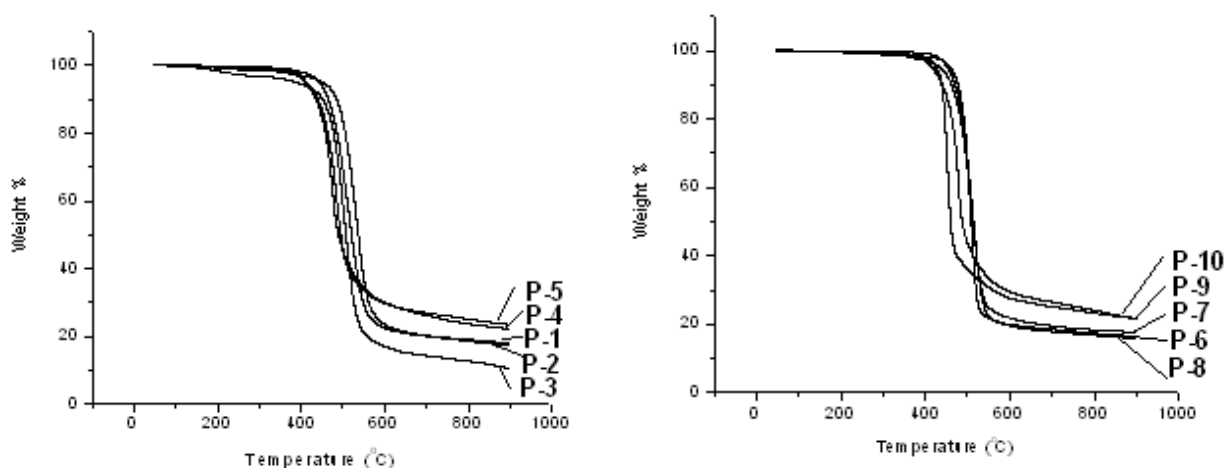
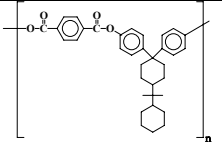
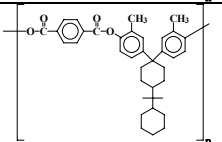
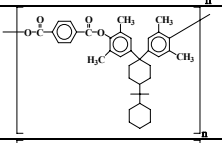
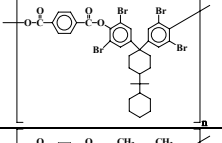
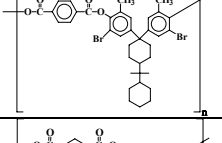
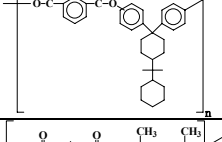
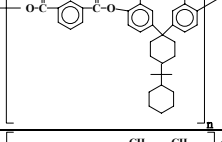
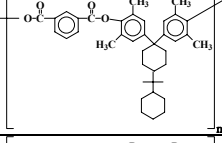
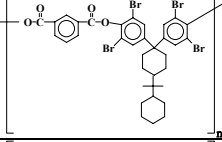
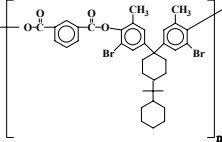


Figure 5.9: TG curves of polyesters derived from perhydrocumyl cyclohexylidene containing bisphenols with terephthalic acid chloride / isophthalic acid chloride

Table 5.5: Thermal properties of polyesters derived from perhydrocumyl cyclohexylidene containing bisphenols and terephthalic acid chloride / isophthalic acid chloride

Polyester	IDT (°C)	T ₁₀ (°C)	T _g (°C)
P-1 	477	485	254
P-2 	453	465	232
P-3 	450	453	267
P-4 	434	440	293
P-5 	434	435	288
P-6 	469	477	213
P-7 	458	470	201
P-8 	454	462	240
P-9 	450	438	272
P-10 	431	440	256

IDT : initial decomposition temperature

T₁₀ : Temperature at 10 % weight loss

Glass transition (T_g) temperature of the polyesters was evaluated by differential scanning calorimetry (DSC). T_g values were obtained from second heating scans of polyester samples at a heating rate of $10^\circ\text{C} / \text{minute}$. DSC curves are reproduced in **Figure 5.10 and 5.11** and T_g values are given in **Table 5.5**. The T_g values were in the range $232\text{-}293^\circ\text{C}$. The glass transition temperature of the polyesters derived from terephthalic acid chloride are higher than their isophthalic acid chloride derived analogues. A review of studies on spatial configuration effects for a variety of polymers suggests that a higher T_g for *para* structure is a general phenomenon.^{26,29} The lower glass transition temperatures of polyesters derived from isophthalic acid chloride than the corresponding polyesters derived from terephthalic acid chloride could be attributed to their more conformational freedom of the main chains than the *para*-linked polymers.

The effect of the symmetric and unsymmetric substitution of the bisphenol rings was observed on the T_g s of polyesters. In case of dimethyl substitution (P-2 and P-7) because of the asymmetric nature the decrease in T_g as compared to unsubstituted bisphenol (P1 and P-5) was observed. T_g increases with tetramethyl substitution (P-3 and P-8). It appears that symmetric bulky substitution retards the long-chain motions in polymer molecule. The presence of bulky, polar bromo-substituent further increased the T_g of polyesters (P-4 and P-9), whereas, unsymmetric dimethyl dibromo containing polyesters (P-5 and P-10) showed lower T_g than that of tetrabromo-substituted ones. T_g followed the following trend in both terephthalic acid chloride and isophthalic acid chloride derived polyesters.



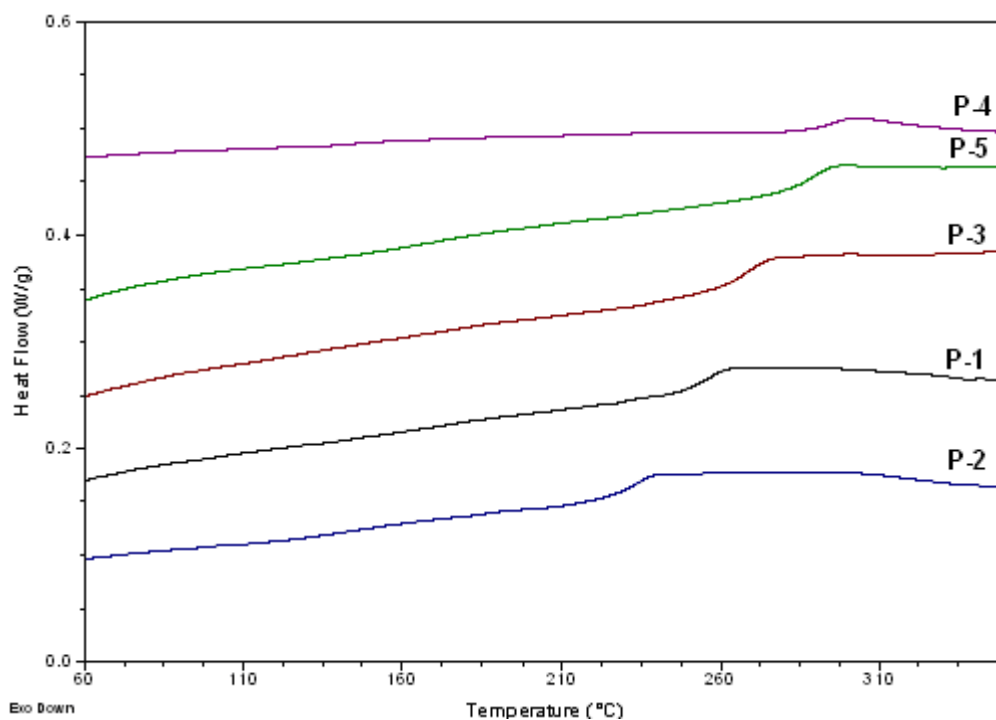


Figure 5.10: DSC curves of polyesters derived from perhydrocumyl cyclohexylidene containing bisphenols and terephthalic acid chloride

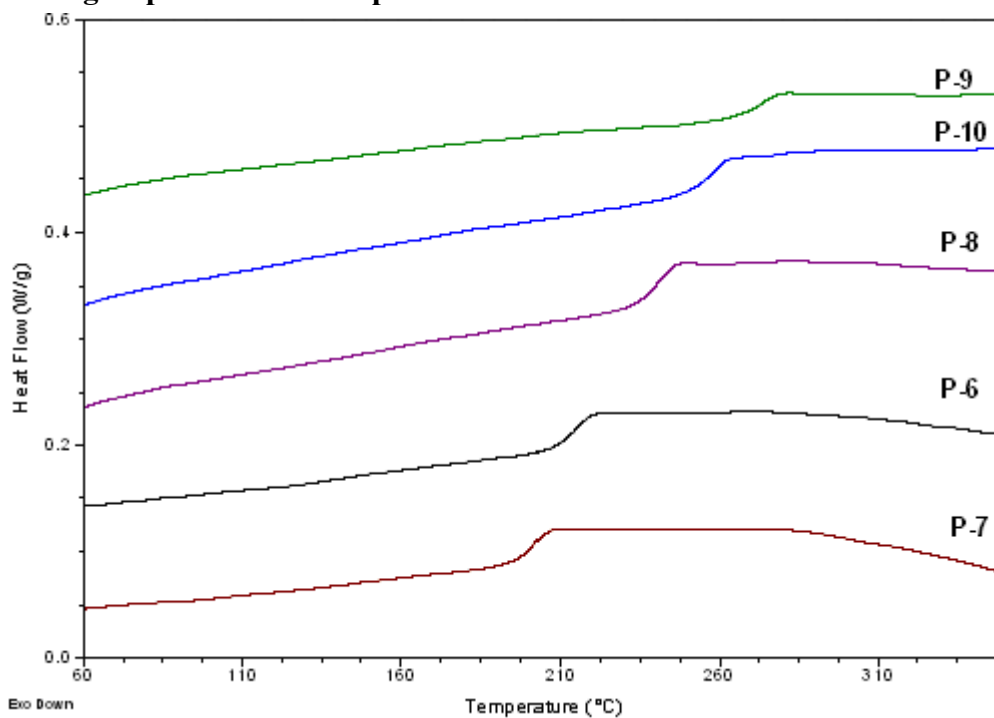


Figure 5.11 DSC curves of polyesters derived from perhydrocumyl cyclohexylidene containing bisphenols and isophthalic acid chloride

5.4.2 Gas permeability studies of polyesters derived from bisphenols containing perhydrocumyl cyclohexylidene moiety and terephthalic acid chloride / isophthalic acid chloride.

Gas separation using membrane technology is useful for a variety of applications, such as hydrogen recovery from reactor purge gas, nitrogen and oxygen enrichment, water vapor removal from air, stripping of carbon dioxide from natural gas, etc. Finding new membrane materials with high permeability and permselectivity has been an active research field for several years. Recent studies indicate that the packing density, the segmental motion of polymer chains and gas-polymer interactions are dominant factors that affect gas transport properties. High permeability is primarily related to high free volume, while significant increase in gas permselectivity may be due to restricted segmental motion. On the basis of this one can design new polymers to combine two favorable factors, thus preparing polymers with both high gas permeability and high permselectivity.

A review of gas permeability studies revealed that, relative to numerous papers on the polymer gas transport properties at room temperature, in recent years, research studies on high-temperature gas separation are rather rare. However, from viewpoint of energy saving, in some cases, e.g. “C₁ chemistry”, it is desirable for the membrane separation process to be operated at the highest allowable temperature, so that the purge streams from synthesis gas production can be regulated in composition and recycled without extensive cooling and reheating prior to recycling to the reactor. Therefore it is necessary to have the polymers with high glass transition temperature so that they can be used for the membrane separation applications at high temperatures.

Gas separation properties of glassy polymer membranes depend to a large extent on the class of polymer used in the separation process and polyimides, polyamideimides, polycarbonates, polysulfones, polyetherketones, aromatic polyesters, etc. have been used for the gas separation processes. Aromatic polyesters offer several advantages over other condensation polymers. The variety of available monomers is much larger and polymer synthesis is relatively straightforward. Aromatic polyesters have high glass transition temperatures and good film forming properties. Previous studies have shown that the aromatic polyesters have high level of permselectivity at moderate levels of permeability.

Some possible disadvantages of aromatic polyesters include low solubility in organic solvents necessary for film casting and tendency to crystallize. Careful molecular design of the polymer structure can help minimize these difficulties.

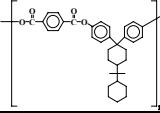
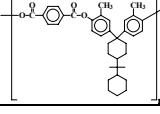
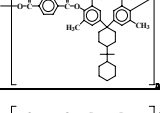
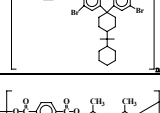
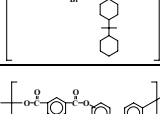
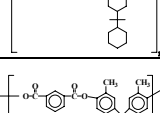
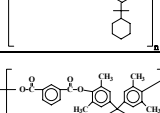
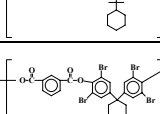
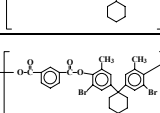
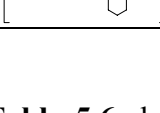
Introduction of the bulky perhydrocumyl cyclohexylidene group along the polymer backbone has resulted in improved solubility of polyesters. The polyesters containing bulky perhydrocumyl cyclohexylidene group exhibited high glass transition temperature. Thus, these polymers are potentially good candidates for gas separation processes.

The results on the gas permeability and structure-property relationship in case of polyesters derived from bulky perhydrocumyl cyclohexylidene bisphenols with various substituents and isophthalic acid chloride / terephthalic acid chloride are presented in this section.

5.4.2.1 Gas permeability analysis

The two series of polyesters based on bisphenols containing bulky perhydrocumyl cyclohexylidene moiety with isophthalic acid chloride / terephthalic acid chloride were studied for the gas permeation measurements. The physical and thermal properties of polyesters are listed in **Table 5.6**. As seen from X-ray diffraction patterns (**Figure 5.8**), all the polyesters are amorphous in nature and crystallinity effects on the physical and transport properties can be eliminated.

Table 5.6 Physical and thermal properties of polyesters derived from perhydrocumyl cyclohexylidene containing bisphenols and terephthalic acid chloride / isophthalic acid chloride.

Polyester	T_g (°C)	d-Spacing (Å)	Density (g/cc)	FFV
P-1 	254	5.6	1.1227	0.350
P-2 	232	5.7	1.1232	0.333
P-3 	267	6.0	1.0656	0.361
P-4 	293	4.6	1.4745	0.383
P-5 	288	5.5	1.2356	0.391
P-6 	213	5.4	1.1518	0.333
P-7 	201	5.6	1.1502	0.317
P-8 	240	6.0	1.1078	0.335
P-9 	272	4.4	1.4873	0.377
P-10 	256	5.4	1.2527	0.383

The data in **Table 5.6** shows polyesters derived from terephthalic acid chloride exhibit slightly higher values of *d*-spacing and FFV than that of isophthalic acid chloride derived polyesters.

In case of tetrabromo-substituted polyesters d-spacing values are smaller than corresponding nonbrominated polyesters. While polar attractions between bromine atoms would tend to draw the polymer chains closer together, the large size of bromine atom as compared with hydrogen opposes this effect and makes this d-spacing result highly unlikely, if not impossible. It appears that average chain d-spacing determined from WAXD may not be representative of the actual chain spacings in these brominated materials. The high X-ray scattering ability of the bromine atom as compared with other atoms in these polymers is probably responsible for of the above noted anomalies.

In all cases polyesters derived from terephthalic acid chloride had higher FFV compared to their isophthalic acid chloride derived analogues. The FFV of tetramethyl-substituted polymers is higher than those of unsubstituted ones, while that of dimethyl-substituted polymers is lowest in the series. This compares well with literature data for dimethyl substituted polyesters and polysulfones.^{25,30} The FFV for dibromo dimethyl substituted polymers is higher than that of tetramethyl substituted ones and is identical to that calculated for tetrabromo-substituted polyesters. These results indicate that asymmetrically substituted monomers pack more efficiently while symmetrically substituted polymers pack less efficiently. This observation is supported by the higher density of the dimethyl substituted polyesters as compared to their tetramethyl substituted analogs.

Pure gas permeability coefficients for three gases and ideal selectivities for gas pairs are given in **Table 5.7**

Table 5.7 Permeability coefficients and ideal selectivities for polyesters derived from perhydrocumyl cyclohexylidene containing bisphenols and terephthalic acid chloride / isophthalic acid chloride at 35±0.1°C and at 10 kg/cm²

No	Polyester	P (barrer ^a)			$\alpha(\text{He}/\text{N}_2)$	$\alpha(\text{He}/\text{O}_2)$	$\alpha(\text{O}_2/\text{N}_2)$
		He	N ₂	O ₂			
P-1	BPPCP TPC	23.3	0.59	2.52	39.4	9.2	4.3
P-2	DMBPPCP TPC	22.0	0.33	1.58	66.7	13.9	4.8
P-3	TMBPPCP TPC	47.3	1.37	5.79	34.6	8.2	4.2
P-4	TBrBPPCP TPC	30.5	0.55	2.86	55.3	10.7	5.2
P-5	DDBPPCP TPC	42.7	0.85	4.1	50.1	10.4	4.8
P-6	BPPCP IPC	21.1	0.34	1.63	61.4	12.9	4.7
P-7	DMBPPCP IPC	19.4	0.21	1.06	91.3	18.3	5.0
P-8	TMBPPCP IPC	42.9	0.83	3.88	51.9	11.0	4.7
P-9	TBrBPPCP IPC	28.6	0.36	2.15	78.7	13.3	5.9
P-10	DDBPPCP IPC	31.1	0.46	2.43	68.3	12.8	5.3

^a: Barrer = 10⁻¹⁰ · [cm³ (STP) · cm/cm² · s · cmHg]

Permeability coefficients of the polyesters derived from terephthalic acid chloride were higher than that of the corresponding polyesters based on isophthalic acid chloride. Several investigators have reported that the polymers containing *meta* substituted phenylene rings have higher packing density and lower permeability to gas as compared to the polymers containing *para* substituted phenylene rings.^{26,29,31,32} The permeability coefficients for the symmetric polyimide PMDA-4,4'-ODA are reported to be about twice that of asymmetric PMDA-3,3'-ODA polymer, while the permselectivity for the asymmetric polymer is almost twice that of symmetric material.³³ The lower permeability and higher selectivity of *meta*-linked polymers may be the result of hindered rotation about the meta-connected linkage. These results are in qualitative agreement with the lower d-spacing and FFV values for the isophthalic acid containing polyesters. The

He/N₂ selectivity has increased by almost 60% for BPPCP-IPC as compared to BPPCP-TPC.

The effect of the dimethyl substitution onto the phenylene rings of bisphenols is very similar to the effect of *meta* bond connection of these rings. In both cases, the asymmetric polyester consistently have lower permeabilities and higher selectivities than their symmetric counter parts. This effect appears to arise from both intermolecular and intramolecular factors. The unsymmetric polyesters are more well packed in the glassy state than their symmetric counter parts; thus, they have lower FFV and permeability.

Amongst the series of polyesters studied in the present work, TBrBPPCP-IPC exhibited highest selectivities for O₂/N₂ and He/N₂. Tetramethyl substituted polyesters have permselectivities similar to their unsubstituted analogue but at higher levels of permeability. Paul et. al. have reported similar observations for polyesters derived from substituted bisphenol-A and isophthalic acid chloride.²⁵

All of the substituted polyesters in this study exhibited either higher permeability, higher selectivity, or both than their unsubstituted analogue.

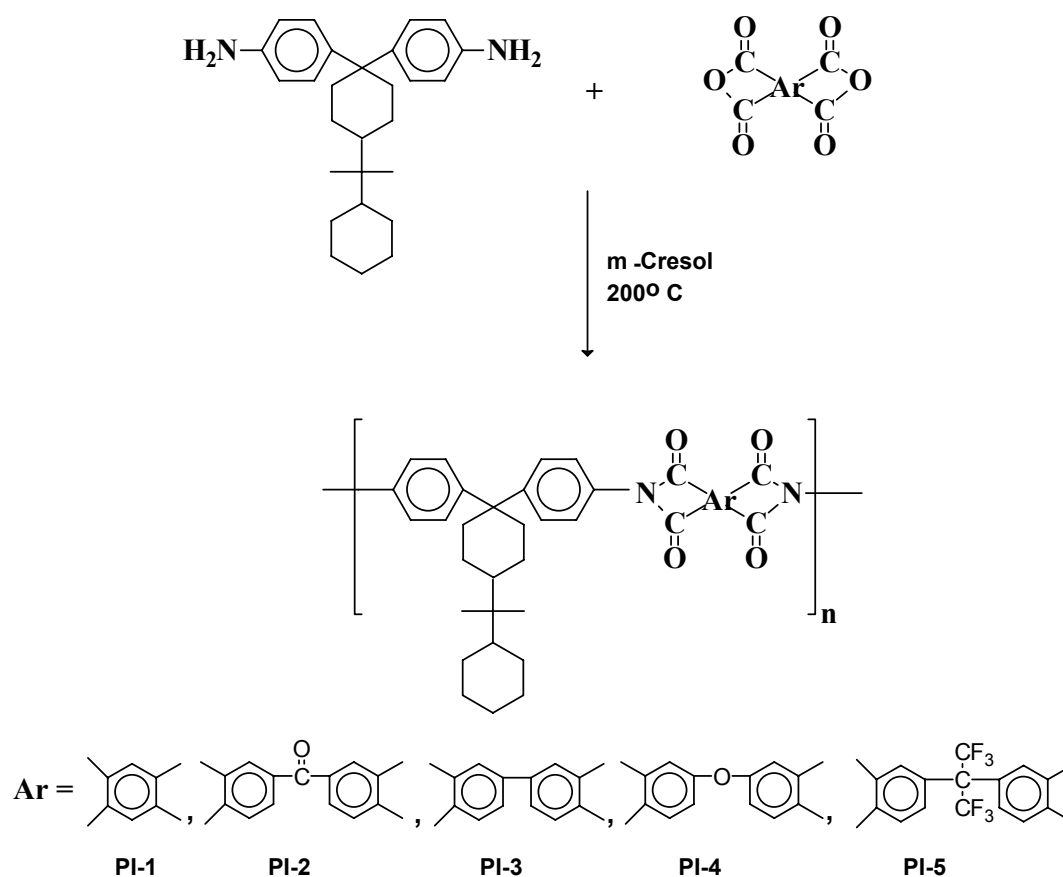
Thus, utility of perhydrocumyl cyclohexylidene containing polyesters as membrane materials for gas separation was demonstrated.

5.4.3 Synthesis and characterization of polyimides from 1,1-bis(4-aminophenyl)-4-perhydrocumyl cyclohexane and commercial dianhydrides

The typical approaches to improve the solubility of aromatic polyimides without sacrifice in their excellent properties are, 1) the insertion of flexible spacers between the rigid units; 2) the insertion of bent or 'crankshaft' units along the polymer backbone and 3) the appending of bulky side groups or flexible side chains along the polymer backbone.

In the present study, bulky perhydrocumyl cyclohexylidene group was introduced along the polymer backbone to improve the processability of polyimides.

In this work, five new polyimides were synthesized by one-step high temperature solution polycondensation of newly synthesized 1,1-bis(4-aminophenyl)-4-perhydrocumyl cyclohexane with five commercial dianhydrides in *m*-cresol (Scheme 5.2).



Scheme 5.2 Synthesis of polyimides from 1,1-bis(4-aminophenyl)-4-perhydrocumyl cyclohexane and commercial dianhydrides

The dianhydrides used in the present study were PMDA, BTDA, BPDA, ODPA and 6-FDA. In a typical experiment, the diamine was dissolved in freshly distilled m-cresol and equimolar quantities of dianhydride was added in portions. The reaction temperature was raised to 80°C and the homogeneous solution was stirred for 1 h. The temperature was raised to 200°C and the reaction mixture was stirred for 6 h. The polymerization reaction carried out under the gentle flow of nitrogen. The water formed during the imidization was removed with the stream of nitrogen.

All the polymerizations proceeded in homogeneous manner. The results of synthesis are summarized in **Table 5.8**

Table 5.8 Synthesis of polyimides from 1,1-bis(4-aminophenyl)-4-perhydrocumyl cyclohexane and commercial dianhydrides

Polyimide	Dianhydride	Yield (%)	η_{inh} (dL/g) ^a	Film quality
PI-1	PMDA	95	0.40	Flexible
PI-2	BTDA	95	0.44	Flexible
PI-3	BPDA	96	0.66	Flexible
PI-4	ODPA	97	0.45	Flexible
PI-5	6-FDA	97	0.35	Flexible

^a: η_{inh} was measured with 0.5 % (w/v) solution of polyimide in TCE at 30±0.1°C

Inherent viscosities were in the range 0.35 to 0.66 dL/g indicating the formation of medium to high molecular weight polyimides. Polyimide PI-5 synthesized from BAPCP and 6-FDA was found to be soluble in chloroform. The number average and weight average molecular weights for PI-5 were 51,800 and 1,03,780 respectively with a polydispersity index of 1.8 as determined by GPC.

Tough, transparent, and flexible films of polyimides could be cast from their TCE solutions.

5.4.3.1 Structural characterization

The formation of polyimides was confirmed by FTIR spectroscopy. As an example, FTIR spectrum of polyimide derived from BAPCP and 6-FDA is reproduced in **Figure 5.12**. The complete imidization was confirmed by the absorption bands at 1785, 1728, 1372 and 721 cm^{-1} , due to symmetric C=O, asymmetric C=O, C-N stretching and imide ring deformation, respectively. These absorption peaks corresponded to previously reported imide ring absorptions. Complete cyclization was also evident by the lack of amide C=O (1640 cm^{-1}) and N-H (1550 cm^{-1}) peaks.

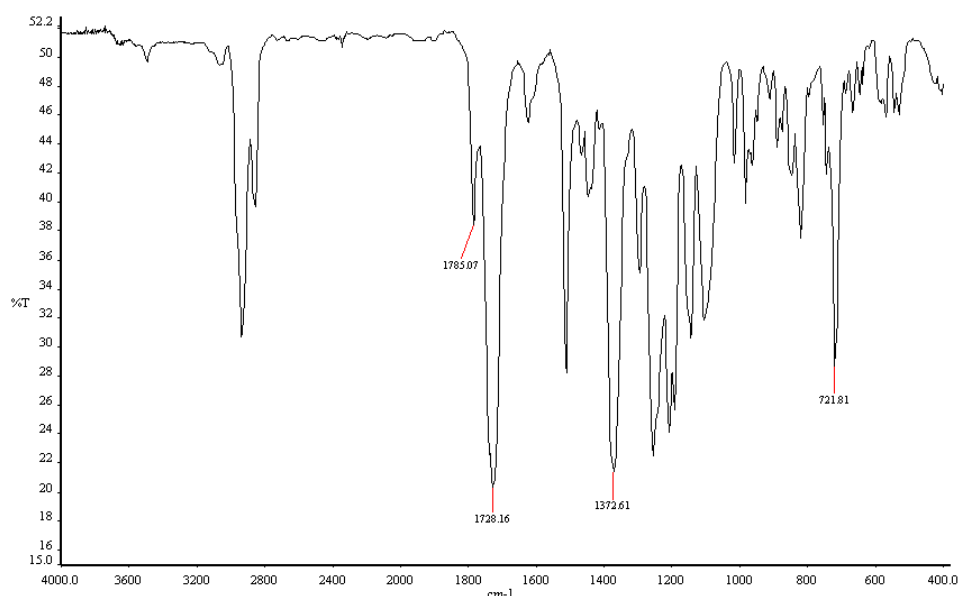
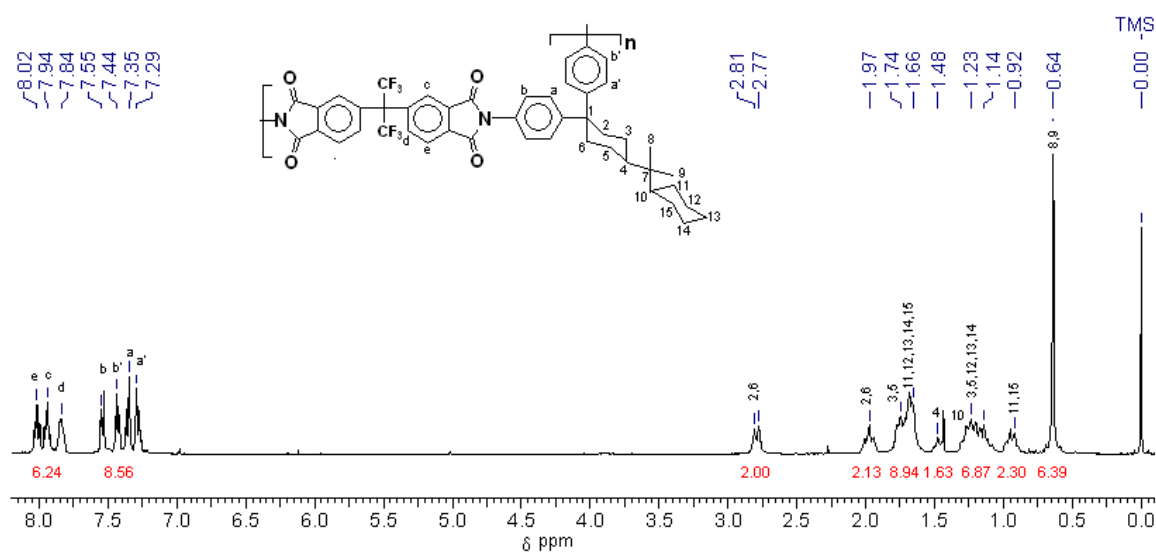
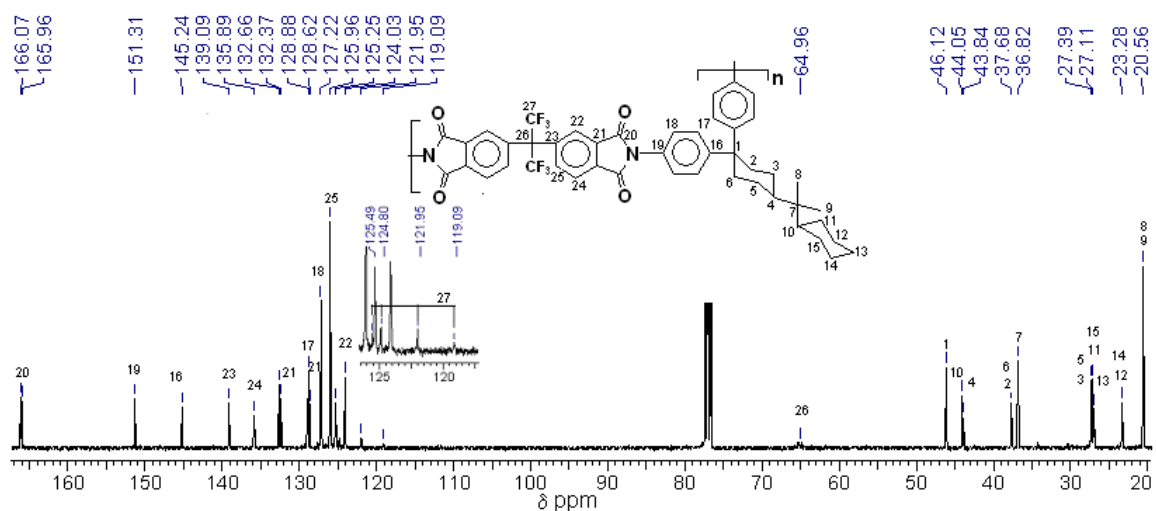


Figure 5.12 FTIR spectrum of polyimide derived from 1,1-bis(4-aminophenyl)-4-perhydrocumyl cyclohexane and 6-FDA (PI-5)

^1H -NMR and ^{13}C -NMR spectra of PI-5 along with assignments are reproduced in **Figure 5.13**



(a) ^1H -NMR spectrum of polyimide PI-5



(b) ^{13}C NMR spectrum of polyimide PI-5

Figure 5.13 ^1H and ^{13}C -NMR spectra of polyimide derived from 1,1-bis(4-aminophenyl)-4-perhydrocumyl cyclohexane and FDA (PI-5)

5.4.3.2 Solubility measurements

Solubility of polyimides was tested in various organic solvents at 3 wt % concentration and data is summarized in **Table 5.9**. BAPCP-based polyimides were soluble in organic solvents such as TCE, *m*-cresol, NMP and ODCB. The literature solubility data for polyimides derived from 1,1-bis(4-aminophenyl)cyclohexane, a diamine containing unsubstituted cyclohexane ring, showed that the polyimides were not soluble in common organic solvents, viz, NMP, *m*-cresol, CHCl₃, etc.¹⁴ That is, introduction of the bulky perhydrocumyl cyclohexylidene group would have decreased the inter-chain interaction of the rigid aromatic polyimides, which resulted in improvement of the solubility. Polyimide derived from BAPCP and 6-FDA was soluble in chloroform, and this can be attributed to both bulky perhydrocumyl cyclohexylidene group and hexafluoroisopropylidene linkage along the polymer backbone.

Table 5.9 Solubility data of polyimides derived from 1,1-bis(4-aminophenyl)-4-perhydrocumyl cyclohexane and commercial dianhydrides.

Polymer	TCE	<i>m</i> -Cresol	ODCB	NMP	DMF	DMAC	CHCl ₃
P-1	++	+-	++	++	+-	+-	--
P-2	++	++	++	++	+-	+-	--
P-3	++	++	++	++	+-	+-	--
P-4	++	++	++	++	+-	+-	--
P-5	++	++	++	++	+-	+-	++

++ soluble at room temperature, +- swelling, -- insoluble

5.4.3.3 X-Ray diffraction studies

X-Ray diffraction patterns of polyimides are shown in **Figure 5.14**. All the polyimides were amorphous in nature. The presence of bulky perhydrocumyl cyclohexylidene group might hinder the packing of the polyimide chains. The amorphous nature of the polyimides was also reflected in their improved solubilities.

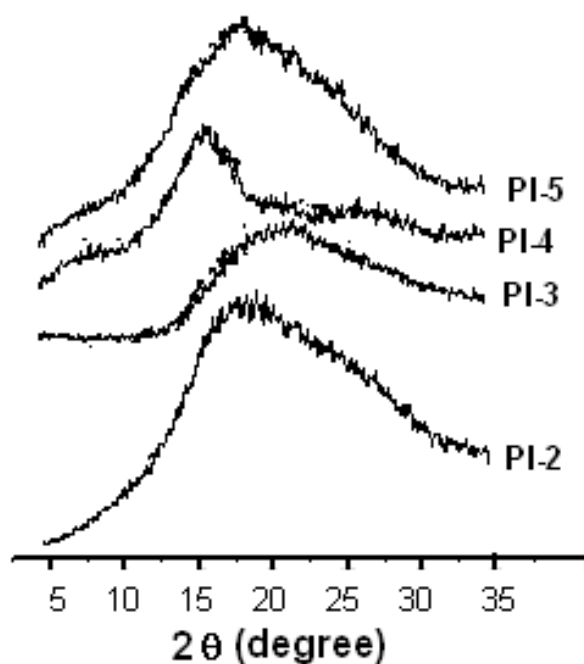


Figure 5.14 X-ray diffraction patterns of polyimides derived from 1,1-bis(4-aminophenyl)-4-perhydrocumyl cyclohexane and commercial dianhydrides

5.4.3.4 Thermal properties

In the present study, thermal stability of polyimides was determined by thermogravimetric analysis (TGA) at a heating rate of 10°C /minute under nitrogen. TG curves for polyimides are shown in **Figure 5.15**. The initial decomposition temperature (IDT) and the decomposition temperature at 10% weight loss (T_{10}) for polyimides are presented in **Table 5.10**. IDT for polyimides was in the range of 475-495°C. T_{10} values of polyimides were in the range 480-511 °C indicating the high thermal stability. Despite the presence of alicyclic group along the polymer backbone, these polyimides showed high thermal stability with the advantage of being soluble in common organic solvents.

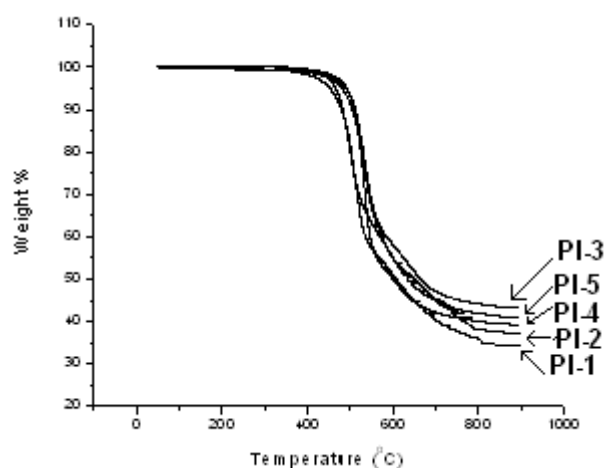


Figure 5.15 TG curves of polyimide derived from 1,1-bis(4-aminophenyl)-4-perhydrocumyl cyclohexane and commercial dianhydrides.

Table 5.10 Thermal properties of polyimides derived from 1,1-bis(4-aminophenyl)-4-perhydrocumyl cyclohexane and commercial dianhydrides

Polyimide	IDT, °C	T ₁₀ , °C	T _g , °C
PI-1	475	480	N.D.
PI-2	478	482	294
PI-3	495	511	310
PI-4	484	505	288
PI-5	495	509	292

N.D.- not detected

DSC curves for the polyimides are reproduced in **Figure 5.16**. The T_g values of polyimides were in the range 288-310°C. Polyimide PI-1 derived from BAPCP and PMDA did not show the glass transition temperature. The T_gs decrease in the following order. BPDA > BTDA > FDA > ODPA. The highest value of T_g of 310°C is obtained for polyimide derived from BPDA in the series, which could be attributed to the more rigid nature of BPDA. Polyimide derived from BAPCP and ODPA exhibited the lowest glass transition temperature of 288 °C in the series of polyimides, which could be attributed to the presence of flexible ether linkage along the polymer backbone.

The comparison of the literature values for T_g of polyimides containing unsubstituted cyclohexane moiety, derived from 1,1-bis(4-aminophenyl)cyclohexane (BACH) indicates

that the glass transition temperature is almost in the same range. The values of glass transition temperature for polyimides derived from BACH with BTDA, ODPDA and 6-FDA are 305, 290 and 293°C, respectively.¹⁴

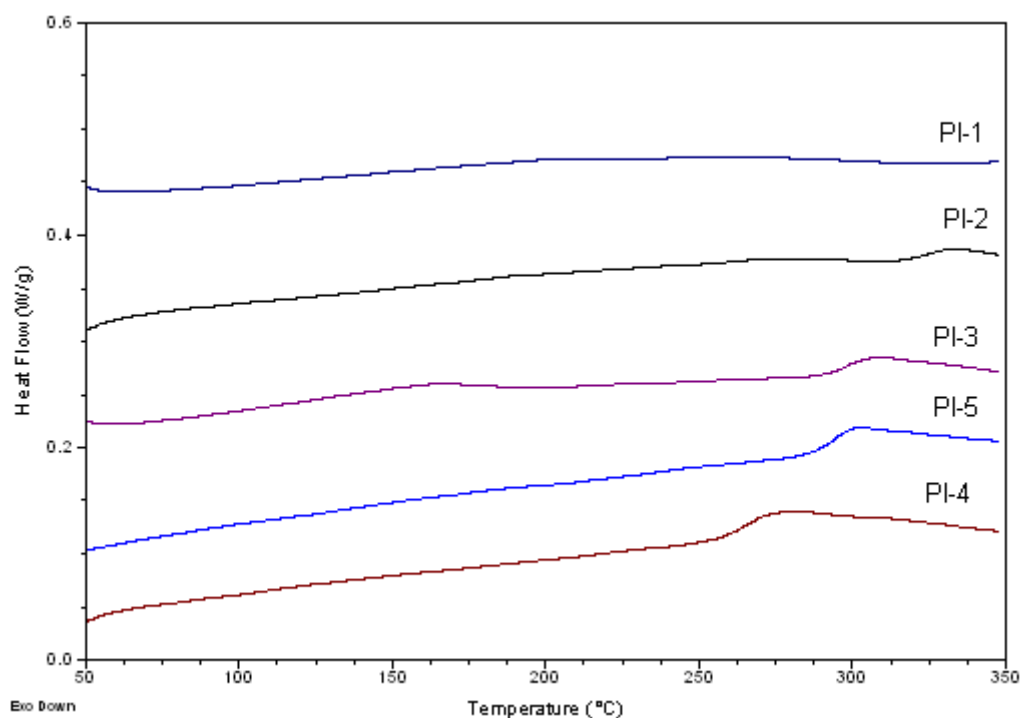


Figure 5.16 DSC curves of polyimides derived from 1,1-bis(4-aminophenyl)-4-perhydrocumyl cyclohexane and commercial dianhydrides

5.4.3.5 Optical properties

In the present study the optical transparencies of selected polyimide films having thickness of ~15 μm were determined by transmission UV-visible spectroscopy. **Figure 5.17** shows UV-visible spectra of BAPCP derived polyimides.

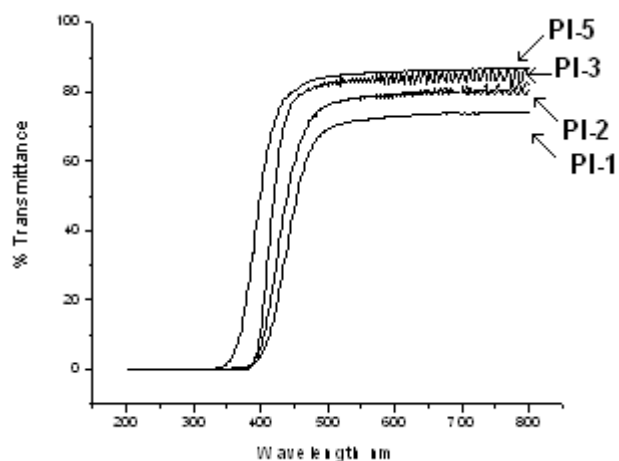
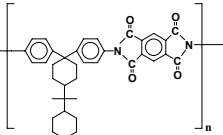
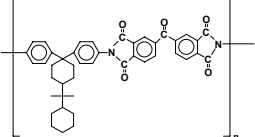
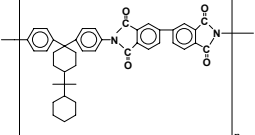
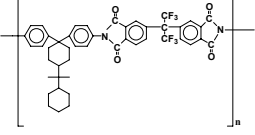


Figure 5.17 UV-vis absorption spectra of polyimide films derived from 1,1-bis(4-aminophenyl)-4-perhydrocumyl cyclohexane and commercial dianhydrides

The cut off wavelength (absorption edge, λ_0), and % transmittance at 500 nm (the solar maximum) are given in **Table 5.11**. Polyimide derived from BAPCP and 6-FDA showed the maximum transparency (84%) and this can be attributed to the bulky perhydrocumyl cyclohexylidene and hexafluoroisopropylidene group along the polymer backbone which might decrease the intermolecular interactions and minimize the formation of charge transfer complexes. All these polyimides exhibited the cut off wavelength (λ_0) between 334-381 nm, which were better than the commercially available polyimide Kapton with onset wavelength at 414 nm.

Table 5.11 Optical properties of polyimides derived from 1,1-bis(4-aminophenyl)-4-perhydrocumyl cyclohexane and commercial dianhydrides

Polyimide	λ_o nm	% Transmittance at 500 nm
 <p>PI-1</p>	364	69
 <p>PI-2</p>	378	76
 <p>PI-3</p>	381	83
 <p>PI-5</p>	334	84

5.4.4 Pretilt angle and electro-optical characteristics of polyimides derived from 1,1-bis(4-aminophenyl) -4-perhydrocumyl cyclohexane and commercial dianhydrides

The liquid crystal cells were prepared as described in **section 4.2.3** and the measurements were done by crystal rotation method.³⁵ The pretilt angle was then calculated from the obtained incident angle.

Uniform alignment of liquid crystals was observed. This opens the route for these polyimides to be used as an alignment layer for liquid crystal displays. The pretilt angles obtained were in the range 0.20-2.43, which is adequate for display applications. Low LC pretilt angle is particularly attractive for In-Plane-Switching or twisted-nematic LCD modes. Organo-soluble polyimides are desirable as their processing temperature is low – a feature particularly important for low temperature poly-silicon-thin-film transistor-liquid crystal display (TFT-LCD) processes.^{36,37}

Figure 5.18 (a) shows a typical transmittance voltage curve for normal incidence of the twisted nematic cell. A typical switching curve is observed with a switching voltage of nearly 3 V. Response and relaxation time of the twisted nematic cell is shown in **Figure 5.18 (b)**, a switching time of about 50-60 ms was observed at 5 V. In the OFF state, black flow effect is visible in the graph because of the 18 μm thick cell.

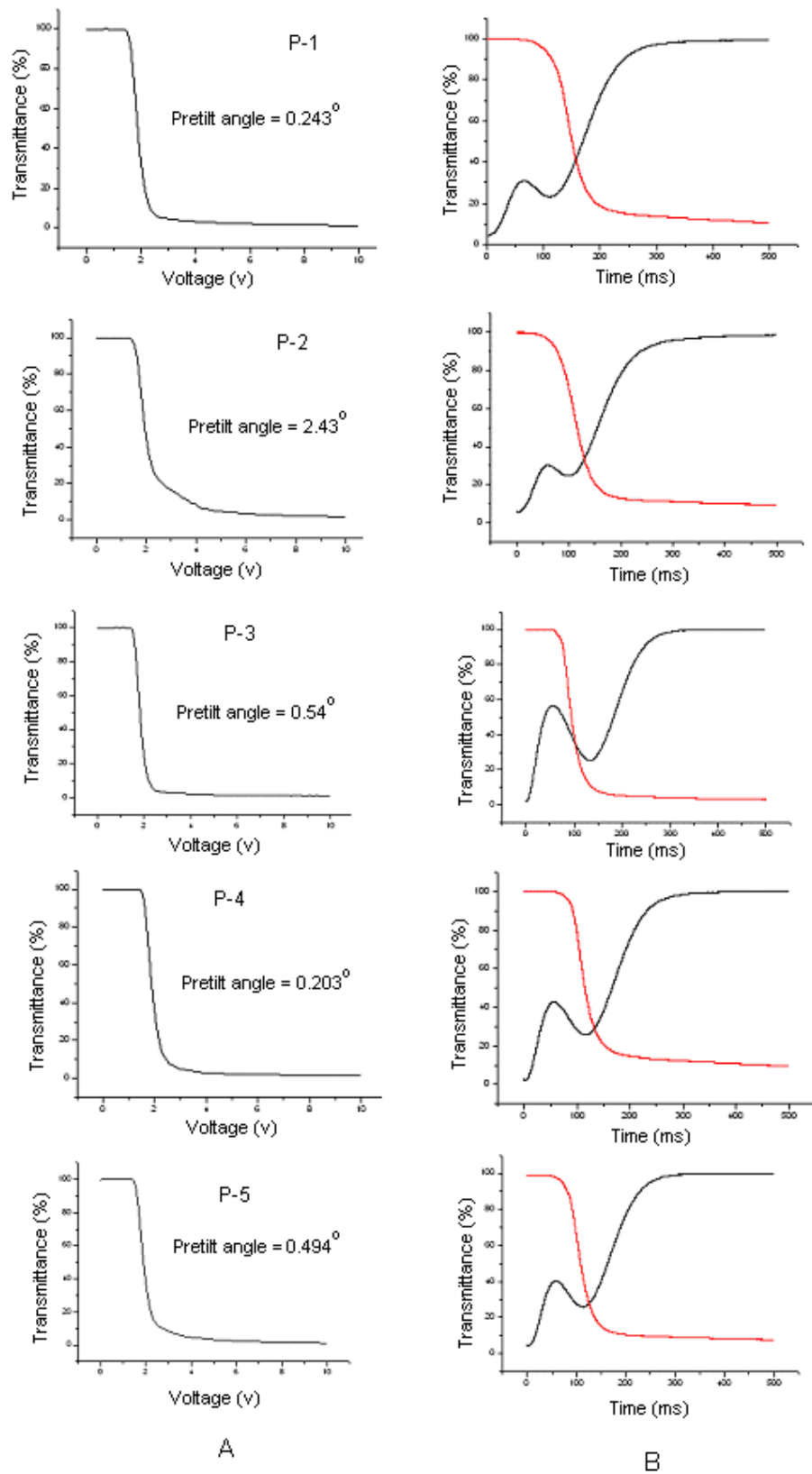


Figure 5.18 (a) Electro-optical characteristics of polyimide orientation layer (b) Response and relaxation times for polyimide orientation layer from the non-select to select state (5V) at a frequency of 1000 Hz

room temperature and BPDA was added in small portions. Reaction mixture was heated to 80°C and stirred for 1 h. The temperature was raised to 200°C and reaction mixture was stirred for 6 h. The reaction was performed under the gentle flow of nitrogen and water formed during imidization was removed with the stream of nitrogen. At the end of 6 h, the reaction mixture was cooled to room temperature and was precipitated in excess methanol. The fibrous polymer obtained was dried in vacuum.

All the polymerizations proceeded in homogeneous manner. The results of polymerizations are summarized in **Table 5.12**.

Table 5.12 Synthesis of polyetherimides from 1,1-bis[4-(4-aminophenoxy)phenyl]-4-per-hydrocumyl cyclohexane and commercial dianhydrides

Polyetherimide	Dianhydride	Yield %	η_{inh} dL/g	Molecular Weight ^b		PDI ^b Mw/Mn
				Mn	Mw	
PEI-1	BPDA	96	0.94	59460	140760	2.4
PEI-2	ODPA	96	0.66	49670	107090	2.2
PEI-3	FDA	94	0.66	57100	122530	2.1

a: η_{inh} was measured with 0.5% (w/v) solution of polyetherimide in chloroform at 30 ± 0.1°C
b: measured by GPC in chloroform, polystyrene was used as the calibration standard

Inherent viscosity values of the polyetherimides were in the range 0.66-0.94 dL/g. All the polyimides synthesized were soluble in chloroform and were used for GPC analysis. The results of GPC measurements on polyetherimides are presented in **Table 5.12**. Number average molecular weights (Mn) were in the range 49670 - 59460 with polydispersity index in the range 2.1-2.4. Inherent viscosity and GPC data indicate the formation of reasonably high molecular weight polymers. However, the molecular weight values provided by GPC should not be taken as absolute as the calibration of GPC was carried out using polystyrene standards.

Tough, transparent, and flexible films of polyetherimides could be cast from their chloroform solutions.

5.4.5.1 Structural characterization

The formation of polyetherimides was confirmed by FTIR, and $^1\text{H-NMR}$ spectroscopy. A representative FTIR spectrum of polyetherimide derived from BAPPHC with BPDA is reproduced in **Figure 5.19**. Absorption bands at approximately 1775, 1721, 1375 and 739 cm^{-1} due to symmetric C=O, asymmetric C=O and C-N stretching and imide ring deformation, respectively confirmed the formation of imide linkages. These wavelengths corresponded to previously reported imide ring absorptions. In addition to the imide bands, C–O–C absorption band was observed at 1242 cm^{-1} indicating the presence of ether linkage along the polymer backbone.

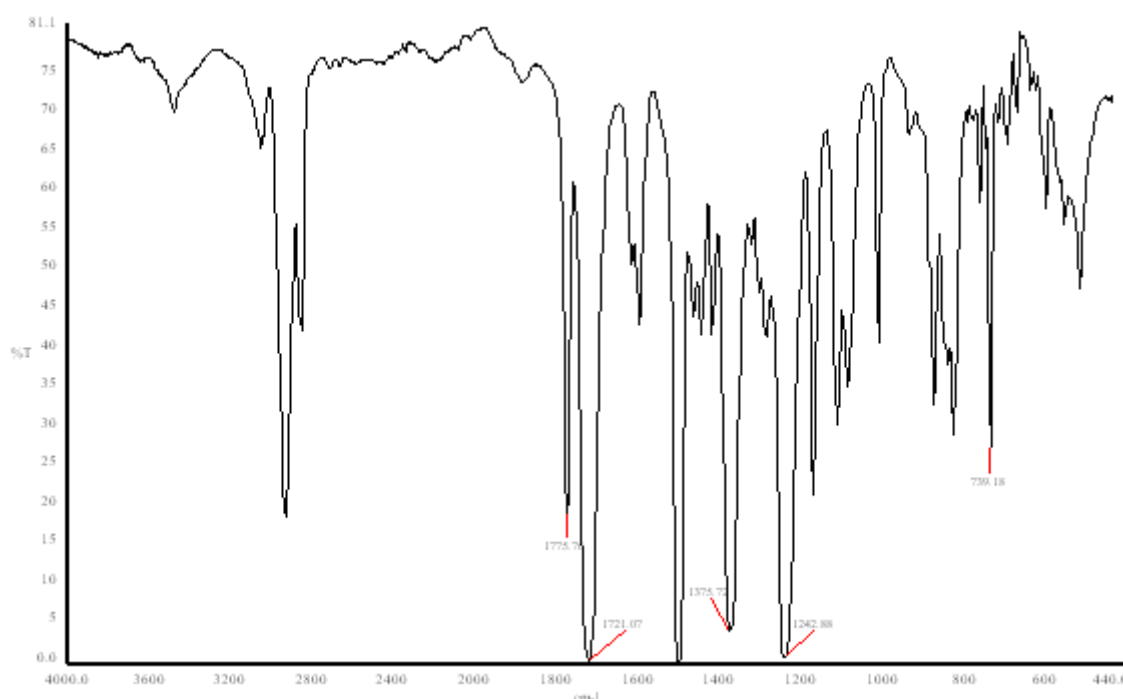


Figure 5.19 FT-IR spectrum of polyetherimide derived from 1,1-bis[4-(4-aminophenoxy)phenyl]-4-per-hydrocumyl cyclohexane and BPDA (PEI-1)

A representative $^1\text{H-NMR}$ spectrum of polyetherimide (PEI-1) along with assignments is reproduced in **Figure 5.20**

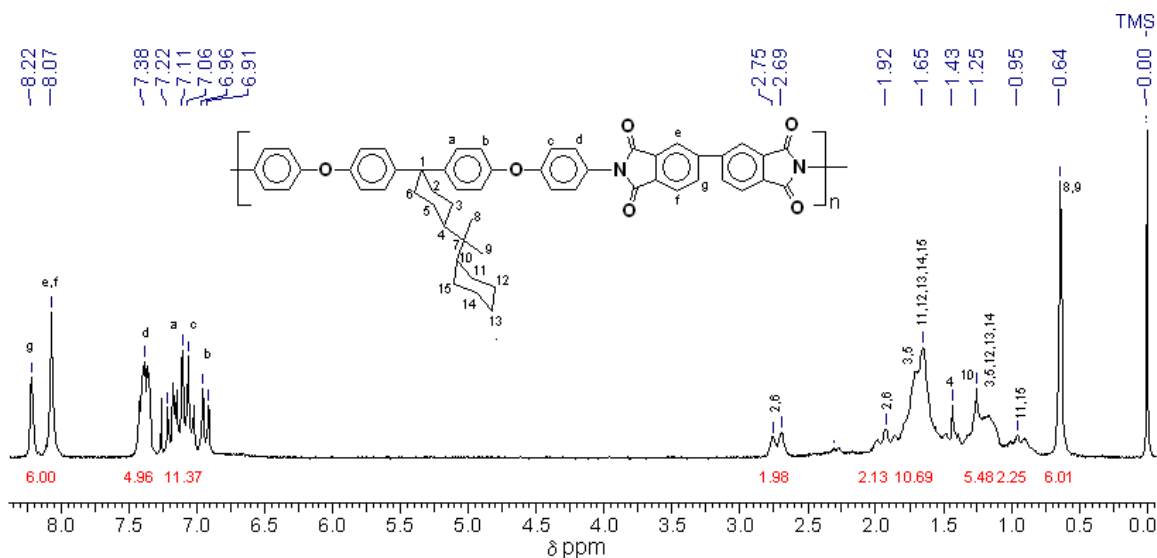


Figure 5.20 $^1\text{H-NMR}$ spectrum of polyetherimide derived from 1,1-bis[4-(4-aminophenoxy)phenyl]-4-per-hydrocumyl cyclohexane and BPDA (PEI-1)

5.4.5.2 Solubility measurements

Solubility of polyetherimides was tested in various organic solvents at 3 wt % concentration and data is summarized in **Table 5.13**. BAPPHC-based polyetherimides were soluble in common organic solvents such as chloroform, TCE, *m*-cresol, NMP and ODCB. That is, introduction of the bulky perhydrocumyl cyclohexylidene group and flexible ether linkage has decreased the inter-chain interaction of the rigid aromatic polyimides, which resulted in improvement of the solubility. All of the polyetherimides were soluble in chloroform, unlike the polyimides without ether linkage (data in **Table 5.9**). This can be attributed to the presence of the flexible ether linkage along the polymer backbone.

Table 5.13 Solubility data for polyetherimides derived from 1,1-bis[4-(4-aminophenoxy)phenyl]-4-per-hydrocumyl cyclohexane and commercial dianhydrides

Polyetherimide	CHCl_3	TCE	ODCB	<i>m</i> -Cresol	NMP	DMF	DMAC
PEI-1	++	++	++	++	++	+-	+-
PEI-2	++	++	++	++	++	+-	+-
PEI-3	++	++	++	++	++	+-	+-

++ soluble, +- swelling

5.4.5.3 X-Ray diffraction studies

X-Ray diffraction patterns of polyetherimides are shown in **Figure 5.21**. All polyetherimides were amorphous in nature. This could be attributed to the presence of perhydrocumyl cyclohexylidene along the polymer backbone, which might hinder packing of the polyimide chain. The amorphous nature of polyimides was also reflected in their improved solubilities.

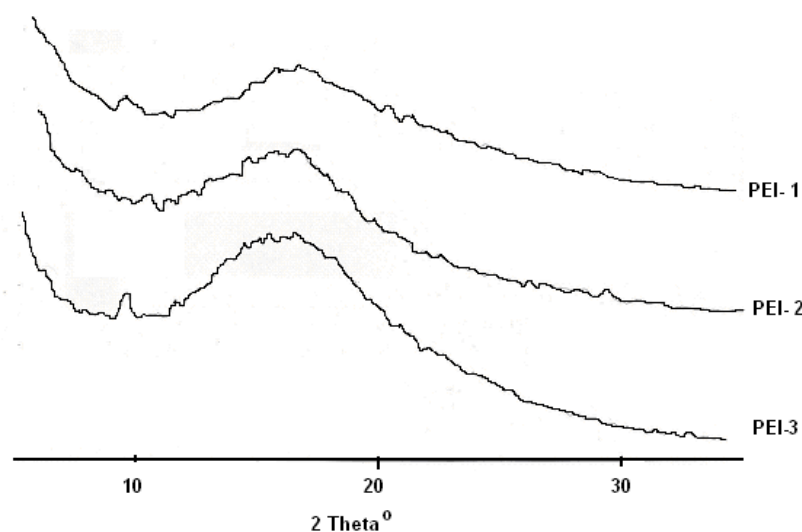


Figure 5.21 Wide angle X-ray diffractograms of polyetherimides synthesized from 1,1-bis[4-(4-aminophenoxy)phenyl]-4-per-hydrocumyl cyclohexane and commercial dianhydrides

5.4.5.4 Thermal properties

In the present study, thermal stability of polyetherimides was determined by thermogravimetric analysis (TGA) at a heating rate of 10°C /minute under nitrogen. **Figure 5.22** shows TG curves for polyetherimides.

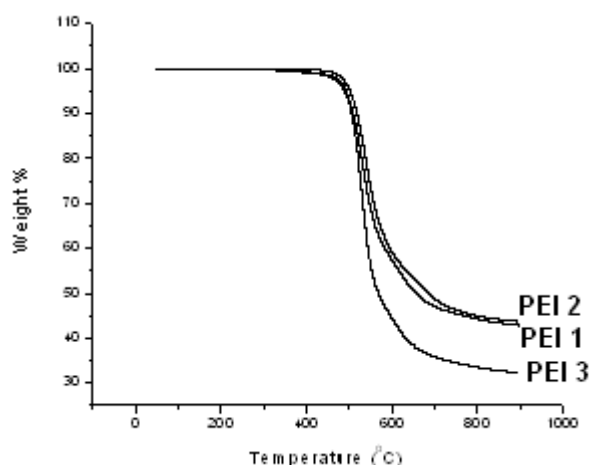


Figure 5.22 TG curves of polyetherimides derived from 1,1-bis[4-(4-aminophenoxy)phenyl]-4-per-hydrocumyl cyclohexane and commercial dianhydrides

The initial decomposition temperature (IDT) and the decomposition temperature at 10% weight loss (T_{10}) for polyetherimides are given in **Table 5.14**. IDT for polyetherimides was in the range 483-489°C. T_{10} values were in the range 505-518 °C, indicating high thermal stability of polyetherimides. The polyetherimide derived from 6-FDA and BAPPHC showed the highest T_{10} in the series. Despite the presence of alicyclic group and ether linkage along the polymer backbone, these polyetherimides showed high thermal stability with the advantage of being soluble.

Table 5.14 Thermal properties of polyetherimides derived from 1,1-bis[4-(4-aminophenoxy)phenyl]-4-per-hydrocumyl cyclohexane and commercial dianhydrides

Polyetherimide	IDT, °C	T_{10} , °C	T_g , °C
PEI-1	483	480	249
PEI-2	489	505	234
PEI-3	495	508	260

DSC curves for polyetherimides are reproduced in **Figure 5.23**. The T_g values of polyimides were in the range 234-260°C. The T_g s decrease in the following order, 6-FDA > BPDA > ODPA.

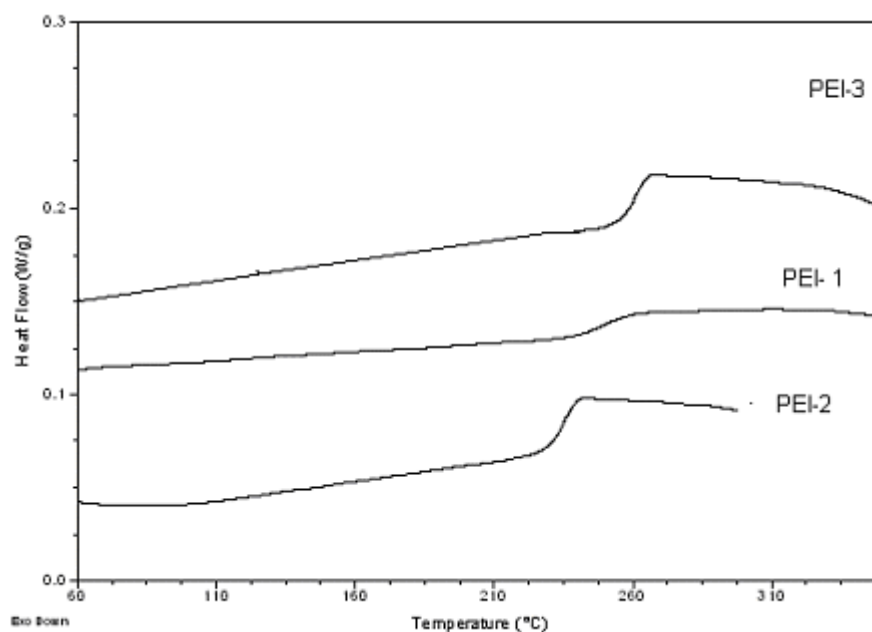


Figure 5.23 DSC curves of polyetherimides derived from 1,1-bis[4-(4-aminophenoxy)phenyl]-4-per-hydrocumyl cyclohexane and commercial dianhydrides

5.4.5.5 Optical properties

In the present study optical transparencies of polyetherimide films of thickness $\sim 10 \mu\text{m}$ were determined by transmission UV-visible spectroscopy. **Figure 5.24** shows UV-visible spectra of the BAPPHC derived polyetherimides.

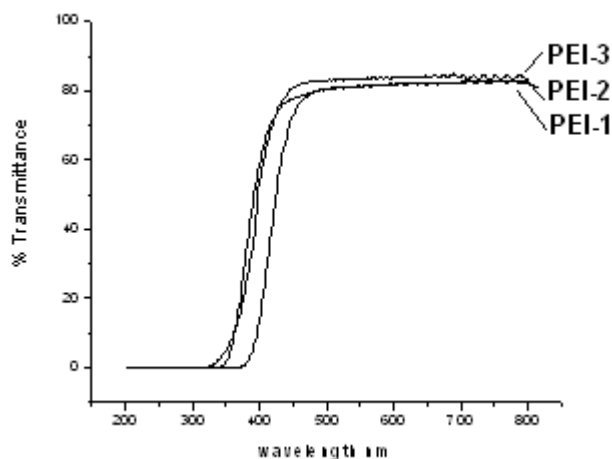
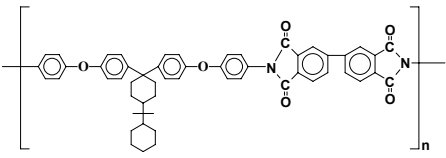
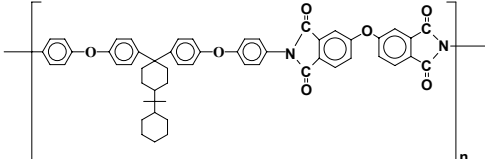
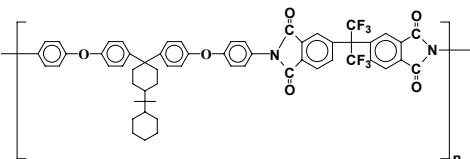


Figure 5.24 UV-visible absorption spectra of polyetherimides derived from 1,1-bis[4-(4-aminophenoxy)phenyl]-4-per-hydrocumyl cyclohexane and commercial dianhydrides

The cut off wavelength (absorption edge, λ_0), and % transmittance at 500 nm (the solar maximum) are given in **Table 5.15**. In the case of all polyetherimides, the transmission of light started below 400 nm. Polyetherimide derived from BAPPHC and 6-FDA showed the maximum transparency (84%) and this could be attributed to the bulky perhydrocumyl cyclohexylidene and hexafluoroisopropylidene group along the polymer backbone which might decrease the intermolecular interactions and thus minimize the formation of charge transfer complexes. All these polyetherimides have cut off wavelength between 321-372 nm, which were better than the commercially available polyimide Kapton with onset wavelength at 414 nm.

Table 5.15 Optical properties of polyetherimides derived from 1,1-bis[4-(4-aminophenoxy)phenyl]-4-per-hydrocumyl cyclohexane and commercial dianhydrides

Polyetherimide	λ_0 nm	% Transmittance at 500 nm
 <p>PEI-1</p>	372	80
 <p>PEI-2</p>	337	80
 <p>PEI-3</p>	321	84

5.5 Conclusions:

1. A series of polyesters with moderate to high molecular weights was synthesized by interfacial polycondensation of bisphenols containing perhydrocumyl cyclohexylidene moiety and terephthalic acid chloride / isophthalic acid chloride.
2. A detailed NMR analysis of polyesters revealed the presence of constitutional isomerism resulting from the different enchainment of the phenyl rings of bisphenol monomer along the polymer chain. The axial and equatorial identity of the phenyl rings of bisphenol monomer was retained in the polymer backbone.
3. All polyesters were readily soluble in chlorinated hydrocarbons such as dichloromethane, chloroform and tetrachloroethane, as well as in *m*-cresol and THF. Perhydrocumyl cyclohexylidene containing polyesters exhibited better solubility than those derived from bisphenol-A or cyclohexylidene bisphenol. Tough, transparent and flexible films of perhydrocumyl cyclohexylidene containing polyesters could be cast from chloroform solutions.
4. The T_{10} for polyesters were in the range 435-485°C indicating the high thermal stability of polyesters.
5. The T_g values were in the range 232-293°C. The glass transition temperature of the polyesters derived from terephthalic acid chloride were higher than their isophthalic acid chloride derived analogues. T_g of polyesters was dependant on the nature of substituent on the bisphenol rings, which followed the following trend. DMBPCP < BPPCP < TMBPPCP < DDBPPCP < TBrBPPCP.
6. The gas permeability studies on the polyesters containing bulky perhydrocumyl group revealed following
 - *meta*-Linked polyesters exhibited lower permeabilites and higher permselectivities than their *para*-linked analogues
 - Dimethyl substitution of each of the bisphenol phenyl rings (TMBPPCP) increases polymer permeability retaining permselectivity of the unsubstituted polymer analogues.
 - Tetrabromo substituted polyesters exhibited highest permselectivities.
7. A series of polyimides was synthesized from BAPCP and commercial dianhydrides by one-step high temperature solution polycondensation in *m*-cresol. Polyimides with moderate molecular weight were obtained.

8. Polyimides were soluble in organic solvents such as, TCE, *m*-cresol, NMP and ODCB. Polyimide derived from BAPCP and 6-FDA was soluble in chloroform. Tough, transparent and flexible films of polyimide could be cast from their TCE solutions.
9. All polyimides exhibited high thermal stabilities and their T_{10} values were in the range 480-511°C.
10. A pretilt angle of 2.43° was observed for polyimide derived from BAPCP and BTDA. This opens the route for this organosoluble polyimide to be used as an alignment layer for liquid crystal displays.
11. Polyetherimides synthesized from BAPPHC and commercial dianhydrides exhibited good solubility in organic solvents, high thermal stabilities (T_{10} values in the range 480-508°C) and high optical transmittance.

References:

1. *Synthetic Methods in Step Growth Polymers*, Rogers, M.E.; Long, T.E.; Eds. John Wiley and Sons : New York , 2003.
2. *Polyimides and Other High Temperature Polymers, Vol. I*, Mittal, H.K., Ed.; VSP BV: The Netherlands, 2001.
3. *Polyimides: Fundamentals and Applications*, Ghosh, M. K.; Mittal, K. L., Eds.; Marcel Dekker: New York, 1996.
4. *Heat Resistant Polymers: Technologically Useful Materials*, Critchley, J. P.; Knight, G. J.; Wright, W. W. Plenum Press: New York, 1983.
5. *Structure-Solubility Relationships in Polymers*, Harris, F.W.; Seymour, R.B., Eds.; Academic Press: New York, 1977.
6. Korshak, V. V.; Vinogradova, S. V.; Vygodskii, Y. S. *J. Macromol. Sci. Rev. Macromol. Chem.* **1974**, C11, 45.
7. Bier, G.; *Polymer* **1974**, 15, 127.
8. Sillion, B. *High Perform. Polym.* **1999**, 11, 417.
9. de Abajo, J.; de la Campa, J. G. *Adv. Polym. Sci.* **1999**, 140, 23.
10. Vinogradova, S.V.; Vasnev, V.A.; Valetskii, P.M. *Russ. Chem. Rev.* **1994**, 63, 833.
11. Morgan, P.W. *Macromolecules* **1970**, 3, 536.
12. Liaw, D.J.; Hsu, C.-Y.; Liaw, B.-Y. *Polymer* **2001**, 42, 7993.
13. Liaw, D.J.; Liaw, B.-Y. *Polym. Prepr.* **2000**, 41, 79.
14. Choi, K. Y.; Yi, M. H. *Macromol. Symp.* **1999**, 142, 193.
15. Liaw, D.J.; Liaw, B.-Y.; Lai, S.-H. *Macromol. Chem. Phys.* **2001**, 202, 807.
16. Yang, C.P.; Chen, J.-A. *Polym. Int.* **2000**, 49, 103.
17. Liaw, D.J.; Liaw, B.Y.; Chung, C.Y. *Macromol. Chem. Phys.* **2000**, 202, 1887.
18. *Purification of Laboratory Chemicals* Perrin, D.D.; Armarego, W.L.F. Pergamon Press: New York, 1989.
19. Yang, C.P.; Oishi, Y.; Kakimoto, M.A.; Imai, Y. *J. Poly. Sci. Polym. Chem.* **1990**, 28, 1353.
20. Mitchell, G.R.; Windle, A.H. *Polymer* **1984**, 25, 906.
21. Windle, A.H. *Pure Appl. Chem.* **1985**, 57, 1627.
22. Pixton, M.R.; Paul, D.R. *J. Polym. Sci. Polym. Phys.* **1995**, 33, 1353.
23. Aguilar-Vega, M.; Paul, D.R., *J. Polym. Sci. Polym. Phys.* **1993**, 31, 1577.

24. Wrasidlo, W. *Macromolecules*, **1971**, *4*, 462.
25. Pixton, M.R.; Paul, D.R. *Macromolecules* **1995**, *28*, 8277.
26. Sheu, F.R.; Chern, R.T. *J. Polym. Sci. Polym. Phys.* **1989**, *27*, 1121.
27. Van Krevelen, D.W.; Hoftyzer, P. J., *Properties of Polymers*, (2nd Ed.), Elsevier Science: Amsterdam, 1972, pp. 378-383.
28. Stern, S.A.; Gareis, P.J.; Sinclair, T.F.; Mohr, P.H. *J. Appl. Polym. Sci.* **1963**, *7*, 2035.
29. Akiten, C.L.; Koros, W.J.; Paul D.R. *Macromolecules*, **1992**, *25*, 3424.
30. McHattite, J.S.; Koros, W.J.; Paul, D.R. *Polymer*, **1991**, *32*,840.
31. Pessan, L.A.; Koros, W.J. *J. Polym. Sci. Polym. Phys.* **1993**, *31*, 1245.
32. Jager, J; Hendriks, A.J.J. *J. Appl. Polym. Sci.* **1995**, *58*, 1465.
33. Stern, S.A.; Mi, H.; Yamamoto, H.; Clair, A.K.St. *J. Polym. Sci. Polym. Phys.* **1989**, *27*, 1887.
34. Omote, T.; Koseki, K.; Yamaoka, T. *Macromolecules*, **1990**, *23*, 4788.
35. Scheffer, T.J.; Nehring, J. *J. Appl. Phys.* **1977**, *48*, 1783.
36. Lee, W.-C.; Chen, J.-T.; Hsu, C-S. *Liquid Crystals* **2002**, *29*, 907.
37. Zhang, W.; Xu, H.-J.; Yin, J.; Guo, X.-X.; Ye, Y.-F.; Fang, J.-H.; Sui, Y.; Zhu, Z.-K.; Wang, Z.-G. *J. Appl. Polym. Sci.* **2001**, *81*, 2814.

Chapter 6. Summary and Conclusions

The main objective of the present research was to design and synthesize processable high performance polymers such as polyimides and polyesters by making use of difunctional monomers containing pendent flexible pentadecyl chain or bulky perhydrocumyl cyclohexylidene group. Another objective was to study the applications of selected (co)polyimides as alignment layers for liquid crystal display devices. Polyesters containing bulky perhydrocumyl cyclohexylidene moiety with a systematic variation of methyl and /or bromo substituent on bisphenol rings were evaluated as membrane materials for gas separations.

Two new difunctional monomers containing pendant pentadecyl chain, namely, 1,1-bis(4-hydroxyphenyl)-3-pentadecylcyclohexane (BPC₁₅) and 1,1-bis(4-aminophenyl)-3-pentadecylcyclohexane (BAC₁₅) were synthesized starting from CNSL, a commercially available, inexpensive and renewable resource material.

Eight new difunctional monomers containing bulky perhydrocumyl substituted cyclohexylidene moiety were synthesized starting from p-cumylphenol, a commercially available raw material.

Thus, total of ten new difunctional monomers were designed and synthesized starting from commercially available raw materials *via* simple reaction steps.

All the new monomers and intermediates involved in their synthesis were characterized by a combination of chemical and spectroscopic techniques, including NMR and single crystal X-ray crystallography. Whenever suitable crystals could be obtained, X-ray crystallography provided unequivocal assignments of chemical structure.

A detailed investigation of spectral and X-ray crystallography data of difunctional monomers containing substituted cyclohexylidene moiety showed the presence of distereotopic phenyl rings, which are magnetically non-equivalent. Both diamine and bisphenol molecules are not symmetrical about a C₂ axis between two phenyl rings. The phenyl rings of both diamine and bisphenol molecules lie in different plane and axial and equatorial phenyl rings could be distinguished. ¹H NMR spectra exhibited two sets of doublets and ¹³C NMR spectra exhibited

four sets of carbon signals in the aromatic region originating from axial and equatorial phenyl rings.

A series of polyesters and polyimides containing pentadecyl substituted cyclohexylidene moiety was synthesized from BPC₁₅ and BAC₁₅, respectively. Polyesters were synthesized by two-phase interfacial polycondensation whereas polyimides were synthesized by one-step high temperature solution polycondensation. Medium to high molecular weight polyesters and polyimides soluble in common organic solvents were obtained. Polyesters derived from BPC₁₅ exhibited constitutional isomerism, which has its origin in the distereotopic nature of BPC₁₅. Glass transition temperatures (T_g) of the polyesters derived from BPC₁₅ and terephthalic acid chloride and isophthalic acid chloride are 94 and 74°C, respectively. The T_g values of polyimides derived from BAC₁₅ were in the range 161-209°C. A comparison of the glass transition values with that of polyesters derived from BPC₁ and polyimides derived from BAC clearly indicated the substantial decrease in the T_g of pentadecyl substituted cyclohexylidene containing polymers. The depression in glass transition temperature of pendant pentadecyl chain containing polyesters and polyimides demonstrated the “plasticizing” ability of pentadecyl chain.

Encouraged by the results of homopolymers, it was of interest to synthesize copolymers with a systematic variation of pentadecyl substituted cyclohexylidene containing monomers and study the effect of comonomer content on the final copolymer properties. High molecular weight copolyesters and copolyimides containing pentadecyl substituted cyclohexylidene moiety were synthesized. The T_g of copolyesters and copolyimides decreased with the increasing content of BPC₁₅ or BAC₁₅, respectively. All of the (co)polyesters and (co)polyimides exhibited high thermal stabilities. A large window between glass transition and polymer degradation temperature was observed. This gives an opportunity for these (co)polymers to be melt-processed or compression molded.

Preliminary experiments for using copolyimides containing pentadecyl substituted cyclohexylidene moiety as alignment layer for liquid crystal display were carried out. Pretilt angles in the range 2.51-2.75° were observed which is adequate for display applications.

A series of new polyesters with a systematic variation of methyl and /or bromo substituent on phenyl rings was synthesized from bisphenols containing bulky perhydrocumyl

cyclohexylidene “cardo” group by two-phase interfacial polycondensation technique. Moderate to high molecular weight polyesters soluble in common organic solvents were obtained. The presence of constitutional isomerism in polyesters containing substituted cyclohexylidene moieties was established by detailed NMR spectral analysis. All the polyesters were amorphous in nature as indicated by their wide angle X-ray diffraction patterns. Polyesters containing perhydrocumyl cyclohexylidene moiety had T_{10} values in the range 435-485°C indicating high thermal stabilities. The glass transition temperature of polyesters derived from isophthalic acid chloride were lower than their terephthalic acid chloride derived analogues, which is due to their more conformational freedom of the main chains than that in case of *para*-linked polymers. Symmetric and asymmetric substitution of bisphenol rings had a effect on Tg values of polyesters. The Tg values of polyesters followed the following trend. DMBPCP<BPPCP<TMBPPCP<DDBPPCP<TBrBPPCP.

The utility of perhydrocumyl cyclohexylidene containing polyesters as membrane materials for gas separation was demonstrated. Polyesters derived from isophthalic acid chloride exhibited lower permeabilities and higher permselectivities than their terephthalic acid chloride derived analogues. The systematic variation of methyl and bromo substituent on phenyl rings revealed that the incorporation of polar groups within polymer structures which inhibit free volume collapse help in increasing gas permeability and permselectivity.

A series of polyimides was synthesized from perhydrocumyl cyclohexylidene containing diamine and commercial dianhydrides by one-step high temperature solution polycondensation in *m*-cresol. Organo-soluble polyimides with inherent viscosity values in the range 0.35-0.66 dL/g were obtained. All the polyimides were amorphous in nature as indicated by their wide angle X-ray diffraction patterns. Polyimides exhibited high thermal stabilities and their T_{10} values were in the range 480-511°C. Optical transmittance of polyimides containing perhydrocumyl substituted cyclohexylidene moiety indicated the good optical transparency. The maximum transparency of 84% was observed for polyimide derived from BAPCP and 6-FDA at 500 nm.

Application of organo-soluble polyimides containing perhydrocumyl cyclohexylidene moiety as alignment layer for liquid crystal display was evaluated in brief. A pretilt angle of 2.43°

was observed for polyimide synthesized from BAPCP and BTDA, which is adequate for display applications.

A series polyetherimides was synthesized from BAPPHC and commercial dianhydrides by one-step high temperature solution polycondensation in *m*-cresol. Polyetherimides exhibited good solubility in common organic solvents, high thermal stabilities (T_{10} values in the range 480-508°C) and high optical transmittance.

Overall, the polymer processability / solubility was improved by the incorporation of pendant pentadecyl chain *via* internal “plasticization”. The incorporation of bulky perhydrocumyl substituted cyclohexylidene “cardo” group resulted into polyimides and polyesters with improved solubility in common organic solvents and higher thermal properties.

Perspectives

High performance / high temperature polymers such as polyimides and polyesters are of great interest in view of their excellent versatility in various applications. In this context an understanding of the structure-property relationship in high performance polymers is of significant contemporary interest. There is a continuing need to examine approaches to address the issues related to their limited solubility in common organic solvents and poor processability.

The present work on synthesis of new difunctional monomers starting from CNSL and *p*-cumylphenol has expanded the range of condensation monomers available for preparation of a host of high performance polymers, viz. polyethersulfones, polyetherketones, polyamides, polyazomethines, polyhydrazides, polyoxadiazoles, polybenzoxazoles, etc.

There are several interesting experiments that could be a continuation of this project.

Diamines synthesized in the present work could easily be converted into diisocyanates which by themselves represent valuable monomers for synthesis of polyurethanes, polyureas, etc.

It is well known that the molecular motions in polymer bulk play an important role in governing the transport properties of the polymers. A detailed DMA study would provide an additional insight into the factors governing molecular motions and transport properties of polyesters and their interrelationship.

Polyimides, as a class represent good dielectric materials. Efforts are being made to develop polyimides with lower dielectric constants than conventional polyimides. Polyimides synthesized in the present work are expected to possess lower dielectric constant by virtue of the presence of aliphatic moieties in their backbone. Studies in these directions would be worthwhile.

Appendix 1

a) Bond distances of 1,1-bis(4-hydroxyphenyl)-3-pentadecylcyclohexane in angstroms

Atom1	Atom2	Distance	Atom1	Atom2	Distance
O (1)	C(10)	1.385(3)	C(7)	C(12)	1.399(3)
O(2)	C(16)	1.385(3)	C(8)	C(9)	1.392(3)
C(1)	C(13)	1.532(3)	C(9)	C(10)	1.377(3)
C(1)	C(7)	1.541(3)	C(10)	C(11)	1.360(3)
C(1)	C(6)	1.547(3)	C(11)	C(12)	1.373(3)
C(1)	C(2)	1.555(3)	C(13)	C(14)	1.379(3)
C(2)	C(3)	1.535(3)	C(13)	C(18)	1.388(3)
C(3)	C(4)	1.523(3)	C(14)	C(15)	1.382(3)
C(3)	C(19)	1.524(3)	C(15)	C(16)	1.376(3)
C(4)	C(5)	1.529(3)	C(16)	C(17)	1.362(3)
C(5)	C(6)	1.530(3)	C(17)	C(18)	1.400(3)
C(7)	C(8)	1.386(3)	C(19)	C(20)	1.522(3)

b) Bond angles of 1,1-bis(4-hydroxyphenyl)-3-pentadecylcyclohexane in degrees

Atom 1	2	3	Angle	Atom 1	2	3	Angle
C(13)	C(1)	C(7)	110.8(2)	C(11)	C(10)	C(9)	120.1(2)
C(13)	C(1)	C(6)	112.28(19)	C(11)	C(10)	O(1)	117.8(2)
C(7)	C(1)	C(6)	109.67(19)	C(9)	C(10)	O(1)	122.1(2)
C(13)	C(1)	C(2)	109.09(19)	C(10)	C(11)	C(12)	120.4(2)
C(7)	C(1)	C(2)	108.51(18)	C(11)	C(12)	C(7)	122.1(2)
C(6)	C(1)	C(2)	106.3(2)	C(14)	C(13)	C(18)	116.0(2)
C(3)	C(2)	C(1)	113.37(18)	C(14)	C(13)	C(1)	120.8(2)
C(4)	C(3)	C(19)	112.2(2)	C(18)	C(13)	C(1)	123.1(2)
C(4)	C(3)	C(2)	108.8(2)	C(13)	C(14)	C(15)	122.7(2)
C(19)	C(3)	C(2)	112.44(18)	C(16)	C(15)	C(14)	119.9(2)
C(3)	C(4)	C(5)	112.0(2)	C(17)	C(16)	C(15)	119.5(3)
C(4)	C(5)	C(6)	111.7(2)	C(17)	C(16)	O(2)	123.1(3)
C(5)	C(6)	C(1)	114.2(2)	C(15)	C(16)	O(2)	117.4(3)
C(8)	C(7)	C(12)	115.9(2)	C(16)	C(17)	C(18)	119.8(2)
C(8)	C(7)	C(1)	123.2(2)	C(13)	C(18)	C(17)	122.0(2)
C(12)	C(7)	C(1)	120.9(2)	C(20)	C(19)	C(3)	114.5(2)
C(7)	C(8)	C(9)	122.4(2)	C(21)	C(20)	C(19)	116.4(2)
C(10)	C(9)	C(8)	119.1(2)				

Appendix 2

a) Bond distances of 1,1-bis(4-hydroxyphenyl) -4-perhydrocumyl cyclohexane in angstroms

Atom1	Atom2	Distance	Atom1	Atom2	Distance
O(3)	C(29)	1.448(4)	C(10)	C(11)	1.367(4)
C(28)	C(29)	1.469(6)	C(11)	C(12)	1.377(3)
O(1)	C(10)	1.376(3)	C(13)	C(18)	1.380(3)
O(2)	C(16)	1.370(3)	C(13)	C(14)	1.382(3)
C(1)	C(7)	1.534(3)	C(14)	C(15)	1.381(3)
C(1)	C(13)	1.535(3)	C(15)	C(16)	1.371(3)
C(1)	C(6)	1.541(3)	C(16)	C(17)	1.371(3)
C(1)	C(2)	1.545(3)	C(17)	C(18)	1.376(3)
C(2)	C(3)	1.520(3)	C(19)	C(21)	1.535(3)
C(3)	C(4)	1.526(3)	C(19)	C(20)	1.538(3)
C(4)	C(5)	1.529(3)	C(19)	C(22)	1.556(3)
C(4)	C(19)	1.557(3)	C(22)	C(27)	1.511(4)
C(5)	C(6)	1.515(3)	C(22)	C(23)	1.519(3)
C(7)	C(8)	1.380(3)	C(23)	C(24)	1.507(4)
C(7)	C(12)	1.388(3)	C(24)	C(25)	1.502(4)
C(8)	C(9)	1.379(3)	C(25)	C(26)	1.498(4)
C(9)	C(10)	1.370(3)	C(26)	C(27)	1.520(4)

b) Bond angles of 1,1-bis(4-hydroxyphenyl) -4-perhydrocumyl cyclohexane in degrees

Atom 1	2	3	Angle	Atom 1	2	3	Angle
O(3)	C(29)	C(28)	109.9(4)	C(18)	C(13)	C(1)	123.88(19)
C(7)	C(1)	C(13)	108.04(17)	C(14)	C(13)	C(1)	120.47(19)
C(7)	C(1)	C(6)	111.02(18)	C(15)	C(14)	C(13)	123.1(2)
C(13)	C(1)	C(6)	111.24(17)	C(16)	C(15)	C(14)	119.6(2)
C(7)	C(1)	C(2)	108.31(17)	O(2)	C(16)	C(15)	123.0(2)
C(13)	C(1)	C(2)	112.85(18)	O(2)	C(16)	C(17)	118.1(2)
C(6)	C(1)	C(2)	105.37(17)	C(15)	C(16)	C(17)	118.9(2)
C(3)	C(2)	C(1)	115.51(18)	C(16)	C(17)	C(18)	120.5(2)
C(2)	C(3)	C(4)	112.22(19)	C(17)	C(18)	C(13)	122.4(2)
C(3)	C(4)	C(5)	106.92(17)	C(21)	C(19)	C(20)	107.7(2)
C(3)	C(4)	C(19)	114.98(18)	C(21)	C(19)	C(22)	110.18(19)
C(5)	C(4)	C(19)	114.73(17)	C(20)	C(19)	C(22)	109.11(19)
C(6)	C(5)	C(4)	112.38(18)	C(21)	C(19)	C(4)	109.33(18)
C(5)	C(6)	C(1)	114.08(18)	C(20)	C(19)	C(4)	109.76(19)
C(8)	C(7)	C(12)	115.7(2)	C(22)	C(19)	C(4)	110.67(18)
C(8)	C(7)	C(1)	123.00(19)	C(27)	C(22)	C(23)	107.7(2)
C(12)	C(7)	C(1)	121.2(2)	C(27)	C(22)	C(19)	115.1(2)
C(9)	C(8)	C(7)	122.2(2)	C(23)	C(22)	C(19)	113.7(2)
C(10)	C(9)	C(8)	120.3(2)	C(24)	C(23)	C(22)	113.2(3)
C(10)	C(9)	H(9)	119.9	C(25)	C(24)	C(23)	110.8(3)
C(11)	C(10)	C(9)	119.2(2)	C(26)	C(25)	C(24)	110.2(3)
C(11)	C(10)	O(1)	118.4(2)	C(25)	C(26)	C(27)	112.3(3)
C(9)	C(10)	O(1)	122.5(2)	C(22)	C(27)	C(26)	112.7(3)
C(10)	C(11)	C(12)	119.9(2)	C(14)	C(13)	C(1)	120.47(19)
C(18)	C(13)	C(14)	115.5(2)				
C(11)	C(12)	C(7)	122.6(2)				

Appendix 3

a) Bond distances of 1,1-bis(4-hydroxy-3,5-dimethylphenyl) -4-perhydrocumyl cyclohexane in angstroms

Atom1	Atom2	Distance	Atom1	Atom2	Distance
O(1)	C(10)	1.3892(18)	C(11)	C(29)	1.503(3)
O(2)	C(16)	1.3933(18)	C(13)	C(18)	1.388(3)
C(1)	C(7)	1.546(2)	C(13)	C(14)	1.387(2)
C(1)	C(2)	1.544(2)	C(14)	C(15)	1.393(2)
C(1)	C(6)	1.545(2)	C(15)	C(16)	1.390(3)
C(1)	C(13)	1.549(2)	C(15)	C(30)	1.502(3)
C(2)	C(3)	1.534(2)	C(16)	C(17)	1.393(3)
C(3)	C(4)	1.536(2)	C(17)	C(18)	1.397(2)
C(4)	C(5)	1.538(3)	C(17)	C(31)	1.506(3)
C(4)	C(19)	1.570(2)	C(19)	C(20)	1.543(3)
C(5)	C(6)	1.525(2)	C(19)	C(21)	1.552(3)
C(7)	C(12)	1.383(3)	C(19)	C(22)	1.555(3)
C(7)	C(8)	1.397(2)	C(22)	C(27)	1.527(2)
C(8)	C(9)	1.394(2)	C(22)	C(23)	1.540(2)
C(9)	C(10)	1.386(3)	C(23)	C(24)	1.504(3)
C(9)	C(28)	1.511(2)	C(24)	C(25)	1.506(3)
C(10)	C(11)	1.385(2)	C(25)	C(26)	1.519(3)
C(11)	C(12)	1.405(2)	C(26)	C(27)	1.511(3)

b) Bond angles of 1,1-bis(4-hydroxy-3,5-dimethylphenyl) -4-perhydrocumyl cyclohexane in degrees

Atom 1	2	3	Angle	Atom 1	2	3	Angle
C(7)	C(1)	C(2)	109.50(12)	C(18)	C(13)	C(14)	116.85(15)
C(7)	C(1)	C(6)	112.00(15)	C(18)	C(13)	C(1)	122.67(14)
C(2)	C(1)	C(6)	104.67(12)	C(14)	C(13)	C(1)	120.37(16)
C(7)	C(1)	C(13)	108.28(11)	C(13)	C(14)	C(15)	123.00(18)
C(2)	C(1)	C(13)	111.52(15)	C(16)	C(15)	C(14)	117.88(16)
C(6)	C(1)	C(13)	110.88(12)	C(15)	C(16)	O(2)	117.40(16)
C(3)	C(2)	C(1)	113.50(12)	C(15)	C(16)	C(17)	121.63(15)
C(2)	C(3)	C(4)	113.86(15)	O(2)	C(16)	C(17)	120.84(17)
C(3)	C(4)	C(5)	110.59(12)	C(16)	C(17)	C(18)	117.75(17)
C(3)	C(4)	C(19)	112.87(15)	C(13)	C(18)	C(17)	122.87(16)
C(5)	C(4)	C(19)	113.14(12)	C(20)	C(19)	C(21)	108.46(17)
C(6)	C(5)	C(4)	113.63(13)	C(20)	C(19)	C(22)	110.48(15)
C(5)	C(6)	C(1)	112.39(15)	C(21)	C(19)	C(22)	108.70(18)
C(12)	C(7)	C(8)	116.46(14)	C(20)	C(19)	C(4)	108.28(17)
C(12)	C(7)	C(1)	123.43(14)	C(21)	C(19)	C(4)	109.80(13)
C(8)	C(7)	C(1)	120.10(15)	C(22)	C(19)	C(4)	111.08(12)
C(9)	C(8)	C(7)	122.75(16)	C(27)	C(22)	C(23)	108.17(14)
C(10)	C(9)	C(8)	118.11(15)	C(27)	C(22)	C(19)	115.04(17)
C(10)	C(9)	C(28)	121.25(15)	C(23)	C(22)	C(19)	114.72(13)
C(8)	C(9)	C(28)	120.59(16)	C(24)	C(23)	C(22)	112.68(15)
C(9)	C(10)	C(11)	121.94(14)	C(23)	C(24)	C(25)	112.3(2)
C(9)	C(10)	O(1)	120.73(14)	C(24)	C(25)	C(26)	110.22(17)
C(11)	C(10)	O(1)	117.31(16)	C(27)	C(26)	C(25)	112.08(18)
C(10)	C(11)	C(12)	117.51(16)	C(26)	C(27)	C(22)	113.2(2)
C(7)	C(12)	C(11)	123.22(15)				

Appendix 4

a) Bond distances of 1,1-bis(4-aminophenyl)-4-perhydrocumyl cyclohexane in angstroms

Atom1	Atom2	Distance	Atom1	Atom2	Distance
N(1)	C(10)	1.396(2)	C(11)	C(12)	1.377(2)
N(2)	C(16)	1.391(2)	C(13)	C(18)	1.378(2)
C(1)	C(7)	1.536(2)	C(13)	C(14)	1.391(2)
C(1)	C(13)	1.537(2)	C(14)	C(15)	1.369(2)
C(1)	C(2)	1.543(2)	C(15)	C(16)	1.388(3)
C(1)	C(6)	1.544(2)	C(16)	C(17)	1.374(2)
C(2)	C(3)	1.519(2)	C(17)	C(18)	1.384(2)
C(3)	C(4)	1.526(2)	C(19)	C(20)	1.530(2)
C(4)	C(5)	1.528(2)	C(19)	C(21)	1.539(2)
C(4)	C(19)	1.556(2)	C(19)	C(22)	1.563(2)
C(5)	C(6)	1.523(2)	C(22)	C(27)	1.518(2)
C(7)	C(8)	1.380(2)	C(22)	C(23)	1.540(2)
C(7)	C(12)	1.385(2)	C(23)	C(24)	1.508(3)
C(8)	C(9)	1.383(2)	C(24)	C(25)	1.501(3)
C(9)	C(10)	1.373(2)	C(25)	C(26)	1.497(3)
C(10)	C(11)	1.382(3)	C(26)	C(27)	1.517(3)

b) Bond angles of 1,1-bis(4-aminophenyl)-4-perhydrocumyl cyclohexane in degrees

Atom 1	2	3	Angle	Atom 1	2	3	Angle
C(7)	C(1)	C(13)	107.81(11)	C(18)	C(13)	C(1)	124.78(13)
C(7)	C(1)	C(2)	107.05(11)	C(14)	C(13)	C(1)	119.43(14)
C(13)	C(1)	C(2)	112.89(12)	C(15)	C(14)	C(13)	122.70(16)
C(7)	C(1)	C(6)	111.72(12)	C(14)	C(15)	C(16)	120.92(15)
C(13)	C(1)	C(6)	110.87(12)	C(17)	C(16)	C(15)	117.08(15)
C(2)	C(1)	C(6)	106.49(11)	C(17)	C(16)	N(2)	121.70(18)
C(3)	C(2)	C(1)	115.53(12)	C(15)	C(16)	N(2)	121.22(16)
C(2)	C(3)	C(4)	111.89(13)	C(16)	C(17)	C(18)	121.52(16)
C(3)	C(4)	C(5)	106.86(11)	C(13)	C(18)	C(17)	122.05(16)
C(3)	C(4)	C(19)	114.43(12)	C(20)	C(19)	C(21)	108.60(15)
C(5)	C(4)	C(19)	115.81(12)	C(20)	C(19)	C(4)	110.09(13)
C(6)	C(5)	C(4)	111.37(12)	C(21)	C(19)	C(4)	108.27(13)
C(5)	C(6)	C(1)	114.36(12)	C(20)	C(19)	C(22)	109.01(14)
C(8)	C(7)	C(12)	115.85(15)	C(21)	C(19)	C(22)	109.57(12)
C(8)	C(7)	C(1)	124.55(14)	C(4)	C(19)	C(22)	111.26(12)
C(12)	C(7)	C(1)	119.54(14)	C(27)	C(22)	C(23)	109.73(13)
C(7)	C(8)	C(9)	122.34(15)	C(27)	C(22)	C(19)	114.12(12)
C(10)	C(9)	C(8)	120.96(16)	C(23)	C(22)	C(19)	113.12(14)
C(9)	C(10)	C(11)	117.50(16)	C(24)	C(23)	C(22)	114.38(16)
C(9)	C(10)	N(1)	121.37(18)	C(25)	C(24)	C(23)	111.88(15)
C(11)	C(10)	N(1)	121.08(17)	C(26)	C(25)	C(24)	109.85(15)
C(12)	C(11)	C(10)	120.98(16)	C(25)	C(26)	C(27)	111.23(17)
C(11)	C(12)	C(7)	122.27(16)	C(26)	C(27)	C(22)	113.12(14)
C(18)	C(13)	C(14)	115.70(14)				

Appendix 5

a) Bond distances of 1,1-bis[4-(4-aminophenoxy)phenyl]-4-per-hydrocumyl cyclohexane in angstroms

Atom1	Atom2	Distance	Atom1	Atom2	Distance
O(1)	C(10)	1.378(4)	C(7)	C(8)	1.387(4)
O(1)	C(28)	1.390(5)	C(7)	C(12)	1.393(4)
O(2)	C(16)	1.385(3)	C(12)	C(11)	1.391(4)
O(2)	C(34)	1.400(4)	C(11)	C(10)	1.372(5)
N(1)	C(31)	1.411(7)	C(10)	C(9)	1.375(5)
N(2)	C(37)	1.396(4)	C(9)	C(8)	1.386(4)
C(1)	C(7)	1.538(4)	C(13)	C(18)	1.392(4)
C(1)	C(13)	1.547(4)	C(13)	C(14)	1.394(4)
C(1)	C(2)	1.548(4)	C(18)	C(17)	1.382(4)
C(1)	C(6)	1.552(4)	C(17)	C(16)	1.383(4)
C(2)	C(3)	1.525(4)	C(16)	C(15)	1.371(4)
C(3)	C(4)	1.536(4)	C(15)	C(14)	1.382(4)
C(4)	C(5)	1.538(4)	C(28)	C(29)	1.351(5)
C(4)	C(19)	1.566(4)	C(28)	C(33)	1.385(7)
C(5)	C(6)	1.526(4)	C(33)	C(32)	1.410(9)
C(19)	C(20)	1.535(4)	C(32)	C(31)	1.342(8)
C(19)	C(21)	1.538(4)	C(31)	C(30)	1.325(6)
C(19)	C(22)	1.562(4)	C(30)	C(29)	1.369(5)
C(22)	C(23)	1.528(4)	C(34)	C(35)	1.367(4)
C(22)	C(27)	1.536(4)	C(34)	C(39)	1.372(5)
C(27)	C(26)	1.517(4)	C(39)	C(38)	1.374(5)
C(26)	C(25)	1.508(4)	C(38)	C(37)	1.372(5)
C(25)	C(24)	1.519(4)	C(37)	C(36)	1.371(5)
C(24)	C(23)	1.518(4)	C(36)	C(35)	1.374(4)

b) Bond angles of 1,1-bis[4-(4-aminophenoxy)phenyl]-4-per-hydrocumyl cyclohexane in degrees

Atom 1	2	3	Angle	Atom 1	2	3	Angle
C(10)	O(1)	C(28)	117.1(3)	C(11)	C(10)	O(1)	116.6(3)
C(16)	O(2)	C(34)	119.4(2)	C(9)	C(10)	O(1)	124.5(4)
C(7)	C(1)	C(13)	109.5(2)	C(10)	C(9)	C(8)	119.9(3)
C(7)	C(1)	C(2)	112.3(2)	C(9)	C(8)	C(7)	123.0(3)
C(13)	C(1)	C(2)	109.0(2)	C(18)	C(13)	C(14)	116.2(3)
C(7)	C(1)	C(6)	110.8(2)	C(18)	C(13)	C(1)	120.8(2)
C(13)	C(1)	C(6)	109.3(2)	C(14)	C(13)	C(1)	123.0(2)
C(2)	C(1)	C(6)	105.8(2)	C(17)	C(18)	C(13)	122.6(3)
C(3)	C(2)	C(1)	114.1(2)	C(18)	C(17)	C(16)	119.4(3)
C(2)	C(3)	C(4)	112.5(2)	C(15)	C(16)	C(17)	119.6(3)
C(3)	C(4)	C(5)	107.9(2)	C(15)	C(16)	O(2)	116.0(3)
C(3)	C(4)	C(19)	113.9(2)	C(17)	C(16)	O(2)	124.4(3)
C(5)	C(4)	C(19)	115.1(2)	C(16)	C(15)	C(14)	120.3(3)
C(6)	C(5)	C(4)	111.7(2)	C(15)	C(14)	C(13)	121.9(3)
C(5)	C(6)	C(1)	113.3(2)	C(29)	C(28)	C(33)	117.7(5)
C(20)	C(19)	C(21)	108.7(3)	C(29)	C(28)	O(1)	120.5(4)
C(20)	C(19)	C(22)	108.7(2)	C(33)	C(28)	O(1)	121.8(4)
C(21)	C(19)	C(22)	109.9(2)	C(28)	C(33)	C(32)	119.4(5)
C(20)	C(19)	C(4)	109.8(2)	C(31)	C(32)	C(33)	121.1(5)
C(21)	C(19)	C(4)	108.9(2)	C(30)	C(31)	C(32)	118.1(6)
C(22)	C(19)	C(4)	110.8(2)	C(30)	C(31)	N(1)	122.5(7)
C(23)	C(22)	C(27)	107.6(2)	C(32)	C(31)	N(1)	119.5(6)
C(23)	C(22)	C(19)	115.6(2)	C(31)	C(30)	C(29)	123.1(5)
C(27)	C(22)	C(19)	114.8(2)	C(28)	C(29)	C(30)	120.7(4)
C(26)	C(27)	C(22)	111.8(2)	C(35)	C(34)	C(39)	119.5(3)
C(25)	C(26)	C(27)	111.7(3)	C(35)	C(34)	O(2)	119.0(3)
C(26)	C(25)	C(24)	111.0(3)	C(39)	C(34)	O(2)	121.2(3)
C(23)	C(24)	C(25)	112.1(3)	C(34)	C(39)	C(38)	120.2(3)
C(24)	C(23)	C(22)	111.9(3)	C(37)	C(38)	C(39)	121.1(3)
C(8)	C(7)	C(12)	115.6(3)	C(36)	C(37)	C(38)	117.7(3)
C(8)	C(7)	C(1)	120.5(3)	C(36)	C(37)	N(2)	121.4(3)
C(12)	C(7)	C(1)	123.8(3)	C(38)	C(37)	N(2)	120.9(3)
C(11)	C(12)	C(7)	122.0(3)	C(37)	C(36)	C(35)	122.0(3)
C(10)	C(11)	C(12)	120.6(3)	C(34)	C(35)	C(36)	119.5(3)
C(11)	C(10)	C(9)	119.0(3)				

Synopsis of the Thesis Entitled “Synthesis of Processable High Performance Polymers”

Introduction:

Plastics are nowadays clearly the material of choice in all applicational sectors. The relative growth of plastics in the last three decades compared to other materials has been phenomenal. Every day we can see the results of innovative plastics technology-technology which creates opportunities for manufacturers and designers to meet new performance and environmental challenges. Modern industry demands advanced materials and products engineered to have special properties that guarantee performance in certain applications. In this respect, high performance polymers (HPPs) have been explored extensively to meet these demands. HPPs can be broadly defined as materials that exhibit unique combination of properties (e.g., strength, high stiffness and impact resistance, high resistivity, low dielectric constants, chemical and solvent resistance, etc.) superior to those of state-of-the-art materials along with better elevated temperature behavior. Many of the important advances in the polymeric materials involve imparting desirable properties through the control of polymer structure.

Aromatic polyimides, polyamides and polyesters are important classes of high performance polymers.¹⁻¹⁰ The high regularity and high rigidity of the backbones of HPPs result in strong chain-chain interactions, high crystallinity, high melting points and low solubility. The processing of HPPs is therefore more challenging. Recently, synthetic research in the area of HPPs has been directed towards the improvement of their processability.¹¹⁻¹⁴

Of the many approaches attempted to improve processability of high performance polymers, introduction of “cardo” groups (pendant loops) into rigid polymer backbones has resulted in much success.¹⁵ The introduction of cardo groups along the polymer backbone has been shown to impart greater solubility as well as better mechanical and thermal properties. These “cardo” groups could be alicyclic or aromatic in nature. The alicyclic groups, viz., cycloalkyl, norbornyl, adamantyl, etc., have been studied in the literature.¹⁶ The alicyclic groups, along with the improvement in processability of polymers impart lighter color, lower

dielectric constants,¹⁷ and better gas barrier properties¹⁸ without significantly affecting thermal stability. The simplest cardo group is cyclohexyl group and it can be introduced into the polymer backbone easily. Monomers containing “cardo” cyclohexyl groups can be easily synthesized and polymerized to get cyclohexyl-cardo containing HPPs. Cyclohexyl ring is conformationally flexible and undergoes chair-boat transformations, allowing polymer chains to pack better.¹⁹ Consequently, cyclohexyl-containing polymers have lower free volumes, which reduces their solubility / processability. The substitution on cyclohexyl ring hinders the packing of polymer chains, which leads to better processability. Therefore, it is desirable to have substituted cyclohexyl rings to get processable HPPs. Substituent can be alkyl,²⁰ aryl,¹⁶ etc. The bulky substituent like t-butyl,²¹ hinder the packing of polymer chains giving them more free volume which in-turn improves processability. If the length of linear alkyl group increases, it acts as an internal plasticizer,²² thus aiding the processability.

The approach adapted in the present work for the synthesis of processable HPPs involves synthesis of difunctional monomers containing cyclohexylidene moiety with (1) flexible pentadecyl, and (2) bulky perhydrocumyl substituents. Flexible pentadecyl chain containing monomers were synthesized for improving polymer processability *via* internal plasticization allowing polymer chains more freedom for flow during processability. The monomers containing bulky perhydrocumyl substituent were targeted for improving processability of resulting polymers by increasing free volume. Thus, various difunctional monomers were designed and synthesized by relatively inexpensive chemical routes with an objective to obtain processable HPPs with specific properties such as high pretilt angle, good gas permeability and lower dielectric constant. The aim of the present investigation was to synthesize processable high performance polymers by incorporating flexible alkyl chain (pentadecyl) or bulky perhydrocumyl – substituted cyclohexylidene moiety and to establish a structure-property relationship.

With above objectives in mind, the following specific work was chosen for the thesis. Objectives of the present thesis:

1. Synthesis of bisphenols and diamines containing substituted cyclohexylidene moiety starting from commercially available chemicals, viz., cashewnut shell liquid (CNSL) and p-cumyl phenol. The substituents were flexible alkyl chain (pentadecyl) or bulky perhydrocumyl group

2. Synthesis and characterization of high performance polymers such as aromatic polyesters, polyimides, etc., containing cyclohexylidene moiety with flexible alkyl (pentadecyl)- substituent.
3. Synthesis and characterization of high performance polymers such as aromatic polyesters, polyimides, polyetherimides, containing cyclohexylidene moiety with bulky perhydrocumyl- substituent.
4. To study the effect of flexible alkyl or bulky perhydrocumyl groups on the solubility and thermal properties of cyclohexylidene -containing high performance polymers.
5. To evaluate a few selected polymers as materials for alignment layers for liquid crystals, and as membrane materials for gas separation.

The thesis has been divided into the following six chapters.

Chapter I: Introduction

A comprehensive review of literature on high performance polymers, viz., aromatic polyesters and polyimides, covering methods of synthesis, structure-property relationship and applications is presented.

Chapter 2: Scope and Objectives

This chapter discusses scope and objectives of the thesis

Chapter 3: Synthesis and Characterization of Condensation Monomers

This chapter describes

- i. Synthesis of bisphenol and diamines containing cyclohexylidene moiety with a flexible pentadecyl- substituent, starting from CNSL – a renewable resource material.
- ii. Synthesis of bisphenols and diamines containing cyclohexylidene moiety with bulky perhydrocumyl- substituent, starting from p-cumyl phenol – a commercially available chemical.

The difunctional monomers and intermediates involved in their synthesis were characterized by IR, $^1\text{H-NMR}$, and $^{13}\text{C-NMR}$. Some of the difunctional monomers were characterized by single crystal X-Ray diffraction analysis.

Chapter 4: Synthesis and Characterization of Processable High Performance Polymers Containing Cyclohexylidene Moiety with Flexible Pentadecyl-Substituent

This chapter describes

- i. Synthesis and characterization of (co)polyesters, and (co)polyimides, containing cyclohexylidene moiety with flexible pentadecyl- substituent.
- ii. Evaluation of selected polymers as alignment layers for liquid crystals.

Chapter 5: Synthesis and Characterization of Processable High Performance Polymers Containing Cyclohexylidene Moiety with Bulky Perhydrocumyl-Substituent

This chapter describes

- i. Synthesis and characterization of polyesters, polyimides and polyetherimides containing cyclohexylidene moiety with bulky perhydrocumyl- substituent.
- ii. Evaluation of selected polymers as alignment layers for liquid crystal displays, interlayer dielectric materials and as membrane materials for gas separation studies.

Chapter 6: Summary and Conclusions

This chapter summarizes the results and salient conclusions of the investigations reported in this thesis.

References:

1. *Synthetic Methods in Step Growth Polymers*, Rogers, M.E.; Long, T.E.; Eds. John Wiley and Sons : New York , 2003.
2. *Polyimides and Other High Temperature Polymers, Vol. I*, Mittal, H.K., Ed.; VSP BV: The Netherlands, 2001.
3. *Polyimides: Fundamentals and Applications*, Ghosh, M. K.; Mittal, K. L., Eds.; Marcel Dekker: New York, 1996.
4. Vinogradova, S. V.; Vasnev, V. A.; Valetskii, P. M. *Russ. Chem. Rev.* **1994**, 63(10), 833.
5. Lin, J.; Sherrington, D. C. *Adv. Polym. Sci.* **1994**, 111, 177.
6. Wartusch, J. *Makromol. Chem. Macromol. Symp.* **1993**, 75, 67.
7. Sroog, C. E. *Prog. Polym. Sci.* **1991**, 16, 561.
8. *Heat Resistant Polymers: Technologically Useful Materials*, Critchley, J. P.; Knight, G. J.; Wright, W. W. Plenum Press: New York, 1983.
9. Hergenrother, P. M. *High Perform. Polym.* **2003**, 15, 3.
10. Bier, G.; *Polymer* **1974**, 15, 127.
11. Sillion, B. *High Perform. Polym.* **1999**, 11, 417.
12. de Abajo, J.; de la Campa, J. G. *Adv. Polym. Sci.* **1999**, 140, 23.
13. Huang, S. J.; Hoyt, A. E. *Trends in Polym. Sci.* **1995**, 3, 262.
14. Cheng, S. Z. D.; Arnold, F. E.; Li, F.; Harris, F. W. *Trends in Polym. Sci.* **1993**, 1, 243.
15. Korshak, V. V.; Vinogradova, S. V.; Vygodskii, Y. S. *J. Macromol. Sci. Rev. Macromol. Chem.* **1974**, C11, 45.
16. Liaw, D. J.; Liaw, B. Y. *Polym. Prepr. (Am. Chem. Soc., Div. Polym. Chem.)* **2000**, 41, 79.
17. Li, J.; Kato, J.; Kudo, K.; Shiraishi, S. *Macromol. Chem. Phys.* **2000**, 201, 2289.
18. Jager, J.; Hendriks, A. J. J. *J. Appl. Polym. Sci.* **1995**, 38, 1465.
19. Zhao, J.; Jones, A.; Inglefield, P. T.; Bendler, J. T. *Polymer*, **1998**, 39, 1339.
20. Choi, K. Y.; Yi, M. H. *Macromol. Symp.* **1999**, 142, 193.
21. Liaw, D. J.; Liaw, B. Y.; Chung, C. Y. *Macromol. Chem. Phys.* **2000**, 14, 1887.
22. Yazdani-Pedram, M; Soto, E.; Tagle, L. H.; Diaz, F. R.; Gargallo, L.; Radic, D. *Thermochimica Acta*, **1986**, 105, 149.

(R. D. Shingte)

Student

(P. P. Wadgaonkar)

Research Guide

List of Publications

1. Polyamides containing s-Triazine rings and fluorene "cardo" groups: synthesis and characterization
A.D. Sagar, R.D. Shingte, P.P. Wadgaonkar and M.M. Salunkhe
***European Polymer Journal* 2001, 37, 1493**
2. One pot, spontaneous and simultaneous synthesis of gold nanoparticles in aqueous and nonpolar organic solvents using a diamine-containing oxyethylene linkage
PR. Selvakannan, P. Senthil Kumar, Arvind S. More, Rahul D. Shingte, Prakash P. Wadgaonkar, and Murali Sastry
***Langmuir* 2004, 20, 295**
3. Free-standing gold nanoparticle membrane by the spontaneous reduction of aqueous chloroaurate ions by oxyethylene linkage-bearing diamines at a liquid-liquid interface
PR. Selvakannan, P. Senthil Kumar, Arvind S. More, Rahul D. Shingte, Prakash P. Wadgaonkar and Murali Sastry
***Advanced Materials*, 2004, 16, 966**
4. 1,1-Bis(4-aminophenyl)-3-alkylcyclohexanes, method for their preparations
Rahul D. Shingte and Prakash P. Wadgaonkar
US Patent 6,790,993 , 2004
5. Process for the preparation of free standing membranes
Kumar Pandian Senthil, Kannan Periasamy Selva, More Arvind, Shingte Rahul, Wadgaonkar Prakash and Sastry Murali
US Patent 0199544 A1, 2005
6. Synthesis and characterization of processable aromatic (co)polyesters derived from 1,1-bis(4-hydroxyphenyl)-3-pentadecylcyclohexane and bisphenol-A
Rahul D. Shingte and Prakash P. Wadgaonkar
Manuscript under preparation
7. New organosoluble polyarylates containing perhydrocumyl cyclohexylidene, "cardo" group: synthesis and characterization
Rahul D. Shingte and Prakash P. Wadgaonkar
Manuscript under preparation
8. Organosoluble Polyetherimides based on 1,1-bis[4-(4-aminophenoxy)phenyl]-4-perhydrocumyl cyclohexane and aromatic dianhydrides
Rahul D. Shingte, C. V. Avadhani and Prakash P. Wadgaonkar
Manuscript under preparation

9. Synthesis and characterization of new organosoluble polyimides based on 1,1-bis(4-aminophenyl)-4-per-hydrocumyl cyclohexane and aromatic dianhydrides
Rahul D. Shingte, Vedavati G. Puranik and Prakash P. Wadgaonkar
Manuscript under preparation

10. Synthesis and characterization of new organosoluble polyimides based on 1,1-bis(4-aminophenyl)-3-pentadecylcyclohexane and aromatic dianhydrides
Rahul D. Shingte and Prakash P. Wadgaonkar
Manuscript under preparation